UNIVERSIDADE TÉCNICA DE LISBOA

INSTITUTO SUPERIOR DE AGRONOMIA

CARACTERIZAÇÃO E FRACCIONAMENTO DA CASCA DE *QUERCUS CERRIS* PARA SEPARAÇÃO DA CORTIÇA TENDO EM VISTA A SUA UTILIZAÇÃO EM AGLOMERADOS

TESE APRESENTADA PARA OBTENÇÃO DO GRAU DE DOUTOR EM ENGENHARIA FLORESTAL E DOS RECURSOS NATURAIS

ALI UMUT ŞEN

ORIENTADORA:DOUTORA HELENA PEREIRA

CO-ORIENTADORA:DOUTORA ISABEL MIRANDA

JÚRI:

Presidente: Reitor da Universidade Técnica de Lisboa

Vogais: Doutora Helena Margarida Nunes Pereira Professora Catedrática Instituto Superior de Agronomia da Universidade Técnica de Lisboa;

Doutora Elizabeth da Costa Neves Fernandes de Almeida Duarte Professora catedrática;
Instituto Superior de Agronomia da Universidade Técnica de Lisboa;
Doutor António Jorge Velez Marques Professor Coordenador Instituto Superior de Engenharia de Lisboa do Instituto Politécnico de Lisboa;
Doutor Bruno Miguel de Morais Lemos Esteves Professor Adjunto Escola Superior de Tecnologia e Gestão do Instituto Politécnico de Viseu;
Doutora Teresa Maria Gonçalves Quilhó Marques dos Santos Investigadora auxiliar Instituto de Investigação Científica Tropical;
Doutora Isabel Maria Silva Sanches de Miranda Técnica Superior do Instituto Superior de Agronomia da Universidade Técnica de Lisboa.

LISBOA

2012

Agradecimentos

Agradeço, em primeiro lugar, à Professora Helena Pereira, minha orientadora, por todo o auxílio que me prestou na elaboração desta tese. A Professora mostrou-se um ser humano admirável, para além de uma excelente orientadora, que qualquer aluno gostaria de ter.

Agradeço também à Professora Isabel Miranda, minha co-orientadora, que esteve sempre disponível para me ajudar durante a realização da tese.

O meu muito obrigado à Professora Teresa Quilhó, que contribuiu com os seus conselhos para o aperfeiçoamento da tese.

Agradeço também ao Professor António Velez Marques, do Instituto Superior de Engenharia de Lisboa, o seu contributo para o trabalho e a realização dos espetros FTIR.

Aos Engenheiros florestais Ali Göçer e Mehmet Demirbağ, da província de Kahramanmaras, e à organização Orman Genel Müdürlüğü (Serviços Florestais da Turquia), que me permitiram recolher amostras que estudei na presente tese.

Ao Professor José Luis Louzada pela fotografia de *Q. cerris* no Jardim Botânico de UTAD, ao Engenheiro Nuno Oliveira pela sua ajuda no Parque da Pena e à colega Chang Liu pela sua prestativa tradução de um artigo em chinês.

Aos colegas Dr. José Ramón Gonzáles Adrados do Instituto Nacional de Investigación y Tecnología Agraria y Alimentaria-Madrid, Manel Pretel Wilson (Diretor Geral) e Patricia Jové (Investigadora) do Institut Català del Suro-Girona, pela disponibilidade de trocar ideias sobre a cortiça.

Agradecimentos

Às lindas e maravilhosas amigas Ana Luísa Luz, Alexandra Lauw, Sofia Leal, Vicelina Sousa, Ana Alves, Rita Simões, Sara Santos, Vanessa Cabral, Ana Lourenço e Sofia Knapic, cujas correções e sugestões ajudaram a melhorar o texto.

A Joaquina Martins, Cristiana Alves, Lidia Silva, Dr. Jorge Gominho, Professora Fátima Tavares, Professor José Graça e à Professor António Fabião que sempre demonstraram o zelo por mim e pelo meu trabalho.

Aos colegas e amigos do ISA com os quais partilhei bons momentos durante estes anos de trabalho.

Aos Professores Osman Engür, Ercan Tanrıtanır e Nusret As da Universidade de Istanbul.

Às Professoras Isabel Villaescusa, Angels Olivella e Nuria Fiol da Universidade de Girona.

Aos grandes amigos Shahram Rahnemoon, Ufuk Yılmaz, Ahmet Çelebi, Hasan Özdemir, Terencio Aguiar Junior, Nurgül Karlıoğlu, Elisianne Campos e David Pujol, com os quais passei momentos importantes da minha vida.

E por último, mas não menos importante, agradeço aos meus pais Fatma Şen e Yusuf Şen, pois sem a ajuda deles não teria chegado até aqui.

NOME: ALI UMUT ŞEN

DOUTORAMENTO EM: ENGENHARIA FLORESTAL E DOS RECURSOS NATURAIS

ORIENTADOR: PROFFESORA DOUTORA HELENA PEREIRA

CO-ORIENTADOR: PROF.PROFESSORA DOUTORA ISABEL MIRANDA

DATA:18.10.2012

TÍTULO DA TESE: CARACTERIZAÇÃO E FRACCIONAMENTO DA CASCA DE *QUERCUS CERRIS* PARA SEPARAÇÃO DA CORTIÇA TENDO EM VISTA A SUA UTILIZAÇÃO EM AGLOMERADOS

RESUMO

Estudou-se a casca de *Quercus cerris* com os seguintes objetivos: i) analisar a anatomia da casca; ii) separar e determinar a composição química da cortiça; iii) analisar o comportamento térmico da cortiça; iv) estudar a cortiça como material de adsorção de poluentes em meio aquoso; e v) comparar os resultados com os da cortiça de *Quercus suber.*

A casca de *Q. cerris* é constituída por floema, periderme e ritidoma. O ritidoma inclui várias peridermes sequenciais, com proporção elevada de cortiça e muito tecido esclerificado. A estrutura da cortiça da *Q. cerris* é semelhante à da *Q.suber*. No entanto, as células são mais pequenas e a fração sólida é mais elevada.

A composição química da cortiça de *Q. cerris* é semelhante à da *Q. suber* mas com menor teor de suberina e formada principalmente por ω-hidroxiácidos.

A degradação térmica iniciou-se a 200°C e aumentou com a temperatura e duração do tratamento. A suberina foi termicamente mais resistente. A cor alterou-se até 40% de perda de massa. Desenvolveu-se um modelo de perda de massa com os valores da alteração de cor.

A cortiça da *Q. cerris* demonstrou ser eficaz para adsorção de hidrocarbonetos aromáticos policíclicos e crómio (VI) em soluções aquosas.

Palavras-chave: *Quercus cerris*, cortiça, composição química, tratamento térmico, adsorção

TITLE: CHARACTERIZATION AND FRACTIONATION OF *QUERCUS CERRIS* BARK FOR SEPARATION OF CORK WITH AN INTENTION TO USE IT IN AGGLOMERATES

ABSTRACT

Quercus cerris bark was studied with the following objectives: i) to study bark anatomy, ii) to separate and determine chemical composition of cork, iii) to analyze the thermal behavior of cork, iv) to investigate the use of cork as adsorbent of pollutants in aqueous environments and v) to compare the results obtained with those from *Quercus suber*.

The bark of *Q. cerris* is composed of phloem, periderm and rhytidome. The rhytidome contains various sequential periderms with large portions of cork and many sclerified tissues. The cork structure is similar to that of *Q. suber*, but the cells are smaller and have higher solid fraction.

The chemical composition of cork of *Q. cerris* is similar to that of *Q. suber* but suberin content is less and it is formed largely by ω-hidroxyacids. The thermal degradation starts at 200°C and increases with temperature and treatment time. Suberin was thermically more resistant. The colour was altered until 40% of mass loss. A mass loss model was developed with colour change values.

The *Q. cerris* cork demonstrated to be efficient for adsorption of polycyclic aromatic hydrocarbons and chromium (VI) from aqueous solutions.

Keywords: *Quercus cerris*, cork, chemical composition, heat treatment, adsorption

Índice

Capítulo 1. Introdução e Objetivos

1.1. Enquadramento geral e justificação do interesse

O género *Quercus* L. tem na Turquia uma área de distribuição de 6,4 milhões de hectares e inclui 18 espécies, entre as quais a *Quercus cerris* L. (OGM, 2006). O carvalho turco (Carvalho da Turquia, *Quercus cerris*) cresce naturalmente na Europa central e no sul até à Asia Menor. A espécie existe em toda a Turquia, exceto na região este e nordeste, com duas variedades: cerris, a mais comum, e *austriaca*, que só existe numa zona no norte do país (Hedge e Yaltırık, 1982). A área total de ocupação desta espécie não é conhecida, uma vez que é inventariada com outras espécies do género Quercus. No entanto, é possível delimitar áreas específicas onde ela é encontrada como espécie dominante, como seja o município de Andırın, no sudeste de Turquia, local de amostragem do presente trabalho. *Q. cerris* tem uma área de distribuição estimada em cerca de 235 mil hectares no sudeste de Turquia, na província florestal de Kahramanmaraş, perto de Andırın (Mıhçıoğlu, 1942).

As árvores de *Q. cerris* não têm atualmente valorização madeireira e são utilizadas pela população local como lenha. Também a casca de *Q. cerris* não é valorizada, mas o facto de apresentar uma quantidade considerável de cortiça poderá torná-la um material importante para a economia da Turquia. Neste país, a cortiça de *Q. cerris* era desconhecida como material até à Segunda Guerra Mundial, altura em que houve grande dificuldade na importação da cortiça de Espanha e Portugal e se equacionou o seu aproveitamento.

As propriedades básicas da cortiça de *Q. cerris* (densidade aparente, elasticidade, etc.) foram consideradas inferiores às da cortiça de *Q. suber* (Mıhçıoğlu, 1942). Realizaram-se alguns trabalhos industriais para utilização da casca de *Q. cerris* e produziram-se rolhas para bebidas e placas isolantes (Kasaplıgil, 1981; Bozkurt e Göker, 1986). Natividade (1950) também referiu a extração da cortiça da *Q. cerris* para o fabrico de rolhas na Turquia. A Turquia recomeçou a importar cortiça da Europa pouco tempo depois da Segunda Guerra Mundial, o que fez com que os trabalhos sobre a utilização deste material terminassem (Kasaplıgil, 1981).

O primeiro trabalho sobre a casca da espécie foi feito pelo engenheiro florestal Kazım Mıhçıoğlu, que assinalou o facto de casca de *Q. cerris* conter uma porção considerável de cortiça e chamou a atenção para o seu potencial de utilização (Kasaplıgil, 1981).

São muito escassos os trabalhos encontrados em bibliografia relativos às propriedades da cortiça de *Q. cerris*, destacando-se o estudo de Telgeren (1976) que compara qualitativamente a casca desta espécie com a de *Q. suber* ou o trabalho realizado por Babos (1979) que analisou as propriedades anatómicas de casca de *Q. cerris* var. *cerris* e *Q. cerris* var. *austriaca* na Hungria, indicando a formação apreciável de cortiça em árvores com 30 anos de idade.

A região sudeste da Turquia é uma das mais pobres do país (Çekiç, 2011). Com o objetivo de atenuar as desigualdades económicas entre as regiões no âmbito do acordo para a integração na União Europeia, foram criadas, em 2006, agências regionais de desenvolvimento na Turquia (Çuhadar, 2010). A Agência de Desenvolvimento do Mediterrâneo Oriental (Dogaka) abrange as cidades de Osmaniye, Hatay e Kahramanmaraş. De acordo com o relatório desta entidade vivem nestas cidades aproximadamente 2,8 milhões de pessoas e o desemprego atinge os 18% (Tanılır, 2010). A valorização dos componentes da casca de *Q. cerris*, particularmente da cortiça, pode constituir um contributo importante para a economia da região, ao mesmo tempo que pode contribuir também para a preservação destas florestas (Guerra et al., 2009).

Assim, pretende-se com este trabalho contribuir para esta valorização através de uma caracterização anatómica e química desta casca e de algumas das suas propriedades relevantes para utilização, em comparação com as propriedades da cortiça de *Q. suber*, cuja utilização é sobejamente conhecida (Pereira, 2007) e que constitui o material de referência.

1.2. Objetivos

Com este trabalho pretende-se adquirir maior conhecimento sobre a casca da *Q. cerris*, nomeadamente da sua fração de cortiça, potencialmente com maior valorização, de modo a contribuir para o desenvolvimento económico local das regiões da sua distribuição assim como para a preservação das suas florestas.

Os objetivos específicos são: investigar as características anatómicas da casca de *Q. cerris* e fazer o seu fracionamento de modo a separar uma fração de cortiça; estudar as propriedades químicas da cortiça e as características da sua estrutura celular; estudar a decomposição térmica de grânulos de cortiça e o impacto na sua estrutura e composição química; avaliar as possibilidades para utilização da cortiça de *Q. cerris* como material de adsorção de poluentes em meio aquoso; e comparar os resultados adquiridos com os da cortiça de *Q. suber*.

1.3. Estrutura do trabalho

O trabalho estrutura-se em quatro capítulos.

Neste Capítulo 1 inclui-se enquadramento geral do trabalho, que justificam os seus objetivos gerais e específicos, assim como a descrição da organização desta tese.

No Capítulo 2 é feita uma revisão de conhecimentos sobre: o carvalho *Q. cerris*; a formação da cortiça em cascas; a caracterização da estrutura celular e a composição química da cortiça; as utilizações atuais da cortiça nomeadamente sob a forma de grânulos, de aglomerados compósitos e aglomerados puros; a adsorção de poluentes utilizando cascas como bioadsorventes.

No Capítulo 3 apresentam-se a metodologia utilizada neste trabalho e os resultados dos trabalhos originais desenvolvidos, sob a forma de oito artigos (sete já publicados e um submetido) em revistas científicas. Os artigos são apresentados com a sua formatação original e organizados sequencialmente

de acordo com o critério temático: anatomia (artigos I e II), composição química (artigo III), tratamento térmico (artigos IV e V) e aplicações como adsorvente de poluentes (artigos VI, VII e VIII).

No Capítulo 4 são apresentadas as conclusões e perspetivas de trabalhos futuros.

Nos anexos são incluídos os resumos dos trabalhos apresentados em congressos internacionais.

Artigos:

I. Şen, A., Quilhó, T., Pereira, H. 2011a. Bark anatomy of *Quercus cerris* L. var. *cerris* from Turkey. Turk J. Bot. 35, 45-55.

II. Şen, A., Quilhó, T., Pereira, H. 2011b. The cellular structure of cork from *Quercus cerris* var. *cerris* bark in a materials perspective. Ind. Crop. Prod. 34(1), 929-936.

III. Şen, A., Miranda I., Santos, S., Graça, J., Pereira, H. 2010. The chemical composition of cork and phloem in the rhytidome of *Quercus cerris* bark. Ind. Crop. Prod. 31, 417-422.

IV. Şen, A., Miranda, I., Pereira, H. 2012a. Temperature-induced structural and chemical changes in cork from *Quercus cerris*. Ind. Crop. Prod. 37, 508-513.

V. Şen, A., Velez Marquez, A., Gominho, J., Pereira, H. 2012b. Study of thermochemical treatments of cork in the 150-400ºC range using colour analysis and FTIR spectroscopy. Ind. Crop. Prod. 38, 132-138.

VI. Olivella, M.A., Jove, P., Şen, A., Pereira, H., Villaescusa, I., Fiol, N., 2011. Sorption performance of *Quercus cerris* cork with polycyclic aromatic hydrocarbons and toxicity testing. BioResources 6(3), 3363-3375.

VII. Şen, A., Olivella, M.A., Fiol, N., Miranda, I., Villaescusa, I., Pereira, H. 2012c. Removal of chromium (VI) in aquaeus environments using cork and heat treated cork samples from *Quercus cerris* and *Quercus suber*. BioResources 7(4), 4843-4857.

VIII. Şen, A., Pereira, H., Olivella, M.A., Villaescusa, I. 2012d. Heavy metal removal in aqueous environments using bark as a biosorbent: a review. Submetido a Water Research.

Capítulo 2. Revisão de conhecimentos

2.1. *Quercus cerris*

O carvalho da Turquia (*Quercus cerris*) é uma árvore folhosa, que pertence à família das Fagaceae, género *Quercus*, subgénero de *Euquercus*, secção de *Cerris* (Figura 1). A espécie *Q. cerris* pertence à mesma secção que o sobreiro (*Quercus suber*).

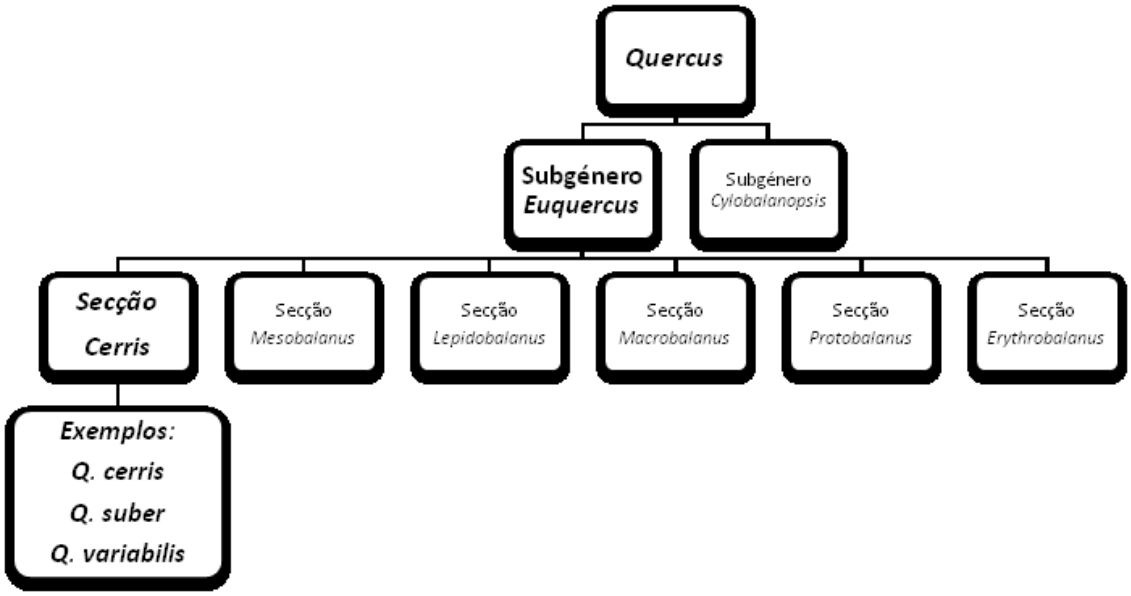

Figura 1. A classificação da *Quercus cerris* (Camus, 1934).

A espécie distribui-se naturalmente na parte sul de França, Itália, Europa central, península Balcânica, Turquia e oeste da Síria e Líbano (Figura 2) (Kasaplıgil, 1981). Atualmente a espécie encontra-se principalmente no sudeste de Europa e na Ásia Menor, e maioritariamente na Turquia (Figura 2) (Cotti, 2008). Itália possui também uma área importante de *Q. cerris*, estimando uma área de distribuição de aproximadamente 500 mil hectares, principalmente no sul de rio Pó, desde região Appenino Tosco-Emiliano até à Calábria, embora seja raro na Sicília e não exista na Sardenha (La Marca et al., 1983; Lo Monaco et al., 2011).

A espécie foi introduzida na Grã-Bretanha, em 1735, como ornamental onde teve muito boa adaptação e é cultivada nos jardins públicos e arboretos

(Royal Botanic Gardens-Kew, 2012). Em Portugal, a espécie apenas existe como alguns exemplares introduzidos como ornamentais. Por exemplo, existem árvores de *Q. cerris* no Parque da Pena-Sintra, Tapada da Ajuda-Lisboa e Jardim Botânico da Universidade de Trás-os-Montes e Alto Douro (UTAD) em Vila Real (Azevedo Gomes, 1960; Liberato et al., 2003, Jardim Botânico-UTAD, 2012). A Figura 3 mostra árvores de *Q. cerris* no Parque da Pena e Jardim Botânico da UTAD.

Nos limites este e sul, na Turquia e no Líbano, respetivamente, a espécie cresce naturalmente entre altitudes de 10 m e 1500 m (Kasaplıgil, 1981; Abi Saleh e Safi, 1988), enquanto que, no limite oeste, em França, o limite de altitude é 1200 m (Rameau et al., 1989). A espécie cresce rápido, é muito resistente a temperaturas baixas e, portanto, é particularmente adequada a plantações em zonas frias (Kasaplıgil, 1981).

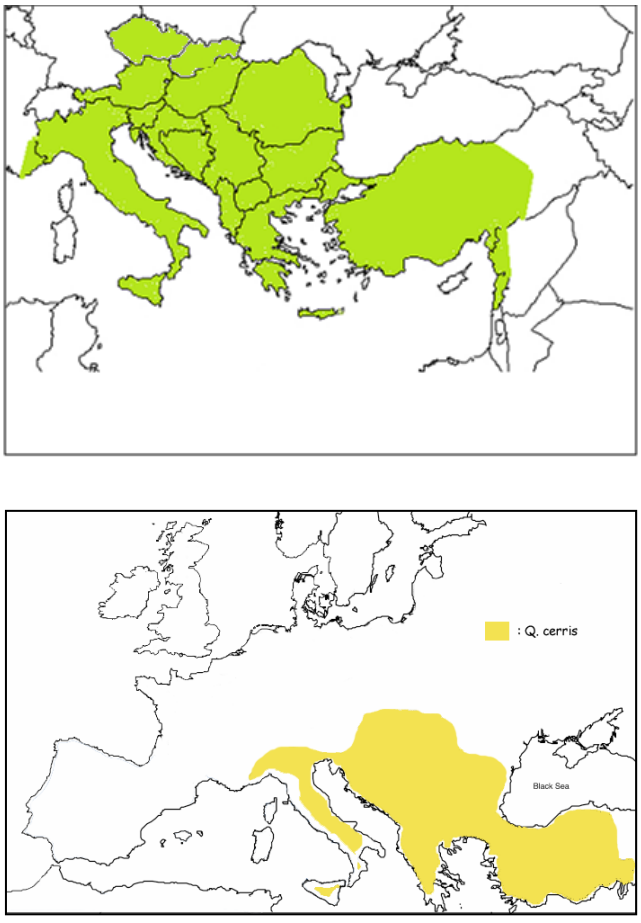

Figura 2. A distribuição da espécie *Quercus cerris* (Kasaplıgil, 1981 em cima, e Cotti, 2008 em baixo)

Figura 3. Exemplares de *Q. cerris* no Jardim Botânico da UTAD (em cima), e no Parque da Pena (diâmetro no DAP, 100 cm) (em baixo)

Q. cerris é uma árvore de porte médio que pode atingir uma altura de 30 m. As folhas são caducas, de cor verde-escura, mais brilhantes nas faces superiores e acinzentadas nas inferiores, alternas, simples, lobadas, oblongas, pinadas e pecioladas (Kasaplıgil, 1981; Yaltırık, 1984). O comprimento e a largura das folhas são entre 7-14 cm e 3-5 cm respetivamente (Cotti, 2008). Na Turquia existem duas variedades, var.

cerris (folhas com lobos profundos) e var. *austriaca* (folhas com lobos pequenas) (Figura 4) (Yaltırık, 1984).

O fruto maduro produz-se nos ramos de ano anterior no segundo ano, tem um comprimento entre 2,5 e 3,6 cm, e possui uma cúpula entre 1,6 e 2,4 cm de diâmetro e entre 1,5 e 1,9 cm de comprimento, com escalas longas entre 4-8 mm de comprimento (Kasaplıgil, 1981; Cotti, 2008).

A casca é espessa (com aproximadamente 5 cm de espessura) (Berkel e Bozkurt, 1961), cinzenta, rija e contém sulcos longitudinais profundos (Figura 5).

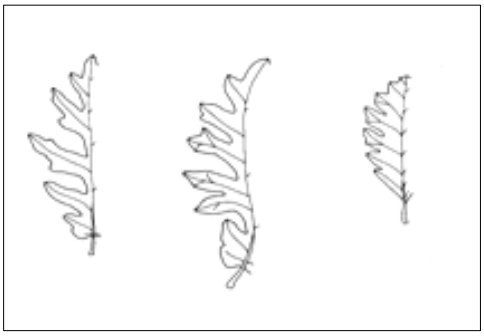

Figura 4. A forma de folha da *Q. cerris* (a esquerda e ao centro var. *cerris* e direta var. *austriaca,* Yaltırık, 1984)

Figura 5. A casca da *Q. cerris* (acima na árvore, em baixo no tronco a secção transversal)

A maioria dos trabalhos científicos sobre a espécie tem sido realizada em Itália, uma vez que a espécie tem grande distribuição neste país.

Atualmente os trabalhos focalizam-se sobre a dendroclimatologia e dendroecologia (Romagnoli e Codipietro, 1996; Di Filippo et al., 2010) e genética (Cotti, 2008; Bagnoli et al., 2009, Fineschi et al., 2011; Gorian et al, 2012). O carvalho turco é sensível, como outras espécies de carvalhos decíduos, às alterações ambientais e regista o mesmo sinal climatológico independentemente da latitude e das circunstâncias ecológicas. A maioria dos anos indicadores (*pointer years)* determinados estão relacionados com a precipitação de primavera e a temperatura de junho (Romagnoli e Codipietro, 1996).

Os haplotipos encontrados a partir de DNA cloroplástico de *Q. cerris* são semelhantes aos de *Q. suber* o que sugere a *introgressão* entre as duas espécies (Gorian et al., 2012). Brüggemann et al. (2009) e Royal Botanic Gardens-Kew (2012) referem a existência dum híbrido de *Q. suber* e *Q. cerris* (*Q. hispanica ou Q. crenata,* carvalho de Lucombe) que tinha sido produzido num viveiro de Exeter na Grã-Bretanha, em 1762, por William Lucombe. Outros híbridos de *Q. cerris* incluem *Q. libanerris* (*Q. cerris* x *Q. libani*), *Q. baenitzii* (*Q. cerris* x *Q. pubescens*), *Q. schneideri* (*Q. cerris* x *Q. trojana)* e *Q. kewensis* (*Q. cerris* x *Q. wislizeni*) (International Oak Society, 2012).

A madeira da espécie é descrita como possuindo: um borne branco e rosa amarelado, bastante ampla e que pode atingir 15-18 cm de espessura e um cerne castanho claro com um tom avermelhado (Bartha, 2011). A espécie não foi valorizada como produtora de madeira, porque a madeira tem propriedades não desejadas no uso final, tais como pouca estabilidade dimensional (retração volumétrica total 12%), ocorrência de rachaduras de secagem (a proporção de retração nas direções tangencial e radial entre 2,3 e 2,4), pouca durabilidade e uma cor irregular e avermelhada, sendo o seu uso principal como lenha (La Marca et al., 1983; Bartha, 2011; Todaro et al, 2012a).

No entanto, a madeira tem uma densidade elevada de 0,80-0,85 g/cm^3 e possui propriedades mecânicas boas (resistências de compressão axial, tração axial e flexão estática de 475-535 daN/cm^2, 1220-1486 daN/cm^2, 793-1086 daN/cm^2 respetivamente) (Bartha, 2011). Fabricaram-se já com madeira de *Q. cerris* painéis de partículas na Bulgária e Itália, painéis de fibras na Roménia, portas e janelas na Hungria e paletes na Itália (La Marca et al., 1983). Lavisci e Scalbert (1991) e Lavisci et al. (1991, 1992) estudaram a colagem da madeira da *Q. cerris,* e referem que a madeira tem pouco polifenóis, os extrativos são principalmente taninos condensados, a madeira colada tem alta resistência ao cisalhamento, mas resistência à fratura da madeira é baixa. La Marca et al. (1983) referem também a possibilidade de utilização de *Q. cerris* para madeira maciça, a casca para extrair taninos e as bolotas como alimento animal.

Atualmente há trabalhos recentes sobre a utilização da sua madeira e melhoria das suas características com tratamento hidrotérmico a temperaturas entre 80 e 180°C (Karastergiou et al., 2006; Lo Monaco et al., 2011; Todaro et al., 2012a, 2012b).

2.2. As cascas das árvores

2.2.1. Formação da casca

A casca inclui todos os tecidos exteriores ao câmbio vascular (Trockenbrodt, 1990; Junikka, 1994; Richter et al., 1996) sendo composta por floema, periderme e ritidoma (Figura 6). Nesta revisão é utilizada a nomenclatura para cascas da IAWA (International Association of Wood Anatomists) (Trockenbrodt, 1990; Junikka 1994).

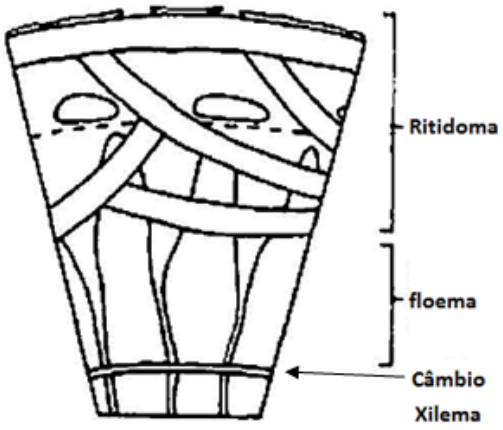

Figura 6. A estrutura da casca (Trockenbrodt, 1990).

Num estado secundário de crescimento, a casca na árvore forma-se a partir de atividade de dois meristemas: o câmbio vascular e o felogénio.

O câmbio vascular é um meristema cujas células se dividem e produzem tecidos secundários por divisões periclinais: xilema para o interior e floema para o exterior. O câmbio origina mais células de xilema do que células de floema, embora a proporção de xilema/floema varie entre espécies: por exemplo, 14:1 em *Abies concolor* e 10:1 em *Quercus alba* (Evert, 2006). No entanto, Beck (2010) referiu que nas coníferas se produz mais floema em relação a xilema (até 1:3) do que nas angiospermas. No câmbio ocorrem também divisões anticlinais das células meristemáticas, formando novas células cambiais de modo a acompanhar o aumento de diâmetro.

O floema é o principal tecido de transporte dos alimentos nas plantas vasculares, tais como açúcares, aminoácidos, lípidos e hormonas. O floema transporta igualmente uma grande quantidade de água para a copa da árvore (Evert, 2006). O floema é constituído por diferentes tipos de células: elementos de tubo crivoso e células companheiras, parênquima axial e radial, fibras e esclereídos (Fahn, 1990).

Os elementos de tubo crivoso e respetivas células companheiras nas folhosas e as células crivosas e de strasburger nas coníferas são responsáveis pela condução da seiva elaborada no floema. As células crivosas têm poros mais pequenos do que os elementos de tubo crivoso e as células de strasburger são mais curtas do que as células companheiras

(Beck, 2010). A ocorrência de uma proteína (*P-protein)* nos elementos de tubo crivoso é característica das angiospermas (Beck, 2010). As fibras e os esclereídos são células de esclerênquima com a função de suporte mecânico. No floema primário as fibras ocorrem nas partes externas do tecido, mas no floema secundário ocorrem várias disposições para as fibras. As fibras vivas servem como células de armazenamento. Os esclereídos aparecem tipicamente nas partes mais velhas do floema como resultado de esclerificação de células de parênquima (Evert, 2006).

A função de armazenamento é assegurada pelas células de parênquima axial e radial, sendo que o parênquima radial acumula também a função de condução no floema, na direção radial. A formação de cristais é comum no floema das folhosas nas células de parênquima e esclerênquima (Roth, 1981).

O floema inclui duas zonas funcional e estruturalmente distintas: o floema condutor e o floema não condutor (também designados floema secundário colapsado e não colapsado) (Junikka, 1994) (Figura 7). De facto, os elementos de tubo crivoso mantem-se fisiologicamente ativos por pouco tempo e apenas uma pequena porção do floema se mantem ativa para a condução (floema condutor) junto ao câmbio vascular. A largura do floema condutor varia entre as espécies: por exemplo 0,14-0,27 mm em *Picea* e 0,20-0,30 mm em *Quercus*. A parte não condutora do floema é estruturalmente diferente da parte condutora: os elementos de tubo crivoso colapsam, as células de parênquima podem dividir-se, dilatar e também esclerificar, originando a formação de raios dilatados (Trockenbrodt, 1991; Quilhó et al., 1999). É frequente a ocorrência de cristais nas células expandidas e nos esclereídos (Roth, 1981; Dickinson, 2000).

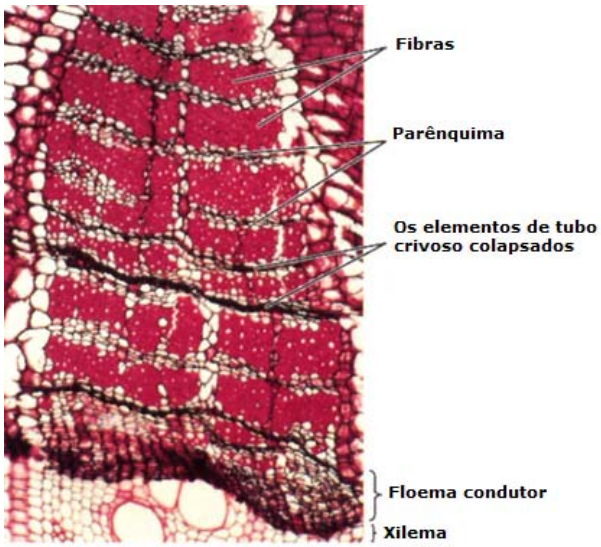

Figura 7. Floema condutor e não condutor (Adaptado de Mauseth, 2011)

A periderme é um tecido protetor que substitui a epiderme que existe num estado primário de crescimento. Estruturalmente, a periderme é constituída por felogénio, feloderme e felema (suber ou cortiça). A periderme ocorre no tronco e nas raízes da árvore e pode também originar-se após um ferimento no tronco, designando-se neste caso periderme traumática (Evert, 2006).

O felogénio é o meristema responsável pela formação da periderme. O felogénio origina-se debaixo de uma (Graça e Pereira, 2004) ou duas camadas de células (Beck, 2010) da epiderme no primeiro ano de crescimento (Figura 8). A formação das células iniciais segue o processo da regressão ao estado meristemático das células de parênquima, seguido pelas divisões periclinais (Beck, 2010).

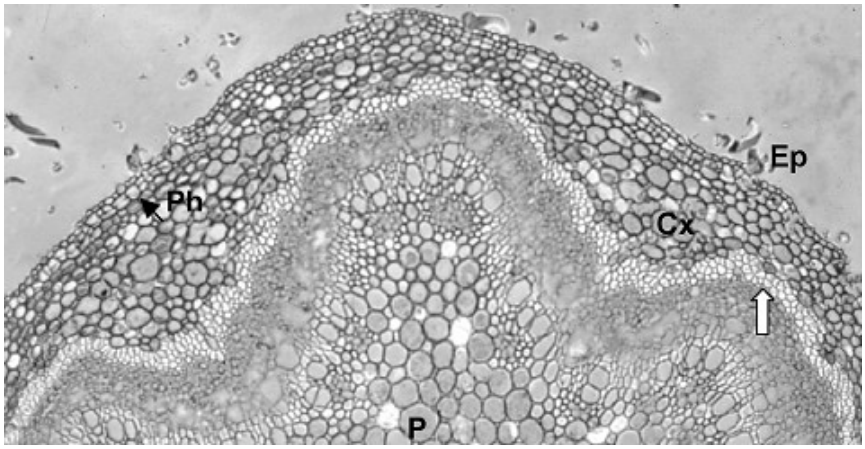

Figura 8. A formação do primeiro felogénio na *Q. suber. Ph: felogénio, Cx: córtex, Ep: Epiderme, P: medula, Seta: fibras* perivasculares (Adaptado de Graça e Pereira, 2004)

Por divisões periclinais das células de felogénio são produzidas as células de feloderme para interior e de felema para exterior. Ao mesmo tempo, por divisões anticlinais das células cambiais, formam-se células intercalares no felogénio para acompanhar o aumento de diâmetro da árvore (Roth, 1981). Ao contrário do câmbio, o felogénio contem só um tipo de células. Na secção tangencial, as células aparecem com um aspeto retangular ou poligonal (Evert, 2006).

A produção de células de felema é maior do que a produção de células de feloderme. Geralmente, a feloderme inclui só algumas células em cada fiada radial, embora em algumas espécies, tal como *Gingko,* seja possível observar até 40 células em cada fiada (Evert, 2006).

O felogénio pode ser contínuo (por exemplo em *Q. suber, Fagus e Prunus*) ou descontínuo ao redor de tronco (Pereira, 2007; Beck, 2010). Em algumas espécies, tais como *Q. suber* (Pereira, 2007), *Fagus*, *Betula* e *Abies* (Roth, 1981), o primeiro felogénio pode manter-se ativo na periderme toda a vida da árvore ou durante muitos anos. No entanto, na maioria das espécies o felogénio tem uma longevidade curta.

Neste caso, ao longo da vida da árvore vão-se formando novos felogénios e peridermes cada vez mais interiormente na casca, isolando portanto funcionalmente os tecidos que lhe ficam para o exterior, ou seja, tecido de floema e peridermes mais antigas. No seu conjunto, estes tecidos isolados

pela última periderme formam o ritidoma. Por exemplo, na macieira (*Malus domestica*) a primeira periderme é substituída pela segunda periderme entre os 6-8 anos e em *Pinus sylvestris* é substituida entre os 8-10 anos (Evert, 2006). Em geral, as espécies das zonas temperadas têm mais peridermes sequenciais do que as espécies das zonas tropicais.

O ritidoma pode apresentar diferentes tipos, de acordo com as características de formação do felogénio da espécie e que se traduzem por diferenças estruturais, visíveis macroscopicamente e utilizadas para descrever o tipo de casca da espécie. O ritidoma pode resultar da sobreposição de várias peridermes ramificadas, anastomosadas e descontínuas e que à medida que se formam, isolam porções de tecido de floema, dando origem a um ritidoma em "escama". Este tipo de ritidoma é muito frequente e ocorre em géneros variados, como por exemplo *Pinus* (Nunes et al., 1996, 1999) e é comum entre os carvalhos (Whitmore, 1962; Howard, 1977; Evert, 2006; Quilhó et al. 2012). Menos frequente é o aparecimento do ritidoma "em anel" que se forma quando as peridermes sucessivas são aproximadamente concêntricas em relação ao eixo da árvore (Evert, 2006). Exemplos deste tipo incluem espécies de *Cupressus*. A terceira forma de ritidoma é uma combinação dos tipos escama e anel, com porções grandes de periderme, de que é exemplo o Plátano (Fahn, 1990).

2.2.2. Estudos sobre cascas de carvalhos

São escassos os trabalhos sobre a casca das espécies do género *Quercus* L. comparativamente aos estudos que existem sobre a madeira.

Evert e Kozlowski (1967) estudaram a proporção de produção xilema/floema (10:1) pelo câmbio de *Q. alba*. Whitemore (1962) indicou um crescimento anual do floema de *Q. robur* de 0,4-1,2 mm. Holdheide (1951) e Huber (1958) referiram a espessura do floema condutor como de 0,2-0,3 mm no género *Quercus*. Holdheide (1951) e Chang (1954) destacaram a importância da disposição das fibras e de cristais no floema como diagnóstico para a identificação de espécies. Trockenbrodt (1995) indicou a formação de drusas na casca de *Q. robur*.

Howard (1977) estudou a estrutura da casca de 10 espécies e uma variadade de *Quercus* (*Q. alba*, *Q. nigra*, *Q. falcata*, *Q. falcata* var. *pagodaefolia*, *Q. rubra*, *Q. velutina*, *Q. marilandica*, *Q. stellata*, *Q. laurifolia*, *Q. coccinea*, e *Q. shumardii*) e concluiu que o floema dos carvalhos é relativamente espesso (entre 3-7 mm), que as fibras se dispõem em faixas tangenciais, e que a sua estrutura é semelhante à das fibras de madeira, embora as fibras de floema sejam mais curtas. Röckle (1986) verificou que o comprimento das fibras na casca de *Q. robur* aumenta nos primeiros 30 anos, permanecendo constante durante alguns anos e depois diminuindo. Howard (1977) assinala que a espessura da periderme depende da duração da atividade do felogénio e que a feloderme que se origina é de espessura reduzida, contendo apenas algumas células em cada fiada.

Tal como Howard (1977), também Evert (2006) faz referência a aspetos relativos ao ritidoma de vários carvalhos, caracterizando-os como um ritidoma do tipo escama. Trockenbrodt (1994) indicou a formação do ritidoma nos carvalhos entre 25 e 35 anos.

Um caso particular no estudo da casca de carvalhos é a do sobreiro, *Q. suber*, e principalmente do seu felema, certamente em resultado da importância económica da produção e indústria de cortiça. Natividade (1950) e Pereira (2007) fizeram descrições detalhadas sobre a formação, e a estrutura da casca de *Q. suber* onde domina o tecido da periderme e não se forma naturalmente o ritidoma (Junikka, 1994). A exploração da cortiça do sobreiro faz-se através da capacidade de regeneração de um felogénio traumático quando se faz a remoção do primeiro felema produzido (Pereira, 2007). O felogénio traumático origina-se no interior do floema aproximadamente 30 dias após a remoção da cortiça no descortiçamento, primeiro em algumas zonas, e depois estende-se até reconstituir uma camada contínua (Fortes et al., 2004). O novo felogénio é também meristemático e produz células de felema para o exterior e células de feloderme para o interior (Fortes et al., 2004). No modelo de exploração do sobreiro como produtor de cortiça, quando o novo felema (cortiça) atinge uma certa espessura adequada para o processamento industrial (aproximadamente 27 mm), remove-se o felema e reinicia-se o processo de regeneração do felogénio (Pereira, 2007).

A única referência encontrada em bibliografia sobre a estrutura da casca de *Q. cerris* é de Babos (1979). Este autor deu uma atenção particular ao desenvolvimento da casca em *Q. cerris* var. *cerris* e *Q. cerris* var. *austriac*a, assinalando a formação da epiderme no primeiro ano de vida, da periderme no segundo e terceiro anos e do ritidoma a partir do terceiro ano. O mesmo autor também apresentou uma descrição sobre a estrutura e organização dos tecidos na casca: por exemplo, evidencia o aparecimento de nódulos pequenos e grandes de esclereídos nos raios, a ocorrência de cristais de forma romboédrica e assinala a formação de anéis de crescimento no floema (133 µm na variedade cerris e 196 µm na variedade austriaca). Apresentou valores médios para o comprimento, largura e espessura da parede das células tais como para os elementos de tubo crivoso e para as fibras: o comprimento e diâmetro dos tubos crivosos são 46-40 µm e 58-45 µm nas variedades cerris e austriaca respetivamente; o diâmetro médio das fibras é 15 e 17 µm respetivamente. Observou a formação de camadas de felema com 10-20 células em cada fiada radial.

2.2.3. Cascas com cortiça

Algumas espécies contem uma casca com uma proporção notável de felema. Para além do *Quercus suber*, exemplos destas espécies incluem *Quercus variabilis*, *Phellodendron amurense*, *Ulmus campestres*, *Pseudotsuga taxifolia*, *Abies lasiocarpa*, *Abies concolor* e algumas espécies tropicais, particularmente do Brasil (Natividade, 1950).

O Brasil possui pelo menos 31 plantas produtoras de cortiça (Almeida, 1946; Natividade, 1950). No entanto, as espécies mais importantes são *Kielmeyera coriacea* (pau-santo), *Agonandra brasiliensis* (pau-marfim), *Pisonia tomentosa* (pau-lepra), *Enterolobium ellipticum* (favela-branca), *Aspidosperma dasycarpum* (pereira-do-campo), *Connarus suberosus*, (cabelo-de-negro), *Erythrina mulungu* (mulungu), *Syplocas lanceolata* (congonha) e *Eugenia dysenterica* (cagaiteira) (Rizzini e Mors, 1995; Almeida et al., 1998; Matheus et al., 2009). Na Figura 9 mostra-se a casca de *K. coriacea*, que foi caracterizada recentemente (Rios, 2011).

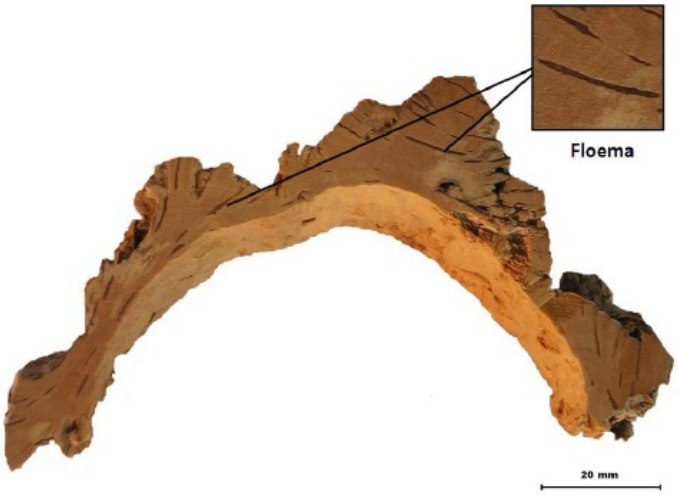

Figura 9. A estrutura da casca de *K. coriacea* (Rios, 2011).

Um dos artigos mais antigos sobre as plantas corticeiras do Brasil é o trabalho de Buttrick (1941) que identifica 7 espécies como corticeiras. Almeida (1946) referiu ainda outras espécies, comparou as propriedades da cortiça das espécies do trabalho de Buttrick com as de *Q. suber*, tendo concluido que a cortiça das espécies do Brasil tem propriedades inferiores às da cortiça do sobreiro (Almeida, 1948). Damas (1949) também desenvolveu um estudo comparativo das cortiças portuguesas e brasileiras, principalmente sobre a sua capacidade de utilização em aglomerados negros. Williams e Erlanson (1959) referem a utilização da cortiça de *K. coriacea* do Brasil para fabrico de materiais de isolamento e linóleo durante a Segunda Guerra Mundial quando ocorreu a dificuldade de importação da cortiça da região do Mediterrâneo.

2.3. Caracterização da cortiça

2.3.1. Caracterização anatómica

A cortiça é um conjunto de células suberizadas, produzidas pelo felogénio da periderme, constituindo o tecido designado anatomicamente por felema. A cortiça do sobreiro foi estudada com grande detalhe do ponto de vista

anatómico e estrutural, quer em trabalhos científicos publicados desde o final do séc. XX, quer em estudos pioneiros de observação no séc. XVII, tal como sumarizado por Pereira (2007).

O primeiro felogénio é formado debaixo de epiderme logo no primeiro ano de crescimento na *Q. suber* e cada célula-mãe produz 3-6 células de felema para o exterior e uma célula de feloderme para o interior (Graça e Pereira, 2004). Nos anos seguintes aumenta a atividade meristemática de produção de células de felema por parte do felogénio, formando camadas uniformes sucessivas. Caso se proceda ao descortiçamento, o que ocorre geralmente quando a árvore tem aproximadamente 20 anos, a cortiça da primeira periderme é removida, destruindo-se o felogénio, e forma-se uma segunda periderme através da atividade de um novo felogénio traumático que se diferencia alguns milímetros no interior do floema (Pereira, 2007).

As células de cortiça são células mortas. A cortiça constitui um tecido bastante regular onde as células se organizam em filas radiais paralelas, sem espaços intercelulares (Figura 10) (Pereira, 2007).

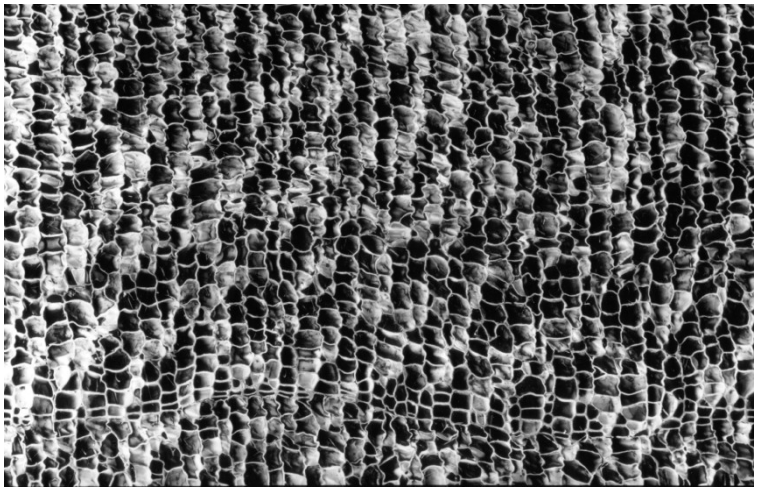

Figura 10. Estrutura da cortiça observada numa secção radial

As células da cortiça apresentam-se geometricamente como poliedros com 14 faces (8 faces com 6 arestas e 6 faces com 4 arestas, o poliedro de Kelvin) (Pereira, 2007) (Figura 11). As células apresentam-se individualmente com a forma de prismas hexagonais, com o eixo orientado

na direção radial e que se dispõem umas sobre outras formando fiadas radiais (Figura 11).

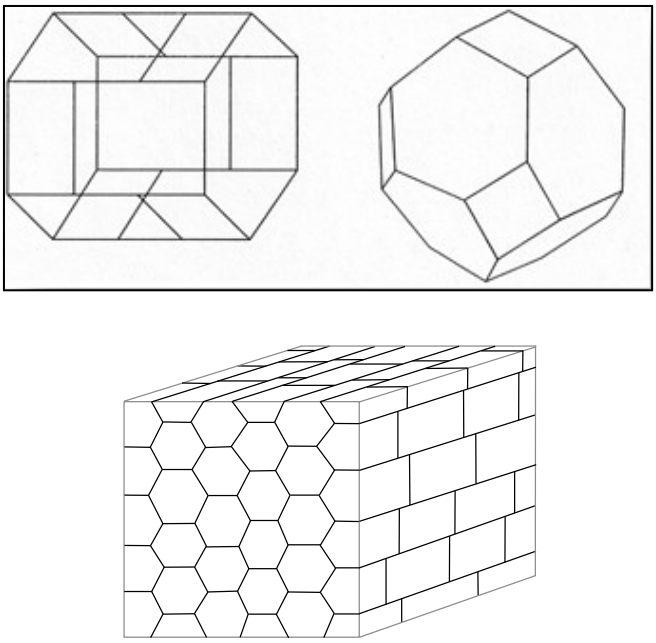

Figura 11. Modelo da célula da cortiça e organização do tecido: a célula individual (em cima à esquerda) e poliedro de Kelvin (em cima à direita) e organização do tecido (em baixo) (Pereira, 2007).

Na secção tangencial, as células da cortiça organizam-se numa estrutura do tipo de favo de mel, em que a maioria das células de cortiça têm 6 arestas, embora ocorram também células com 5 e 7 arestas. As secções radiais e transversais são semelhantes: as células alinham-se em filas radiais e apresentam-se como retângulos, tendo a maioria das células 6 arestas (Figura 12) (Pereira, 2007).

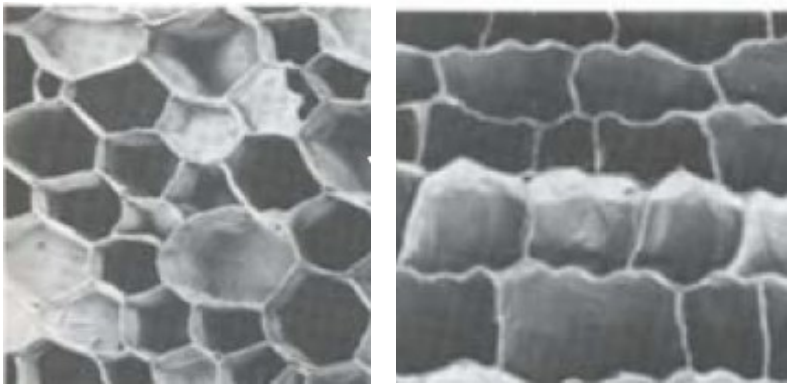

Figura 12. Secção tangencial (a esquerda) e secção não tangencial (a direita) das células da cortiça (Adaptado de Pereira et al., 1987).

Em *Q. suber*, o felogénio produz uma camada inicial de felema com células de maior comprimento radial e paredes finas (cortiça inicial) e uma camada final de felema com células de menor comprimento radial e paredes mais espessas (cortiça final), resultando a formação dos anéis de crescimento na cortiça. No entanto, nem sempre se observam anéis de crescimento no felema: por exemplo, em algumas espécies existe só um tipo de felema com células com paredes espessas, como em *Ceratonia,* ou só com células com paredes finas como em *Pseudotsuga* (Evert, 2006).

As células da cortiça têm dimensões que variam entre as células, embora uma célula ideal da *Q. suber* tenha 40 μm de altura de prisma, 20 μm de aresta da base, 1 μm de espessura de célula (Gibson et al., 1981; Pereira, 2007). No Quadro 1 resumem-se as dimensões das células de início e de fim de estação da cortiça de *Q. suber.* Considerando as dimensões celulares é possível calcular a fração sólida na cortiça. Pereira (2007) referiu uma fração sólida de 8-9% na cortiça inicial e 15-22% na cortiça final da *Q. suber*.

Quadro 1: As dimensões das células de *Q. suber* (Pereira, 2007)

	Cortiça inicial	Cortiça final
Altura de prisma	30-40 μm	10-15 μm
Aresta da base	13-15 μm	13-15 μm
Espessura da parede	1-1.5 μm	2-3 μm
Numero das células por cm^3	4-7 X 10^7	10-20 X 10^7

Cortiças de outras espécies mostram o mesmo tipo de estrutura celular e de biometria celular embora com algumas diferenças. Por exemplo, as células da cortiça inicial de *K. coriacea* são maiores e têm paredes mais espessas do que as de *Q. suber* (40-70 μm e 1,5-2,0 μm respetivamente) (Rios et al, 2011); enquanto as células da cortiça de *Q. variabilis* são mais pequenas (15-35 μm) e têm espessura de parede semelhante à de *Q. suber* (Yafang et al, 2009; Miranda et al. 2012).

2.3.2. Caracterização química

A cortiça caracteriza-se quimicamente por possuir suberina como componente estrutural da parede celular, distinguindo-se assim de outros tecidos lenhocelulósicos, por exemplo do floema ou da madeira.

A composição química sumativa da cortiça é constituída por cinzas, extrativos, suberina, lenhina e polissacáridos. A composição da cortiça varia com a espécie, como se mostra do Quadro 2 para as cortiças de *Quercus suber*, *Quercus variabilis*, *Calotropis procera, e Kielmeyera coriacea*. Verificam-se grandes diferenças entre o teor dos diferentes componentes: por exemplo o teor de suberina varia entre cerca de 40% (*Q. suber*) a 5% (*C. procera*). No caso do sobreiro, cuja cortiça tem sido a mais estudada, a composição diferencia-se também entre os diferentes tipos de cortiça, tendo a cortiça virgem, em geral, mais extrativos e menos suberina relativamente à cortiça amadia (Quadro 3).

Quadro 2. A composição química das cortiças de diferentes árvores (Pereira, 1988b; Pereira, 2007; Rios, 2007, Miranda et al., 2012)

Componente	*Q. suber*	*Q. variabilis*	*C. procera*	*K. coriacea*
Cinzas	1%	1,1%	21,5%	0,9%
Extrativos	14-17%	9,6%	11,1%	24,6%
Suberina	33-40%	34,8%	5,3%	20,6%
Lenhina	21-23%	19,1%	40,0%	25,9%
Polissacarídeos	18-21%	-	25,7%	28,0%

Quadro 3. A composição química da cortiça de *Q. suber* (Pereira, 1988a)

Componente	Cortiça virgem	Cortiça amadia
Cinzas	0,7%	1,2%
Extrativos	15,0%	14,2%
Suberina	38,6%	39,4%
Lenhina	21,7%	23,0%
Polissacarídeos	18,2%	19,9%

A parede celular da cortiça é constituída por uma lamela média e parede primária muito lenhificadas, uma parede secundária, que contém suberina e lenhina e possivelmente monómeros gordos extratáveis, e uma parede

terciária, constituída essencialmente por polissacáridos (Figura 13). A parede primária e a parede terciária são finas, enquanto a parede secundária é bastante mais espessa (Pereira, 2007).

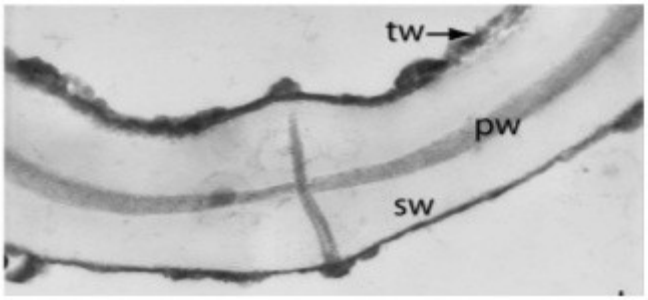

Figura 13. Estrutura da parede celular da cortiça de *Q. suber*: pw – lamela média e parede primária, sw – parede secundária, tw- parede terciária (Teixeira e Pereira, 2009)

A suberina é o principal componente das células da cortiça, constituindo cerca de 40% de massa da cortiça do sobreiro e sendo o principal componente estrutural da parede celular (Pereira, 1988b). *Q. suber* tem o maior teor de suberina entre as diferentes cortiças (Quadro 2).

A suberina é uma macromolécula estrutural, com ligações do tipo éster glicerídicas, que contém uma parte alifática que é acompanhada por outra parte aromática. A composição monomérica da parte alifática inclui, para além do glicerol, ácidos carboxílicos com 16-26 átomos de carbono, principalmente ω-hidroxi ácidos e α,ω-diácidos. A composição monomérica da suberina de *Q. suber* resume-se no Quadro 4. A informação sobre a composição da parte aromática de suberina é ainda insuficiente (Pereira, 2007).

Quadro 4. A composição monomérica da suberina de *Q. suber* (Graça e Pereira, 2000)

Monómeros	Massa (%)
Glicerol	14,2
Açúcares e fenólicos	1,1
1-Alcanois	0,4
Ácidos alcanóicos	1,1
α,ω-Diácidos saturados	8,7
α,ω-Diácidos substituídos	36,8
ω-hidroxiácidos saturados	11,4
ω-hidroxiácidos substituídos	14,9
Monoacilgliceróis	0,5
Triterpenóides	0,5
Outros	0,4
Não identificados	10,0
Total	100,0

Embora a composição da suberina na cortiça de diferentes espécies seja no seu essencial semelhante, encontram-se diferenças na proporção monométrica de diferentes grupos de monómeros. Assim, na suberina da *K.* coriacea os monómeros mais abundantes são ω-hidroxiácidos (54% de mistura de monómeros) (Rios, 2011), enquanto que na suberina da *Pseudotsuga menziesii* os monómeros dominantes são α,ω-diácidos (Graça e Pereira, 1999).

O segundo componente mais importante da cortiça é a lenhina. A lenhina da cortiça não é semelhante à lenhina extraída da madeira das folhosas (que é uma lenhina guaiacílica-siringílica ou tipo G-S) mas antes semelhante à lenhina da madeira das coníferas (uma lenhina guaiacílica, ou tipo G). A composição monomérica da lenhina da cortiça é 95% G, 2% H e 3% S, sendo a sua fórmula molecular $C_9H_{8.74}O_{2.82}(OCH_3)_{0.85}$ (Marques et al., 1994,1999; Pereira, 2007).

O teor dos polissacáridos é mais baixo na cortiça, quando comparado com o da madeira (cerca de 20% e 80%, respetivamente). Os monómeros mais abundantes são glucose, xilose e arabinose. Os teores de celulose e hemiceluloses podem ser estimados através dos teores de monómeros, correspondendo a celulose a cerca de metade dos polissacáridos. A

proporção de glucose/xilose é aproximadamente 1,5 na cortiça, constatando-se valores superiores a 3 na maioria das madeiras de folhosas (Pereira, 1988a).

Os extractivos são moléculas com peso molecular baixo e médio que podem ser removidos das células por solubilização sem danificar a estrutura celular. O teor dos extrativos varia entre 8% e 24% na cortiça, com valores médios de 14%-18% (Pereira, 2007). Os extrativos da cortiça podem-se agrupar em alifáticos (extraídos por solventes não polares) e fenólicos (extraídos por solventes polares) que constituem um terço e dois terços dos extrativos totais na cortiça da *Q. suber* (Pereira, 2007).

O teor de cinzas (material inorgânico) varia entre 1% e 2% na cortiça da *Q. suber*. No entanto, em outras espécies, o valor varia muito e pode ser elevado: por exemplo 0,9% na *Kielmeyera coriacea* e 21,5% na *Calotropis procera* (Quadro 2). O cálcio é o elemento mais importante (60% de total inorgânicos), destacando-se igualmente o fósforo e o potássio.

2.4. Utilizações da cortiça

A cortiça é um material com um conjunto de propriedades interessantes baseadas nas suas características anatómicas e químicas que lhe permitem diferentes áreas de utilização (Fortes et al., 2004; Pereira, 2007). A cortiça constitui um dos mais importantes produtos florestais não lenhosos (NWFP, *non-wood forest products*) e baseia-se na exploração sustentável do sobreiro (*Quercus suber*). Estima-se anualmente uma produção mundial de aproximadamente 200 mil toneladas de cortiça. Portugal é responsável aproximadamente por metade desta produção (Apcor, 2012).

A principal utilização da cortiça é o fabrico de rolhas que constitui o suporte económico da sua fileira industrial. Anualmente produzem-se 15 mil milhões de rolhas no mundo. Assim, o objetivo fundamental da produção de cortiça e da sua transformação industrial é produzir rolhas naturais para vinhos (Pereira, 2007; Gete, 2008). A matéria-prima que não é apropriada para o fabrico das rolhas naturais por não ter espessura suficiente ou não ter a

qualidade necessária, assim como os subprodutos do seu fabrico, são triturados e o granulado de cortiça é aglomerado com um adesivo para produzir rolhas aglomeradas e aglomerados de revestimento (Fortes et al., 2004). O granulado de cortiça é também aproveitado na produção de aglomerados puros (aglomerados negros) que consistem em aglomerados obtidos após tratamento térmico com vapor sobre aquecido sem adição de adesivo (Pereira, 2007).

A Figura 14 apresenta esquematicamente o fluxograma de processamento da cortiça.

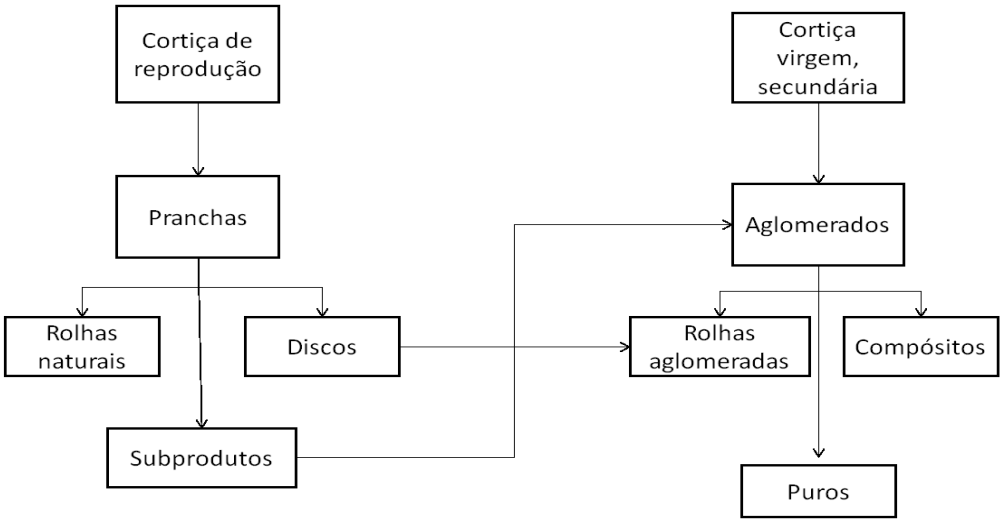

Figura 14**.** O esquema geral de utilizações da cortiça (Adaptado de Pereira, 2007).

2.4.1. Rolhas de cortiça

As rolhas naturais têm como matéria-prima as pranchas de cortiça amadia. A cortiça amadia corresponde à terceira cortiça extraída da árvore e às tiradas subsequentes. A primeira cortiça (cortiça virgem, que corresponde ao felema da periderme original produzida pelos sobreiros jovens) e a cortiça secundeira (cortiça contida na periderme traumática formada depois da retirada da cortiça virgem) não se utilizam para a produção de rolhas porque a sua estrutura é pouco homogénea e apresentam numerosas fissuras. Para o fabrico de rolhas utiliza-se a cortiça amadia (cortiça de reprodução, contida nas sucessivas peridermes traumáticas formadas após a retirada da cortiça secundeira). Procura-se que a cortiça de reprodução

tenha uma espessura de cortiça com pelo menos 27 mm (o diâmetro da rolha é em geral 24 mm, mas pode variar entre 20 e 32 mm) (Pereira, 2007).

Para além das rolhas de cortiça naturais, produzem-se também rolhas de cortiça aglomerada e, por combinação de discos de cortiça natural com aglomerados, as chamadas rolhas técnicas. As rolhas aglomeradas podem ser produzidas por moldagem ou por extrusão. Nas rolhas técnicas incluem-se as rolhas de champanhe (um corpo cilíndrico de aglomerado e um ou dois discos de cortiça natural colados no topo inferior) ou as rolhas 1+1 (ou twin-top) correspondendo a um corpo aglomerado e a um disco de cortiça em cada um dos topos. Há também rolhas especiais em que as rolhas de cortiça se combinam com madeira, plástico, ou outros materiais.

2.4.2. Aglomerados compósitos

Os aglomerados compósitos são feitos por combinação dos grânulos de cortiça e um adesivo (Fortes et al., 2004). Os aglomerados compósitos também se denominam aglomerados brancos, porque os aglomerados têm a cor natural da cortiça (não foram sujeitos a tratamento térmico a temperatura elevada, e portanto não tem a cor escura). O objetivo do fabrico dos aglomerados compósitos é conseguir um produto semelhante à cortiça natural, porém permitindo maiores dimensões e formas geométricas mais complexas (Fortes et al., 2004). Deste modo é possível produzir vários materiais incluindo componentes para calçado, acessórios para escritório e casa, juntas de dilatação/contração, juntas de vedação, etc (Corticeira Amorim, 2012a).

Em geral, os aglomerados brancos têm três utilizações principais: o fabrico de rolhas aglomeradas, painéis e folhas da cortiça para revestimento (Fortes et al., 2004).

Para o fabrico dos aglomerados brancos são utilizados os grânulos de cortiça de melhor qualidade, resultantes da trituração dos subprodutos da

produção de rolhas e discos, dos bocados e refugos da cortiça amadia e da cortiça secundeira e virgem.

O adesivo, cujo teor varia entre 3% e 8%, pode ser um polímero termofixo (urea, melamina ou fenol-formaldeído) ou um polímero termo-elástico (poliuretanos). Os polímeros termofixos são utilizados em aglomerados de revestimento de pavimentos, enquanto os poliuretanos são utilizados em rolhas e nos materiais mais flexíveis (Pereira, 2007).

Os aglomerados brancos podem ser feitos por prensagem em moldes, por extrusão ou por prensagem a quente por placas ou de forma continua. As condições específicas variam de acordo com os produtos pretendidos e o adesivo utilizado (Pereira, 2007).

No processo de prensagem em moldes, os grânulos da cortiça são colocados num misturador onde se adiciona o adesivo por um pulverizador. A mistura é vazada para o molde e o molde é fechado e prensado. A prensagem reduz o volume da mistura e facilita o contacto entre o adesivo e os grânulos. A duração da prensagem depende do tipo e características do adesivo. O molde prensado é aquecido em estufa para facilitar a polimerização do adesivo. Depois do tempo de estabilização da cura após a saída da estufa, o bloco de aglomerado compósito é cortado em lâminas de dimensões diferentes (Fortes et al., 2004).

Na extrusão, a mistura dos grânulos da cortiça e o adesivo é introduzida continuamente num tubo, onde é comprimida por um pistão. No tubo de extrusão existe uma zona de aquecimento para polimerização do adesivo e uma zona de arrefecimento para estabilização da cura e forma-se continuamente um bastão do aglomerado. Muitos dos aglomerados para rolhas são produzidos por extrusão.

Também existe um outro tipo de prensagem, que se chama moldação em tubo. Neste processo, a mistura é comprimida em tubos que são aquecidos em estufas para polimerização do adesivo, após o que se faz a desmoldação (Fortes et al., 2004).

A prensagem a quente de forma contínua é semelhante à produção de placas de aglomerados de partículas de madeira, a temperaturas de 100-150°C e pressões de 5-15 kg/cm2 durante 3-8 minutos (Pereira, 2007; Gete, 2008).

Nos últimos anos desenvolveram-se novos compósitos com integração de cortiça com outros materiais, que incluem compósitos sanduíche, cortiça-resíduo de papelão de bebidas, cortiça-termoplástico, cortiça-hidroxipropilcelulose, cortiça-resina de lenhina, pó de cortiça, resinas sintéticas-cortiça, cortiça-materiais lenhocelulósicos, cortiça-carvão, cortiça-gipsita, e cortiça-poliuretanos. (Gil, 2009). Em 2009, foi concedida uma patente, (PT-nº 104704) sobre os compósitos de cortiça reforçados com fibras naturais ou sintéticas, usadas para melhorar as propriedades mecânicas do compósito, permitindo a sua utilização na indústria de construção, transportes, etc. (INPI, 2012a).

2.4.3. Aglomerados puros

Os granulados de cortiça utilizados na fabricação dos aglomerados puros são os de menor qualidade e incluem os resultantes da trituração da cortiça virgem de falca, de desperdícios de cortiça amadia e as aparas de costa provenientes da produção de discos (Fortes et al., 2004). Os granulados utilizados contêm impurezas de madeira. O tamanho dos grânulos é maior do que o dos grânulos dos aglomerados brancos, em geral, entre 4-22 mm (Pereira, 2007). Para os aglomerados acústicos, térmicos e vibráticos utilizam-se respetivamente as seguintes granulometrias: 5-10 mm, 5-32 mm e 5-32 mm (Fortes et al., 2004).

Nos aglomerados puros, a colagem dos grânulos de cortiça é conseguida sem utilizar adesivos, através da sua aglutinação por efeito de temperatura. No processo de fabrico ocorre perda da massa e expansão da cortiça (Pereira e Ferreira, 1989; Pereira, 1992) pelo que estes aglomerados se designam também aglomerados expandidos, ou ainda aglomerados negros devido à sua cor escura (Fortes et al., 2004, Pereira, 2007).

Os aglomerados puros têm como principal utilização o isolamento de acordo com a sua densidade: 80-100 kg/m3, 100-150 kg/m3 e 175-320 kg/m3 para isolamentos acústico, térmico e vibrático respetivamente (Fortes et al., 2004).

Os aglomerados puros são fabricados numa autoclave. Os grânulos são compactados antes do tratamento térmico para conseguir a densidade final após de tratamento. O tratamento térmico é feito em autoclave com admissão de vapor de água sobreaquecido (40 kPa) a 300-350°C durante cerca de 20 minutos. Durante o tratamento térmico, as células da cortiça expandem e a espessura das células diminui, resultando num material leve (conteúdo de vazio entre 45-50%), o que é ideal para isolamentos. Os isolantes produzidos utilizam-se para aumentar a resistência de elementos de construção (isolante térmico), para absorção de energia sonora (isolante acústico) e para reduzir a energia transmitida através de um elemento estrutural (isolante vibrático) (Fortes et al., 2004; Pereira, 2007).

A condutividade térmica do isolante térmico, medida a 20°C é 0,035 kcal $(m.\ h.\ °C)^{-1}$, sendo semelhante à da cortiça natural. O módulo de Young dos aglomerados negros varia entre 1-2 MPa para os aglomerados acústicos e térmicos e 4-8 MPa para os aglomerados vibráticos (Fortes et al., 2004).

2.4.4. Adsorção de poluentes

Nos últimos anos, as cascas têm vindo a ganhar importância na adsorção de poluentes em meio aquoso (Martin-Dupont et al., 2006), tendo-se feito estudos com cascas de diferentes espécies (Kumar, 2006). Os granulados de cortiça, sem pré-tratamento ou após tratamento térmico/químico, foram também testados para a purificação de águas contaminadas (Chubar, 2004a, 2004b; Villaescusa et al., 2000; Fiol et al., 2003).

Os adsorventes podem ser agrupados como absorventes hidrofóbicos (para recuperar poluentes apolares) e adsorventes para todos os líquidos (para recuperar poluentes polares e apolares) (Cedre 2012a). A cortiça corresponde ao segundo tipo de adsorventes.

A cortiça já foi testada para adsorver metais pesados, pesticidas, hidrocarbonetos poliaromáticos policíclicos (HAPs ou PAHs) e óleos (Pereira, 2007; Pintor et al. 2012, Corticeira Amorim 2012b).

A capacidade da cortiça para adsorver metais pesados é mais baixa do que a de outros materiais lenhocelulósicos (por exemplo, madeira). Os grupos carboxílicos são os principais responsáveis pela adsorção e pré-tratamentos com cloreto de sódio e ativação a 700-800°C aumentaram a adsorção (Chubar, 2004b; Pereira, 2007).

A cortiça revelou eficiência na remoção do pesticida bifentrina, sendo a sua capacidade para adsorver este pesticida mais alta do que a do carvão ativado (Domingues et al., 2005). Considerando a estrutura não polar deste poluente, a suberina e os extrativos alifáticos podem ser responsáveis pela ligação do pesticida sobre a cortiça (Pereira, 2007). A lenhina pode igualmente contribuir para as ligações não polares dos efluentes (Pintor et al., 2012).

Os extrativos de cortiça (particularmente, os extrativos fenólicos), que podem ser úteis na adsorção dos poluentes, podem simultaneamente ser tóxicos para os organismos presentes nas águas (Aoyama e Tsuda, 2001). Foram testados vários métodos de pré-tratamentos de cascas para fixar os extrativos, nomeadamente um tratamento com formaldeído (Vázquez et al., 2002), embora se deva ter em linha de conta a toxicidade do formaldeído e os custos inerentes.

A cortiça já tem sido também utilizada na adsorção de óleos derramados. Por exemplo, o produto “Corksorb” da Corticeira Amorim é comercializado para a adsorção de óleos e solventes orgânicos (Corticeira Amorim, 2012b) (Figura 15). Uma patente de invenção nacional (PT-nº103492) foi concedida em 2006 para granulados de cortiça para absorção/adsorção de óleos. A patente apresenta um modelo para estimar a quantidade de cortiça natural necessária para a absorção/adsorção de óleos, utilizando os valores de granulometria, densidade do óleo e o ângulo de contacto do óleo na cortiça.

Os grânulos de cortiça podem variar de dimensão e também ser submetidos a tratamentos químicos ou físicos para aumentar a capacidade de absorção/adsorção (INPI, 2012b).

A baixa densidade e a capacidade de flutuação dos grânulos de cortiça são particularmente importantes nos tratamentos de óleos que ficam na superfície das águas. A organização Cedre (2012b) indicou Corksorb G01006 (granulados escuros de cortiça) e Corksorb G02025 (granulados pouco escuros de cortiça) para utilizações como adsorventes flutuantes e que se podem utilizar no mar, canais e lagos, segundo a norma AFNOR NFT 90-360.

Figura 15. Os produtos Corksorb para tratamentos seletivos dos poluentes em meio aquoso (www.corksorb.com)

Capítulo 3. Trabalho original

3.1. Metodologia geral

A metodologia geral deste trabalho consistiu na análise da casca da *Quercus cerris* var. *cerris* em termos da sua constituição anatómica e do estudo detalhado da componente de cortiça presente no ritidoma quanto às características da sua estrutura celular e composição química, assim como quanto às características de comportamento importantes em possíveis vias de utilização, tais como o comportamento durante tratamentos térmicos e estudos de bioadsorção de poluentes. A realização destes estudos foi precedida de amostragem em campo das cascas de *Q. cerris*, na Turquia, e da sua preparação para análise. A Figura 16 apresenta esquematicamente o fluxograma do trabalho experimental.

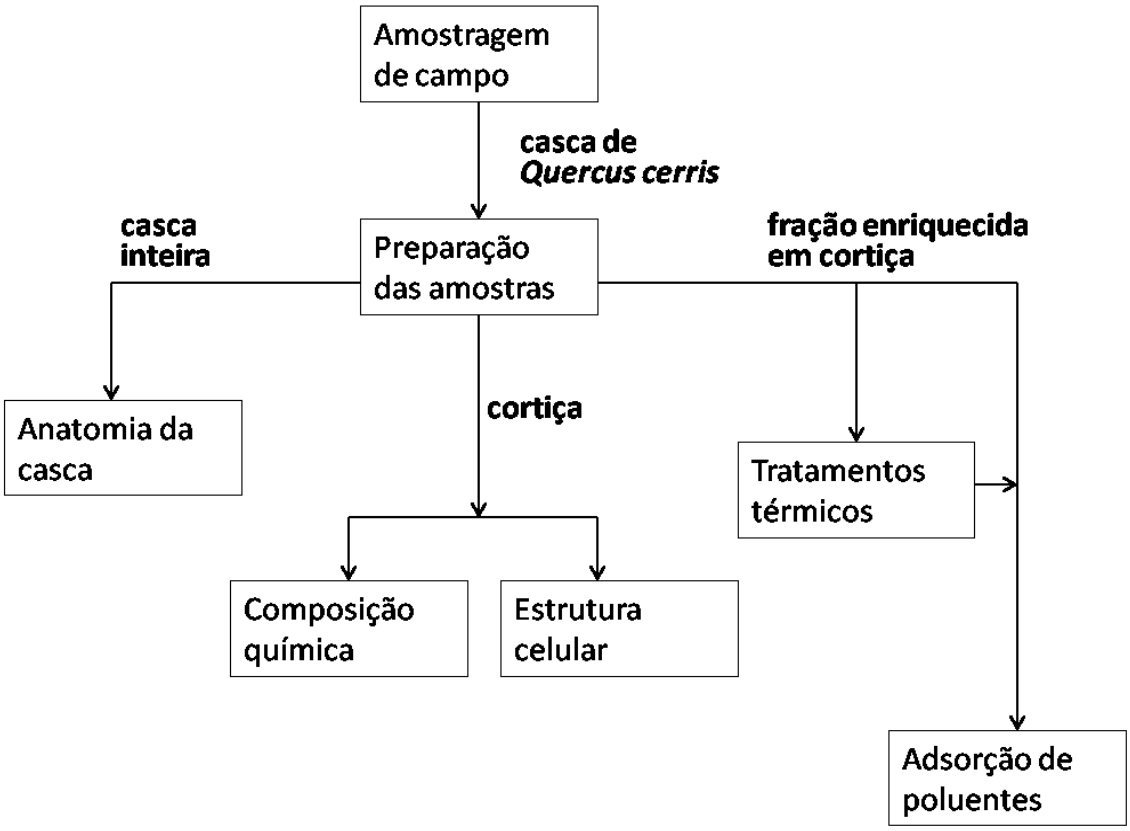

Figura 16**.** Apresentação esquemática da estrutura do trabalho experimental

As amostras de cascas foram recolhidas em três locais na unidade florestal de Andirin (Província florestal de Kahramanmaraş) no sudeste da Turquia (Figura 17) com uma altitude média de 1000 m, uma precipitação anual de

662 mm e temperatura média de 16.5 ºC: Tiril (37º35'49"N, 36º18'32"E), Okçu (37º43'48"N, 36º22'01"E) e Armutkuyusu (37º32'01"N, 36º16'07"E). Em cada local foram selecionadas aleatoriamente árvores de *Quercus cerris* var. *cerris* com a seguinte classe de idade e diâmetro à altura do peito (DAP), respectivamente: 75 anos e 45 cm em Tiril (6 árvores), 70 anos e 35 cm em Okçu (três árvores), 80 anos e 40 cm em Armutkuyusu (três árvores).

A zona de amostragem corresponde a florestas dominadas por carvalhos *Q. cerris*, sob jurisdição estatal por parte dos Serviços Florestais e geridas de acordo com os respetivos planos de gestão. Dado o baixo valor comercial das árvores de *Q. cerris*, cuja madeira é vendida localmente para utilização como lenha, não existe um plano de gestão específico de valorização madeireira. Neste caso, a floresta teve um corte seletivo de grande intensidade por volta de 1975, que apenas deixou em pé árvores para semente. Verificou-se desde então regeneração natural pelo que atualmente as florestas possuem árvores com diferentes classes de idade.

A caracterização de uma parcela do inventário florestal nesta unidade de Andirin, e que se assemelhará às características dos locais de amostragem, dá as seguintes informações: tipo de solo argila sobre rocha calcária, altitude média 1000 m, inclinação 35-40%, precipitação anual 662,2 mm, máxima precipitação mensal 133,1 mm em Janeiro, mínima precipitação mensal 0,9 mm em Julho, humidade relativa 58%, temperatura anual média 16.5°C, temperatura máxima mensal 42.6°C em Julho, temperatura mínima mensal -9°C em Fevereiro. Quanto às características florestais, elas são as seguintes: ocorrência natural, incremento médio 1,532 m^3/ha, diâmetro médio 40 cm, altura média 20 m, densidade 158 árvores/ha, espécies secundárias *Juniperus*.

Figura 17. As províncias do Serviço Florestal (à esquerda) e a unidade Andirin (à direita) da Turquia (OGM, 2012).

As amostras de cascas foram retiradas a uma altura de 1,3 m do solo, manualmente com a ajuda de um machado, de modo a separar um quadrado de casca com aproximadamente 30 cm de lado, a partir do câmbio (Figura 18).

Figura 18**.** Aspeto da floresta de *Quercus cerris* onde foi feita a amostragem e modo de retirada da casca.

Para o estudo anatómico da casca foram utilizadas secções completas, do câmbio até ao exterior, nas quais se cortaram sucessivamente na direção radial as amostras como cubos (2x2x2 cm).

Para o estudo químico e da estrutura celular preparam-se manualmente amostras de cortiça que foram cortadas a partir do ritidoma da casca. Dada

a dificuldade de separação duma fração pura de cortiça sem resíduos de floema, fez-se uma trituração em moinho de facas Retsch da fração de cortiça e uma suspensão em água: a camada mais leve sobrenadante foi considerada cortiça e a fração mais densa, que sedimentou, material do floema do ritidoma.

O estudo do comportamento térmico, entre 150ºC e 400ºC, da cortiça de *Q. cerris* foi feito nas amostras de casca inteira após trituração num moinho de facas de tipo industrial com crivo de saída de 3 mm x 25 mm. Este triturado foi crivado, separando a fração com granulometria acima de 2 mm. Esta fração foi suspensa em água, e retirado o sobrenadante que foi seco e inspecionado visualmente para separar manualmente partículas de floema aparentes, constituindo uma fração que se verificou ser e se designou como "enriquecida em cortiça".

Estudou-se a composição química dos grânulos sujeitos a tratamentos com diferentes temperaturas e tempos, a respetiva alteração de cor e da estrutura celular.

Para o estudo de adsorção de poluentes, utilizou-se a fração de cortiça preparada anteriormente para os tratamentos térmicos. Utilizaram-se grânulos tal qual e após tratamento térmico, que foram moídos e crivados. Foi utilizada a fração 40-60 mesh para tratamento com soluções de poluentes orgânicos (quatro hidrocarbonetos aromáticos policíclicos) e um poluente inorgânico (crómio (VI)), determinando-se a sua capacidade para adsorver estes compostos.

Os detalhes analíticos dos procedimentos utilizados nos diferentes estudos encontram-se nos artigos correspondentes.

3.2. Resultados

3.2.1. Bark anatomy of *Quercus cerris* L. var. *cerris* from Turkey

Şen, A., Quilhó, T. & Pereira, H.

Turkish Journal of Botany, 35: 45-55

2011

TÜBİTAK

Research Article

Turk J Bot
35 (2011) 45-55
© TÜBİTAK
doi:10.3906/bot-1002-33

Bark anatomy of *Quercus cerris* L. var. *cerris* from Turkey

Ali ŞEN[1], Teresa QUILHÓ[2,*], Helena PEREIRA[3]

[1]İstanbul University, Faculty of Forestry, Department of Forest Biology and Wood Protection Technology, 33473 Bahçeköy, İstanbul - TURKEY

[2]Centre of Forest and Forest Products, Tropical Research Institute, Tapada da Ajuda 1349-017 Lisbon - PORTUGAL

[3]Forest Research Centre, Institute of Agronomy, Technical University of Lisbon, Tapada da Ajuda 1349-017 Lisbon - PORTUGAL

Received: 12.02.2010
Accepted: 29.06.2010

Abstract: *Quercus cerris* L. var. *cerris* has a conspicuous bark which is generally thicker than that of other *Quercus* L. species in Turkey. The present study aimed to provide detailed anatomical characterisation of the bark of this species, which is necessary to assess its potential. The anatomical studies were conducted on the bark samples of nine 70- to 80-year-old trees growing in 3 sites of Andırın district from Kahramanmaraş province in Turkey. For microscopic observation transverse and longitudinal sections were prepared and individual specimens were taken for maceration. The bark is composed of phloem, periderm, and a very substantial rhytidome. The rhytidome has sequential periderms with phloem tissue between them, and includes compact nodules of sclerified tissues. The phellem has typical cork cells arranged regularly in radial rows and showing rings. The phelloderm is poorly developed. The phloem is layered regularly from cambium until the last formed periderm in successive tangential bands of fibres and groups of sclereids alternated with axial parenchyma and sieve tubes. Uniseriate phloem rays transverse the fibre groups, and fused phloem rays originate conspicuous broad rays. The dilatation growth showed large and conspicuous sclereids. Numerous crystals and druses in axial parenchyma cells were also observed. Full illustration of this species is given.

Key words: Phloem, periderm, rhytidome, *Quercus cerris*

Türkiye'deki *Quercus cerris* L. var. *cerris*'in kabuk anatomisi

Özet: *Quercus cerris* L. var. *cerris* Türkiye'deki diğer *Quercus* L. türlerinden genel olarak daha kalın olan belirgin bir kabuğa sahiptir. Bu çalışmada, bu kabuğun kullanım potansiyelini değerlendirmek üzere gerekli olan, kabuğun detaylı anatomik karakterizasyonunun sağlanması amaçlanmıştır. Anatomik çalışmalar Türkiye'de Kahramanmaraş'ın Andırın ilçesindeki üç ayrı bölgeden alınan 70-80 yaşlarındaki dokuz kabuk örneğinde gerçekleştirilmiştir. Mikroskobik gözlem için enine ve boyuna kesitler hazırlanmış ve bireysel örnekler maserasyon için ayrılmıştır. Kabuk, floem, periderm ve önemli miktarda ritidomdan oluşmaktadır. Ritidom aralarında floem dokusu bulunan sıralı peridermlere sahiptir ve sklereid hücrelerine dönüşmüş dokulardan oluşan kompakt nodüller içermektedir. Fellem, radyal sıralar halinde düzenli olarak sıralanmış karakteristik mantar hücrelerine sahiptir ve gelişim halkaları görülmektedir. Felloderm gelişimi zayıftır. Floem, kambiyumdan en son oluşan periderme kadar, ardışık teğet sıralı lif ve sklereid grupları ve bunlar ile yer değiştiren boyuna paranşim ve kalburlu borular ile düzenli olarak tabakalıdır. Tek sıralı floem ışınları lif grupları arasından geçmekte, birleşik floem ışınları da belirgin geniş ışınları oluşturmaktadır. Genişleme bölgesinde büyük ve belirgin sklereidler görülmektedir. Boyuna paranşim hücrelerinde aynı zamanda çok sayıda kristal ve druzlar gözlenmiştir. Bu türün tüm tanım resimleri sunulmaktadır.

Anahtar sözcükler: Floem, periderm, ritidom, *Quercus cerris*

* E-mail: terisantos@isa.utl.pt

Introduction

Quercus L. is one of the most important woody genera in the northern hemisphere, namely in North America, Europe, and especially in Eastern Asia, where the highest diversity can be found with about 250 species (Özcan, 2007).

In Turkey, *Quercus* species have a natural distribution of about 6.5 million ha area including many subspecies, varieties, and natural hybrids (Özcan & Bayçu, 2005). Hedge and Yaltırık (1982), who classified the *Quercus* species existing in Turkey, considered a total number of 18 species, which was a reduction from the previously accepted 35 *Quercus* species. However, nomenclatural and typification problems are still unresolved (Borazan & Babaç, 2003), because widespread hybridisation and introgression have much obscured specific limits (Hedge & Yaltırık, 1982).

Turkey oak (*Quercus cerris* L.) grows naturally from central and south-eastern Europe to Asia Minor. In Turkey, except in the eastern and north-eastern areas, it grows in all the regions with 2 varieties, *Q. cerris* var. *cerris* and *Q. cerris* var. *austriaca* (Wild.) Louden (Yaltırık, 1984). The distribution area for *Q. cerris* var. *cerris* is unknown after its new classification (previously *Q. cerris* var. *pseudocerris*) (Hedge & Yaltırık, 1982; Borazan & Babaç, 2003). In the Andırın district the distribution area of *Q. cerris* var. *cerris* is about 235,000 ha (Mıhçıoğlu, 1942).

Q. cerris especially *Q. cerris* var. *cerris* in the southern region of Anatolia has a conspicuous bark which is generally thicker than that of other *Quercus* species in Turkey. Morphological and anatomical studies were recently conducted to compare endemic Turkish species (Cabi, 2010; Güvenç & Duman, 2010).

The bark of *Q. cerris* var. *cerris* contains in its rhytidome substantial, albeit not continuous, regions of cork tissue that are clearly visible to the naked eye. Because of this and due to cork products shortage, *Q. cerris* bark was used in Turkey as an alternative to cork from *Q. suber* L. for production of agglomerates for insulation during World War II (Mıhçıoğlu, 1942), and later for production of bottle stoppers.

In general, the bark anatomy of *Q. cerris* has received little attention. The bark of *Q. cerris* var. *cerris* was briefly studied in the beginning of the 20th century and compared with *Q. suber*, leading to reports that it was of inferior quality (Mıhçıoğlu, 1942; Telgeren, 1976). Babos (1979a) also analysed the bark structure of *Q. cerris* var. *cerris* and compared it with *Q. cerris* var. *austriaca* from Hungary. However, such studies remained insufficient to enable a realistic evaluation of *Q. cerris* cork properties and potential uses. Overall there is a limited number of bark anatomical studies in other *Quercus* species (e.g. Howard, 1977; Trockenbrodt, 1991, 1994, 1995a, 1995b). An exception is the knowledge and the research effort made on *Q. suber* bark, which constitutes a model for cork in barks (e.g. Natividade, 1950; Pereira et al., 1987, 1992; Costa et al., 2002; Graça & Pereira, 2004). Recently, Pereira (2007) compiled the available knowledge on cork of this species in a review book.

This study presents a detailed analysis on the structure and anatomical characteristics of *Q. cerris* var. *cerris* bark from Turkey. This characterisation of *Q. cerris* var. *cerris* bark is a first step within the knowledge development that is necessary to assess its potential exploitation and products.

Materials and methods

The anatomical studies were conducted on the barks of 9 *Quercus cerris* var. *cerris* trees, growing in 3 sites of the Andırın district from Kahramanmaraş province in Turkey, with an altitude of 1000 m, 662.2 mm annual rainfall, and 16.5 °C mean temperature: Tiril (37°35′49″N, 36°18′32″E), Okçu (37°43′48″N, 36°22′1″E) and Armutkuyusu (37°32′1″N, 36°16′7″E). Three trees were randomly selected in each site, with the following age and mean diameter at breast height: 75 years and 45 cm in Tiril, 70 years and 35 cm in Okçu, and 80 years and 40 cm in Armutkuyusu.

The bark samples were collected at 1.30 m of height from the main trunks of *Q. cerris* var. *cerris* trees. The samples were impregnated with DP 1500 polyethylene glycol and transverse and longitudinal microscopic sections of approximately 17 μm thickness were prepared with a Leica SM 2400 microtome using Tesafilm 106/4106 adhesive for sample retrieval (Quilhó et al., 1999). The sections were stained with malachite green and hematoxylin, as well as with a triple staining of chrysodine/acridine red and astra blue. The sections were mounted on

glycerine Kaiser and after 24 h drying, the lamellas were submerged in xylol for 30 min to remove the Tesafilm adhesive, dehydrated on alcohol 96% and alcohol 100%, and mounted on Eukitt. Sudan 4 was used for selective staining of suberin.

Individual specimens were taken sequentially from the cambium towards the periphery and macerated in a solution of 30% H_2O_2 and CH_3COOH 1:1 at 60 °C for 48 h and stained with astra blue.

Light microscopic observations were made using Leica DM LA and photomicrographs were taken with a Nikon Microphot-FXA.

The terminology follows mainly Trockenbrodt (1990) and Richter et al. (1996).

Results and discussion

All the *Q. cerris* var. *cerris* trees that were analysed revealed a similar bark structure and the description here is therefore integrative. The bark is thick (3-7 cm) with a brown greyish colour, hard to the touch, and longitudinally furrowed with short deep furrows as in other *Quercus* species (Withmore, 1962; Howard, 1977). This results from the formation and growth of several periderms, the spatial development of phellem, and the amount of tissues cut off by each periderm (Junika, 1994).

The bark is composed of phloem and a very substantial rhytidome that can be clearly distinguished in transverse sections of the stem (Figure 1).

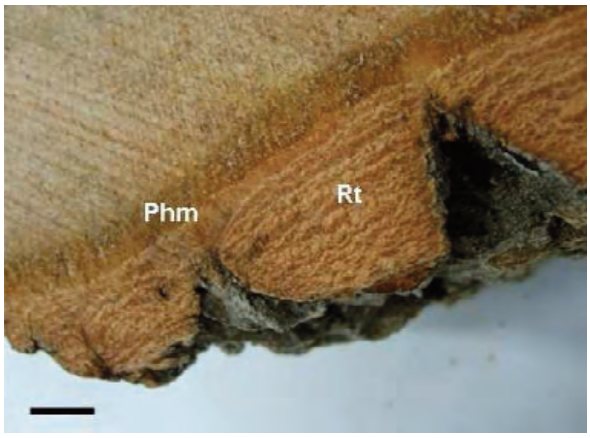

Figure 1. Phloem (Phm) and rhytidome (Rt) of *Quercus cerris* var. *cerris*. Scale bar = 25 mm.

Rhytidome and periderms

The rhytidome of *Q. cerris* var. *cerris* (Figure 2a, b) consists of various sequential periderms (3 to 4) with dead phloem tissue between them (Figure 2a). Taking into account the tree age of 70-80 years, we estimate a phellogen lifespan in *Q. cerris* var. *cerris* of about 25 years in accordance with a rhytidome formation at 30 years of age (Babos, 1979a) or the 25-35 years reported for oaks (Roth, 1981; Trockenbrodt, 1994).

No shedding of the outermost periderms of the rhytidome was observed. Therefore thickness of rhytidome increased with tree age and can provide tree protection, namely against extreme temperatures and fire (Roth, 1981; Dickison, 2000). The rhytidome shows a dark coloration resulting from abundant deposits of materials (Figure 2b).

The periderms of *Q. cerris* are very conspicuous due to the presence of prominent phellem layers (Figure 2a) that are clearly identified macroscopically as cork tissues.

The phellem layer curved slightly, forming discontinuous arching layers in cross section (Figure 2a). The phellogen is composed of rectangular and thin-walled cells in transverse section but is difficult to distinguish in the periderm. Figure 3a shows the differentiation of phellogen cells by tangential cell division. A narrow phelloderm formed by 2 or 3 cell layers of rectangular to round cells is developed, sometimes with thickened walls (Figure 3b) that often cannot be distinguished from the neighbouring parenchyma cells unless by their evident radial alignment. Roth (1981) stated that a very thick cork usually excludes a thick phelloderm and vice versa.

Rings were visible in the phellem layer in each periderm, which included 2-5 growth rings and each ring was composed of 6-12 layers of phellem cells with a more or less radial alignment without intercellular voids. The phellem cells are suberised and have thin walls with a uniform thickness in the tangential and radial walls, and sometimes are radially flattened. At the beginning of a growth ring the phellem cells are larger and have thinner walls in contrast to the narrow and thicker walled phellem cells of the end of the growth ring, as also occur in *Q. suber* (Pereira et al., 1987). However, both species differ markedly on the intensity of phellem growth. In *Q. suber* each

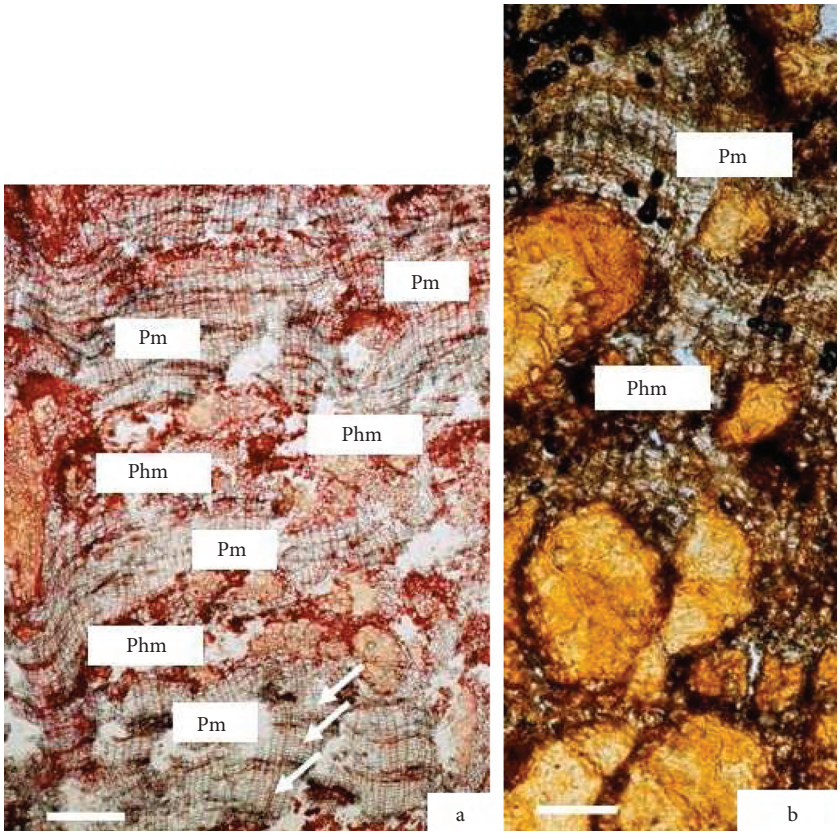

Figure 2. Transverse section of rhytidome of *Quercus cerris* var. *cerris*. a - Various sequential periderms conspicuous due to the presence of wide phellem layers (Pm) with phloem tissue (Phm) between them. Phellem with growth rings (arrows). b - phellem layers (Pm); phloem tissue (Phm). Scale bars; a = 125 µm; b = 50 µm.

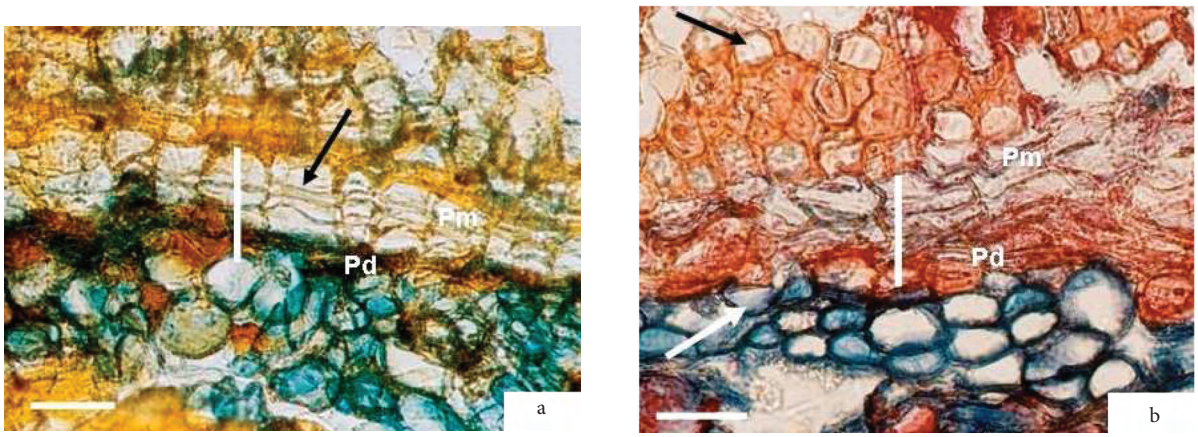

Figure 3. Transverse section of bark of *Q. cerris* var. *cerris*. Vertical bar showing one periderm with phellem (Pm) and phelloderm cells (Pd). a - differentiation of phellogen cells, tangential divisions (black arrow). b - Sc = sieve tubes and phloem parenchyma cells (white arrow). F = fibres and crystals (black arrow). Scale bars; a and b = 25 µm.

phellogen mother cell produces annually about 10-20 phellem cells in young plants (Graça & Pereira, 2004) and many more (up to about 100 cells) in mature trees (Pereira et al., 1992). In *Q. cerris* var. *cerris* the phellogen meristematic activity was much smaller with production in 1 ring of only 6-12 phellem cells in each radial row. The variation in phellem ring width that was found in our samples may be related with external conditions in parallel to what has been reported for *Q. suber* cork, where drought or temperature, or both, can limit cork growth (Costa et al., 2002).

A few (1-2 layers) of the phellem cells in the limit of each growth ring could thicken up to heavily lignified cells. Figure 4 shows lignified phellem cells. This feature was not noted in *Q. suber* cork although lignified thickened cells in phellem are observed in other species, i.e. *Eucalyptus globulus* Labill. (Quilhó et al., 1999) and various tropical barks (Roth, 1981).

Dark stained material was observed in the phellem cells of all the trees (Figure 2b), presumably phenolic compounds. Alonso and Machado (2008) also reported phenolic compounds in phellem cells in tropical species.

The occurrence of lenticular channels crossing radially the periderm was rare, and observed only in one sample of *Q. cerris* var. *cerris* and without filling material (Figure 5). This clearly differs from *Q. suber* cork, where lenticular channels are numerous, variable in number and size, and a key feature for the visual appreciation and quality classification of cork (Pereira, 2007). Their ontogeny was studied by Graça and Pereira (2004). The fact that the cork layers in *Q. cerris* var. *cerris* do not build a continuous cylindrical envelop around the tree stem, as is the case in *Q. suber* where cork makes up a tight impermeable coating, may be the reason why gas exchange between the living tissues underneath and the exterior does not require such a channel system.

In many cases, and especially near the last formed periderm, it was possible to recognise the regular and organised structure of the phloem, i.e. stratified tangential bands of fibres, sclereids, and broad phloem rays.

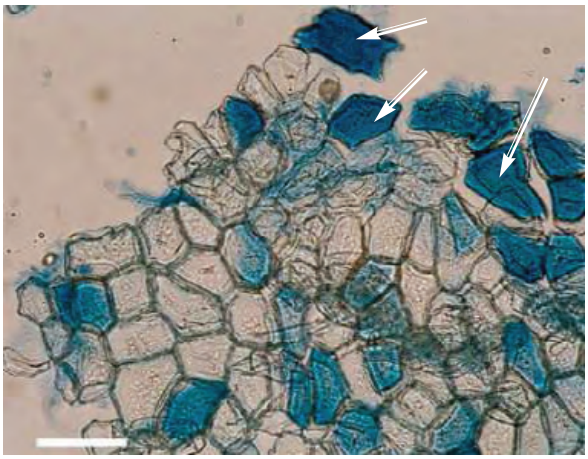

Figure 4. Thick-walled and heavily lignified phellem cells in macerated bark of *Q. cerris* var. *cerris* (arrows). Scale bar = 25 µm.

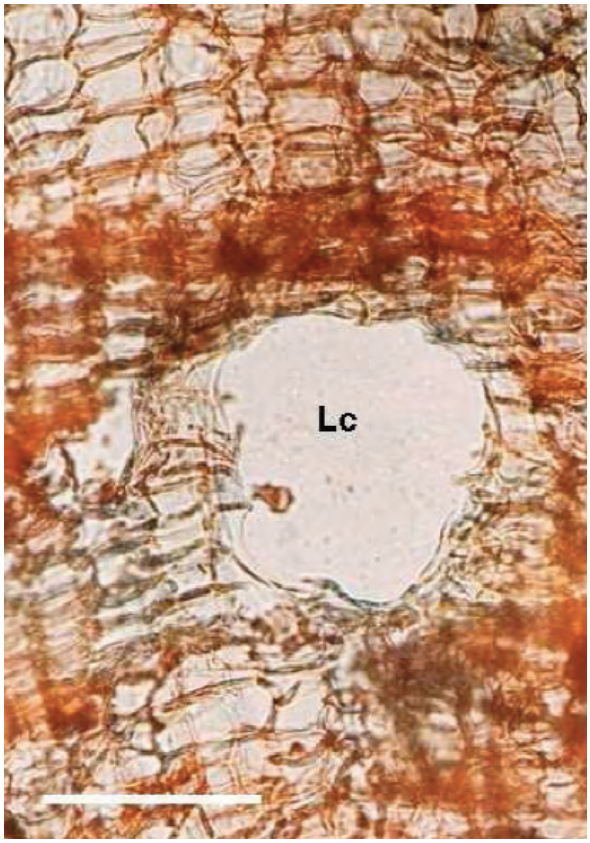

Figure 5. Tangential section of bark of *Q. cerris* var. *cerris*. a - lenticular channel (Lc) without filling material in the phellem of one periderm. Scale bar = 25 µm.

Phloem

The phloem included the non-collapsed phloem and the collapsed phloem layered regularly from the vascular cambium towards the periphery with growth rings marked by non lignified cells (Figure 6). Babos (1979a) referred to the occurrence of phloem rings in *Q. cerris* var. *cerris* and *Q. cerris* var. *austriaca*. Growth rings were also observed in the phloem of *Q. robur* by Trockenbrodt (1991).

At the beginning of each growth ring sieve tubes and axial parenchyma were generally formed followed by tangential bands of fibres and groups of sclereids, while at the end of the ring only a narrow layer of axial parenchyma was formed. According to Barlow and Luck (2006), the tangential banding of the different cell types within the phloem indicates synchrony of cellular development.

Therefore, the phloem of *Q. cerris* var. *cerris* is characterised in the transverse section by the occurrence of successive tangential bands of fibres and groups of sclereids arranged parallel to the cambium, and alternated with axial parenchyma and sieve tubes until the last formed periderm. Uniseriate phloem rays transverse the fibre groups (Figure 6) and fused phloem rays were observed forming conspicuous broad rays (Figure 7).

This structure remained more or less unaltered towards the periderm, mainly in the non-collapsed phloem, which is responsible for the active conduction and represents only a narrow band close to the vascular cambium as in other *Quercus* spp., i.e. *Q. velutina*, *Q. rubra*, *Q. alba*, and *Q. coccinia* (Howard, 1977).

The collapsed phloem in *Q. cerris* var. *cerris* starts not far from the cambium, and shows collapsed sieve tube cells that ceased their conductive function and a disorganised tissue arrangement, as also described in

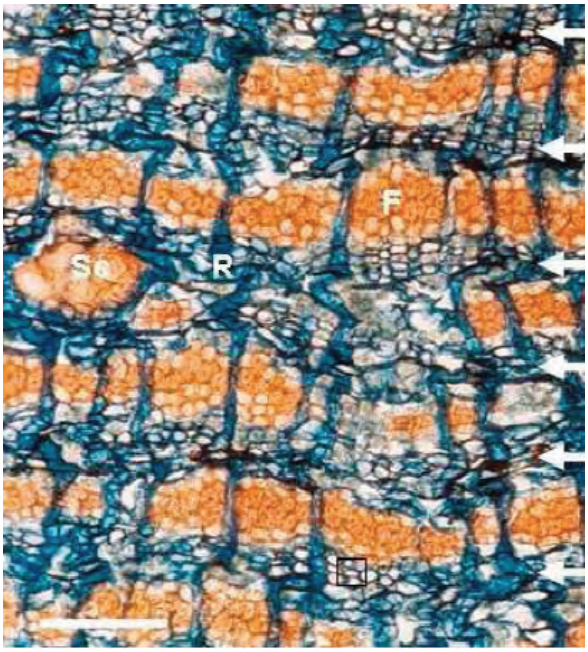

Figure 6. Transverse section of phloem of *Q. cerris* var. *cerris*. Growth rings marked by non lignified cells (arrows). Successive tangential bands of fibres (F) and groups of sclereids (Sc) arranged parallel to the cambium, alternated with axial parenchyma and sieve tubes (¤). Uniseriate phloem rays (R) undulated with moderate dilatation. Scale bar = 50 µm.

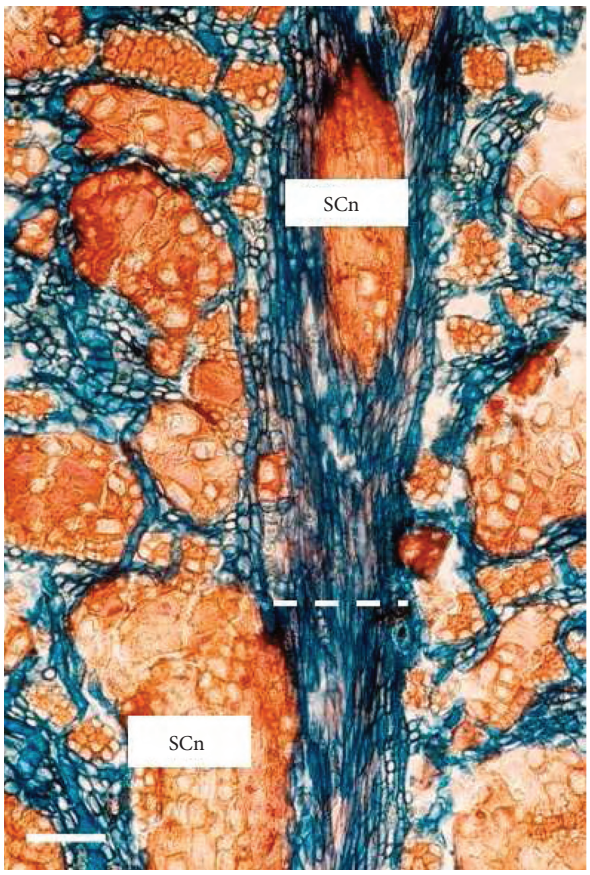

Figure 7. Transverse section of bark of *Q. cerris* var. *cerris*. Fused phloem rays (—). Sclerification of radial parenchyma cells, formation of nodules of sclereids (SCn) within and near the broad rays. Scale bar = 50 µm.

other *Quercus* spp. (Howard, 1977; Trockenbrodt, 1991). A slight distortion of rays was observed that was accompanied by dilatation tissue resulting from expanded axial and radial parenchyma cells and subsequent sclerification. The sclereids form prominent nodules near the fibres and the wide rays. Such structural alterations in the phloem are a consequence of stem radial growth (Quilhó et al., 1999) as described in the genus *Quercus* by Whitmore (1962), Howard (1977), and Trockenbrodt (1991).

Nevertheless, a structural pattern is recognised in the collapsed phloem of *Q. cerris* var. *cerris* with parallel bands of sclerified tissues, i.e. secondary fibres, gross nodules of cluster sclereids, and broad rays with ray sclerified cells, probably providing mechanical support of the tissue. The occurrence of sclerenchyma as a mechanical barrier against collapse of living cells was mentioned in the phloem of *Q. suber* (Quilhó et al., 2003) and in tropical species (Machado et al., 2005).

Sieve tubes, companion cells and sieve plates are of the same type of those described for *Quercus* spp. (Howard, 1977). Sieve tubes with companion cells are solitary or in groups of 2-3 elements with a tangential arrangement. The companion cells are difficult to recognise in transverse and longitudinal sections. The sieve elements have a round to irregular shape in transverse section and the cell walls are thin and unlignified, and may frequently be confused with axial parenchyma. Sieve plates are inclined, compound, and scalariform with 4-8 sieve areas per plate (Figure 8) and numerous sieve pores; several lateral sieve areas are also present.

Fibres are arranged parallel to the vascular cambium in continuous tangential bands, about 3 to 4 cells wide, sometimes interrupted by groups of sclereids (Figure 6). The fibres are slender with tapered overlapping end with narrow lumens (Figure 9a), occasionally forked. They are usually thick walled, lignified, accompanied by chambered and crystalliferous parenchyma cells of approximately equal length at their inner and outer sides (Figure 9b).

The fibre morphology and arrangement are in accordance with observations by Babos (1979a, b) while various fibre arrangements occur in other *Quercus* spp. i.e. fairly continuous, regular, tangential layers of fibres in *Q. robur,* scattered sparse clusters in *Q. encleisocarpa* (Whitmore, 1962) or fibres in small groups in widely spaced, discontinuous tangential bands (Howard, 1977).

Axial parenchyma cells are round to rectangular in transverse section (Figure 3b). They have thin walls and round pit fields and occur near the sieve elements making tangential bands of 2-3 cells in width. In the outer portion of the phloem close to the periderm, these cells proliferated and expanded forming the tissue of dilatation growth.

Prismatic crystals occur profusely in chambered parenchyma cells as strands of up to 10 cells near the fibres (Figure 9b). The strands of crystal-bearing parenchyma along the margins of the fibre band were also described by Howard (1977) and Trockenbrodt (1991) and illustrated in *Q. suber* by Quilhó et al. (2003). The abundance of druses and polygonal crystals (Figure 10), probably of calcium oxalate, found in the phloem of *Q. cerris* var. *cerris* is also found in the bark of oaks as a by product of metabolism (Howard, 1977; Trockenbrodt, 1991, 1995a, 1995b) although depending on environment and plant development (Marcati & Angyalossi, 2005).

Uniseriate rays (Figure 11a) are about 3 cells high, but frequently up to 10 cells, with procumbent cells (Figure 11b). Rays are undulated at the beginning of

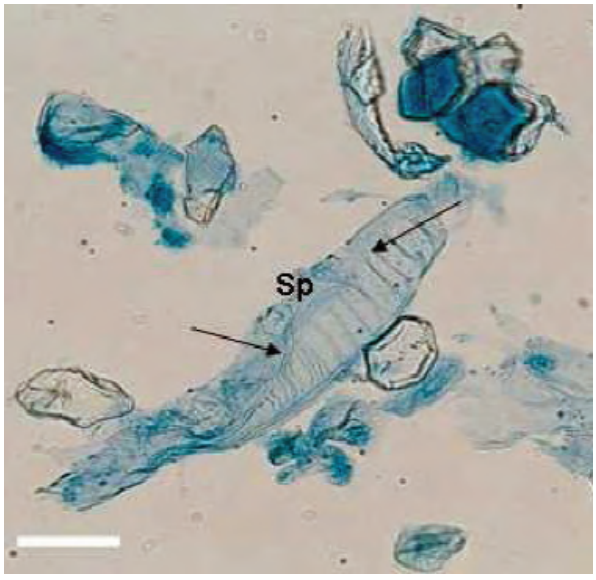

Figure 8. Sieve element of *Q. cerris* var. *cerris* with sieve plates (Sp) and sieve areas (arrow). Scale bar = 25 μm.

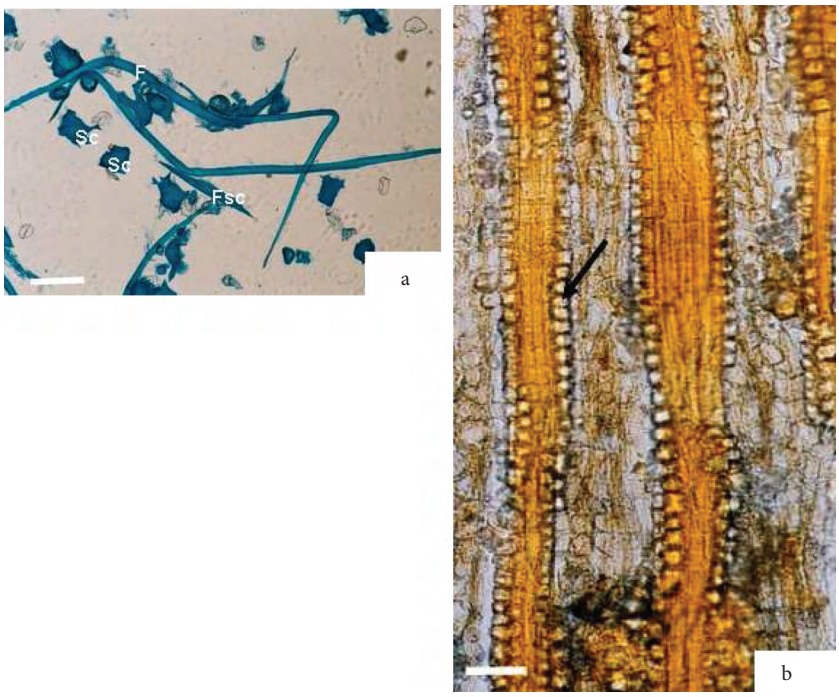

Figure 9. Bark of *Q. cerris* var. *cerris* bark. a - fibres (F) fibrosclereid (Fsc) and sclereids (Sc) in maceration. b - radial section of phloem with fibres (F) accompanied by chambered and crystalliferous parenchyma cells (arrow). Scale bars; a and b = 50 μm.

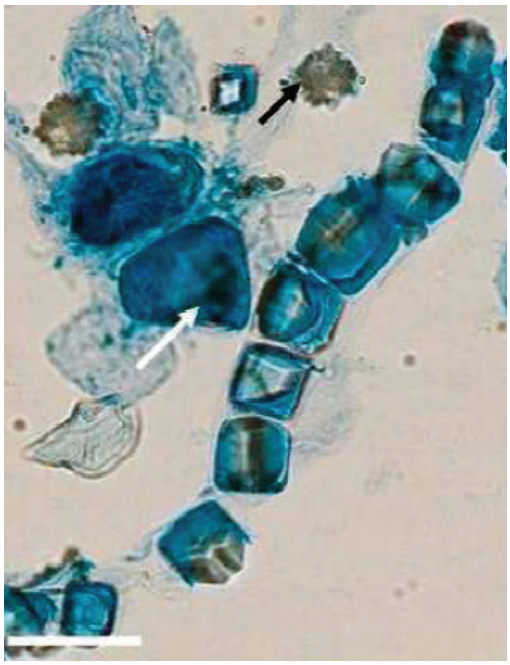

Figure 10. Maceration of *Q. cerris* var. *cerris* bark; crystalliferous parenchyma cells (arrow); druses (black arrow) and a sclerified cell filled with a crystal (white arrow). Scale bar = 125 μm.

the growth ring and show a moderate dilatation (Figure 6) towards the periderm due mainly to the tangential expansion and sometimes division of their cells. In the outer phloem close to the periderm, the ray dilatation tissue may be confused with axial parenchyma cells. Some cells develop thick, lignified secondary walls (Figure 11c).

Sclerification of radial parenchyma cells occurred near the cambium and groups of sclereids accompanied the broad rays (Figure 7) forming radial groups of sclereids (e.g. Figure 12). This was described by Babos (1979a) in his work on *Q. cerris* var. *cerris* as rays with a so-called "palm" formation. The sclerification of phloem ray cells is also present in *Q. suber* (Graça & Pereira, 2004) and in other *Quercus* spp. (Howard, 1977).

Sclereids (Sc) are abundant and occur mostly in clusters. A high proportion of sclereids was observed in all the bark samples. In general sclereids are isodiamteric (Figure 9a), although they attain various shapes and sizes with thickened and polylamellate walls transversed by minute pit channels. They

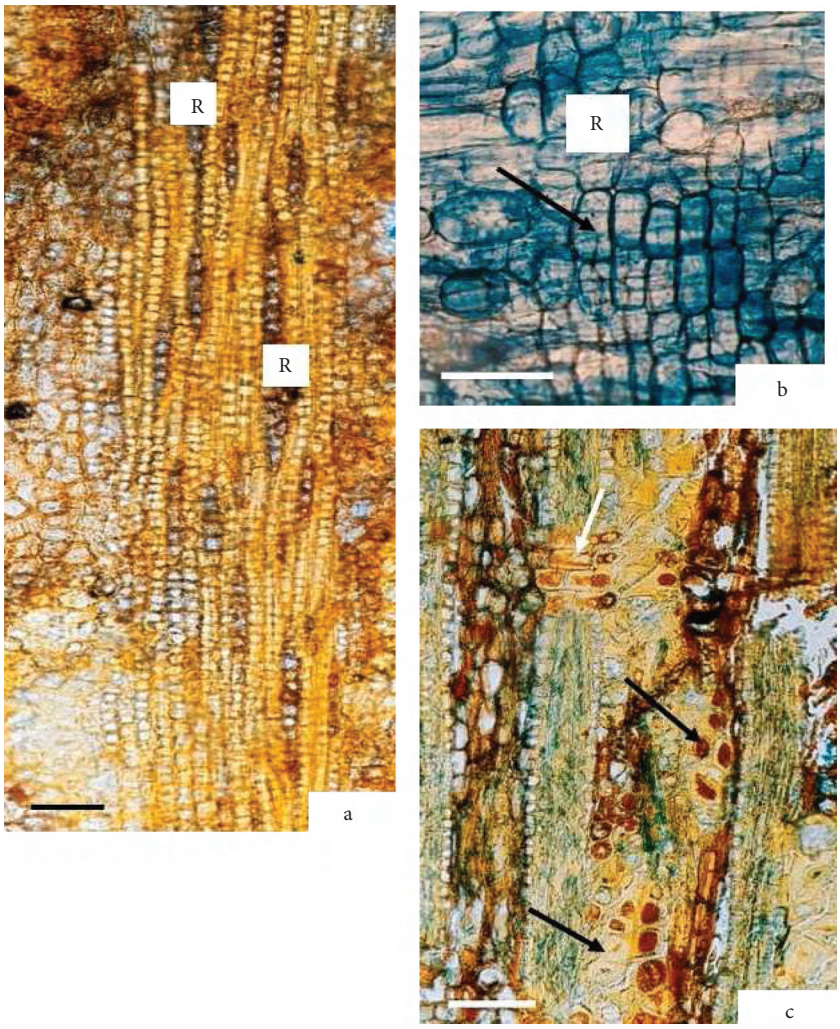

Figure 11. Rays in bark of *Quercus cerris* var. *cerris*. a - Tangential section of secondary phloem; uniseriate rays (R). b - Radial section of secondary phloem; ray (R) with procumbent cells (arrow). c - Sclerified radial parenchyma cells (white arrow) and sclerified axial parenchyma cells (black arrow) with phenolic compounds. Scale bars; a and c = 50 µm; b = 25 µm.

frequently include large prismatic crystals (Figure 10), and phenolic compounds (Figure 11c). Groups of sclereids sometimes form prominent nodules with large tangential or radial diameters. In the transverse section, nodules of clustered sclereids have a tangential or radial arrangement: they are adjacent to the fibre groups, or form radial bands near or even within the broad rays (Figures 7, 12). Fibre sclereids (Fs) are similar to the fibres but shorter and were only distinguish in macerated bark (Figure 9a).

Sclereids originate from axial and radial parenchyma, which gradually enlarge and thicken their radial and tangential cell walls and compact masses of sclereids are clearly visible on cut surfaces of *Quercus* barks (Trockenbrodt, 1991; Howard, 1977; Graça & Pereira, 2004). These cells give bark rigidity and brittleness but cause substantial problems during processing (Roth, 1981) and are one of the causes for the reported inferior quality of *Q. cerris* var. *cerris* bark in comparison with *Q. suber* (Mıhçıoğlu, 1942).

Figure 12. Nodules of sclereids (SCn) in bark of *Q. cerris* var. *cerris*. Transverse section of secondary phloem near the vascular cambium. A narrow band close to the vascular cambium, responsible for the active conduction (arrow). Scale bars = 125 μm.

Conclusions

The findings in this study enhance our understanding of *Q. cerris* var. *cerris* bark and show that the tissue structural complexity is a key feature that has to be taken into account when envisaging bark uses. A careful fractioning of the non-phellemic tissue will be a requirement whenever cork is the targeted component to be valued. The presence of numerous sclereids and crystal inclusions is an important characteristic that lowers the quality of *Q. cerris* var. *cerris* cork and calls for an adequate processing design.

Acknowledgments

We thank the Andırın Unit of the Turkey General Directory of Forestry for the field sampling, and Cristiana Alves and Claudia Santos for technical assistance. The work was carried out with funding by Fundação para a Ciência e Tecnologia, Portugal, to Centro de Estudos Florestais (FEDER/POCI 2010 programme) and Centro das Florestas e Produtos Florestais (POR/3.1.002/DRELVT-ME/IICT), and by the Research Fund of İstanbul University Project Number: 1823.

References

Alonso AA & Machado SR (2008). Stem protective tissue in *Erythroxylum tortuosum* (Erythroxylaceae). A fire tolerant species from cerrado. *IAWA J* 29: 69-77.

Babos K (1979a). Anatomische *Unter*suchungen der Rinde bei den Stammen von *Quercus cerris* var. *cerris* Loud. und *Quercus cerris* var. *austrica* (Willd.) Loud. *Folia Dendrol* 6: 60-78.

Babos K (1979b). Fibre characteristics of some cuba hardwoods. *IAWA Bull* 2/3: 61-62.

Barlow PW & Luck J (2006). Patterned cell development in the secondary phloem of dicotyledonous trees: a review and Hypothesis. *J Plant Res* 119: 271-291.

Borazan A & Babaç MT (2003). Morphometric leaf variation in oaks (*Quercus*) of Bolu, Turkey. *Ann Bot Fennici* 40: 233-242.

Cabi E, Doğan M, Mavi Ö, Karabacak E & Başer B (2010). *Elymus sosnowskyi* (Hackel) Melderis (Poaceae), a rare endemic species in Turkey. *Turk J Bot* 34: 105-114.

Costa A, Pereira H & Oliveira A (2002). Influence of climate on the seasonality of radial growth of cork oak during a production cycle. *Ann For Sci* 59: 429-437.

Dickison WC (2000). *Integrative Plant Anatomy*, USA. Elsevier Publ.

Graça J & Pereira H (2004). The periderm development in *Quercus suber*. *IAWA J* 25: 325-335.

Güvenç A & Duman H (2010). Morphological and anatomical studies of annual taxa of *Sideritis* L. (Lamiaceae), with notes on chorology in Turkey. *Turk J Bot*, 34: 83-104.

Hedge IC & Yaltırık F (1982). *Flora of Turkey and the East Aegean Islands*. Edinburg: Edinburgh Univ Press.

Howard ET (1977). Bark structure of the Southern Upland Oaks. *Wood and Fiber* 9: 172-183.

Junikka L (1994). Survey of English macroscopic bark terminology. *IAWA J* 15: 3-45.

Machado SR, Marcati CR, Morretes BL & Angyalossi V (2005). Comparative bark anatomy of root and stem in *Styrax Camporum* (Styracaceae). *IAWA J* 26: 477-487.

Marcati CR & Angyalossi V (2005). Seazonal presence of acicular crystals in the cambial zone of *Citharexylum myrianthum* (Verbenaceae). *IAWA J* 25: 93-98.

Mıhçıoğlu K (1942). Türkiye'de Saçlı Meşeden Mantar İstihsaline Dair Bir Araştırma. *Orman ve Av* 1: 151-166.

Natividade JV (1950). *Subericultura*. Lisboa Ministério da Economia, Direccão Geral dos Servicos Florestais e Aquícolas.

Özcan T (2007). Characterization of Turkish *Quercus* L. taxa based on fatty acid compositions of the acorns. *J Amer Oil Chem Soc* 84: 653-662.

Özcan T & Bayçu G (2005). Some elemental concentration in the acorns of Turkish *Quercus* L. (Fagaceae) taxa. *Pak J Bot* 37: 361-371.

Pereira H (2007). *Cork: Biology, Production and Uses*. Amsterdam. Elsevier Publ.

Pereira H, Graça J & Baptista C (1992).The effect of growth rate on the structure and compressive properties of cork from *Quercus suber* L. *IAWA Bull* 13: 389-396.

Pereira H, Rosa ME & Fortes MA (1987). The cellular structure of cork from *Quercus suber* L. *IAWA Bull* 8: 213-218.

Quilhó T, Lopes F & Pereira H (2003). The effect of tree shelter on the stem anatomy of cork oak (*Quercus suber*) plants. *IAWA J* 24: 385-395.

Quilhó T, Pereira H & Richter HG (1999). Variability of bark structure in plantation- grown *Eucalyptus globules*. *IAWA J* 20: 171-180.

Richter HG, Mazzoni-Viveiros SC, Alves ES, Luchi AE & Costa CG (1996). Padronização de critérios para a descrição anatómica da casca: lista de características e glossário de termos. *Ver Inst Flor IF Série Reg* 16: 1-25.

Roth I (1981). *Structural Patterns of Tropical Barks*. Berlim. Gebr. Borntraeger

Telgeren G (1976). Memleketimizde yetişen saçlı meşe ağaçlarının kabuklarından yararlanma olanakları. *Ormancılık Araştırma Enstitüsü Dergisi* 22: 114-127.

Trockenbrodt M (1990). Survey and discussion of the terminology used in bark anatomy. *IAWA Bull* 11: 141-166.

Trockenbrodt M (1991). Qualitative structural changes during bark development in *Quercus robur*, *Ulmus glabra*, *Populus tremula* and *Betula pendula*. *IAWA Bull* 12: 5-22.

Trockenbrodt M (1994). Quantitative changes of some anatomical charcters during bark development in *Quercus robur, Ulmus glabra, Populus tremula* and *Betula pendula IAWA J* 15: 387-398.

Trockenbrodt M (1995a). Calcium oxalate crystals in the bark of *Quercus robur*, *Ulmus glabra*, *Populus tremula* and *Betula pendula*. *Ann of Bot* 75: 281-284.

Trockenboldt M (1995b). Structure and identification of root bark of *Quercus robur* L. *Trees* 9: 341-347.

Withmore TC (1962). Studies in systematic bark morphology IV. The bark of beech, oak and sweet chestnut. *New Phytol* 62: 161-169.

Yaltırık F (1984) *Türkiye Meşeleri Teşhis Kılavuzu*. İstanbul Yenilik Basımevi

3.2.2. The celular structure of cork from *Quercus cerris* var. *cerris* bark in a material's perspective

Şen, A., Quilho, T., & Pereira, H.

Industrial Crops and Products, 34:929-936

2011

Industrial Crops and Products 34 (2011) 929–936

Contents lists available at ScienceDirect

Industrial Crops and Products

journal homepage: www.elsevier.com/locate/indcrop

The cellular structure of cork from *Quercus cerris* var. cerris bark in a materials' perspective

Ali Şen[a,c], Teresa Quilhó[b,*], Helena Pereira[c]

[a] Istanbul University, Faculty of Forestry, Department Forest Biology and Wood Protection Technology, 33473 Bahçeköy, Istanbul, Turkey
[b] Centro das Florestas e Produtos Florestais. Instituto de Investigação Científica Tropical, Tapada da Ajuda, 1349-017 Lisboa, Portugal
[c] Centro de Estudos Florestais, Instituto Superior de Agronomia, Universidade Técnica de Lisboa, Tapada da Ajuda, 1349-017 Lisboa, Portugal

ARTICLE INFO

Article history:
Received 4 January 2011
Received in revised form 17 February 2011
Accepted 19 February 2011
Available online 24 March 2011

Keywords:
Quercus cerris
Cork
Cellular structure
Bark
Quercus suber

ABSTRACT

Cork in the outer bark of trees is among the valuable raw materials of biological origin due to properties that result mainly from its cellular structure. Large scale commercial utilization of cork has been only achieved with cork from *Quercus suber*. Another oak species, *Quercus cerris*, also contains substantial, albeit not continuous, regions of cork that are clearly visible to the naked eye but are so far considered as a waste material.

Bark samples of *Q. cerris* var. *cerris* trees were collected from the Andırın province, Turkey. Cork portions were separated and their cellular structure was investigated with optical and electron scanning microscopy observations. The results were compared with *Q. suber* cork.

Q. cerris cork has the typical features of cork tissues with a regular and radially aligned structure of suberized cells without intercellular voids, showing a ring structure and a distinction of earlycork and latecork cells. Solid volume fraction was estimated at 25% (22% in earlycork, 36% in latecork).

In *Q. cerris* cork cells are smaller, cell wall thickness and solid volume fraction are higher, and the tissue is less homogeneous with a higher content of lignified inclusions than in *Q. suber* cork. These factors will negatively influence quality in regard to density and mechanical properties associated to elasticity. However, this does not impair its use for production of granulates and agglomerates, e.g. for insulation and energy absorption. Separation of the cork fraction from the bark is a step required before further processing and use.

1. Introduction

Cork is a cellular material with closed cells. The understanding of the behaviour of a cellular material requires the quantitative description of its structural features (Gibson and Ashby, 1997) since their properties depend on the way the solid is distributed in the cell faces and edges, on the geometry and dimensions of the cells, as well as on their three-dimensional arrangement.

Cork is of biological origin, formed by the secondary meristem phellogen in the outer bark of trees as part of the periderm (Esau, 1969). Each phellogen mother-cell gives by cellular division cork cells (phellem cells in plant anatomy nomenclature) that grow unidirectionally outwards in the tree's radial direction.

Cork is known world wide as the material produced by the cork oak (*Quercus suber* L.) that is used as sealant in wine bottles, as well as in insulation and surfacing products. Its structure, chemical composition and properties have been thoroughly studied and a recent review book gathered the available knowledge on formation, production, properties and uses of cork (Pereira, 2007).

Structurally cork has small thin walled cells in the form of hexagonal prisms (prism height 30–40 μm, base edge 13–15 μm and wall thickness 1–1.5 μm) that are stacked base to base in regular rows, arranged parallel without intercellular voids (Pereira et al., 1987). There are periodic variations in cell size and density during the annual growth season with formation of growth rings (Cumbre et al., 2000). Discontinuities may occur in the cork tissue namely of biological origin, i.e. the lenticular channels and inclusions of phloem tissue (Graça and Pereira, 2004; Pereira et al., 1996). Many of the properties of cork may be related to the characteristics of its cellular structure and are determinant for the use of cork products, i.e. as sealants, floating and insulation materials (Anjos et al., 2008; Pereira et al., 1992; Rosa et al., 1990; Pereira and Ferreira, 1989).

Other tree species contain cork tissues in their outer barks, i.e. *Betula pendula* (Ekman, 1983; Pinto et al., 2009), *Pinus pinaster* (Nunes et al., 1996) and *Pseudotsuga menziesii* (Hergert and Kurth, 1952; Krahmer and Wellons, 1973; Litvay and Krahmer, 1977). The bark of *Q. cerris* var. *cerris* (Turkey oak) also contains large areas of

* Corresponding author.
E-mail address: terisantos@isa.utl.pt (T. Quilhó).

0926-6690/$ – see front matter © 2011 Elsevier B.V. All rights reserved.
doi:10.1016/j.indcrop.2011.02.015

Fig. 1. Photograph of the bark of *Q. cerris* var. *cerris* showing the successive layers of cork (lighter coloured regions) and of phloem (dark coloured regions) in the thick rhytidome that lies to the outside of the bark phloem (shown at the bottom of the photo).

cork tissue as part of the successive periderms that constitute its thick rhytidome (Şen et al., 2011).

Q. cerris var. *cerris* grows naturally in central and south-eastern Europe and Asia Minor. In Turkey, the *Q. cerris* var. *cerris* covers about 235 000 ha in the Andirin province in Anatolia (Mıhçıoğlu, 1942). The bark of *Q. cerris* var. *cerris* contains substantial, albeit not continuous, regions of cork tissue that are clearly visible to the naked eye. It was already used in Turkey at a very small scale as an alternative to cork from *Q. suber* for production of insulation agglomerates (Mıhçıoğlu, 1942) and later for production of stoppers for the alcoholic raki drink. However, the comparisons made with *Q. suber* led to reports that the bark of *Q. cerris* was of less quality (Mıhçıoğlu, 1942; Telgeren, 1976). At present there is no specific forest management towards the exploitation of *Q. cerris* and its bark is not used.

In this paper we describe the structure of the cork tissue from the bark of *Q. cerris* var. *cerris* from Turkey based on scanning electron microscopy observations and optical microscopy, and characterize it in relation to geometry and size of the individual cells, as well as their two- and three-dimensional arrangement. A comparison is made with the cellular characteristics of cork from *Q. suber* which is the benchmark for this type of material. It is the objective to establish basic knowledge on the cellular characteristics of *Q. cerris* var. *cerris* cork that will framework its potential utilization.

2. Materials and methods

Bark samples were collected at breast height level from nine *Quercus cerris* var. *cerris* mature trees with 70–80 years of age, in the south-eastern part of Turkey, in the Andirin Province of Kahramanmaraş (altitude of 1000 m, 662.2 mm annual rainfall and 16.5 °C mean temperature). The cork and phloem portions of the rhytidome were separated manually, and the cork fractions were kept for observation.

Small cubes with approximately 5 mm of edge were cut with a sharp razor blade. These dimensions were selected in order to have pure cork samples without phloem regions. The cubes were mounted on stubs (ProSciTech, Australia) and sputter coated (Polaron E 5100 E, USA) with gold palladium for 3 min at 20 mA with their faces oriented so that the observation surface corresponded to transverse, radial and tangential sections.

The cubes were vacuum dried and gold was vapour sprayed making up an approximately 450 Å thick coating. The surfaces were

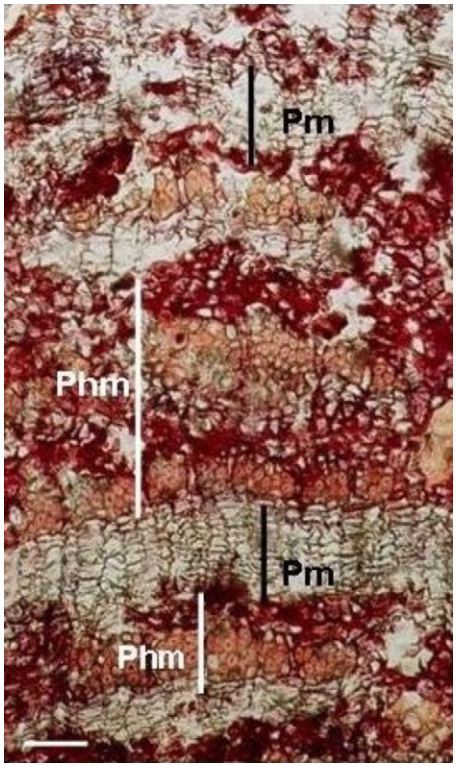

Fig. 2. Optical microscopy photograph of the bark rhytidome of *Q. cerris* var. *cerris* showing the successive layers of cork (Pm) and of phloem (Phm) in the thick rhytidome. (—) Scale bar: 125 μm.

observed in an electron scanning microscope Hitachi S-2400 at magnifications ranging from 50 to 1000×, and the images were recorded in digital format.

The cell measurements were made on the images using image analysis software (Leica Qwin Plus) on approximately 900 cell-samples. On the tangential sections, the number of edges of each cell was counted and the average cell area was calculated. On the transverse sections ring width was measured and the following measurements were made separately on earlycork and latecork cells: number of edges of each cell, radial and tangential dimensions of the lumen of each cell, radial width of the growth ring. The radial and tangential cell wall thickness was calculated as (cell dimension − lumen dimension)/2.

The distribution function of the number of edges of each cell was calculated for the tangential and the non-tangential (radial and transverse) sections as

$$f_i = \frac{N_i}{\sum N_i}$$

where N_i represents the number of cells with i edges. The dispersion of the function in relation to the mean was calculated as $\mu^2 = \sum (i-6)^2 f_i$.

Considering the average dimensions of the cellular units, it can be calculated how much of the cork volume is occupied by the solid. The individual cell is taken as a hexagonal prism, and the solid volume V_s as the difference between total volume V and the empty (lumen) volume V_0, as given by

$$V = \left(\frac{3\sqrt{3}}{2}\right) \times l^2 \times h$$

$$V_0 = \left(\frac{3\sqrt{3}}{2}\right) \times \left(l - \left(\frac{e}{\sqrt{3}}\right)\right) \times (h - e)$$

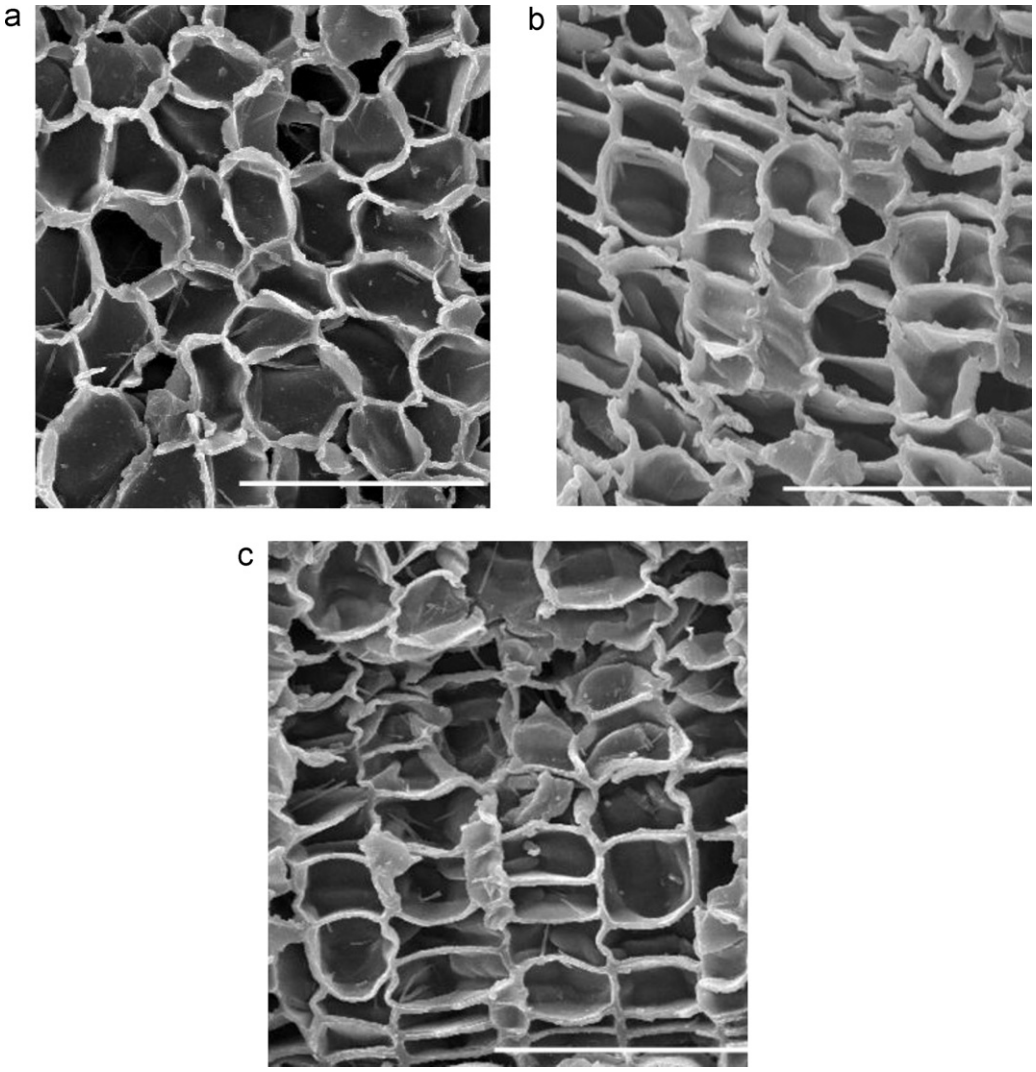

Fig. 3. Scanning electron microscopy observations of cork from the bark of *Q. cerris* var. *cerris*: (a) tangential section; (b) transverse section; (c) radial section. (—) Scale bar (a, b and c): 100 μm.

$$V_s = V - V_0$$

with l as the base edge, h the prism height and e the total wall thickness (between two cells) (Fortes et al., 2004).

Additional optical microscopic observations were also made. The rhytidome samples were impregnated with DP 1500 polyethylene glycol and transverse and longitudinal microscopic sections of approximately 17 μm thickness were prepared with a Leica SM 2400 microtome using Tesafilm 106/4106 adhesive for sample retrieval. The sections were stained with a triple staining of chrysodine/acridine red and astra blue. The sections were mounted on Kaiser glycerin and after 24 h drying were submerged in xylol for 30 min to remove the adhesive, dehydrated in 96% and 100% ethanol, and mounted on Eukitt (Quilhó et al., 1999). Sudan 4 was used for selective staining of suberin. Specimens were also taken from the bark samples and macerated in a solution of 30% H_2O_2 and CH_3COOH 1:1 at 60 °C for 48 h for cell dissociation and stained with astra blue.

The light microscopic observations were made using a Leica DM LA microscope and photomicrographs were taken with a Nikon Microphot-FXA.

3. Results

The layers of cork are part of the successive periderms that constitute the thick rhytidome of *Q. cerris* var. *cerris* and their location in the bark is shown in Fig. 1. The cork layers (phellem layers) are interspersed with phloem layers of variable thickness and do not show spatial continuity in the radial direction (Fig. 2) nor in the tangential, e.g. along the circumference, and axial directions.

3.1. Structure

The structure of the cork contained within the rhytidome of *Q. cerris* var. *cerris* as observed by scanning electron microscopy in the

Table 1
Frequency distribution of the number of edges of cells in the tangential and non-tangential sections of cork from *Q. cerris* var. *cerris*.

Number of edges	Tangential	Non-tangential
4	0.029	0.280
5	0.296	0.385
6	0.486	0.312
7	0.168	0.036
8	0.019	0.002
μ_2	0.656	0.754

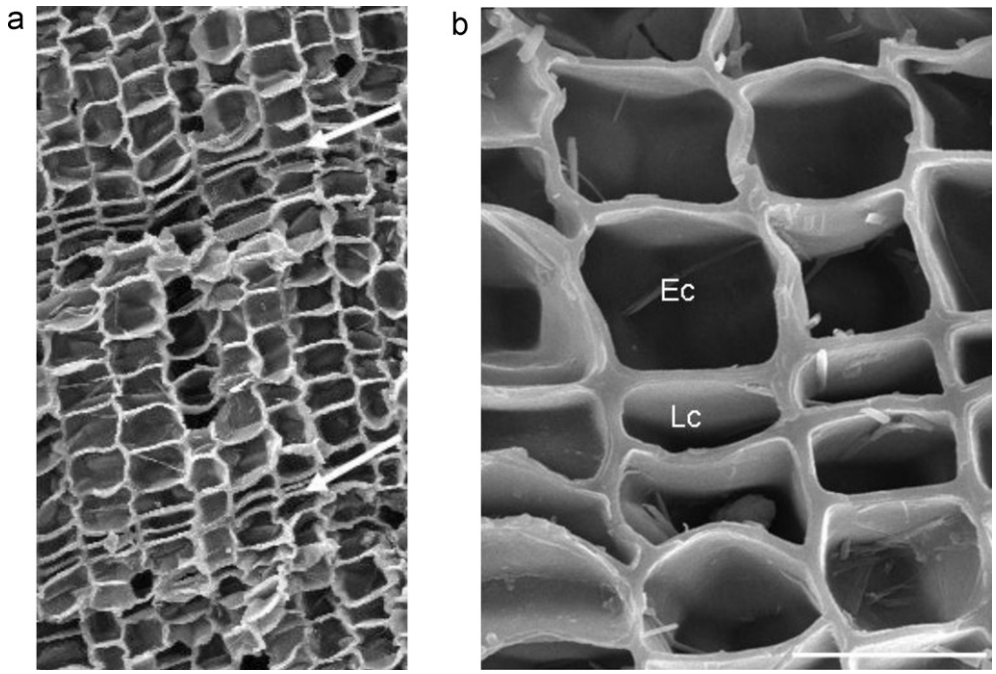

Fig. 4. SEM images of cork from the bark of *Q. cerris* var. *cerris* showing a ring organization with alternating layers of earlycork (Ec) and latecork (Lc) cells (a); a ring boundary (b). Scale bar: (a) 300 μm; (b) 30 μm.

three principal sections is shown in Fig. 3. In each section the cells formed a bidimensional network of edges and vertices, arranged without gaps or intercellular voids.

In the tangential section, the cork cells appear as polygons arranged in a honeycomb-type structure (Fig. 3a). About half of the cells have six sides, with five- and seven-sided polygons making up most of the other cases (Table 1). The dispersion around the average of the number of polygonal edges is low, reflecting a large homogeneity of cell shape in this section. This means that in the majority of cases three cells meet at each vertex of the network.

The radial and transverse sections of cork look very similar and may be referred to as non-tangential sections (Fig. 3b and c). They differ from the tangential section, since the individual cells are approximately rectangular and aligned in parallel rows with a brick wall appearance. Their topological description shows some differences in relation to the tangential section (Table 1): the number of sides of each cell is on average five with a distribution that shows a substantial fraction of cells with four edges. Therefore in these sections and in most of the cases four cells meet at each vertex.

3.2. Cork rings

The cork shows a layered structure of rings with a cell size variation within each ring that distinguishes the cells formed in the first period of growth from the cells formed at the end of the previous growing season, named, respectively, earlycork and latecork cells (Fig. 4a). Earlycork cells are larger and have thinner walls while latecork cells have thicker walls and a much smaller prism height (Fig. 4b). Optical microscopy observations showed that 1–2 layers of the phellem cells in the limit of each growth ring may be heavily lignified (Fig. 5).

The cork rings comprised approximately 7–9 earlycork cells and 2–4 latecork cells in each radial row. Typical measurements of the ring width averaged 201 μm, with a range from 160 μm to 236 μm.

3.3. 3D-structure

The three sections observed in cork allow visualizing its three-dimensional structure (Fig. 3, Table 1). In general terms, cork may be described as being formed by hexagonal prisms that are stacked base-to-base forming rows. The cell rows are assembled in a parallel position in a compact space-filling arrangement. The rows are aligned in the radial direction and therefore the individual cells have the prism height oriented in the radial direction and the prism base in a tangential plane. In adjacent rows the prism bases are frequently coincident and in other cases lay in staggered positions.

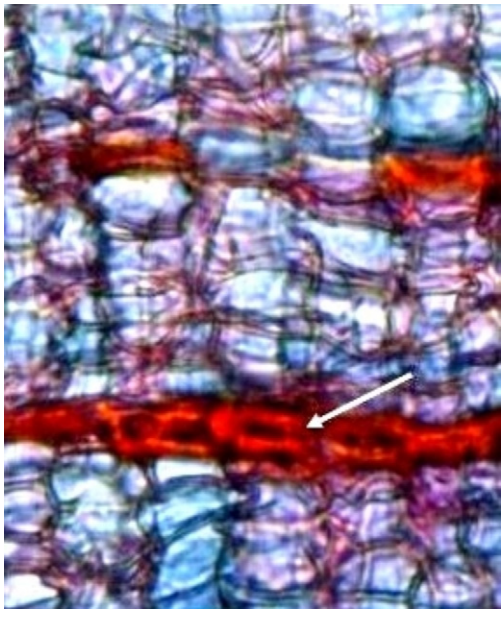

Fig. 5. Optical microscopy observation showing thick lignified phellem cells (arrow) in the limit of the growth ring. (—) Scale bar: 25 μm.

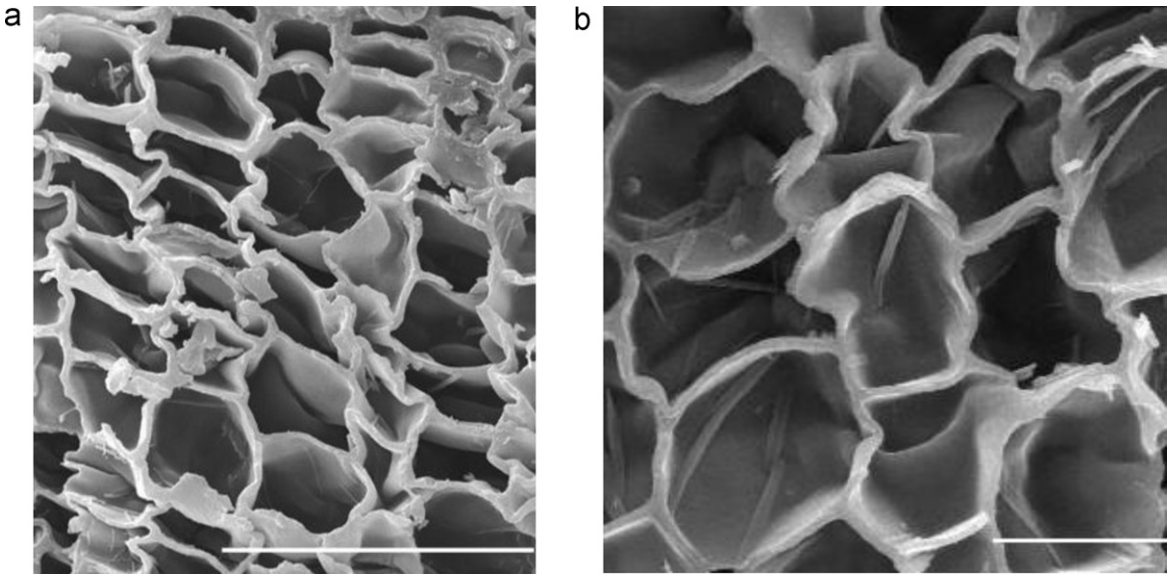

Fig. 6. Scanning electron microscopy observations of cork from the bark of *Q. cerris* var. *cerris* showing the undulations of cell walls. Scale bar: (a) 100 μm; (b) 30 μm.

3.4. Undulation

In the radial and transverse sections of cork it can be observed that the cell sides that are roughly oriented along the radial direction, i.e. the prism lateral faces, in most cases are not straight but show some cell wall undulation (Fig. 6a and b). Usually one to two corrugations per face can be seen especially in the earlycork cells but the amplitude of the corrugations is variable within and between samples. In some regions the cells were heavily compressed in the radial direction or may show distortion of cells in other directions (Fig. 7).

In the tangential section the sides of the cells did not usually show corrugations, although some buckling may occur.

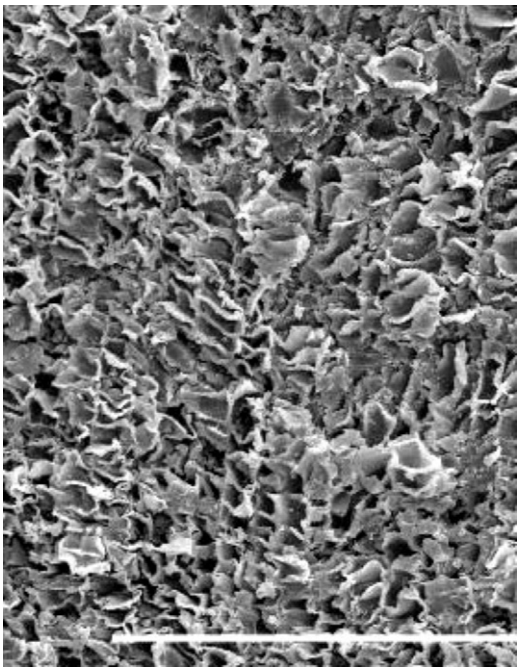

Fig. 7. Scanning electron microscopy observations in the transverse section of cork from the bark of *Q. cerris* var. *cerris* showing heavy cell corrugation and distortion. (—) Scale bar: 300 μm.

3.5. Cell dimensions

The cell dimensions in earlycork and latecork are summarized in Table 2. On average in earlycork the prism height is 25 μm, the base edge 16 μm and the cell wall thickness 2–3 μm; in latecork the prism height is reduced to 14 μm, and the cell wall thickness increased to 3–5 μm. However, the cork dimensions were far from uniform and there were large variations within the sample and between samples.

The aspect ratio of the cells (h/l) is about 1.5–2 in earlycork cells and close to 1 in latecork cells.

3.6. Solid volume

The solid distribution in faces and edges is uniform and the cell edges have substantially the same cell wall thickness as faces, apart from a slight rounding that is observed at the inner side of cells at face junction (Fig. 8a and b). The wall thickness differs for the cell faces lying in the tangential plane (the prism base) which are thinner than those in the radial direction (prism sides), corresponding, respectively, to 2.1 and 2.9 μm in earlycork and 2.8 and 5.2 μm in latecork.

Considering the average dimensions of the cellular units, it can be calculated how much of the cork volume is occupied by the solid. The solid fraction in the cork calculated in percent volume is approximately 22.3% in the earlycork and 35.8% in the latecork region.

Table 2
Mean and standard deviation (in parenthesis) of the cellular dimensional characteristics of the cork cells from *Q. cerris* var. *cerris* measured on transverse sections in the radial and tangential directions.

	Earlycork	Latecork
Radial width, μm	24.6 (5.6)	14.0 (6.6)
Radial lumen width, μm	20.5 (5.9)	8.5 (4.2)
Radial cell wall thickness, μm	2.1 (1.3)	2.8 (2.0)
Tangential width, μm	30.2 (6.3)	30.0 (5.8)
Tangential lumen width, μm	24.4 (6.8)	20.0 (7.8)
Tangential cell wall thickness, μm	2.9 (1.6)	5.2 (3.8)

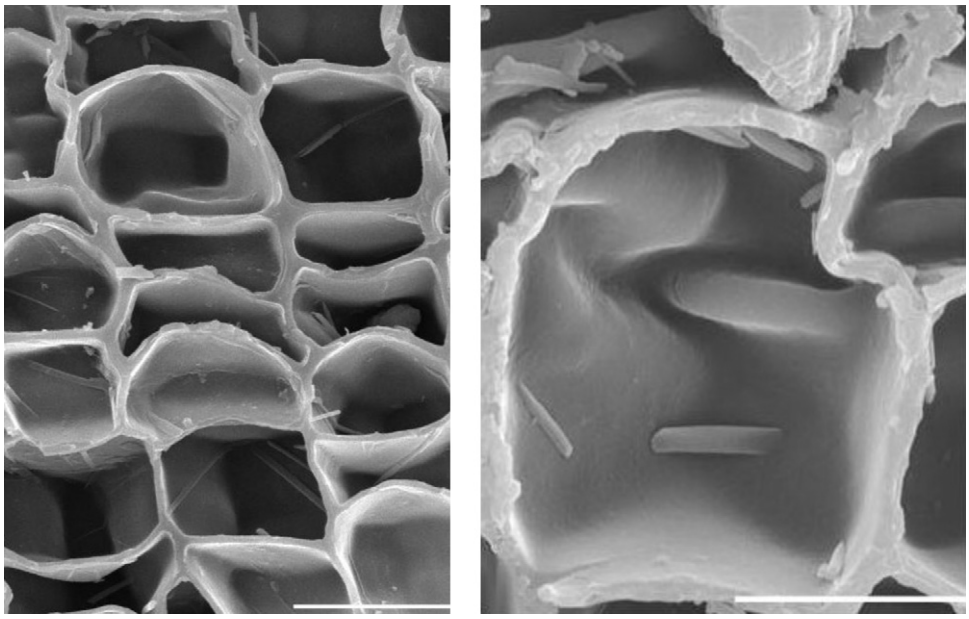

Fig. 8. Scanning electron microscopy observations in the transverse section of cork from the bark of *Q. cerris* var. *cerris* showing the solid distribution in the cell wall of contiguous cells. Scale bar: (a) 30 μm; (b) 10 μm.

3.7. Structural discontinuities

Within the cork tissue there are lenticular discontinuities with an approximate circular section in the tangential section as shown in Fig. 9, and extending as channels in the radial direction. These channels are filled with thin walled cells with a loose arrangement.

The cork tissue frequently also includes lignified phloem cells (fibers and sclereids). Sclereids may occur in the phellem mass in aggregates of a few cells, sometimes forming prominent nodules with large tangential or radial diameters (Fig. 10). In general sclereids are approximately isodiametric although with various shapes and sizes, and have almost no lumen and very thickened and polilamellated cell walls transversed by minute pit channels (Fig. 10). They frequently include large prismatic crystals and phenolic compounds (Fig. 11).

4. Discussion

The anatomy of the bark of *Q. cerris* var. *cerris* was recently described (Şen et al., 2011) and shown to contain a thick rhytidome formed by successive periderms with conspicuous cork layers as depicted in Fig. 1. It is this important content of cork in the bark of *Q. cerris* that has triggered interest in its possible utilization and on the characterization of its cellular structure as a determining factor for defining properties and performance, as shown in detail for *Q. suber* cork (Pereira, 2007) and in general for cellular materials (Gibson and Ashby, 1997).

The results of this paper bring a description of *Q. cerris* var. *cerris* cork cells and structure that was not yet available, therefore allowing a comparison with the known features of the commercial valuable *Q. suber* cork. However, taking into account the bark and rhytidome structure (Figs. 1 and 2), the use of the *Q. cerris* cork fraction will require a fractionation process and be limited to cork granulates. The need for a careful bark fractionation was already advised when considering the chemical

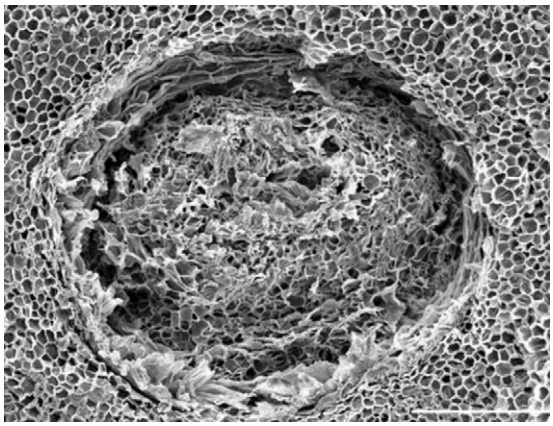

Fig. 9. Scanning electron microscopy observations in the tangential section of cork from the bark of *Q. cerris* var. *cerris* showing one lenticular pore. Scale bar: 300 μm.

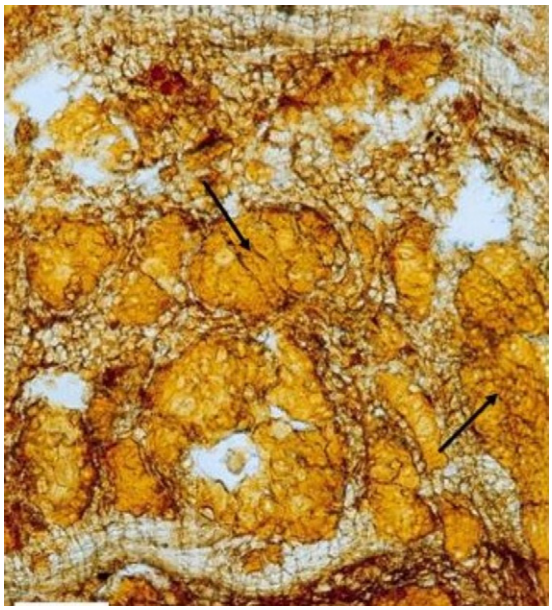

Fig. 10. Inclusions of lignified cells within the cork tissue as observed by optical microscopy in thin sections. Scale bar: 50 μm.

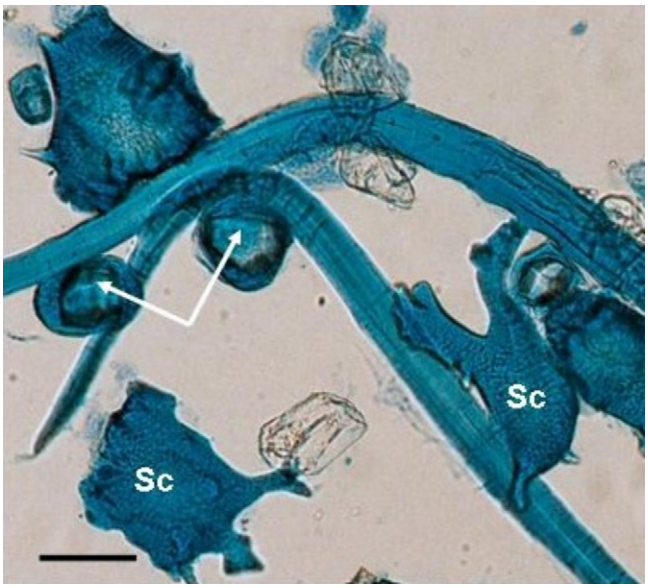

Fig. 11. Sclereids (Sc) observed by optical microscopy in dissociated cells and prismatic crystals (arrows). Scale bar: 50 μm.

composition of the *Q. cerris* rhytidome components (Sen et al., 2010).

Overall the cellular structure of *Q. cerris* cork is similar to that found in corks of other species namely in *Q. suber* (Pereira et al., 1987; Pereira, 2007) with a regular and compact arrangement of small closed cells. Some differences are, however, present as discussed in sequence.

The cell dimensions of *Q. cerris* cork (Table 2) are smaller than those of *Q. suber* in relation to the prism height in the earlycork cells (25 μm vs. 30–40 μm), while cell wall thickness is higher (2–3 μm vs. 1–1.5 μm). The fraction of solid material in *Q. cerris* cork (22% and 36%, respectively, in earlycork and latecork, Table 3) can be estimated at an average of about 25% by assuming that the volume ratio earlycork:latecork is about 0.82:0.18, taking into account the number of both cell types and their dimensions. This solid fraction is much higher compared with the 10% of *Q. suber* cork (Pereira, 2007). In consequence *Q. cerris* cork has a higher density and therefore looses the competitive advantage of a very low density of *Q. suber* cork and other cellular materials used for insulation.

The topology of *Q. cerris* cork as regards the distribution of the number of cells in each section (Table 1) shows a higher dispersion in the non-tangential sections. In these sections the cells are mostly 5- and 6-sided but with a substantial proportion of 4-sided cells, leading to the frequent location of the prism base of cells in contiguous rows in the same tangential plane (Fig. 3a). This differs from *Q. suber* cork where the three sections are topologically very similar (Pereira et al., 1987).

Another difference in the cellular characteristics of *Q. cerris* cork lies in a more irregular undulation of the cell walls (Figs. 6a,b and 7) in comparison to *Q. suber*. This is a consequence of the thicker cell walls but also of the less regular stress distribution of radial growth in the bark tissue due to the presence of phloemic layers between the cork regions (Figs. 1 and 2).

Table 3
Dimensional characteristics of the cork cells from *Q. cerris* var. *cerris*.

	Earlycork	Latecork
Prism height, μm	24.6	14.0
Prism base edge, μm	15.5	15.5
Average base area, μm^2	620.9	620.9
Total cell volume, μm^3	15355	8738
Number of cells per cm^3	6.5×10^7	11.4×10^7
Solid volume fraction, %	22.25	35.84

Rings were visible in the phellem layer in each periderm (2–5 rings, Fig. 4a). Previous anatomical studies of *Q. cerris* var. *cerris* bark estimated that the phellogen lifespan in each periderm was about 25 years (Şen et al., 2011). This means that the phellogen activity will not have an annual regularity and the rings shown in the phellem are not annual rings as it is the case in *Q. suber*. The lignified layers of phellem cells in the limit of each ring (Fig. 5) are not noticed in *Q. suber* cork although they are observed in other species, i.e. *E. globulus* (Quilhó et al., 1999) and various tropical barks (Roth, 1981).

The intensity of phellem growth in each periderm was moderate, with only 9–13 cells produced by one phellogen mother cell during one ring period. This differs markedly from *Q. suber* where each phellogen mother cell produces annually about 10–20 phellem cells in young plants and many more (up to about 100 cells) in mature trees (Graça and Pereira, 2004; Pereira et al., 1992).

Q. cerris var. *cerris* also showed a great amount of lignified and sclerified phloem cells within the cork tissue as compared with *Q. suber* (Fig. 10). Sclereids originate from axial and radial parenchyma, which enlarge and thicken and compact masses of sclereids are clearly visible on cut surfaces of *Quercus* barks (Trockenbrodt, 1991; Howard, 1977; Graça and Pereira, 2004). From a material's point of view, the sclerified nodules are defects that will negatively impact on the mechanical properties of the cork tissue and are one of the causes for the reported inferior quality of *Q. cerris* var. *cerris* bark in comparison with *Q. suber* (Mıhçıoğlu, 1942).

On the contrary very few lenticular channels were observed crossing the cork layers (Fig. 9). Therefore they will not be the determining quality parameter as it is the case for *Q. suber* cork (Pereira et al., 1996).

The combined characteristics of *Q. cerris* cork cells and structure will influence the material's properties, behaviour during processing and performance in use, as detailed for *Q. suber* cork (Pereira, 2007). Overall the quality may be considered as lower than that of *Q. suber* in what relates to density and mechanical properties associated to elasticity. However, consequences should not be overwhelming since the potential use of *Q. cerris* cork has to be directed to the production of granulates and agglomerates, where such properties will have less impact.

5. Conclusions

The cork of *Q. cerris* var. *cerris* shows typical features of bark cork tissues with a regular and radially aligned structure of suberised cells without intercellular voids. These characteristics support its use as a cellular material namely for insulation and energy absorption. Separation of the cork fraction from the rhytidome is a step required before further processing and use.

Taking as reference the cork from *Q. suber*, the cells of *Q. cerris* var. *cerris* are smaller leading to a higher solid volume fraction, and the tissue is less homogeneous with a higher content of lignified inclusions.

Acknowledgements

We thank the Andırın Unit of the Turkey General Directory of Forestry for the field sampling; Isabel Dias Nogueira for assistance in SEM analysis and Cristiana Alves for preparation of microtomed sections. The work was carried out with funding by Fundação para a Ciência e Tecnologia, Portugal, to Centro de Estudos Florestais (FEDER/POCI 2010 programme) and Centro das Florestas e Produ-

tos Florestais (POR/3.1.002/DRELVT-ME/IICT), and by the Research Fund of Istanbul University, Project Number: 1823.

References

Anjos, O., Pereira, H., Rosa, M.E., 2008. Effect of quality, porosity and density on the compression properties of cork. Holz Roh Werkst. 66 (4), 295–301.

Cumbre, F., Lopes, F., Pereira, H., 2000. The effect of water boiling on annual ring width and porosity of cork. Wood Fiber Sci. 32 (1), 125–133.

Ekman, R., 1983. The suberin monomers and triterpenoids from the outer bark of *Betula verrucosa* Ehrh. Holzforschung 37 (4), 205–211.

Esau, K., 1969. The Phloem Handbuch der Pflanzenanatomie, vol. 2. Gebr. Bomtraeger, Berlin/Stuttgart.

Fortes, M., Rosa, M.E., Pereira, H., 2004. A Cortiça. IST Press, Lisboa.

Gibson, L.J., Ashby, M.F., 1997. Cellular Solids. Structure and Properties, 2nd ed. Cambridge University Press, Cambridge.

Graça, J., Pereira, H., 2004. The periderm development in *Quercus suber*. IAWA J. 25 (3), 325–335.

Hergert, H., Kurth, E., 1952. The chemical nature of cork from Douglas fir bark. Tappi 35, 59–66.

Howard, E.T., 1977. Bark structure of the Southern Upland Oaks. Wood Fiber 9, 172–183.

Krahmer, R., Wellons, J., 1973. Some anatomical and chemical characteristics of Douglas-fir cork. Wood Sci. 6, 97–105.

Litvay, J., Krahmer, R., 1977. Wall layering in Douglas-fir cork cells. Wood Sci. 9, 167–173.

Mıhçıoğlu, K., 1942. Türkiye'de Saçlı Meşeden Mantar İstihsaline Dair Bir Araştırma. Orman. Av. 1, 151–166.

Nunes, E., Quilhó, T., Pereira, H., 1996. Anatomy and chemical composition of *Pinus pinaster* bark. IAWA J. 17 (2), 141–149.

Pereira, H., 2007. Cork: Biology Production and Uses. Elsevier Publications, Amsterdam, p. 336.

Pereira, H., Ferreira, E., 1989. Scanning electron microscopy observations of insulation cork agglomerates. Mater. Sci. Eng. A 111, 217–225.

Pereira, H., Graça, J., Baptista, C., 1992. The effect of growth rate on the structure and compressive properties of cork. IAWA Bull. 13 (4), 389–396.

Pereira, H., Lopes, F., Graça, J., 1996. The evaluation of the quality of cork planks by image analysis. Holzforschung 50 (2), 111–115.

Pereira, H., Rosa, M.E., Fortes, M.A., 1987. The cellular structure of cork from *Quercus suber* L. IAWA Bull. 8 (3), 213–218.

Pinto, P.C.R.O., Sousa, A.F., Silvestre, A.J.D., Neto, C.P., Gandini, A., Eckerman, C., Holmbom, B., 2009. *Quercus suber* and *Betula pendula* outer barks as renewable sources of oleochemicals: a comparative study. Ind. Crops Prod., 29126–29132.

Quilhó, T., Pereira, H., Richter, G., 1999. Variability of bark structure in plantation-grown *Eucalyptus globulus*. IAWA J. 20 (2), 171–180.

Rosa, M.E., Pereira, H., Fortes, M.A., 1990. Effects of hot water treatments on the structure and properties of cork. Wood Fiber Sci. 22 (2), 149–164.

Roth, I., 1981. Structural Patterns of Tropical Barks. Encyclopedia of Plant Anatomy Part 3, vol. IX. Gebr. Borntraeger, Berlin, p. 609.

Sen, A., Miranda, I., Santos, S., Graça, J., Pereira, H., 2010. The Chemical composition of cork and phloem in the rhytidome of *Quercus cerris* bark. Ind. Crop Prod. 31, 417–422.

Şen, A., Quilhó, T., Pereira, H., 2011. Anatomical characterization of the bark of *Quercus cerris* var. *cerris*. Turk. J. Bot. 35, 45–55.

Telgeren, G., 1976. Memleketimizde yetişen saçlı meşe ağaçlarının kabuklarından yararlanma olanakları. Orman. Araştırma Enstitüsü Derg. 22 (2), 114–127.

Trockenbrodt, M., 1991. Qualitive structural changes during bark development in *Quercus robur*, *Ulmus glabra*, *Populus tremula* and *Betula pendula*. IAWA Bull. 12, 5–22.

3.2.3. The chemical composition of cork and phloem in the rhytidome of *Quercus cerris* bark

Şen, A., Miranda, I., Santos, S., Graça, J., & Pereira, H.

Industrial Crops and Products, 31: 417-422

2010

Industrial Crops and Products 31 (2010) 417–422

Contents lists available at ScienceDirect

Industrial Crops and Products

journal homepage: www.elsevier.com/locate/indcrop

The chemical composition of cork and phloem in the rhytidome of *Quercus cerris* bark

Ali Şen[a], Isabel Miranda[b,*], Sara Santos[b], José Graça[b], Helena Pereira[b]

[a] Istanbul University, Faculty of Forestry, Dept. Forest Biology and Wood Protection Technology, 33473 Bahçeköy, Istanbul, Turkey
[b] Centro de Estudos Florestais, Instituto Superior de Agronomia, Universidade Técnica de Lisboa, Tapada da Ajuda, 1349-017 Lisboa, Portugal

ARTICLE INFO

Article history:
Received 7 December 2009
Received in revised form 7 January 2010
Accepted 11 January 2010

Keywords:
Quercus cerris
Cork
Phloem
Bark
Suberin
Chemical composition

ABSTRACT

Quercus cerris is an important oak species in Eastern Europe and Minor Asia that has a thick bark with a substantial content of cork tissues in its rhytidome. The chemical composition of the cork and of the interspersed phloemic tissues in the rhytidome of *Q. cerris* var. *cerris* from mature trees from Turkey was investigated in relation to summative composition, monomeric composition of suberin, non-polar extractives composition, elemental analysis and ash composition. *Q. cerris* cork has 2.6% ash, 16.7% extractives, 28.5% suberin (fatty monomers) and 28.1% lignin. The non-cellulosic monosaccharide composition shows the predominance of xylose (27.8% of total neutral sugars) with arabinose and galactose (11.5% and 7.9%). Suberin is composed mainly by long-chain ω-hydroxyacids representing 90% of all long-chain monomers and include α,ω-diacids (less than 8%), and small amounts of alkanoic acids in C16 and C18 and alkanols in C20, C22 and C24.

The phloemic tissues have a different composition with a high content of ash (13.0%) and a lignin–cellulose–hemicellulose cell wall composition. Separation of cork from phloem will therefore be a pre-requisite for use of *Q. cerris* cork.

1. Introduction

Tree barks are complex biomass components that have a large potential for utilization mostly based on their chemical composition.

In the outer bark, the periderm results from the activity of the phellogen, a secondary meristem that produces cork to the outside and phelloderm to the inside (Esau, 1977; Fahn, 1990). In most species, the phellogen has a short lifespan of a few years and is periodically renewed in internal regions of the phloem. This originates layers of successive periderms interspersed by phloemic tissues that constitute the so-called rhytidome of tree barks.

This structural organisation has been shown in many tree species, and in some the cork layers contained in the successive periderms are substantial and conspicuous to the naked eye, i.e. in *Pinus pinaster* (Nunes et al., 1996), *Betula pendula* (Ekman, 1983; Pinto et al., 2009), *Pseudotsuga menziesii* (Hergert and Kurth, 1952; Krahmer and Wellons, 1973; Litvay and Krahmer, 1977). This is also the case of *Quercus cerris* where successive periderms are seen in the outer bark with a clearly differentiated cork tissue, as described for the first time by Şen et al. (submitted for publication). *Quercus suber* makes up a special case with production of a very thick cork layer in a persistent periderm (Pereira, 2007).

Cork is a closed-cell material with a set of specific properties that result to a large extent from its chemical composition, i.e. very low permeability, hydrophobic behaviour, biological inertia, large elastic compression and dimensional recovery (Silva et al., 2005). Cork has been extensively studied in the cork oak (*Q. suber*), due to its economic importance for production of wine stoppers and insulation materials, and its structure, chemistry and properties have been recently reviewed in a reference book (Pereira, 2007).

Chemically cork is characterized by the presence of suberin as a major cell wall structural component. Its content varies with species, i.e. 40% in *Q. suber* (Pereira, 1988a), 33% in *P. menziesii* (Graça and Pereira, 2000b), 5% in *Calotropis procera* (Pereira, 1988b), 45% in *B. pendula* (Pinto et al., 2009).

Suberin is a macromolecule formed by the ester coupling of fatty alcohols, fatty acids and diacids, hydroxy fatty acids and glycerol, including also ferulic acid and eventually other phenolic components (Graça and Pereira, 1997, 1998, 2000a; Pereira, 2007). The monomeric composition of suberin is also species dependent as shown, i.e. for *Q. suber* (Graça and Pereira, 2000b), *P. menziesii* (Graça and Pereira, 1999), *B. pendula* (Holloway and Deas, 1973; Ekman, 1983; Gandini et al., 2006) or *Solanum tuberosum* (Graça and Pereira, 2000c). The cork cell wall further includes as structural

* Corresponding author.
E-mail addresses: umutsen@istanbul.edu.tr (A. Şen), Imiranda@isa.utl.pt (I. Miranda), helenapereira@reitoria.utl.pt (H. Pereira).

0926-6690/$ – see front matter © 2010 Elsevier B.V. All rights reserved.
doi:10.1016/j.indcrop.2010.01.002

components lignin and the polysaccharides cellulose and hemicelluloses, and a considerable amount of extractives (Pereira, 1988a; Conde et al., 1998). The soluble compounds that may be extracted from cork include mainly polar compounds, i.e. low molecular weight phenolics and tannins (Conde et al., 1997; Cadahía et al., 1998) as well as a lipophilic fraction contain waxes and triterpenes (Conde et al., 1999; Castola et al., 2002, 2005; Sousa et al., 2006).

There are relatively few chemical studies of tree bark periderms, namely of their cork tissues, which could constitute a basis for their use. This study aims to enlarge this knowledge by chemically analysing the cork fractions contained in the periderms of *Q. cerris* bark rhytidome. *Q. cerris* is an important oak species in Eastern Europe and Minor Asia that has a thick bark with a substantial content of cork tissues in its rhytidome, namely the var. *cerris* that includes large, albeit not continuous, regions of cork tissue, clearly visible to the naked eye. Since significant amounts of phloemic tissues are present between the cork layers, these were also chemically analysed. This study constitutes a basis for a possible utilization of *Q. cerris* bark, namely of its cork fraction, as a suggestion made a few decades ago (Mıhçıoğlu, 1942) but not followed by any research. Nothing was published so far on the cork from *Q. cerris* and this will be the first report on its chemical composition.

2. Materials and methods

2.1. Samples

Bark samples were collected from *Q. cerris* var. *cerris* mature trees with 70–80 years of age, in the South-eastern part of Turkey, in the Andırın Province of Kahramanmaraş. The cork and phloem portions were separated manually, ground in a Retsch SK hammer mill, sieved and the 40–60 mesh fractions were kept for analysis. The fractions were purified by suspending in water for a short time for further separation of the cork (floating layer) and phloem (sedimenting material). The resulting fractions were dried at 60 °C for 2 days before chemical analysis.

2.2. Chemical summative analyses

Chemical summative analyses included determination of ash, extractives, suberin, klason and acid-soluble lignin, and monomeric composition of polysaccharides.

Ash content was determined according to TAPPI Standard T 15 os-58 using 2.0 g of cork and phloem materials that were incinerated at 450–500 °C overnight and the residues weighted.

Extractives were determined by successive Soxtec extractions with dichloromethane, ethanol and water during 1.5 h with each solvent. The solvents were recovered and the extractives content determined from mass of residue after drying at 105 °C and reported as a percentage of original samples.

Suberin content was determined in extractive-free material by use of methanolysis for depolymerisation. A 1.5 g of extractive-free material was refluxed with 100 ml of a 3% methanolic solution of $NaOCH_3$ in CH_3OH during 3 h. The sample was filtrated and washed with methanol. The filtrate and the residue were refluxed with 100 ml CH_3OH for 15 min and filtrated again. The combined filtrates were acidified to pH 6 with 2 M H_2SO_4 and evaporated to dryness. The residues were suspended in 50 ml water and the alcoholysis products recovered with dichloromethane in three successive extractions, each with 50 ml dichloromethane. The combined extracts were dried over anhydrous sodium sulphate (Na_2SO_4), and the solvent was evaporated to dryness (Pereira, 1988a). Suberin extracts were quantified gravimetrically, and results were expressed in percent of cork dry weight. These include the fatty acid and fatty alcohol monomers of suberin.

Klason and acid-soluble lignin, and carbohydrates contents were determined on the extracted and desuberinised materials. Sulphuric acid (72%, 3.0 ml) was added to 0.35 g of extracted and desuberinised sample and the mixture was placed in a water bath at 30 °C for 1 h after which the sample was diluted to a concentration of 3% H_2SO_4 and hydrolysed for 1 h at 120 °C. The sample was vacuum filtered through a crucible and washed with boiling purified water. Acid-soluble lignin was determined on the combined filtrate by measuring the absorbance at 206 nm using a UV–vis spectrophotometer. Klason lignin was determined by the mass of residue after drying at 105 °C. Measurements were reported as a percentage of the original sample and klason lignin and acid-soluble lignin were combined to give the total lignin content.

The polysaccharides were calculated based on the amount of the neutral sugar monomers released by total hydrolysis, after derivatisation as alditol acetates and separation by gas chromatography with a method adapted from Tappi 249 cm. The hydrolysed carbohydrates were derivatized as alditol acetates and separated by GC (HP 5890A gas chromatograph) equipped with a FID detector, using helium as carrier gas (1 ml/min) and a fused silica capillary column S2330 (30 m × 0.32 mm ID; 0.20 μm film thickness). The column program temperature was 225–250 °C, with 5 °C/min heating gradient, and the temperature of injector and detector was 250 °C. For quantitative analysis the GC was calibrated with pure reference compounds and inositol was used as an internal standard in each run.

2.3. Composition of lipophilic extractives

Aliquots of the dichloromethane extracts (1–5 ml) were taken and filtered through Anatop 10 membranes (pore dimensions 0.2 μm, Merck). The filtrate was evaporated under N_2 flow and dried under vacuum at room temperature. The residues were dissolved in 250 μl of pyridine per mg of dry mass and the compounds containing hydroxyl and carboxyl groups were trimethylsilylated into trimethylsilyl (TMS) ethers and esters, respectively, by adding 250 μl of bis(trimethylsily)-trifluoroacetamide. The reaction mixture was heated at 60 °C for 30 min in an oven. The derivatized extracts were immediately analysed by GC–MS.

The derivatized solution was injected in a GC–MS (Agilent 5973 MSD) with the following GC conditions: DB5-MS column (60 m, 0.25 mm; ID, 0.25 μm film thickness), injector 320 °C, oven temperature program, 100 °C (5 min), rate of 8 °C/min up to 250 °C, rate of 2.5 °C/min up to 320 °C (20 min). The MS source was kept at 220 °C and the electron impact mass spectra (EIMS) taken at 70 eV of energy.

Compounds were identified as TMS derivatives by comparing their mass spectra with a GC–MS spectral library (Wiley, NIST), and by comparing their fragmentation profiles with published data (Eglinton and Hunneman, 1968; Kolattukudy and Agrawal, 1974). For semi-quantitative analysis, the area of peaks in the total ion chromatograms of the GC–MS analysis were integrated and their relative proportions expressed as percentage.

2.4. Suberin composition

Aliquots of methanolic cork extract and the respective organic phases (ca. 1 ml) were evaporated under N_2 flow and dried under vacuum at room temperature. The residue was dissolved in 250 μl of pyridine and components containing hydroxyl groups were trimethylsilylated into their trimethylsilyl (TMS) ethers with 250 μl bis-(trimethylsilyl)trifluoroacetamide) during 15 min in an oven at 60 °C. The methyl ester TMS ethers were immediately analysed by GC–MS to avoid degradation of the sample. The acidic monomers

Table 1
Summative chemical composition (% o.d. material) of the cork and phloem fractions of *Quercus cerris* var. *cerris* rhytidome.

	Cork	Phloem
Ash	2.6	13.0
Extractives		
Total	16.7	6.5
Dichloromethane	(10.9)	(1.7)
Ethanol	(3.4)	(3.6)
Water	(2.4)	(1.3)
Suberin[a]	28.5	5.5
Lignin		
Total	28.1	35.4
Klason lignin	(26.9)	(32.4)
Soluble lignin	(1.2)	(3.0)
Polysaccharides[b]	16.5	30.6

[a] Suberin only includes fatty acids and alcohols.
[b] Polysaccharides only include the neutral monosaccharides.

were analysed in the organic phase and glycerol in the methanolic extract.

The derivatized solution was injected in a GC–MS (Agilent 5973 MSD) with the following GC conditions: DB5-MS column (60 m, 0.25 mm; ID, 0.25 μm film thickness), injector 320 °C, oven temperature program, 100 °C (5 min), rate of 8 °C/min up to 250 °C, rate of 2.5 °C/min up to 320 °C (20 min). The MS source was kept at 220 °C and the electron impact mass spectra (EIMS) taken at 70 eV of energy.

A semi-quantitative analysis was made in the GC–MS chromatograms as described above for the dichloromethane extract. Identification of compounds was based on commercial mass spectra libraries (Wiley, NIST), by comparison with previously published data and interpretation of mass spectra.

2.5. Ash composition

Nitrogen was determined by the Kjeldahl method (Jackson, 1958) in a Tecator equipment (Herdon, VA, USA). After a hydrochloric digestion of the ash (Marti and Muñoz, 1957), phosphorus was determined by molecular absorption spectrometry in a Hitachi U-2000 VIS/UV equipment, and all the other minerals were determined by atomic absorption spectrophotometer in a Pye Unicam SP-9 apparatus (Cambridge, UK) equipped with a graphite furnace GF95.

3. Results and discussion

The thick rhytidome in the bark of *Q. cerris* var. *cerris* mature trees consists of two fractions, cork and phloem, as interspersed layers that result from the formation of successive periderms (Şen et al., submitted for publication). These periderms are very conspicuous due to their substantial amount of cork disposed as discontinuous layers around the stem. The cork and phloem tissues were fractionated in a first step manually and then, after grinding, by density using water as a floating medium. This methodology allowed separating cork, i.e. the floating layer only consisted of cork particles as controlled microscopically, but on the contrary the phloemic fraction still entrapped small regions of cork tissue.

3.1. Summative chemical composition

The summative chemical composition of the cork and phloemic fractions is shown in Table 1, and their carbohydrate composition in Table 2. There are considerable differences in the chemical composition of the cork and phloem samples of *Q. cerris* bark rhytidome, namely in terms of ash, extractives and suberin contents.

Table 2
Monosaccharide composition of the cork and phloem fractions in *Quercus cerris* var. *cerris* rhytidome, in % of total neutral monosaccharides detected by GC.

Monosaccharide	Cork	Phloem
Glucose	49.7	47.2
Mannose	2.4	1.3
Galactose	7.3	3.6
Rhamnose	1.2	1.0
Xylose	27.9	40.3
Arabinose	11.5	6.6

Cork has approximately 2.5 times more extractives than phloem (16.7% and 6.5%, respectively). This difference is mainly due to an accumulation in cork of dichloromethane soluble compounds that represented 65.3% of the total extractives (26.1% in phloem). The dichloromethane extractives content of *Q. cerris* cork (10.9%) is higher than in *Q. suber* cork, the later ranging from 3.6% (Sousa et al., 2006) to 7.9% (Pereira, 1988a). On the contrary, ethanol soluble extractives showed a relatively higher proportion in phloem (55.4% of the total extractives in phloem and 20.3% in cork) while the proportion of water soluble in the total extractives of phloem and cork was similar (14.4% and 20.0% of the total extractives, respectively).

The cork fraction of *Q. cerris* bark contained a considerable amount of suberin (28.5% of the material, representing 34.1% of extractive-free cork). This cork suberin content, measured as the organic phase of the methanolysates, is smaller than comparable determinations for *Q. suber* cork suberin, 33–40% (Pereira, 1988a; Pinto et al., 2009). The phloem samples contained a very small amount of suberin (5.5% of the material). The presence of suberin in the phloemic fractions shows that the full fractioning was not achieved and that a small proportion of cork tissues remained in the sample. A similar occurrence was found when analysing the phloemic tissue of the outer layer of reproduction cork of *Q. suber*, where a 4.3% suberin content was also found due to the incomplete separation of cork (Pereira, 1987).

The cork and phloem fractions showed similar lignification of the cell wall structural composition: lignin content was 37.8% of extractive-free phloem and 33.7% of extractive-free cork. A striking chemical difference between cork and phloem is related to their polysaccharide content, with phloem with approximately twice the content of cellulose and hemicelluloses, as an evidence of the lignocellulosic nature of the phloem and of the predominance of a lignosuberinic matrix in the cork cell walls.

The carbohydrate composition was similar in cork and phloem (Table 2). The major monosaccharide was glucose (49.7% of the total neutral monomeric sugars in cork and 47.2% in phloem) while xylose was the dominating non-cellulosic sugar, indicating the presence of xylans as the main hemicelluloses although in a higher proportion in phloem (27.8% and 40.3% of total neutral monosaccharides in cork and phloem, respectively). The arabinogalactan hemicellulosic family was more present in cork than in phloem (arabinose and galactose represented 18.8% and 10.2% of the total content of neutral sugars, respectively in cork and phloem).

There are few published references on the chemical composition of hardwood outer barks that separate cork and phloem, with the exception of *Q. suber* for which several studies have been made (as compiled in Pereira, 2007). The composition of *Q. cerris* cork is within the general range reported for cork of *Q. suber*, albeit with some differences. The content of extractives is similar to the 14–17% reported for *Q. suber* although the proportion of non-polar compounds extracted by dichloromethane is higher in *Q. cerris* cork extractives (42% of total extractives in *Q. suber*) (Pereira, 1988a). The suberin content is at the low limit of the range found for *Q. suber* (23–49%, Pereira, 2007) while lignin is slightly above the average values of 21–23% reported for *Q. suber* (Pereira, 1988a). The monosaccharide composition

Table 3
Suberin composition of cork and phloem fractions of *Quercus cerris* bark rhytidome, in % of the chromatographic peak areas of the compounds detected by GC–MS.

Chemical class and compounds	Cork	Phloem
Alkanols		
Eicosanol	0.4	
Docosanol	0.5	7.3
Tetracosanol	0.5	
Alkanoic acids		
Hexadecanoic acid	0.8	
Octadecanoic acid	1.0	
Saturated diacids		
Hexadecanedioic acid	0.7	
Unsaturated diacids		
Octadec-9-enedioic acid	1.4	3.6
Substituted diacids		
9,10-Dihydroxyoctadecanedioic acid	5.3	
Saturated ω-hydroxyacids		
16-Hydroxyhexadecanoic acid	0.8	
22-Hydroxydocosanoic acid	19.7	24.7
24-Hydroxytetracosanoic acid	1.8	
Unsaturated ω-hydroxyacids		
18-Hydroxyoctadec-9-enoic acid	10.8	28.0
Substituted ω-hydroxyacids		
9,10,18-Trihydroxyoctadecanoic acid	52.8	18.1
Ferulic acid	0.7	3.0
Unidentified	2.7	15.3
Total	100.0	100.0

of *Q. cerris* cork was very similar to that reported for *Q. suber* cork: glucose 41–51%, xylose 32–34%, arabinose 6–13%, galactose 4–5%, and mannose 3–4% and rhamnose 1–2% (Pereira, 1988a). This suggests that the main hemicelluloses in *Q. cerris* cork may be structurally of the type of 4-O-methylglucuronoxylans, arabino-4-O-methylglucuronoxylans and 4-O-methylglucurono-arabinogalactoglucoxylans, as determined for *Q. suber* cork by Asensio (1987a,b, 1988a,b). This is further confirmed by the non-cellulosic monomeric composition determined by Pinto et al. (2009) for the outer bark of *B. pendula* and *Q. suber* cork reporting the presence of 4-O-methylglucuronic acid and galacturonic acid.

3.2. Suberin composition

The results obtained for the composition of suberin, based in peak areas of the GC–MS ion chromatograms of the organic phases of the acidified methanolysates, are presented in Table 3. The suberin of *Q. cerris* cork is dominated by ω-hydroxyacids, that make up about 90% of all long-chain suberin monomers. The single most abundant compound is the *vic*-diol mid-chain substituted ω-hydroxyacid in C18: the 9,10,18-trihydroxyoctadecanoic acid represents 54% of all long-chain monomers. The saturated ω-hydroxyacid in C22 represented 20% of the integrated areas and the unsaturated ω-hydroxyacid 18-hydroxyoctadec-9-enoic acid 11%.

The α,ω-diacids account for less than 8%, corresponding mainly to the *vic*-diol substituted 9,10-dihydroxyoctadecanedioic acid with 5% of the long-chain monomers.

Alkanoic acids in C16 and C18 as well as alkanols in C20, C22 and C24 were present in small relative proportions.

Glycerol was found in significant quantities in the direct analysis of the methanolysates, but its relative proportion to the long-chain acid monomers was not quantified.

The suberin of *Q. cerris* cork has substantially more ω-hydroxyacids and less α,ω-diacids in comparison with the suberin of *Q. suber* cork where these chemical classes represent, respectively 36% and 62% of the long-chain monomers (Graça and Pereira, 2000b). Comparable relative quantities of alkanols and alkanoic acids were found for both suberins, as well as small quantities of ferulic acid. As regards chain length, C18 monomers are in majority followed by C22 monomers (74% and 20% of long-chain monomers, respectively). This is similar to *Q. suber* suberin where C18 and C22 compounds represent, respectively 71% and 10% of the long-chain monomers (Graça and Pereira, 2000b).

The suberin from the phloem samples showed a similar composition and seems to be, as discussed above, derived from the incomplete separation of the cork tissue.

Table 4
Composition of dichloromethane extracts of cork and phloem fractions of *Quercus cerris* bark rhytidome, in % of the chromatographic peak areas of the compounds detected by GC–MS.

Compound	Cork	Phloem
Sugar	2.6	–
Cyclic alkane	9.1	8.8
Alkane C20	–	2.6
Alkane C23	3.5	6.5
Alkane C24	5.2	9.3
Alkane C25	5.7	10.3
Alkane C26	4.8	9.1
Alkane C27	3.5	7.7
Alkane C28	3.1	4.4
Alkane C29	2.3	2.9
Azelaic acid	1.0	–
Hexadecanoic acid	12.6	11.3
Octadecanoic acid	18.5	22.2
Oleic acid	1.5	–
Hexadecanedioic acid	3.7	–
Octadec-9-enedioic acid	4.5	–
18-Hydroxyoctadec-9-enoic acid	2.8	–
9,10-Dihydroxyoctadecanedioic acid	1.4	–
9,10,18-Trihydroxyoctadecanoic acid	2.0	–
22-Hydroxydocosanoic acid	2.6	–
Eicosanol	0.9	–
Docosanol	2.5	–
Friedelin	6.2	4.9
Total	100.0	100.0

3.3. Lipophilic extractives

The results of the GC–MS analysis of the dichloromethane extracts are shown in Table 4. In cork, this extract included n-alkanes (29.1%), fatty acids (32.6%), other aliphatic acids identical to the suberin monomers (17%), fatty alcohols (3.4%) and friedelin (6.2%). The n-alkanes had chain-lengths of both odd and even carbon numbers, between C20 and C29. The fatty acids were mostly saturated, C16 (palmitic acid) and C18 (stearic acid) monoacids, together with a small quantity of the mono-unsaturated oleic acid. Many of the long-chain acid monomers found after suberin depolymerisation were also present as free acids in the dichloromethane extract.

The triterpene friedelin, detected here in a fair quantity in these non-polar extractives of *Q. cerris* bark cork, is also the main compound found in the corresponding dichloromethane extract of *Q. suber*, where it represents between 1% (Castola et al., 2002, 2005) and 2.3% of the cork (Sousa et al., 2006).

3.4. Ash composition

Ash content was 5 times higher in phloem than in cork (Table 1) as a result of their different physiological role in the tree. The presence of ash-forming elements is the result of biochemical processes, the mineral uptake from soil and the transport in the wood (xylem sap) and in the inner part of bark (phloem sap) where the elements are trapped in the cell wall or precipitate as inorganic salts (Kozlowski and Pallardy, 1996).

Table 5
Nitrogen contents and elemental constituents of ash in cork and phloem fractions of *Quercus cerris* bark rhytidome (Ca in %, all the other elements in mg/kg of o.d. material).

	Cork	Phloem
N, %	0.4	0.3
Ca, %	2.19	5.35
Mg, mg/kg	77.16	143.94
P, mg/kg	84.51	65.0
K, mg/kg	207.4	265.34
Na, mg/kg	116.4	151.48
Fe, mg/kg	36.17	35.36
Cu, mg/kg	11.57	6.56
Zn, mg/kg	4.82	6.57
Mn, mg/kg	95.01	118.18
Ni, mg/kg	<0.02	<0.02
Pb, mg/kg	0.90	1.41
Cr, mg/kg	2.32	2.37
Cd, mg/kg	0.08	0.009

Table 5 presents the ash composition of cork and phloem tissues of *Q. cerris* bark. The ashes of both cork and phloem are dominated by the presence of Ca which is considered to be immobile in the phloem sap, and therefore accumulates in the bark. Ca content was 2 times higher in phloem than in cork, the same occurring with Mg. The conspicuous presence of many crystals of calcium oxalate in the phloem of *Q. cerris* was shown by Şen et al. (submitted for publication). On the contrary, the easily translocated nutrients, e.g. K and Na, showed similar contents in phloem and in cork.

The ash content in *Q. cerris* cork is higher than the value reported for *Q. suber* cork (1% [Pereira, 1988a]) but its composition is overall similar to that reported for *Q. suber* cork, with values in the same of order of magnitude for the different elements with the exception of K (2.1×10^{-2}% in *Q. cerris* and 2.3×10^{-1}% in *Q. suber*) and Ca (2.2% and 0.6%, respectively) (Mata et al., 1986). The phloemic fractions in the rhytidome of *Q. suber* (the so-called back of cork planks) also show an increased content of mineral elements (Marques et al., 1986).

This aspect should be taken into account when considering *Q. cerris* bark processing given the wear that a high mineral content induces in the cutting equipment, as it is the case in the *Q. suber* cork industry (Pereira, 2007).

4. Conclusions

Cork in *Q. cerris* var. *cerris* bark was chemically characterized for the first time. It is similar to cork of *Q. suber*, with suberin as the main cell wall structural component, although showing some differences. The main differentiating features of *Q. cerris* cork are a high content of lignin that nears that of suberin, and a high content of extractives, with a predominant proportion of non-polar compounds.

The suberin of *Q. cerris* cork is composed mainly by ω-hydroxyacids, that make up about 90% of all long-chain monomers, with a *vic*-diol mid-chain substituted ω-hydroxyacid in C18 as the single most abundant compound representing 54% of long-chain monomers.

The cork fraction of *Q. cerris* is closely associated with phloem tissues in the rhytidome, and therefore extensive fractionation of these two tissues will be necessary when envisaging the use of *Q. cerris* cork. In fact the phloem fraction has a quite different chemical composition, with high ash content and has a lignin–polysaccharidic cell wall structure.

Acknowledgements

We thank the Laboratório de Química Agricola e Ambiental from Instituto Superior de Agronomia for the elemental and ash composition analysis, Joaquina Martins for her help in the chemical laboratory. The work was carried out with the base funding to Centro de Estudos Florestais given by Fundação para a Ciência e Tecnologia, Portugal, under the FEDER/POCI 2010 programme.

References

Asensio, A., 1987a. *Quercus suber* polysaccharides.1. Structural studies of the hemicellulose-A from the cork of *Quercus suber*. Carbohydr. Res. 161 (1), 167–170.
Asensio, A., 1987b. *Quercus suber* polysaccharides. 2. Structural studies of a hemicellulose-B fraction from the cork of *Quercus suber*. Carbohydr. Res. 165 (1), 134–138.
Asensio, A., 1988a. Polysaccharides from the Cork of *Quercus suber*, II. Hemicellulose. J. Nat. Prod. 51 (3), 488–491.
Asensio, A., 1988b. Structural studies of a hemicellulose B fraction (B-2) from the cork of *Quercus suber*. Can. J. Chem. 66 (3), 449–453.
Cadahía, E., Conde, E., Simón, B.F.S., Garcia-Vallejo, M.C., 1998. Changes in tannic composition of reproduction cork *Quercus suber* throughout industrial processing. J. Agric. Food Chem. 46, 2332–2336.
Castola, V., Marongiu, B., Bigelli, A., Floris, C., Lai, A., Casanova, J., 2002. Extractives of cork (*Quercus suber* L.): chemical composition of dichloromethane and supercritical CO_2 extracts. Ind. Crops Prod. 15, 15–22.
Castola, V., Bigelli, A., Rezzi, S., Melloni, J., Gladiali, S., Desjobert, J.M., Casanova, J., 2005. Composition and chemical variability of the triterpene fraction of dichloromethane extracts of cork (*Quercus suber* L.). Ind. Crops Prod. 21, 65–69.
Conde, E., Cadahía, E., García-Vallejo, M.C., de Simon, B.F., Adrados, J.R.G., 1997. Low molecular weight polyphenols in cork of *Quercus suber*. J. Agric. Food Chem. 45, 2695–2700.
Conde, E., Cadahía, E., Garcia-Vallejo, M.C., Adrados, J.R.G., 1998. Chemical characterization of reproduction cork from Spanish *Quercus suber*. J. Wood Chem. Technol. 18, 447–469.
Conde, E., García-Vallejo, M.C., Cadahía, E., 1999. Waxes composition of *Quercus suber* reproduction cork from different Spanish provenances. Wood Sci. Technol. 33, 270–283.
Eglinton, G., Hunneman, D., 1968. Gas chromatographic–mass spectrometric studies of long-chain hydroxy acids-I. Phytochemistry 7, 313–322.
Ekman, R., 1983. The suberin monomers and triterpenoids from the outer bark of *Betula verrucosa* Ehrh. Holzforschung 37 (4), 205–211.
Esau, K., 1977. Anatomy of Seed Plants, 2nd ed. Wiley, New York.
Fahn, A., 1990. Plant Anatomy, 4th ed. Pergamon Press, Oxford, UK.
Gandini, A., Neto, C.P., Silvestre, A.J.D., 2006. Suberin: a promising renewable resource for novel macromolecular materials. Prog. Polym. Sci. 31, 878–892.
Graça, J., Pereira, H., 1997. Cork suberin: a glyceryl based polyester. Holzforschung 51 (3), 225–234.
Graça, J., Pereira, H., 1998. Feruloyl esters of ω-hidroxyacids in cork suberin. Wood Sci. Technol. 18 (2), 207–217.
Graça, J., Pereira, H., 1999. Glyceryl-acyl and aryl-acyl dimers in *Pseudotsuga menziesii* bark suberin. Holzforschung 53 (4), 397–402.
Graça, J., Pereira, H., 2000a. Diglycerol alkanedioates in suberin: building units of a poly(acylglycerol) polyester. Biomacromolecules 1 (4), 519–522.
Graça, J., Pereira, H., 2000b. Methanolysis of bark suberins: analysis of glycerol and acid monomers. Phytochem. Anal. 11 (1), 45–51.
Graça, J., Pereira, H., 2000c. Suberin structure in potato periderm: glycerol, long-chain monomers and glyceryl and feruloyl dimers. J. Agric. Food Chem. 48 (11), 5476–5483.
Hergert, H., Kurth, E., 1952. The chemical nature of cork from Douglas fir bark. Tappi J. 35, 59–66.
Holloway, P.J., Deas, A.H.B., 1973. Epoxyoctadecanoic acids in plant cutins and suberins. Phytochemistry 12 (7), 1721–1735.
Jackson, M.L., 1958. Soil Chemical Analysis. Prentice-Hall, Inc., Madison, Wisconsin.
Kolattukudy, P., Agrawal, V., 1974. Structure and composition of aliphatic constituents of potato tuber skin (suberin). Lipids 9, 682–691.
Kozlowski, T.T., Pallardy, S.G., 1996. Physiology of Woody Plants, 2nd ed. Academic Press, San Diego, California.
Krahmer, R., Wellons, J., 1973. Some anatomical and chemical characteristics of Douglas-fir cork. Wood Sci. 6, 97–105.
Litvay, J., Krahmer, R., 1977. Wall layering in Douglas-fir cork cells. Wood Sci. 9, 167–173.
Marques, A.V., Mata, F., Pereira, H., 1986. Composição química mineral dos desperdícios de cortiça provenientes da indústria de granulados. Bol. Inst. Prod. Florestais, Cortiça. 576, 233–238.
Marti, F., Muñoz, J., 1957. Flame Photometry. Elsevier Publishing Company, London.
Mata, F., Marques, A.V., Pereira, H., 1986. Influência da granulometria na determinação de elementos minerais na cortiça. Bol. Inst. Prod. Florestais, Cortiça. 569, 68–72.
Mıhçıoğlu, K., 1942. Türkiye'de Saçlı Meşeden Mantar İstihsaline Dair Bir Araştırma. Orman ve Av. 1, 151–166 (in Turkish).

Nunes, E., Quilhó, T., Pereira, H., 1996. Anatomy and chemical composition of *Pinus pinaster* bark. IAWA J. 17 (2), 141–149.
Pereira, H., 1987. Composição química da raspa em pranchas de cortiça de reprodução amadia. Bol. Inst. Prod. Florestais, Cortiça. 587, 231–233.
Pereira, H., 1988a. Chemical composition and variability of cork form *Quercus suber* L. Wood Sci. Technol. 22 (3), 211–218.
Pereira, H., 1988b. Structure and chemical composition of cork from *Calotropis procera* (Ait.) R. Br. IAWA Bull. 9 (1), 53–58.
Pereira, H., 2007. Cork: Biology, Production and Uses. Elsevier Publications, Amsterdam.
Pinto, P.C.R.O., Sousa, A.F., Silvestre, A.J.D., Neto, C.P., Gandini, A., Eckerman, C., Holmbom, B., 2009. *Quercus suber* and *Betula pendula* outer barks as renewable sources of oleochemicals: a comparative study. Ind. Crops Prod. 29, 126–132.
Şen, A., Quilhó, T., Ramazan, K., Pereira, H., submitted for publication. Anatomical characterization of the bark of *Quercus cerris* var. *cerris*. Ann. For. Sci.
Silva, S.P., Sabino, M.A., Fernandes, E.M., Correlo, V.M., Boesel, L.F., Reis, R.L., 2005. Cork: properties, capabilities and applications. Int. Mater. Rev. 50 (6), 345–365.
Sousa, A.F., Pinto, C.R., Silvestre, A.J., Neto, C.P., 2006. Triterpenic and other lipophilic components from industrial cork products. J. Agric. Food Chem. 54, 6888–6893.

3.2.4. Temperature-induced structural and chemical changes in cork from *Quercus cerris*

Şen, A., Miranda, I., & Pereira, H.

Industrial Crops and Products, 37: 508-513 2012.

Industrial Crops and Products 37 (2012) 508–513

Contents lists available at ScienceDirect

Industrial Crops and Products

journal homepage: www.elsevier.com/locate/indcrop

Temperature-induced structural and chemical changes in cork from *Quercus cerris*

Ali Şen, Isabel Miranda, Helena Pereira*

Centro de Estudos Florestais, Instituto Superior de Agronomia, Universidade Técnica de Lisboa, Tapada da Ajuda, 1349-017 Lisboa, Portugal

ARTICLE INFO

Article history:
Received 8 June 2011
Received in revised form 15 July 2011
Accepted 23 July 2011
Available online 15 August 2011

Keywords:
Quercus cerris
Cork
Temperature
Cellular structure
Suberin

ABSTRACT

The effects of temperature on anatomical and chemical characteristics of *Quercus cerris* cork were examined. Cork samples were subjected to isothermal air heating between 150 °C and 400 °C and analyzed for mass loss, cellular structure and chemical composition.

The thermal decomposition of *Q. cerris* cork is similar to that of *Q. suber* cork. Cork is thermally stable below 200 °C and after that degradation depended on temperature and heating time with increasing mass loss, i.e. 3% at 200 °C 10 min and 46% at 350 °C 60 min. With temperature and starting at 200 °C, cells expanded, cell wall thickness was reduced and corrugations were lost.

Extractives degraded at lower temperatures, although aliphatic extractives were found to be more stable. Suberin from *Q. cerris* was more heat resistant than *Q. suber* suberin, while lignin showed similar resistance.

These results provide a basis for studies on the production of *Q. cerris* bark expanded cork agglomerates for insulation purposes.

1. Introduction

Cork is a cellular material of biological origin contained in tree barks that has been used as an heat insulator since early antiquity. In plant anatomy cork is also named phellem. Its remarkable insulation properties arise from the anatomical and chemical characteristics of the cork cells: the small, non-communicating (at micrometer or higher levels) and air filled cells give cork a low density of about 0.14–0.17 g cm^{-3} and a low heat transfer coefficient of approximately 0.040–0.045 W/mK (Pereira, 2007).

Today, most cork used for thermal insulation, i.e. by the construction industry, is in the form of expanded cork agglomerates. These are cork-only materials, composed by cork granules that are thermally self-bonded without addition of synthetic adhesives at temperatures of about 300–350 °C (Pereira and Ferreira, 1989). The thermal properties of expanded cork agglomerates are comparable with those of synthetic commercial foams but with significant advantages regarding durability and thermal stability.

Cork is also used in composites as adhesive-bonded agglomerates, that are applied for flooring and surfacing, and in special combinations, i.e. with fire proof minerals to reinforce its properties for harsher temperature conditions such as in ablative insulators for space vehicles.

In either case, the thermal behaviour of cork is an important aspect. Temperature-induced structural and chemical changes occur that may affect the material's properties and its behaviour in use. Upon heating the cork cells expand and cell wall thickness decrease (Rosa and Pereira, 1994). Mass loss is relatively small until 200 °C but increases with temperature and exposure time until complete carbonization at approximately 450 °C (Pereira, 1992). The cell wall components have different thermal stabilities, with lignin and suberin being the most resistant while extractives and hemicelluloses are more heat sensitive (Bento et al., 1992; Pereira, 1992).

All the studies made until now on the thermal behaviour of cork have used cork from the cork oak (*Quercus suber*) which is the only cork material that is produced and processed commercially at significant scale (Pereira, 2007). However other tree species contain cork in their barks and may therefore be envisaged as potential producers of this type of raw material.

This is the case of the Turkish oak (*Quercus cerris*), an important tree species in Eastern Europe and Minor Asia, that has a substantial content of cork tissues in its thick bark, especially the var. *cerris* that includes large, albeit not continuous, regions of cork that are clearly visible to the naked eye (Şen et al., 2010).

Recent studies on *Q. cerris* cork have shown that its chemical and anatomical properties are close to those of *Q. suber* cork (Şen et al., 2010, 2011a). This triggered the interest to use *Q. cerris* cork as an insulating material, as suggested already a few decades ago (Telgeren, 1976), but no further development occurred and the bark of *Q. cerris* is still left unused.

* Corresponding author. Tel.: +351 21 881 19 00; fax: +351 21 881 19 94.
E-mail address: helena.pereira@reitoria.utl.pt (H. Pereira).

0926-6690/$ – see front matter © 2011 Elsevier B.V. All rights reserved.
doi:10.1016/j.indcrop.2011.07.028

In this study, the effects of temperature on the chemical and structural properties of *Q. cerris* cork were examined. Mass loss and the change in chemical composition and cellular structure were followed for different treatment times in the temperature range of 150–400 °C using granulated cork material obtained by grinding and fractioning of *Q. cerris* bark. The aim is to obtain the information basis for the potential production of expanded cork agglomerates for insulation purposes using *Q. cerris* barks as the cork raw-material source.

2. Materials and methods

2.1. Samples

Bark samples were collected from *Q. cerris* var. *cerris* mature trees with 70–80 years of age, in the Andırın district of Kahramanmaraş, located in the south-eastern part of Turkey. The samples were dried in the open air and stored at room temperature prior to granulation with an industry-type hammer mill (screen dimensions: 3 mm × 25 mm).

The granulated samples were sieved with a Retsch Analytical Sieve Shaker AS 200. The granulometric fraction above 2 mm was taken and purified by suspending in water for a short time for separation of the cork granules (floating layer) from the phloem (sedimenting material).

This material was dried at 60 °C for 3 days prior to a further visual inspection that was made to separate manually any apparent residual phloem particles from the cork sample. The resulting cork fraction was used in the subsequent heat treatments.

2.2. Heating treatment

Isothermal treatment in air in a temperature controlled furnace was made using 2 g samples at temperatures from 150 °C to 400 °C, and with treatment times from 5 to 90 min. Mass loss was determined gravimetrically after each treatment. Six replicated samples were separately tested for each set of experimental conditions. The mass loss repeatability of treatments was on average 0.85.

2.3. Chemical summative analyses

The heat-treated cork samples and one untreated control sample were ground and sieved to separate the 40–60 mesh size fractions that were used in chemical analyses. Chemical summative composition included determination of extractives, suberin, klason and acid soluble lignin.

Extractives were determined by successive Soxtec extractions of 2 g samples with dichloromethane, ethanol and water during 1.5 h with each solvent. The solvents were recovered and the extractives content determined from mass of residue after drying at 105 °C and reported in percent of original samples. Duplicate determinations were made in all cases and the results are the mean value.

Suberin content was determined in extractive-free material by use of methanolysis for depolymerization. A 1.5 g aliquot of extractive-free material was refluxed with 100 ml of a 3% methanolic solution of $NaOCH_3$ in CH_3OH during 3 h. The sample was filtrated and washed with methanol. The filtrate and the residue were refluxed with 100 ml CH_3OH for 15 min and filtrated again. The combined filtrates were acidified to pH 6 with 2 M H_2SO_4 and evaporated to dryness. The residues were suspended in 50 ml water and the alcoholysis products recovered with dichloromethane in three successive extractions, each with 50 ml dichloromethane. The combined extracts were dried over anhydrous sodium sulphate (Na_2SO_4), and the solvent was evaporated to dryness (Pereira, 1988). Suberin extracts were quantified gravimetrically, and results were expressed in percent of cork dry weight. These include the fatty acid and fatty alcohol monomers of suberin.

Table 1
Chemical composition (in % of sample dry mass) of cork of *Quercus cerris* after 10 min treatments at different temperatures and their corresponding mass loss (in % of untreated material, mean and standard deviation).

	Untreated	250 °C	300 °C	350 °C
Mass loss	–	13.4 ± 2.2	26.2 ± 3.2	47.9 ± 3.0
Extractives				
Total	7.01	4.98	3.84	2.54
Dichloromethane	2.50	3.08	2.82	1.82
Ethanol	3.48	1.69	0.86	0.52
Water	1.03	0.21	0.16	0.20
Suberin	11.84	19.36	22.63	11.39
Lignin				
Total	32.34	51.96	70.51	80.28
Klason	29.44	49.71	69.01	78.61
Acid soluble	2.90	2.25	1.50	1.66

Klason lignin and acid soluble lignin, and carbohydrate contents were determined on the extracted and desuberinised materials. Sulphuric acid (72%, 3.0 ml) was added to 0.35 g of an extracted and desuberinised sample, and the mixture was placed in a water bath at 30 °C for 1 h after which the sample was diluted to a concentration of 3% H_2SO_4 and hydrolysed for 1 h at 120 °C. The sample was vacuum-filtered through a crucible and washed with boiling purified water. Acid soluble lignin was determined on the combined filtrate by measuring the absorbance at 206 nm using a UV/VIS spectrophotometer. Klason lignin was determined by the mass of residue after drying at 105 °C. Measurements were reported in percent of the original sample and Klason lignin and acid soluble lignin were combined to give the total lignin content.

2.4. SEM observations

Cork granules of the heat treated samples were separated and cut with a sharp knife to obtain a plain surface. The samples were vacuum-dried and gold was vapour-sprayed making up an approximately 450 A thick coating. The surfaces were observed in an electron scanning microscope Hitachi S-2400 at magnifications ranging from 50 to 1000×, and the images were recorded in digital format. The cell measurements were made on the images using image analysis software (Leica Qwin Plus) by measuring the radial total width and the lumen width in the radial and tangential directions in early cork and late cork cells. Cell wall thickness was calculated by difference of cell width and lumen width. A total of 120 cells was measured in each sample.

3. Results and discussion

The cork material that was fractionated from the bulk granulates of *Q. cerris* bark, showed a summative chemical composition (Table 1) that can be compared to the composition of "pure" cork and phloem tissues separated previously from *Q. cerris* bark (Şen et al., 2010). The results show that the obtained crude cork granulate is not fully made up of cork tissue and still contains a substantial proportion of phloemic material. This can be seen in the differences in the content in extractives and suberin which were lower than those of pure cork, i.e. suberin content in the granulate was 11.8% (Table 1) and in pure cork is 28.5%.

Although this was not the aim of this work, the result of this fractionation process confirms that it will be feasible from a practical point of view to separate a cork-enriched fraction from the other bark components after the grinding of *Q. cerris* whole bark using air or water fractionation. In fact any industrial use of the *Q. cerris* cork has to pass through a bulk grinding of the bark and

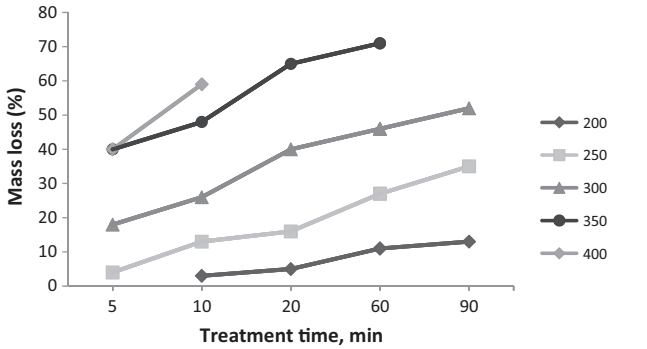

Fig. 1. Variation of mass loss of cork granules from *Quercus cerris* upon air heating at different temperatures and treatment times.

its fractioning. However further developments on the fractionating procedure might improve the purity of the cork fraction.

3.1. Mass loss

Fig. 1 summarizes the results for the mass loss for the temperature range 200–400 °C. At 150 °C mass loss was negligible representing only 3% after 90 min treatment. At 200 °C the effect was also small for short treatments, e.g. 3% mass loss occurred after 10 min, but became significant with longer treatment times e.g. 11% and 13% mass loss were recorded after 60 and 90 min respectively. At higher temperatures mass loss occurred for shorter treatment times. For instance, at 250 °C 13% mass loss occurred after 10 min, while at 300 °C and 350 °C, after 5 min, mass losses of 18% and 40% were already recorded.

With increasing temperature, the mass loss became larger. Approximately 50% of mass loss occurred after 90 min at 300 °C and after 10 min at 350 °C. At 350 °C the mass loss was rapid and attained very large values, e.g. 65% in 20 min and 71% in 60 min of treatment. At 400 °C, already 59% of the cork mass was lost during the first 10 min of treatment.

The thermal degradation of *Q. cerris* cork showed a similar decomposition pattern to that of *Q. suber* cork, where the extent of degradation depended on the temperature and time of exposure (Pereira, 1992). During the process, and in an extent determined by the conditions, it was found that the cells underwent expansion and cell walls became thinner as a result of the chemical degradation of cell wall components and overall mass loss.The mass loss values due to the thermal degradation by volatilization of *Q. cerris* cork were found to be in agreement with those reported for *Q. suber* cork (Pereira, 1992; Rosa and Fortes, 1988). The cork is thermally stable below 200 °C and loss of material starts at this temperature and increases with time of exposure to temperature. The rate of mass loss increased significantly with temperature (Fig. 1).

3.2. Structural changes

In the mildest conditions of heating, corresponding to small mass losses, the structural features of the cork tissue were maintained. For instance, at 200 °C for short treatment times with mass loss of about 3% no differences were observed between untreated and heat treated cork samples. The radial structural arrangement was maintained; the cork cells preserved their dimensions and showed corrugations of cell walls (Fig. 2).

With increasing treatment time and temperature, and along with increased mass loss, clear effects were observed on the cellular organization and cell dimensions (Figs. 3–7).

Upon heating, the cork cells expanded (Fig. 3). The effect was first noticed in the increased dimensions in the radial direction, together with straightening of cell walls and disappearance of corrugations.

Cells enlarged in the radial direction in conjunction with mass loss, i.e. for samples treated 10 min at 200 °C and 350 °C, the radial dimensions in earlycork were respectively 26.2 μm and 37.6 μm, and in latecork 11.6 μm and 21.3 μm respectively (Fig. 4). The tangential cell width remained relatively constant until 60 min treatment at 300 °C but enlarged for harsher conditions.

As a result of the heavy cell enlargement, the cells appear inflated and with stretched cell walls and the overall structure lost somewhat its clear radial alignment of cell rows in the radial and transverse sections which became more similar to the typical honeycomb arrangement of the tangential section. Fig. 5 shows fully expanded cells in a sample where the cell volume was increased approximately by a factor of 2 corresponding to a sample heat treated 10 min at 350 °C.

Physical damage of the cell walls started at approximately 40% mass loss e.g. 300 °C and 60 min, and increased at higher temperatures and for longer treatment times. The cell walls were torn and cracks were formed (Fig. 8).

The loss of material resulted into a significant reduction of the cell wall thickness (Fig. 6). *Q. cerris* cork cells have a wall thickness of 2.5 μm in the earlycork region (Şen et al., 2011b) that was reduced steadily with increasing intensity of the thermal treatment starting at 1.7 μm for 3% mass loss and reaching 0.6 μm for about 50% mass loss.

In latecork cell wall thickness was approximately 1.9 μm until 10% mass loss and decreased subsequently to 1.2 μm (Fig. 7). The temperature-induced effect of cell wall stretching due to expansion of cell volume also contributed to the decrease of cell wall thickness, as seen in Fig. 5.

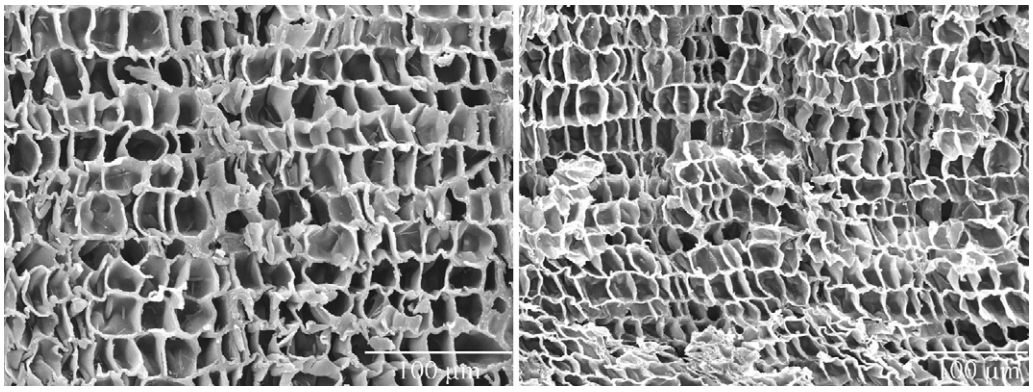

Fig. 2. SEM photographs of the transverse section of untreated *Q. cerris* cork (left) and of heat treated sample during 10 min at 200 °C (right) showing similar radial arrangement of cell rows and cell corrugations.

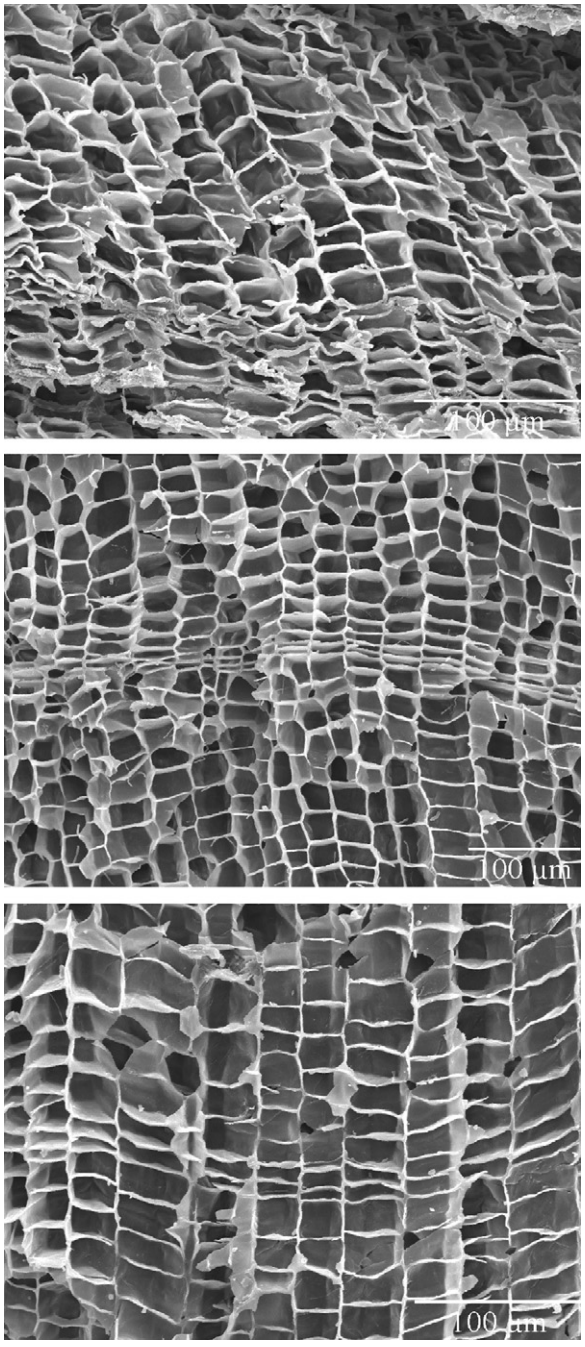

Fig. 3. SEM photographs of the transverse section of *Q. cerris* cork samples that were heat treated during 60 min at 200 °C (top), 250 °C (middle) and 300 °C (bottom) showing the progressive expansion of cell dimensions and the disappearance of cell corrugations.

The SEM observations showed clearly that the cellular structure of cork was altered with the heat treatment, although only for exposures above 10 min at 200 °C (Figs. 2 and 3). The cells expanded, the cell walls straightened loosing the corrugations that were found in the original cork as described by Şen et al. (2011b).

The same effect was observed for the cork of *Q. suber* for which prior studies showed also a cell volume expansion leading to smaller densities in heat-treated cork especially in the cases of cork with many corrugations such as virgin cork in comparison with reproduction cork (Pereira, 1992; Pereira and Ferreira, 1989; Rosa and Fortes, 1988). In *Q. cerris* cork the highest cell

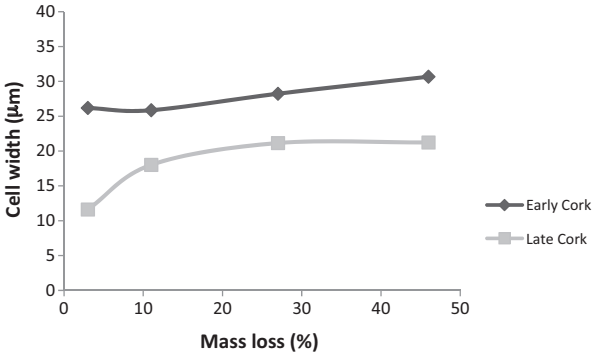

Fig. 4. Variation of cell dimensions width in the radial direction in earlycork and latecork of *Q. cerris* cork with mass loss during heat treatment.

expansion occurred at 350 °C while it occurred at 300 °C in *Q. suber* cork (Pereira, 1992).

3.3. Thermochemical degradation

The summative chemical composition of the heat treated cork samples is summarized in Tables 1–3.

Extractives were the most heat sensible compounds. Starting at 7.0% in untreated cork, extractives were rapidly lost with heating and represented only 0.7% in the sample treated 60 min at 350 °C. Approximately 50% of the extractives were lost in the first 60 min of treatment at 200 °C (Table 2). In relation to the different types of extractives, some difference in degradation rate was found: the non-polar extractives soluble in dichloromethane were comparatively more heat stable than the more polar compounds, as can be seen by the composition of samples treated at 200 °C (Table 2). The explanation may derive from their chemical composition because they are aliphatic extractives composed of *n*-alkanes, fatty acids identical to suberin monomers, fatty alcohols and friedelin and the fact that extractives also include heat sensitive carbohydrates in addition to phenolics (Şen et al., 2010).

Suberin was relatively resistant to thermal degradation until 250 °C, and therefore the heat treated samples showed a higher suberin content than the untreated sample (Table 1). Suberin content only decreased for the 350 °C treated samples, to which corresponded over 50% mass loss (Table 1). For instance the untreated sample contained 11.8% of suberin, while a heat treated sample 60 min at 250 °C contained 22.4% suberin. The results are in agreement with the findings obtained for *Q. suber* cork although in this case suberin content decreased already after 200 °C. Another

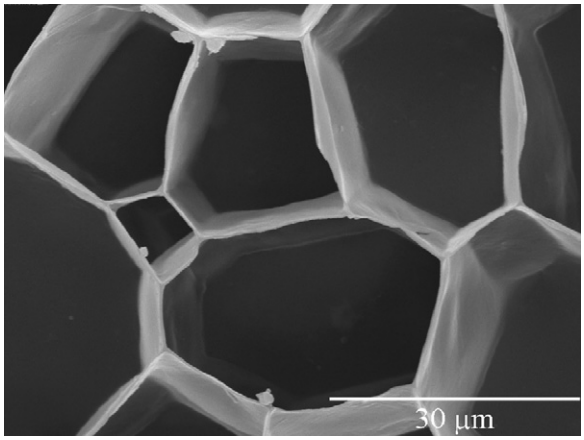

Fig. 5. Expanded cork cells of *Q. cerris*, as observed in the tangential section, after 10 min at 350 °C.

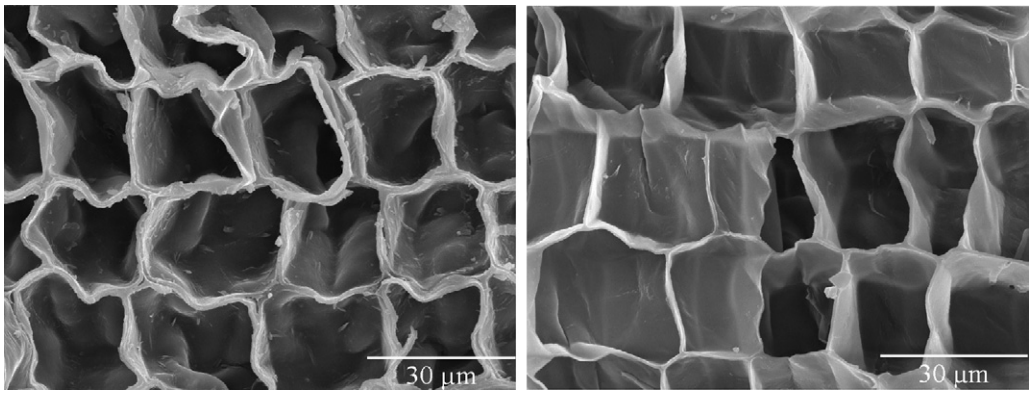

Fig. 6. Comparison of cell wall thickness of heat treated *Q. cerris* cork samples 10 min at 200 °C (left) and 60 min at 300 °C (right).

interesting difference of *Q. cerris* cork is that at 300 °C and higher temperatures, more suberin remained in the samples than in *Q. suber* cork: at 300 °C, 6.7% and 14.2%, and at 350 °C 1.1% and 2.8% for *Q. suber* and *Q. cerris* cork respectively (Pereira, 1992). This may be the result of differences in the monomeric composition of suberin of both corks: *Q. cerris* cork suberin was found to be composed mainly of ω-hydroxyacids and, contrary to *Q. suber* cork, the α–ω diacids content was found to be much smaller (Pereira, 2007; Şen et al., 2010).

Lignin content increased with temperature in all the heat treated samples and was the most heat resistant component, especially the acid insoluble lignin (Table 3). In the heat treated samples with large thermal degradation, the acid insoluble material determined as lignin was by far the dominant component e.g. 85% in the sample treated 60 min at 350 °C (Table 2).

Lignin content is slightly higher in *Q. cerris* cork (28%) as compared to *Q. suber* cork (21–23%) (Pereira, 1988). In the present study lignin content was found to be higher (32%), because of the phloemic inclusions. Lignin content increased with temperature: at 250 °C lignin content reached two times the value of untreated samples and at 300 °C and 350 °C lignin represented 80–85% of the sample. The results are in agreement with those obtained with *Q. suber* cork (Pereira, 1992). These high values of lignin should be taken with care since they do not represent lignin with its original chemical composition structure but rather a transformed lignin that underwent heat-induced chemical alteration. Lignin in *Q. suber* cork was found to be decomposed at temperatures of approximately 250–350 °C (Neto et al., 1995). The lignin determined after heating treatments should therefore be regarded as a transformed lignin (Pereira, 1992).

Table 2
Chemical composition (in % of sample dry mass) of cork of *Q. cerris* after 60 min treatment at different temperatures, and their corresponding mass loss (in % of untreated material, mean and standard deviation).

	Untreated	200 °C	250 °C	300 °C	350 °C
Mass loss	–	11.2 ± 0.9	26.5 ± 5.0	46.0 ± 2.0	71.1 ± 5.9
Extractives					
Total	7.01	3.64	2.21	1.80	0.70
Dichloromethane	2.50	1.48	1.41	1.19	0.36
Ethanol	3.48	1.47	0.60	0.34	0.17
Water	1.03	0.69	0.20	0.26	0.17
Suberin	11.84	16.50	22.43	14.22	2.80
Lignin					
Total	32.34	51.75	75.74	86.41	86.28
Klason	29.44	48.91	74.11	84.98	84.84
Acid soluble	2.90	2.84	1.63	1.44	1.44

Table 3
Chemical composition (in % of sample dry mass) of cork of *Q. cerris* after treatment with different times at 200 °C, and their corresponding mass loss (in % of untreated material, mean and standard deviation).

	Untreated	10 min	60 min	90 min
Mass loss	–	3.5 ± 0.8	11.2 ± 0.9	13.2 ± 3.6
Extractives				
Total	7.01	6.63	3.64	2.67
Dichloromethane	2.50	2.77	1.48	1.10
Ethanol	3.48	2.41	1.47	1.04
Water	1.03	1.45	0.69	0.53
Suberin	11.84	12.60	16.50	14.35
Lignin				
Total	32.34	33.10	51.75	54.46
Klason	29.44	30.27	48.91	51.90
Acid soluble	2.90	2.83	2.84	2.57

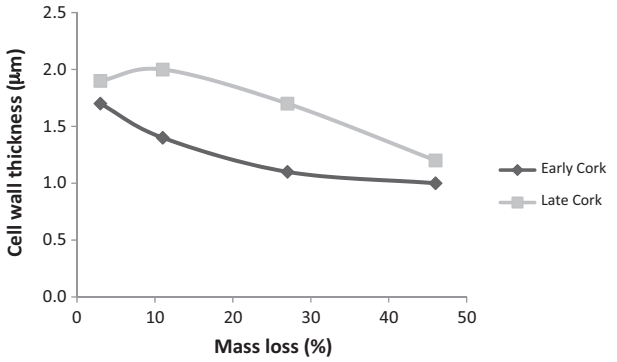

Fig. 7. Variation of cell wall thickness in earlycork and latecork of *Q. cerris* with mass loss during heat treatments.

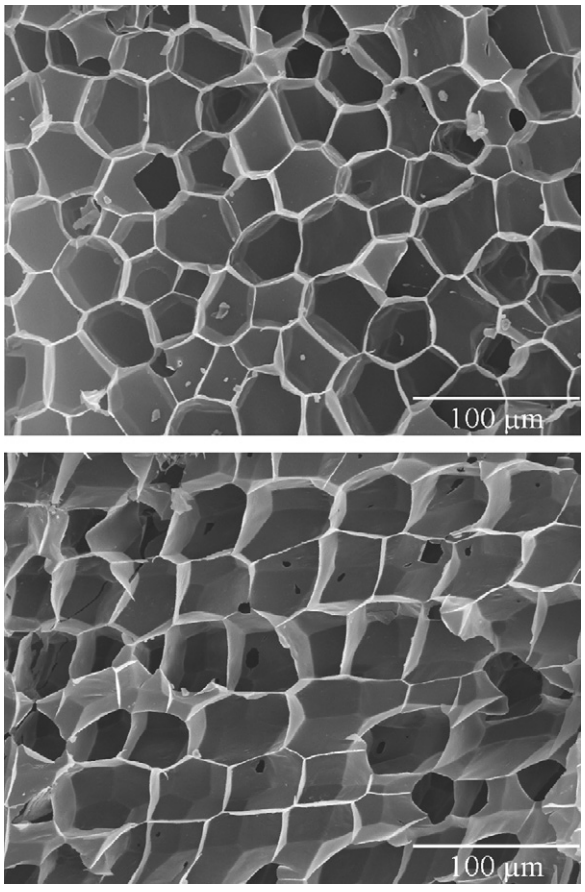

Fig. 8. Formation of cell wall rupture and cracks in the cork of *Q. cerris* as seen in the tangential section (above) and in the radial section (bottom) after 10 min at 350 °C.

Overall the results showed that cork from *Q. cerris* behaves upon heating in a way similar to the cork of *Q. suber* with cellular expansion and density decrease, and chemical changes that enhance lignin and suberin contents. Therefore this opens the possibility of using *Q. cerris* cork as a raw-material for the production of insulation agglomerates, using an autoclave thermal treatment where self-expansion and adhesion of the cork granules will result into an agglomerate, as it is done for the production of the expanded insulation agglomerates of *Q. suber* cork (Pereira and Ferreira, 1989). Improving the enrichment in cork of the granulate will increase process yields and quality of the agglomerate since the phloemic content affects adversely the self agglomeration process as shown for *Q. suber* cork (Pereira and Baptista, 1993).

4. Conclusions

The cork of *Q. cerris* showed similar temperature-induced alterations as the cork of *Q. suber*. Exposure to temperature induces thermal degradation with mass loss and chemical alteration of the cell wall with suberin and lignin as the more stable components. The structural effects included cell expansion and cell wall thickness reduction.

The higher suberin content in elevated temperatures in *Q. cerris* cork is a promising feature for its potential higher temperature stability.

Acknowledgements

We thank Joaquina Martins for her help in the chemical laboratory. The work was carried out with the base funding to Centro de Estudos Florestais given by Fundação para a Ciência e Tecnologia, Portugal, under the FEDER/POCI 2010 programme.

References

Bento, M.F., Cunha, M.A., Moutinho, A.M.C., Pereira, H., Fortes, M.A., 1992. A mass spectrometry study of thermal dissociation of cork. Int. J. Mass Spectrom. Ion Process. 112 (2–3), 191–204.

Neto, C.P., Rocha, J., Gil, A., Cordeiro, N., Esculcas, A.P., Rocha, S., Delgadillo, I., de Jesus, J.D., Correia, A.J., 1995. ^{13}C solid-state nuclear magnetic resonance and Fourier transform infrared studies of the thermal decomposition of cork. Solid State NMR 4, 143–151.

Pereira, H., 1988. Chemical composition and variability of cork form *Quercus suber* L. Wood Sci. Technol. 22 (3), 211–218.

Pereira, H., 1992. The thermochemical degradation of cork. Wood Sci. Technol. 26, 259–269.

Pereira, H., 2007. Cork: Biology Production and Uses. Elsevier Publications, Amsterdam.

Pereira, H., Baptista, C., 1993. Influence of raw material quality and process parameters in the production of insulation cork agglomerates. Holz. Roh.-Werkst. 51 (5), 301–308.

Pereira, H., Ferreira, E., 1989. Scanning electron-microscopy observations of insulation cork agglomerates. Mater. Sci. Eng. A 111, 217–225.

Rosa, M.E., Fortes, M.A., 1988. Temperature induced alterations of the structure and mechanical properties of cork. Mater. Sci. Eng. 100, 69–78.

Rosa, M.E., Pereira, H., 1994. The effect of long-term treatment at 100 °C–150 °C on structure, chemical composition and compression behavior of cork. Holzforschung 48, 226–232.

Şen, A., Miranda, I., Santos, S., Graça, J., Pereira, H., 2010. The chemical composition of cork and phloem in the rhytidome of *Quercus cerris* bark. Ind. Crops Prod. 31, 417–422.

Şen, A., Quilhó, T., Pereira, H., 2011a. Bark anatomy of *Quercus cerris* L. var. *cerris* from Turkey. Turk. J. Bot. 35, 45–55.

Şen, A., Quilhó, T., Pereira, H., 2011b. The cellular structure of cork from *Quercus cerris* var. *cerris* bark in a materials' perspective. Ind. Crops Prod. 34, 929–936.

Telgeren, G., 1976. Memleketimizde yetişen saçlı meşe ağaçlarının kabuklarından yararlanma olanakları. Orman. Araştırma Enstitüsü Derg. 22 (2), 114–127 (in Turkish).

3.2.5. Study of thermochemical treatments of cork in the 150-400°C range using colour analysis and FTIR spectroscopy

Şen, A., Velez Marques A., Gominho J.,& Pereira, H.

Industrial Crops and Products, 38: 132-138
2012

Industrial Crops and Products 38 (2012) 132–138

Contents lists available at SciVerse ScienceDirect

Industrial Crops and Products

journal homepage: www.elsevier.com/locate/indcrop

Study of thermochemical treatments of cork in the 150–400 °C range using colour analysis and FTIR spectroscopy

Ali Şen [a], António Velez Marques [b], Jorge Gominho [a], Helena Pereira [a,*]

[a] Centro de Estudos Florestais, Instituto Superior de Agronomia, Universidade Técnica de Lisboa, Tapada da Ajuda, 1349-017 Lisboa, Portugal
[b] Centro de Investigação em Engenharia Química e Biotecnologia, Instituto Superior de Engenharia de Lisboa, 1959-007 Lisboa, Portugal

ARTICLE INFO

Article history:
Received 20 October 2011
Received in revised form 8 January 2012
Accepted 21 January 2012

Keywords:
Quercus cerris
Cork
Heat treatment
Colour analysis
FTIR

ABSTRACT

A study of chemical transformations of cork during heat treatments was made using colour variation and FTIR analysis. The cork enriched fractions from *Quercus cerris* bark were subjected to isothermal heating in the temperature range 150–400 °C and treatment time from 5 to 90 min. Mass loss ranged from 3% (90 min at 150 °C) to 71% (60 min at 350 °C). FTIR showed that hemicelluloses were thermally degraded first while suberin remained as the most heat resistant component.

The change of CIE-Lab parameters was rapid for low intensity treatments where no significant mass loss occurred (at 150 °C L^* decreased from the initial 51.5 to 37.3 after 20 min). The decrease in all colour parameters continued with temperature until they remained substantially constant with over 40% mass loss. Modelling of the thermally induced mass loss could be made using colour analysis. This is applicable to monitoring the production of heat expanded insulation agglomerates.

1. Introduction

Cork is a renewable raw material finding many application areas because of its unique set of properties (Pereira, 2007). At present cork is obtained commercially from the bark of cork oak (*Quercus suber* L.) but it is also possible to extract cork from the bark of other tree species especially when the rhytidome contains substantial amounts of cork material. An example is the bark of *Quercus cerris* that includes cork with structural and chemical properties close to those of *Q. suber* cork (Şen et al., 2010, 2011a,b). The possibility of its use in insulation agglomerates after thermal treatment has been suggested (Şen et al., 2012). This could increase the valorisation of *Q. cerris* and of other similar cork containing barks, as well as enlarge the raw material basis for the production of cork-based insulation materials.

The thermal treatment used for the production of cork insulation agglomerates induces alterations in the chemical composition and cellular structure of cork (Pereira, 2007). Upon heating the cells expand, their walls stretch and the cell wall components undergo degradation at different rates with extractives and hemicelluloses as the most heat sensitive components (Pereira, 1992). Heating causes mass losses by volatilisation of compounds; the amount of mass loss is a measure of the intensity of the thermally induced effect i.e. it may be significant for high temperatures. The effect of temperature on the cork of *Q. cerris* was found similar to that on *Q. suber* cork although with a higher heat resistance of suberin (Şen et al., 2012).

Temperature has also an effect on the colour of cork, as experienced in the production of the thermal expanded cork agglomerates, the so-called "black" cork agglomerates (Pereira, 2007). Darkening by heat treatment occurs also on wood as a result of coloured degradation products originated from hemicelluloses and extractives as well as oxidation products namely of lignin (Esteves et al., 2008, 2011). The degree of colour change depends on the heating process (dry heating or hydro-thermal heating), the timber species and wood density (Boonstra et al., 2006).

The extent of the thermal effects may be assessed by monitoring colour variation and chemical changes. Colour may be measured using the CIELAB system, developed by the *Commission Internationale d'Eclairage* to rapidly control colour variations of various materials including wood (Pastore, 2004). The system is based on the measurement of three coordinates: lightness L^* between 0 (black) and 100 (white); a^* representing red-green levels (+60 red, −60 green) and b^* representing yellow-blue levels (+60 yellow, −60 blue). The colour of a material is a mixture of these three parameters (Tolvaj and Faix, 1995; Esteves et al., 2008).

FTIR spectroscopy has also been applied to various lignocellulosic materials to evaluate chemical composition and to monitor chemical transformations during heat treatments (Nishimiya et al., 1998; Tjeerdsma and Militz, 2005; Ishimaru et al., 2007; Chen et al., 2010). FTIR spectra of cork have also been used during sample manipulation and to ascertain the purity of isolated components (Pereira, 2007; Lopes et al., 2000; Faix, 1988).

* Corresponding author.
E-mail addresses: hpereira@isa.utl.pt, helena.pereira@reitoria.utl.pt (H. Pereira).

0926-6690/$ – see front matter © 2012 Elsevier B.V. All rights reserved.
doi:10.1016/j.indcrop.2012.01.018

The aim of this paper is to study the chemical transformations of cork during heat treatments using colour variation and FTIR spectral changes as monitoring tools since they may allow a rapid assessment of the intensity of the thermal effect on cork, namely on mass loss. Their application to process monitoring during thermal treatments in production of insulation cork agglomerates is obvious as well as to product quality control and cork performance prediction in various applications.

For this purpose, cork samples from *Q. cerris* bark were subjected to isothermal heating treatments with different intensity by varying temperature and treatment time and the resulting samples were analysed in terms of mass loss, colour variation and chemical composition.

2. Materials and methods

2.1. Samples

Bark samples from *Q. cerris* var. *cerris* were collected from mature trees with 70–80 years of age, from the south-eastern part of Turkey. A bulk bark granulate with particle dimensions between 2 mm and 10 mm was obtained by grinding with an industry-type hammer mill and sieving with a Retsch Analytical Sieve Shaker AS 200. The granulated material was purified by suspending in water for a short time for separation of cork-enriched granules (floating layer) from the phloem (sedimenting material). After drying at 60 °C for three days and visual inspection to separate any conspicuous phloem particles, the cork-enriched granulate was submitted to thermal treatments.

In addition two pure samples of cork and of phloem were carefully prepared manually by precise excision from the rhytidome of the *Q. cerris* barks. These samples were used for comparative purposes to estimate the cork proportion in the studied granulated fraction.

2.2. Heat treatment

Isothermal treatment was made in air using a temperature controlled furnace, at temperatures from 150 °C to 400 °C, and with treatment times from 5 to 90 min, using 2 g samples. Mass loss was determined after each treatment.

2.3. FTIR analysis

Aliquots of 500 mg of the heat treated samples and of an untreated sample as well as of the cork and phloem samples were ground with a Retsch MM200 mixer mill for 20 min. After grinding the samples were dried at 105 °C for 24 h before pellet preparation.

Samples with 2.3 ± 0.1 mg were mixed with 250 ± 2 mg KBr, ground with the Retsch MM200 mill for 2 min and dried for 24 h in vacuum over anhydrous P_2O_5. An amount of 150 ± 1 mg of the mixture was used for preparing KBr pellets. The resulting pellets were analysed in absorption mode FTIR in the 500–4000 cm^{-1} range with a resolution of 4 cm^{-1} and 64 scan accumulation. All spectra were normalised for the highest band in the 500–4000 cm^{-1} range.

2.4. Colour determination

1.5 g of the heat-treated samples and of the untreated control sample was ground and sieved to a 40–60 mesh size prior to colour determination. The colour parameters *L*, *a* and *b* were determined according to the CIELAB method using a Minolta cm-3630 visible reflectance spectrophotometer. The measuring range was between 360 and 720 nm with a 10 nm spectral resolution. Total colour differences (ΔE) were calculated using the following formula (Bekhta and Niemz, 2003; Fan et al., 2010):

$$\Delta E = \sqrt{\Delta L^2 + \Delta a^2 + \Delta b^2}$$

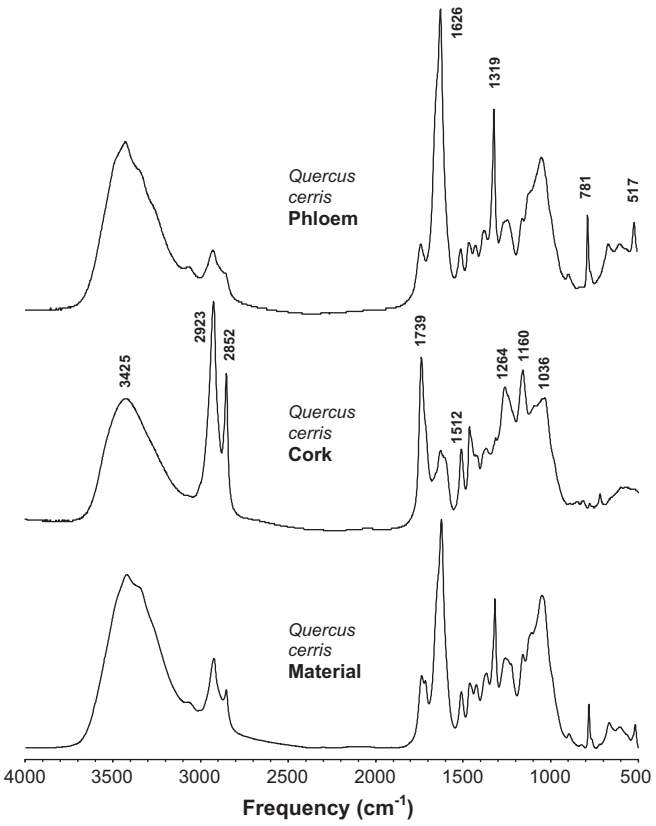

Fig. 1. FTIR spectra of phloem, cork and of the *Quercus cerris* cork-enriched material.

3. Results and discussion

3.1. Characterisation of the cork-enriched fraction

Fig. 1 shows the FTIR spectra of the manually separated cork and phloem tissues, and of the cork-enriched material fractionated from the bulk granulates of *Q. cerris* bark and used for the heat treatment study.

FTIR spectra of the phloem and the cork-enriched material show four acute bands at 1626 cm^{-1}, 1319 cm^{-1}, 781 cm^{-1} and 517 cm^{-1} which clearly do not belong to a lignocellulosic material. These bands and the pattern of the OH stretching band may be assigned to calcium oxalate monohydrate, whewellite (Pinales et al., 2011; Conti et al., 2010). This mineral is widely distributed in plants including bark tissues (Webb, 1999; Trockenbrodt, 1995) i.e. in the stone cells of phloem (D'Antonio et al., 2009). It was observed by optical microscopy in the phloem of *Q. cerris* bark as inorganic prismatic crystals (Şen et al., 2011a).

The oxalate bands are absent in the FTIR spectrum of *Q. cerris* cork. This spectrum has the features of a cork material with sharp intense bands at 2923 cm^{-1}, 2852 cm^{-1}, 1739 cm^{-1}, 1264 cm^{-1} and 1160 cm^{-1}, characteristic of C—H and O—C=O vibrations in aliphatic fatty esters, a medium band at 1512 cm^{-1} characteristic of G-lignin aromatic ring vibrations and medium 3425 cm^{-1} and 1035 cm^{-1} bands from carbohydrates and lignin O—H and C—O vibrations (Marques et al., 1996, 2006; Faix, 1991). These spectral features are similar with those of corks of *Q. suber* and *Pseudotsuga meziesii* (Marques et al., 1996, 2006).

Table 1
Mass loss (% of initial dry mass) by thermal treatment at different temperatures and times of a cork enriched fraction obtained from *Quercus cerris* bark granulates (%).

Temperature	Time (min)				
	5	10	20	60	90
150 °C			2.8		2.7
200 °C		3.5	4.7	11.2	13.2
250 °C	3.7	13.4	15.9	26.5	34.9
300 °C	18.4	26.2	40.5	46.0	52.2
350 °C	39.5	47.9	65.3	71.1	
400 °C	36.0	59.3			

When comparing the FTIR spectra of cork, phloem and the cork-enriched material, it is evident that the fraction obtained from the bulk granulates of *Q. cerris* bark is not pure cork but still contains a very substantial proportion of phloemic material. A rough summative spectral analysis based on the spectra of cork and phloem estimated the composition of the material around 20% cork and 80% phloem. This corroborates the result obtained by wet chemical analysis of a similarly obtained cork-enriched fraction of *Q. cerris* bark granulate and a pure cork material using suberin as "cork-marker", although in this case the cork proportion was higher at about 40% (Şen et al., 2010, 2012).

The results show that the bulk grinding of *Q. cerris* bark into 2–10 mm sized granules with a single fractionation step by floating, although allowing separating a cork-enriched fraction, yields a material still with a high amount of phloemic tissue. Therefore uses in which cork will be the target component or the component responsible for the desired properties will require further refinements in fractionation that have to take into account the specific bark structural features (Şen et al., 2011a).

3.2. Thermochemical degradation

Table 1 includes the results obtained for the mass loss that occurred upon heating of the *Q. cerris* cork-enriched material for the temperature range 150–400 °C.

The intensity of degradation and volatilisation increased with temperature and heating time. At 150 °C mass loss was negligible i.e. 3% after 90 min treatment. At 200 °C the effect was small for short treatments but increased to 13% after 90 min. At higher temperatures, substantial mass loss occurred already with short treatment times and increased rapidly with treatment temperature (e.g. 18% and 40% for 5 min at 300 °C and 350 °C) until substantial mass loss (52% after 90 min at 300 °C and 71% after 60 min at 350 °C). At 400 °C, 59% of the cork mass was already lost during the first 10 min of treatment. For a given mass loss value, each 50 °C increase in treatment temperature reduced the heating time by a factor of about 5.The mass loss values due to the thermal degradation and volatilisation of *Q. cerris* cork components are in agreement with those reported for *Q. suber* cork (Pereira, 1992; Rosa and Fortes, 1988). The cork is thermally stable below 200 °C and loss of material starts at this temperature and increases with time of exposure to temperature (Pereira, 2007).

The FTIR spectra of the heat treated cork material are given in Figs. 2–4, while Table 2 summarises the main trends of the bands and their functional group assignment.

The oxalate bands were always the highest (Figs. 2–4). Calcium oxalate is resistant at the used temperatures and so its presence in the heat treated samples was amplified due to the selective loss of organic material. For this reason all the spectra were normalised for the oxalate band at 1626 cm^{-1} (in the figures this band is shown only for the untreated sample, for reasons of clarity).

The higher content of oxalate in the heat treated samples was seen in the 300 °C and 350 °C treated samples (Figs. 3 and 4) by the higher and more defined OH band pattern with the clear revelation of the characteristic five OH bands from hydration water of calcium oxalate monohydrate (Conti et al., 2010).

The largest modification in the chemical composition as observed in the FTIR spectra was the substantial and systematic intensity reduction in the OH (3000–3800 cm^{-1}) and CO (1000–1200 cm^{-1}) bands with temperature and treatment time. The polysaccharide bands at 1051 cm^{-1} and 1110 cm^{-1} showed a rapid decrease with the heat treatment. After 300 °C 10 min treatment (26% mass loss), the 1051 cm^{-1} band disappeared and after 300 °C 20 min treatment (40% mass loss) the 1110 cm^{-1} band also disappeared. The band at 3425 cm^{-1} which is originated from O—H group vibration, showed a continuous decrease through heating (Figs. 2–4). This means that carbohydrate content reduced substantially with temperature by volatilisation of pyrolysis derived light products and by condensation in char. Suberin was relatively resistant to thermal degradation. The FTIR spectra (Figs. 2–4) show that the CH bands resisted to the temperature and only disappeared for the treatment at 350 °C for 60 min which corresponded over 50% mass loss (Fig. 4).

The results are in agreement with the findings obtained using wet chemical summative analysis for heat-treated *Q. suber* cork (Pereira, 1992) and *Q. cerris* cork (Şen et al., 2012). It was found that suberin was more thermally resistant, and more in the case of *Q. cerris* probably as the result of differences in the monomeric composition of suberin of both corks (Pereira, 2007; Şen et al., 2010). The high presence of the calcium oxalate may also cause some modification in the pyrolysis reactions pattern (Ponder and Richards, 1991).

Suberin was found to be less labile by temperature than lignin. With 10 s pyrolysis at 550 °C of *Q. suber* cork, the lignin derived aromatic products were 4.5 times more than the suberin derived aliphatic products while at 850 °C this relation was reduced to 0.9 times (Marques, 2010).

Lignin content of heat treated cork samples measured as the acid insoluble residue was reported to increase with temperature, and in samples with large thermal degradation the acid insoluble material determined as lignin was by far the dominant component (Pereira, 1992; Şen et al., 2012). The FTIR spectra of the present study showed that lignin only apparently is the most heat resistant component. In fact the bands at 1510 cm^{-1}, 1461 cm^{-1} and 1259 cm^{-1} increased through heating until a certain point but decreased subsequently: it can be observed that the band at 1512 cm^{-1} decreased substantially for treatments above 250 °C (Figs. 3 and 4). This is in accordance with the report that lignin in *Q. suber* cork decomposes at approximately 250–350 °C (Neto et al., 1995). The large acid insoluble residue found in the lignin determination of highly thermally degraded cork samples can be justified by the formation of char with such temperature treatments. Marques (2010) observed that 550 °C pyrolysis of *Q. suber* cork powder formed 27% of char.

3.3. Colour variations

Cork changed colour when exposed to heating that could be visually appreciated by what may be expressed as a darkening effect. This thermal effect was found already in the samples treated at the lowest temperature: for instance, at 150 °C lightness (L^*) decreased rapidly from the initial value of 51.5–37.3 (after 20 min treatment) with also a small decrease in the a^* and b^* parameters (Table 3).

The thermally induced colour changes of cork can also be appreciated in detail by analysis of the reflectance spectra in the wavelength region of 360–720 nm (Fig. 5). Untreated cork reflects a small proportion of violet and blue radiation (until about 480 nm) and also of the green radiation (until about 510 nm).

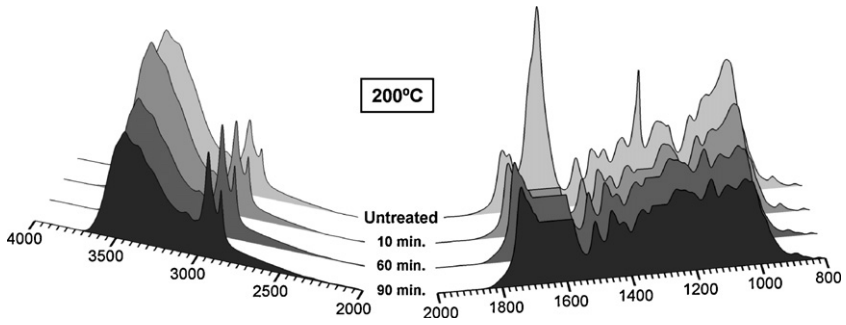

Fig. 2. FTIR spectra for the untreated and thermal treated samples of a cork-enriched material obtained by fractionation of *Quercus cerris* bark for treatment at 200 °C for 10, 60 and 90 min. For better clarity of the spectra comparison, the oxalate bands at 1626 cm^{-1} and 1319 cm^{-1} were cut off for the treated samples.

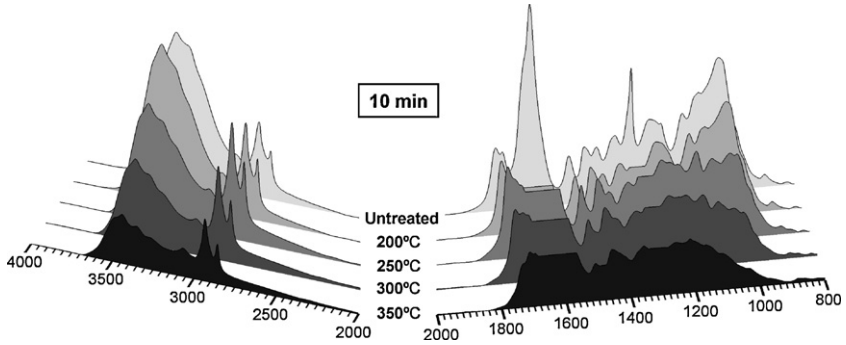

Fig. 3. FTIR spectra for untreated and thermal treated samples of a cork-enriched material obtained by fractionation of *Quercus cerris* bark for 10 min treatment at 200 °C, 250 °C, 300 °C and 350 °C. For better clarity of the spectra comparison, oxalate bands at 1626 cm^{-1} and 1319 cm^{-1} were cut off for the treated samples.

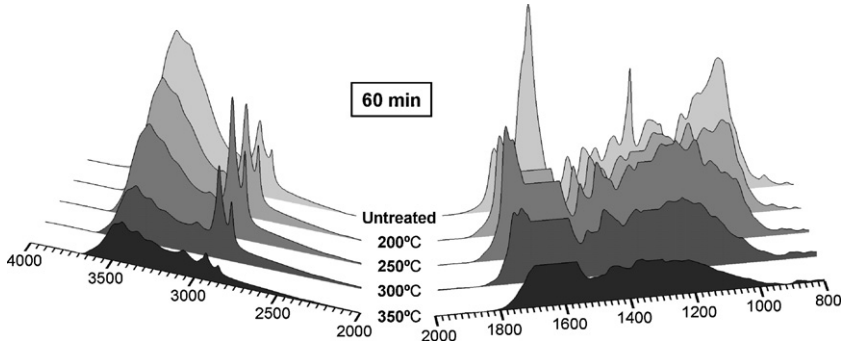

Fig. 4. FTIR spectra for untreated and thermal treated samples of a cork-enriched material obtained by fractionation of *Quercus cerris* bark for 60 min treatment at 200 °C, 250 °C, 300 °C and 350 °C. For better clarity of the spectra comparison, oxalate bands at 1626 cm^{-1} and 1319 cm^{-1} were cut off for the treated samples.

Table 2
FTIR absorbance peak assignments of the spectra of cork enriched fraction obtained from *Quercus cerris* bark granulates and the effect caused by heating on absorbance intensity (Schwanninger et al., 2004; Pereira, 2007).

Frequency range (cm^{-1})	Functional Group	Origin	Heating effect on absorbance intensity
3420–3429	O—H stretch	Polysaccharides	Decrease
2923–2925	Asymmetric C—H vibration	Suberin	Increase
2852–2854	Symmetric C—H vibration	Suberin	Increase
1733–1737	C=O stretch	Suberin	Increase
1625	C—O stretch	Calcium oxalate	Unchanging
1510–1514	Aromatic skeletal vibrations	Guaiacyl lignin	Increase
1461–1463	Asymmetric C—H deformations	Guaiacyl lignin	Increase
1423–1429	H—C—H scissoring	Cellulose	Decrease
1363–1375	C—H stretch	Syringyl lignin	Increase
1317–1319	H—C—H rocking vibration	Syringyl lignin	Increase
1259–1267	C=O stretch	Suberin	Increase
1159–1172	Asymmetric C—O—C vibration	Suberin	Increase
1110–1116	C—C and C—O stretching	Polysaccharides	Decrease
1037–1066	C—O valence vibration	Polysaccharides	Decrease

Table 3
CIELAB colour parameters L^*, a^* and b^* of the heat treated cork enriched fraction obtained from *Quercus cerris* bark granulates and ΔE values in relation to the untreated sample.

Heating temperature/heating time (min)		L	a	b	ΔE
Untreated		51.47	14.04	22.72	0
150 °C	20	37.28	12.10	15.70	15.95
	90	40.35	13.40	17.72	12.21
200 °C	10	36.46	10.89	15.95	16.76
	20	33.98	10.31	14.72	19.59
	60	27.26	7.27	11.48	27.54
	90	27.99	7.43	11.57	26.82
250 °C	5	38.45	11.16	15.90	14.98
	10	25.64	5.52	9.29	30.34
	20	24.57	5.39	8.89	31.46
	60	19.80	3.90	6.52	36.99
	90	17.60	2.95	4.67	39.95
300 °C	5	21.79	3.58	6.52	35.40
	10	20.89	2.96	5.70	36.71
	20	17.67	1.80	3.82	40.61
	60	16.62	1.72	3.35	41.74
	90	16.49	1.37	2.52	42.33
350 °C	5	18.86	1.98	4.47	39.27
	10	18.07	1.74	4.13	40.16
	20	17.52	1.54	3.58	40.93
	60	16.95	1.34	2.31	42.06
400 °C	5	18.24	1.88	4.13	39.98
	10	18.22	1.93	3.64	40.21

Reflectance increases steadily thereafter in the yellow and orange region (570–590 nm) towards the red (650 nm). The effect caused by the 150 °C heating was a decrease of the reflectance curves and a shift towards higher wavelengths (about 570 nm) of the region of increasing reflectance (Fig. 5).

When increasing temperature to 200 °C, the decrease of reflectance over the full spectrum was enhanced as well as the shift of the inflecting point of the curve and the horizontal flattening of the curve especially for the longer treatments at 60 min (Fig. 5). These effects were found also in the samples treated at 250 °C, for which treatments of longer durations (over 20 min) led to linear spectral curves under reflectance values of 10%. For temperatures at 300 °C and above there are only small reflectance values at all wavelengths (Fig. 6).

The summary of the CIELAB colour parameters shows this thermal induced colour change (Table 3). The decrease in all colour parameters (L^*, a^* and b^*) continued with the temperature increase until 300 °C 20 min treatment and remained substantially constant thereafter. At this point cork approximately reached its final colour value and higher temperatures or longer treatments changed colour only slightly. The colour variation measured by the ΔE values followed this trend by increasing steadily until reaching a rather constant value of 40–42 (Table 3).

The colour changes at low mass values (i.e. 150 °C and 200 °C) when cork did not undergo significant chemical decomposition should originate from extractives and hydrolysed carbohydrates and their reactions with cork cell wall components particularly with cork lignin, while above 200 °C decomposition of hemicelluloses and formation of oxidation products contribute to the colour change of the cork (Sundqvist, 2004; Esteves et al., 2008, 2011). The FTIR spectra corroborated that hemicelluloses were degraded almost entirely at that level (Figs. 3 and 4).

When plotting colour parameters in function of the intensity of the thermal degradation measured by mass loss (Fig. 7), three regions of variation could be observed. For mass loss values until about 10% there was an abrupt decrease of lightness (from 52 to about 27), of the a^* parameter (from 14 to about 6) and of the b^* parameter (from 23 to about 10); for mass loss between 10 and 30%, the reduction rate was smaller (L^* to 20, a^* to 3, b^* to 5); for mass loss over 30% the variation was small (L^* remained constant at about 18, a^* varied between 3 and 2, and b^* between 5 and 3). The variation of colour measured by ΔE with mass loss (Fig. 7) also shows a more rapid change for mass losses until about 15%, followed by a decrease of variation until 40% mass loss, after which ΔE remained constant.

Modelling of mass loss (*ML*) using the variation of the colour parameters *L*, *a* and *b* was made with the data until 40% mass loss, because the ΔE did not show any significant variation over this

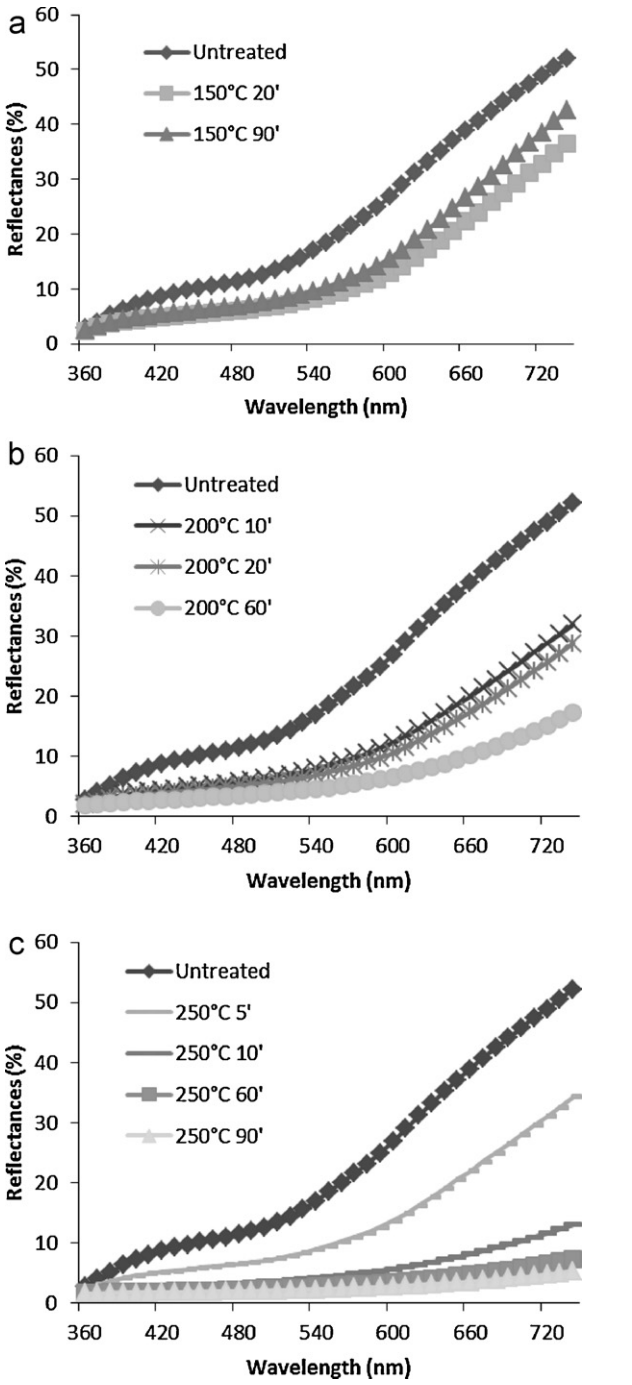

Fig. 5. Variation of spectral reflectance values by thermal treatment at 150 °C, 200 °C and 250 °C of a cork-enriched material obtained by fractionation of *Quercus cerris* bark.

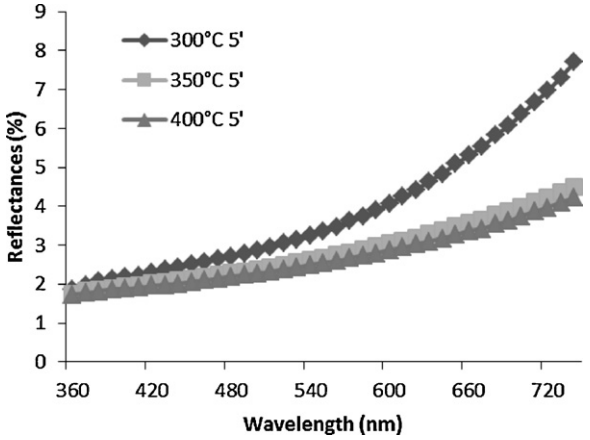

Fig. 6. Variation of spectral reflectance values by thermal treatment during 5 min at 300 °C, 350 °C and 400 °C of a cork-enriched material obtained by fractionation of *Quercus cerris* bark.

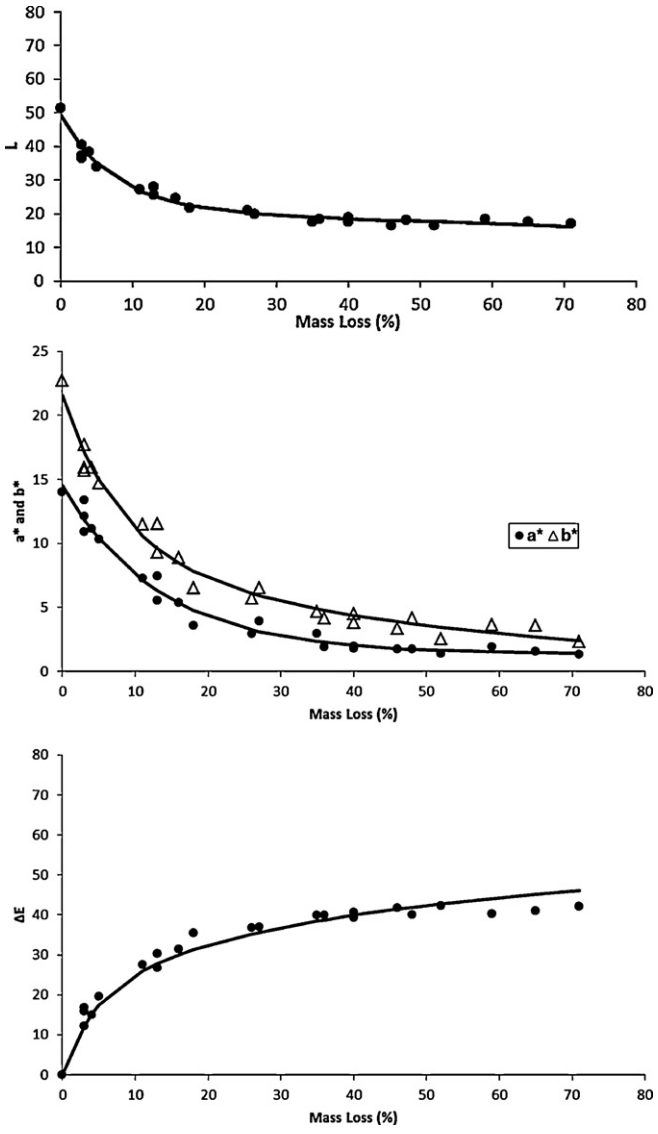

Fig. 7. Variation of the colour parameters *L*, *a*, *b* and ΔE with mass loss obtained by thermal treatment at different temperatures and times of a cork-enriched material obtained by fractionation of *Quercus cerris* bark.

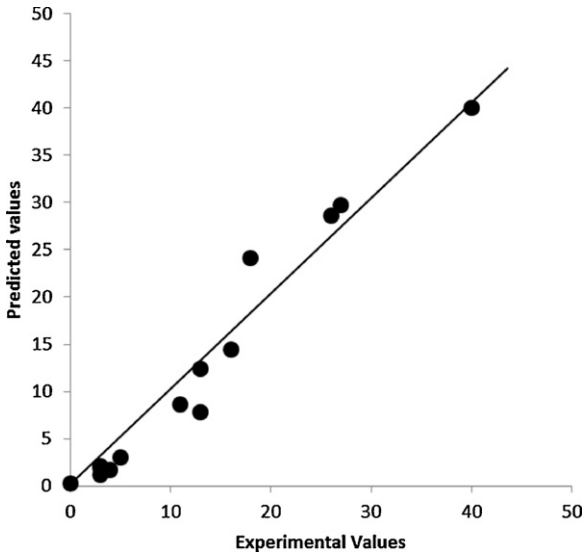

Fig. 8. Predicted mass loss values by thermal treatment at different temperatures and times of a cork-enriched material obtained by fractionation of *Quercus cerris* bark by using an exponential colour variation model.

mass loss point. The exponential model was obtained by fitting the experimental values to the following formula:

$$ML = f(\Delta E) = \alpha.\exp^{k.\Delta E}$$

where $\alpha = 0.535$, $k = 0.107$, $R = 0.89$ and $N = 14$.

With this model it will be possible to estimate mass loss of cork materials during heating treatments until 40% mass loss using change in the colour parameters, as shown by the plot of predicted vs. measured mass loss values (Fig. 8), thereby allowing monitoring thermal treatments.

Since the response to temperature of the *Q. cerris* cork material is similar to that of *Q. suber* cork as regards mass loss and chemical changes (Şen et al., 2012), it can be extrapolated that such models can be applied in industrial black cork agglomerate production. This will be of immediate practical importance. This also opens up the possibility of using colour change to measure extent of mass loss in other lignocellulosic materials, such as wood for the production of heat-treated wood, provided that the specific model parameters are obtained after experimental data acquisition.

4. Conclusions

Heat treatments changed chemical composition and colour of cork-enriched granulates of *Q. cerris*.

The FTIR spectroscopy showed that hemicelluloses were lost first while suberin remained as the most heat resistant component.

The change of CIE-Lab colour parameters was rapid for low intensity treatments, while colour remained rather constant over 40% mass loss.

Colour analysis could be used for modelling the thermally induced mass loss to monitor heat treatments of cork or cork-enriched fractions, such as in the production of heat expanded insulation agglomerates.

FTIR spectral features may be used to check the cork purity of the fractionated material.

Acknowledgements

The work was carried out with the base funding to Centro de Estudos Florestais given by Fundação para a Ciência e Tecnologia, Portugal, under the PEst-OE/AGR/UI0239/2011 programme.

We thank Kahramanmaraş Regional Forest Directorate, Turkey, for their help in field sampling and Ph.D. student Ana Lourenço for her help in colour measurements.

References

Bekhta, P., Niemz, P., 2003. Effect of high temperature on the change in color, dimensional stability and mechanical properties of spruce wood. Holzforschung 57, 539–546.

Boonstra, M.J., Rijsdijk, J.F., Sander, C., Kegel, E., Tjeerdsma, B.F., Militz, M., van Acker, J., Stevens, M., 2006. Microstructural and physical aspects of heat treated wood. Part 1. Softwoods. Maderas: Ciencia y tecnología 8 (3), 192–207.

Chen, H., Ferrari, C., Angiuli, M., Yao, J., Raspi, C., Bramanti, E., 2010. Qualitative and quantitative analysis of wood samples by Fourier transform infrared spectroscopy and multivariate analysis. Carbohydr. Polym. 82, 772–778.

Conti, C., Brambilla, L., Colombo, C., Dellasega, D., Diego Gatta, G., Realinia, M., Zerbib, G., 2010. Stability and transformation mechanism of weddellite nanocrystals studied by X-ray diffraction and infrared spectroscopy. Phys. Chem. Chem. Phys. 12 (43), 14560–14566.

D'Antonio, M.C., Wladimirsky, A., Palacios, D., Coggiola, L., Gonzáles-Baró, A.C., Baran, E.J., Mercader, R.C., 2009. Spectroscopic investigations of iron(II) and iron(III) oxalates. J. Braz. Chem. Soc. 20 (3), 445–450.

Esteves, B., Velez Marquez, A., Domingos, I., Pereira, H., 2008. Heat-induced colour changes of pine (*Pinus pinaster*) and eucalypt (*Eucalyptus globules*) wood. Wood Sci. Technol. 42, 369–384.

Esteves, B., Videira, R., Pereira, H., 2011. Chemistry and ecotoxicity of heat-treated pine wood extractives. Wood Sci. Technol. 45, 661–676.

Faix, O., 1988. Practical uses of FTIR spectroscopy in wood science and technology. Microchim. Acta (Wien) 1, 21–25.

Faix, O., 1991. Classification of lignins from different botanical origins by FTIR spectroscopy. Holzforschung 45 (Suppl.), 21–27.

Fan, Y., Gao, J., Chen, Y., 2010. Colour responses of black locust (*Robinia pseudoacacia* L.) to solvent extraction and heat treatment. Wood Sci. Technol. 44, 667–678.

Ishimaru, K., Hata, T., Bronsveld, P., Meier, D., Imamura, Y., 2007. Spectroscopic analysis of carbonization behaviour of wood, cellulose and lignin. J. Mater. Sci. 42, 122–129.

Lopes, M.H., Pascoal Neto, C., Barros, A.S., Rutlege, D., Delgadillo, I., Gil, A.M., 2000. Quantitation of aliphatic suberin in *Quercus suber* L. cork by FTIR spectroscopy and solid state ^{13}C-NMR spectroscopy. Biopolymers 57, 344–351.

Marques, A.V., Pereira, H., Meier, D., Faix, O., 1996. Isolation and characterization of a guaiacyl lignin from saponified cork of *Quercus suber* L. Holzforschung 50, 393–400.

Marques, A.V., Pereira, H., Rodrigues, J., Meier, D., Faix, O., 2006. Isolation and comparative characterization of a Björkman lignin from the saponified cork of Douglas fir bark. J. Anal. Appl. Pyrol. 77, 169–176.

Marques, A.V., 2010. Pyrolytic bio-oil from industrial cork powder wastes. In: IETS International Workshop in "Energy Optimization in Industry and Reduction of CO_2 Emissions", Lispolis, Lisbon, 3 November 2010.

Neto, C.P., Rocha, J., Gil, A., Cordeiro, N., Esculcas, A.P., Rocha, S., Delgadillo, I., de Jesus, J.D., Correia, A.J., 1995. ^{13}C solid-state nuclear magnetic resonance and Fourier transform infrared studies of the thermal decomposition of cork. Solid State NMR 4, 143–151.

Nishimiya, K., Hata, T., Imamura, Y., Ishihara, S., 1998. Analysis of chemical structure of wood charcoal by X-ray photoelectron spectroscopy. J. Wood Sci. 44, 56–61.

Pastore, T.C.M., 2004. Estudos do Efeito da Radiação Ultravioleta em Madeiras Por Espectroscopias Raman (FT-Raman), de Refletância Difusa no Infravermelho (Drift) e no Visível (CIE-$L^*a^*b^*$). Post Graduation Thesis. Universidade de Brasília, Instituto de Química.

Pereira, H., 1992. The thermochemical degradation of cork. Wood Sci. Technol. 26, 259–269.

Pereira, H., 2007. Cork: Biology, Production and Uses. Elsevier Publications, Amsterdam.

Pinales, L.A., Chianelli, R.R., Durrer, W.G., Pal, R., Narayanb, M., Manciua, S.F., 2011. Spectroscopic study of inhibition of calcium oxalate calculi growth by *Larrea tridentata*. J. Raman Spectrosc. 42, 259–264.

Ponder, G.R., Richards, G.N., 1991. Thermal synthesis and pyrolysis of a xylan. Carbohydr. Res. 218 (30), 143–155.

Rosa, M.E., Fortes, M.A., 1988. Temperature-induced alterations of the structure and mechanical properties of cork. Mater. Sci. Eng. 100, 69–78.

Schwanninger, M., Rodrigues, J.C., Pereira, H., Hinterstoisser, B., 2004. Effects of short time ball milling on the shape of FT-IR spectra of wood and cellulose. Vib. Spectrosc. 36, 23–40.

Şen, A., Miranda, I., Santos, S., Graça, J., Pereira, H., 2010. The chemical composition of cork and phloem in the rhytidome of *Quercus cerris* bark. Ind. Crops Prod. 31, 417–422.

Şen, A., Quilhó, T., Pereira, H., 2011a. Bark anatomy of *Quercus cerris* L. var. *cerris* from Turkey. Turk. J. Bot. 35, 45–55.

Şen, A., Quilhó, T., Pereira, H., 2011b. The cellular structure of cork from *Quercus cerris* var. *cerris* bark in a materials' perspective. Ind. Crops Prod. 34 (1), 929–936.

Şen, A., Miranda, I., Pereira, H., 2012. Temperature-induced structural and chemical changes in cork from *Quercus cerris*. Ind. Crops Prod., doi:10.1016/j.indcrop.2011.07.028.

Sundqvist, B., 2004. Colour changes and acid formation in wood during heating. Ph.D. Thesis. Lulea University of Technology.

Tjeerdsma, B.F., Militz, H., 2005. Chemical changes in hydrothermal treated wood: FTIR analysis of combined hydrothermal and dry heat-treated wood. Holz Roh Werkstoff 63, 102–111.

Tolvaj, L., Faix, O., 1995. Artificial ageing of wood monitored by DRIFT spectroscopy and CIE-$L^*a^*b^*$ color measurements. Holzforschung 49, 397–404.

Trockenbrodt, M., 1995. Calcium-oxalate crystals in the bark of *Quercus robur*, *Ulmus glabra*, *Populus tremula* and *Betula pendula*. Ann. Bot. 75 (3), 281–284.

Webb, M.A., 1999. Cell-mediated crystallization of calcium oxalate in plants. Plant Cell 11, 751–761.

3.2.6. Sorption performance of *Quercus cerris* cork with polycyclic aromatic hydrocarbons and toxicity testing

Olivella, M.A., Jové, P., Şen, A., Pereira, H., Villaescusa, I., & Fiol, N.

Bioresources, 6 (3): 3363-3375

2011

SORPTION PERFORMANCE OF *QUERCUS CERRIS* CORK WITH POLYCYCLIC AROMATIC HYDROCARBONS AND TOXICITY TESTING

M. Àngels Olivella,[a,*] Patrícia Jové,[b] Ali Şen,[c] Helena Pereira,[c] Isabel Villaescusa,[d] and Núria Fiol [d]

Quercus cerris is an important oak species extended in large areas of Eastern Europe and Minor Asia that has a thick bark which is not utilized at all. The sorption performance of cork from *Quercus cerris* bark with four polycyclic aromatic hydrocarbons (PAHs) (acenaphthene, fluorene, phenanthrene, and anthracene) was investigated. *Quercus cerris* cork was characterized for elemental analysis, acidic groups, and summative chemical composition, and the results were compared with *Quercus suber* cork. A Microtox® test was carried out to test for the release of any toxic compounds into the solution. All isotherms fit the Freundlich model and displayed linear *n* values. *Quercus cerris* exhibited a high efficiency for sorption of PAHs for the studied concentrations (5 to 50 µg/L) with 80-96% removal, while the desorption isotherms showed a very low release of the adsorbed PAHs (<2%). In relation to *Quercus suber* cork, K_F values of *Quercus cerris* cork are about three times lower. The quantity of *Quercus cerris* cork required to reduce water pollution by PAHs was estimated to be less than twice the quantity of other adsorbents such as aspen wood and leonardite. Toxicity tests indicated that non-toxic compounds were released into the solution by the Quercus *cerris* and Quercus *suber* cork samples. Overall the results indicate the potential use of *Quercus cerris* cork and of *Quercus suber* cork as effective and economical biosorbents for the treatment of PAH-contaminated waters.

Keywords: Quercus cerris; Quercus suber; Biosorbent; Sorption-desorption; Polycyclic aromatic hydrocarbons (PAHs); Toxicity

Contact information: (a) Department of Chemistry, University of Girona, Campus Montilivi s/n, 17071 Girona, Spain; (b) Catalan Cork Institute, C/Miquel Vincke Meyer, 13, 17200, Palafrugell, Girona, Spain; (c) Centro de Estudos Florestais, Instituto Superior de Agronomia, Universidade Técnica de Lisboa, Tapada da Ajuda, 1349-017, Lisbon, Portugal; (d) Department of Chemical Engineering, Escola Politècnica Superior, University of Girona, Avda Lluis Santaló , s/n 17071, Girona, Spain.
**Corresponding author: angels.olivella@udg.edu*

INTRODUCTION

Polycyclic aromatic hydrocarbons (PAHs) are contaminants that originate from the combustion of fossil fuels. Highly suspected to be probable carcinogens, they are transported by the atmosphere into surface waters (Olivella 2006). Because of their persistence and low solubility they may be accumulated in the food chain (García-Falcón and Simal-Gándara 2005; García-Falcón et al. 2005; Rey-Salgueiro et al. 2007; Rey-Salgueiro et al. 2009a,b). Although activated carbon is probably one of the most effective conventional methods for the removal of PAHs from water (Derbyshire et al. 2001;

Kyriakopoulos y Doulia 2006), the treatment of large amounts of wastewater and stormwater streams makes the treatment highly expensive.

In recent years there has been an increasing interest in removing contaminants, including PAHs, from aqueous environments with low-cost materials. The use of low-cost sorbents and the search of available natural materials are very attractive in terms of their contribution to decrease the costs of operation, therefore helping environmental protection. Depending on the hydrophilic or hydrophobic character of the contaminant, different materials have been applied (Rodríguez-Cruz et al. 2009). The most common adsorbent used so far has been activated carbon, but other cost-efficient and effective options have been tested (Olivella et al. 2011; Ratola et al. 2003; Boving and Zhang 2004; Domingues et al. 2005; Wang et al. 2006; Zeledón et al. 2007).

One of the cost-effective organic materials that has been used to remove PAHs from wastewaters is cork, an industrial raw material extracted from the bark of cork oak trees (*Quercus suber*) and known worldwide as the material used to seal wine bottles (Pereira 2007). Cork is mainly composed of lignin and suberin (hydrophobic biopolymers) and hydrophilic polysaccharides (cellulose and hemicellulose). This heterogeneous chemical composition provides numerous bonding possibilities for a wide range of pollutants.

The cork industry is highly dependent on one application and, therefore dependent on the fate of the stopper market which has lost a big share to alternative closures, aluminum screw caps, and synthetic stoppers. In fact, wine corks only represent 15% of the cork usage by weight but 66% of the revenue. The significant amounts of low-cost residues generated by the cork industry are valued for insulation and surfacing purposes, but their capacity to remove liquid contaminant has also been demonstrated (Domingues et al. 2005; Olivella et al. 2011; Psareva et al. 2005). While cork oak is the species currently providing cork, the bark of other oak species, such as the Turkey oak (*Quercus cerris*), also contains substantial, albeit not continuous, regions of cork and may therefore be considered as a new source of cork (Şen et al. 2010, 2011a). Cork from *Quercus cerris* has cellular and chemical features similar to those of cork from *Quercus suber* and can be used as an adsorbent even though the differences require a different experimental approach.

In this study, the sorption performance regarding PAHs from water environment of *Quercus cerris* cork has been investigated and compared to cork from *Quercus suber* and to other sorbent materials. In addition, acidic surface functional groups were characterized, and tests were carried out to assess the toxicity of aqueous solutions after contact with both *Quercus cerris* and *Quercus suber* cork samples in the same conditions used in the PAH sorption experiments in order to study a potential release of toxic substances from the sorbents into the solution.

EXPERIMENTAL PROCEDURE

Samples

The *Quercus cerris* cork samples were obtained from the bark of trees that were 70 to 80 years old, in the Andırın district of Kahramanmaraş province, in the southeastern

part of Turkey. The cork layers within the *Quercus cerris* bark were separated manually from the phloem regions within the periderms (Şen et al. 2011b).

The *Quercus suber* cork sample was taken from factory-supplied cork strips originating from boards of reproduction cork used to produce stoppers. The cork strips were cut into three layers with a hand saw at three radial positions: the outermost layer (the back), 6-10 mm thick; the middle part used for cork stoppers, 26-32 mm thick; and the innermost layer of cork (the belly), 3-5 mm thick. In this study, only the belly layer was used (Jové et al. 2011).

Each sample was cut into small pieces (<10 mm) and milled using a ZM-200 ultracentrifugal mill (Retsch). The granulated samples were sieved, and the 40-60 mesh granulometric fraction (0.25-0.42 mm grain size) was used for the subsequent analyses.

Reagents

Standard samples of selected PAHs (acenaphthene, fluorene phenanthrene, and anthracene) and deuterated phenanthrene (phenanthrene-d_{10}) at concentrations of 500 µg/mL each one and 2000 µg/mL, respectively were purchased from Supelco (Bellefonte, PA, USA). Chemical properties of the selected PAHs are shown in Table 1.

Deionized water was used for standard solutions and batch experiments. Methanol was Super Purity grade from Romil (Cambridge, UK). Solid phase microextraction (SPME) fibers of 65 µm polydimethylsiloxane/divinylbenzene (PDMS/DVB) were supplied by Supelco (Bellefonte, PA, USA).

Table 1. Chemical Properties of Selected PAHs for this Study. Values presented are obtained from Mackay et al. (2004).

	Name	Abbreviation	Structure	M_w g/mol	logK_{ow} [a]	S [b] mg/L
1	Acenaphthene	Ace	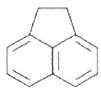	154.21	3.92	3.8
2	Fluorene	Flu	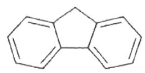	166.2	4.18	1.9
3	Phenanthrene	Phe	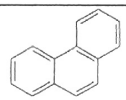	178.24	4.57	1.1
4	Anthracene	Ant	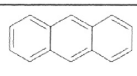	178.24	4.54	0.045

[a] K_{ow} is the octanol-water partition coefficient
[b] S is the solubility

Characterization of the Cork Samples

The C, H, N, and S contents were determined using a Perkin Elmer EA2400 series II elemental analyzer. Oxygen content was calculated by mass difference. The H/C, O/C, C/N, and (O + N)/C atomic ratios were calculated. The detection limits for N and S were 1.20% and 0.44%, respectively.

Acidic surface properties of the cork were determined by the Boehm method (Psareva et al. 2005). According to Boehm, the acidic surface properties derive from the presence of different surface groups: both strong and weak carboxyl groups, carbonyl, lactonic, enolic, and phenolic groups. These groups have different acidity: strongly acidic (carboxylic groups), versus weakly acidic (carboxylic, lactonic and enolic). Acidic groups can be differentiated by neutralization with solutions of $NaHCO_3$, Na_2CO_3, and NaOH. According to the protocol only strongly acidic carboxylic acid groups are neutralized by sodium bicarbonate; those neutralized by sodium carbonate are lactones, lactol, and the carboxylic groups (strong and weak acidic groups). The weakly acidic phenolic groups only react with strong alkali, such as sodium hydroxide. Thus, the difference between NaOH and Na_2CO_3 consumption corresponds to the weakly acidic phenolic group, and the difference between the values for Na_2CO_3 and for $NaHCO_3$ corresponds to the concentration of the weak carboxylic groups.

The chemical characterization of the samples included determinations of: extractives using dichloromethane for solubilization of aliphatic extractives and ethanol and water for extraction of phenolics; suberin; total lignin, including acid insoluble and soluble lignin; and holocellulose. The methods for the chemical characterization of these samples have been described elsewhere (Şen et al. 2010; Jové et al. 2011).

Adsorption Isotherms

For sorption studies in this research, four PAHs were analyzed: acenaphthene [Ace], fluorene [Flu], phenanthrene [Phe], and anthracene [Ant]. The batch equilibrium technique was used for the adsorption experiments. A sample of 0.3 g of cork was weighed into a Pyrex glass bottle and put into contact with 100 mL of an aqueous solution of a PAH mix with different concentrations (5, 10, 20, and 50 μg/L). In all the cases the methanol concentration in solution was 1% or lower. Four points were enough in the studied range for the calculation of isotherms due to the acceptable linearity and reproducibility obtained (< 10%). In a previous study, the equilibrium time for *Quercus suber* was one hour (Jové et al. 2011) and in this study for *Quercus cerris* less than two hours (data not shown). To ensure the full sorption process three hours was chosen as equilibrium time.

The glass bottles were closed, wrapped with aluminum foil, and mixed with a "Vibromatic" shaker at 700 oscillations/min. After shaking, liquid aliquots of 18 mL were collected using a glass luer tip syringe of 20 mL coupled to a stainless steel syringe needle (length 6 in., size 22 gauge) and analyzed for the PAH content, as described below. The amount of adsorbed PAH was considered to be the difference between the initial PAH concentration of the solution and the PAH concentration in the liquid phase at equilibrium.

Three blanks were performed following the same procedure used for the samples: (1) 100 mL of deionized water plus 1 μg/L PAHs; (2) 0.3 g of cork plus 100 mL of deionized water; and (3) 100 mL of deionized water.

Sorption data were fitted to the Freundlich equation in the linearized form according to the equation $\log q = \log K_F + n \log C_{eq}$, where q is the adsorbed amount (μg/g); C_{eq} is the equilibrium concentration of adsorbate in solution after adsorption (μg/L); K_F is an indication of the adsorbent capacity $[(\mu g/g)/\mu g/L)]^{1/n}$; and n is the nonlinearity coefficient.

The distribution coefficient (K_d) is the ratio between the content of the substance in the solid phase and the mass concentration of the substance in the aqueous solution when adsorption equilibrium is reached. K_d values were calculated from the slope of the isotherms.

Desorption Isotherms

Desorption isotherms were studied to assess the degree of reversibility of the sorption process. In the adsorption experiments after equilibrium was attained, the aqueous phase was removed by vacuum filtration and the contaminated cork was put in a glass bottle with 100 mL of deionized water. The content of this bottle was shaken during 6 h, and the solution was analyzed, following the same procedure used for the sorption isotherms.

Solid Phase Microextraction (SPME) and GC-MS Analysis

The extraction of PAHs and the GC-MS analysis were performed following the procedure described by Fernández et al. (2007). For the SPME extraction, 18 mL of deionized water in 20 mL vials, capped with polytetrafluoroethylene (PTFE)-coated septa were analyzed. The fibers were immersed into the aqueous phase with agitation at 60°C for 60 min. After extraction, the fiber was thermally desorbed for 10 min into the liner of the GC injector port at 300°C. The splitless time was set at 4 min, and the desorption time at 10 min. GC was performed with a 6890N Agilent chromatograph equipped with a MPS2 Gerstel autosampler and coupled to a MS 5973N mass spectrometer. The separation was achieved using an HP-5MS column (30m, 0.25mm, 0.25μm film thickness) (J&W Scientific, Folsom, CA, USA), and the GC oven program was: 50°C (3 min), increased by 6°C/min to 325°C (held for 20 min). The carrier gas was helium (99.999%) from Abello Linde with a constant flow rate of 1 mL/min. The transfer line temperature was set at 300°C and the ion source temperature at 250°C. The mass spectrometer was operated in selected ion monitoring mode (SIM). The quantification of PAHs was based on comparisons of the areas for the monitored molecular ions to that of the internal standard, with calibration response curves generated from five different concentrations (0.05, 0.1, 0.5, 1, and 5 μg/L) of each target PAH. The calibration curves for the compounds were linear ($r > 0.99$) over the established range.

Ecotoxicity Test

The possible toxicity added to the solution due to the eventual release of components from the cork was tested with the standard Microtox® bioassay. This test, which consists of measuring the decrease in light emission by *Vibrio fischeri* bacteria

exposed to noxious chemicals, is claimed to be reliable, rapid, and sensitive. Although the toxicity is not commonly controlled in low-cost sorbents, it should be essential to check it, especially in wastes that have suffered some kind of processes. Indeed, extractives of cork with hot water have been reported to show an acute toxicity ranging from 4.1 to 12.3 toxic units for bacterium *Vibrio fischeri* (Anselmo et al. 2001). Some phenolic extractives, namely the group of tannins, are responsible of this toxicity (Mendonça et al. 2004).

After 0.3 g of cork was mixed with 100 mL of deionized water and exposed to 1 h adsorption contact time, an aliquot of 10 mL was collected from each glass bottle, filtered, and analyzed using ecotoxicity tests. Both *Quercus suber* and *Quercus cerris* cork samples were tested. The pH of the samples were between 6 and 8, as required for the Microtox experiments.

The tests were performed using the Microtox Model 500 Toxicity Analyzer System from Azur Environmental (Carlsbad, USA) following the protocols for the basic or 100% test, according to the standard operating procedure (Azur Environmental 1998). The freeze-dried luminescent bacteria, reconstitution solution, osmotic adjusting solution (OAS), diluent, and cuvettes were purchased from Azur Environmental (Carlsbad, USA). Light measurements were taken at 0, 5, and 15 minutes.

The toxicity analyzer is equipped with a 30-well temperature-controlled incubator block set at 15°C and a storage cell kept at around 5°C for the reconstituted bacteria before dilution. The light intensity was digitally recorded. The test consists of adding 10 µL of reagent (Vibrio fischeri bacteria) to four different dilutions of the sample after their osmotic adjustment to get 2% NaCl concentration, which is the required medium for the bioassay. The sample concentration in the four tested dilutions is within the range 45 - 6.25%. A blank consisting in ultrapure water adjusted at 2% NaCl is used to assess the loss of light due to time of exposure. Light measurements were taken at 5 and 15 minutes. The effective concentration, EC50, at which a 50% loss of light emission is observed, is determined with a 95% level of confidence by using the Gamma (Γ) function, which is defined as the ratio of light lost to light remaining, by a specific computer program. The EC50 is the concentration at which Γ=1 (Microbics corporation 1992).

The freeze-dried luminescent bacteria, reconstitution solution, osmotic adjusting solution (OAS), diluent, and cuvettes were purchased from Azur Environmental, (Carlsbad, USA).

RESULTS AND DISCUSSION

Characterization of the Cork Samples

Given that lignin, containing primarily aromatic moieties, and extractives showed great affinity for PAHs (Wang et al 2007; Olivella et al. submitted), a *Quercus suber* sample with a similar percentage of lignin and total extractives was selected for comparison in the sorption studies (Jové et al. 2011). The elemental composition and chemical composition of the *Quercus cerris* and *Quercus suber* cork samples are shown in Table 2.

Table 2. Chemical Composition, Elemental Analysis and Atomic Ratios of Cork from *Quercus suber* and *Quercus cerris*

	Quercus suber	*Quercus cerris*
Extractives*		
Aliphatic, %	5.6	10.9
Phenolic, %	10.8	5.8
Suberin, %	44.1	28.5
Total lignin, %	25.7	28.1
Holocellulose, %	5.0	16.5
Elemental analysis		
C, %	61.0	50.7
H, %	8.7	7.3
Atomic ratios		
H/C	1.70	1.73
O/C**	0.37	0.62

*Aliphatic extractives were extracted with dichloromethane and phenolic extractives were extracted with ethanol and water (Jové et al. 2011; Şen et al. 2010).
** Oxygen was calculated by the mass difference.

Carbon content was lower in the *Quercus cerris* cork sample (50.7 vs. 61.0%), leading to a much higher O/C ratio (0.62 vs. 0.37). The results for N and S were below the determination limits of the equipment and were therefore not considered.

The polarity coefficient (O+N)/C is an important parameter to predict sorption. This parameter was shown to be negatively correlated with the sorption capacity of biopolymers for hydrophobic pollutants (Wang et al. 2007). The values found here for the cork samples are in range of some commercial lignins (0.33-0.94) (Wang et al. 2007) and lower than those obtained for untreated aspen wood (0.754) (Huang et al. 2006).

The difference in elemental composition of the two corks derives from the differences in their chemical composition. Suberin content is higher in *Quercus suber* cork (44.1% vs. 28.5%), while the polysaccharide content is lower (5.0% vs. 16.5% measured as holocellulose). Since lignin content was rather similar in both cork samples, these differences explain the higher polarity of *Quercus cerris* cork.

The results obtained from the determination of acidic groups are listed in Table 3.

Table 3. Distribution of Acidic Functional Groups in Cork from *Quercus suber* and *Quercus cerris*

	Surface Acid Concentration, mmol/g	
	Quercus suber	*Quercus cerris*
Total acid groups	1.8805	1.5520
Strong acids	0.7330	0.8520
Phenolic OH groups	0.9155	0.6815
Weak acid groups	0.2320	0.0185

It is shown that *Quercus suber* cork has a higher concentration of total acidic groups (1.88 mmol/g and 1.55 mmol/g). This difference is mainly attributed to the concentration of phenolic groups and weak carboxylic groups. The content of strong acid groups was, however, higher in *Quercus cerris* cork, in accordance with its higher content of hemicellulosic polysaccharides.

In comparison with other natural materials the total acidic groups found in these *Quercus* samples were in the range of those found in the husk of the mango pit (1.38 mmol/g) and lower than those found in a mango pit/seed (3.15 mmol/g) (Elizalde-González and Hernández-Montoya 2007).

Adsorption/Desorption Isotherms

Adsorption isotherms of PAHs for the *Quercus cerris* cork were obtained (Fig. 1). The equilibrium sorption curves for PAHs fit the Freundlich equation well, following an almost linear C-type curve according to the classification of Giles et al. (1960). The C-type isotherms point to a partitioning mechanism of the adsorbate in the adsorbent, and have been seen for different pesticides (Iglesias et al. 1997; Rodríguez-Cruz et al. 2007), phenols (Ahmaruzzaman and Sharma 2005), and chlorophenols (Severtson and Banerjee 1996).

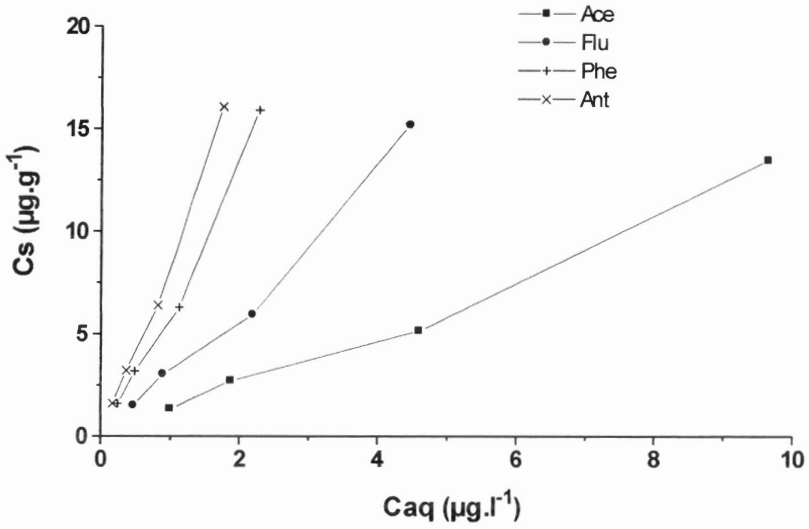

Fig. 1. Adsorption isotherms of acenaphthene (Ace), fluorene (Flu), phenanthrene (Phe), and anthracene (Ant) of cork from *Quercus cerris*

A high percentage of removal was obtained (Table 4), indicating a large affinity of the cork to remove PAHs, and a high effectiveness of the adsorption treatment of the contaminated aqueous solutions.

The sorption coefficients (K_F) for the four tested PAHs, Ace<Flu<Phe<Ant, increased by a factor of about six between Ace and Ant. This trend is in relation to the different polarities of the PAHs. For the *Quercus suber* cork sample the sorption coefficients were K_F = 5 for Ace, K_F = 11 for Flu, K_F =21 for Phe, and K_F =23 for Ant. Thus, *Quercus suber* cork exhibits higher affinity (about three times more) for sorption of

these PAHs than *Quercus cerris* cork. The lower holocellulose content in *Quercus suber* cork (5%) than in *Quercus cerris* cork (16.5%) would favor adsorption because it is located in the primary cell wall and the formation of water clusters via H-bonding could prevent the access of molecules to the bonding sites.

Table 4. Adsorption Coefficients of PAHs on *Quercus cerris* Cork Determined by the Freundlich Equation (K_F, n), correlation coefficients (r), distribution coefficients (K_d), and mean removal percentage calculated at 1, 5, 10, 20, and 50 µg/L

PAHs*	K_F±SD ([(µg/g)/µg/L)]$^{1/n}$)	n±SD**	r	K_d (L/g)	% Removal
Ace	1.4±0.2	1.03±0.02	0.98	1.3±0.1	80
Flu	3.2±0.4	1.01±0.02	0.99	3.3±0.2	90
Phe	6.4±1.0	0.98±0.03	0.99	6.8±0.6	95
Ant	8.8±1.0	1.02±0.02	0.99	8.9±0.9	96

*Abbreviations: acenaphthene [Ace], fluorene [Flu], phenanthrene [Phe], anthracene [Ant]
** SD, standard deviations of triplicate experiments.

The desorption isotherms (not shown) were also well fitted to the Freundlich equation. Table 5 shows the desorption coefficients.

Table 5. Desorption Coefficients of PAHs on *Quercus cerris* Cork Determined by Freundlich Equation (K_{FD}, n_D), Coefficients of Determination (r^2) and Mean Percentage of PAHs Released into the Solution Calculated at 5, 10, 20, and 50 µg/L

PAHs*	K_{FD}±SD ([(µg/g)/µg/L)]$^{1/n}$)	n_D±SD**	r^2	% Released
Ace	33±4	1.02±0.01	0.98	0.99
Flu	23±1	0.96±0.02	1.00	1.53
Phe	77±4	1.02±0.05	1.00	0.41
Ant	97±5	1.08±0.05	1.00	0.27

* Abbreviations: acenaphthene [Ace], fluorene [Flu], phenanthrene [Phe], anthracene [Ant]
** SD, standard deviations of triplicate experiments.

The K_{FD} values (sorbed amounts of PAHs remaining after desorption) were greater for Phe and Ant, which are less soluble (1.1 mg/L and 0.045 mg/L, respectively) than Ace and Flu (3.8 mg/L and 1.9 mg/L, respectively). After a predetermined equilibrium desorption time of 6h, both samples released low percentages of PAHs into the solution (<2%), reflecting the difficulty of PAH desorption from the cork matrix.

Estimation of Sorbent Usage

Table 6 shows the amount of *Quercus cerris* and *Quercus suber* cork that is required to reduce PAHs pollution of 1 L of water from 50 µg/L to 0.1 µg/L. The amount of *Quercus cerris* cork needed is about 1.4 times less than the amount of leonardite and 2 times less than the amount of aspen wood fibers; it is however 3 to 4 times higher than the amount of *Quercus suber* cork. Thus, the results indicate that *Quercus cerris* could be used as an effective biosorbent for the removal of PAHs from wastewater. In addition, its utilization would give an added-value to this natural material.

Table 6. Comparison of the Amount of Biosorbent Needed to Reduce PAHs Pollution from 50 µg/L to 0.1 µg/L and Comparison with Other Materials Reported in the Literature

PAHs*	*Quercus cerris* usage (g/L)	*Quercus suber* (g/L)	Aspen wood fibers usage (g/L)	Leonardite usage (g/L)
Ace	334	80		
Flu	153	39		218 [b]
Phe	82	22	166 [a]	
Ant	54	20		

* Abbreviations: acenaphthene [Ace], fluorene [Flu], phenanthrene [Phe], anthracene [Ant]

[a] Huang *et al.* 2006

[b] Zeledón *et al.* 2007

Ecotoxicity test

Emission of light by the bacteria after 5 and 15 minutes of contact with 45% (the upper concentration that can be tested in the Microtox® basic test protocol) of both *Quercus suber* and *Quercus cerris* cork suspensions decreased by 25%. The same light emission decrease was observed in the control solution (ultrapure water). Therefore, EC_{50} could not be calculated by the computer program, and both *Quercus suber* and *Quercus cerris* cork suspensions were considered as being non-toxic to the bacteria. These results put into evidence that the use of both corks as sorbents does not contribute to any additional toxicity to the treated PAH-contaminated water.

CONCLUSIONS

The sorption performance of *Quercus cerris* cork in relation to polycyclic aromatic hydrocarbons (PAHs) in aqueous solutions was assessed and compared to that of *Quercus suber* cork. Results obtained indicate that:

1. *Quercus cerris* exhibits a high percentage of removal for the selected PAHs (80-96%).
2. The total acidic groups was quantified as 1.552 mmol/g.
3. The amount of *Quercus cerris* used to reduce a PAH-water contaminated was less than twice the amount of leonardite and aspen wood and between 3 and 4 times higher the *Quercus suber* sample.
4. No significant toxicity could be detected by using the bioassay Microtox® test when the concentration of both types of cork in the sample was 3 g/L.

The results obtained in this study are the basis for future studies based on the use of the *Quercus cerris*, whose bark is not used at all, as an effective and economical biosorbent for the removal of PAHs in PAH-contaminated waters. Future studies are mainly focused on developing a technology based on cork filters for treatment of stormwater.

ACKNOWLEDGMENTS

This research was funded by the Spanish Ministry of Science and Innovation as part of the project CTM CTM2010-15185. Thanks to the Cork Center Laboratory for its technical support. Thanks to Dr. Pere Sarquella for his assistance for the toxicity tests. The authors would like to thank AECORK for providing the cork samples.

REFERENCES CITED

Ahmaruzzaman, M., and Sharma, D. K. (2005). "Adsorption of phenols from wastewater," *J. Colloid Interface Sci.* 287, 14-24.

Anselmo, A. M., Gil, E., and Mendonça, E. (2001). "Águas residuais da cozedura da cortiça – caracterização e perspectiva ambiental," *Água e Ambiente* 35(10), Separata Á&A Ciência (1), 1-4.

Azur Environmental (1988). "The Microtox® Acute Basic, DIN, ISO and Wet Test procedures," Carlsbad, California, 1998.

Boving, T. B., and Zhang, W. (2004). "Removal of aqueous-phase polynuclear aromatic hydrocarbons using aspen wood fibers," *Chemosphere* 54 , 831-839.

Derbyshire, F., Jagtoyen, M., Andrews, R., Rao, A., Martín-Gullón, I., and Grulke, E. (2001). "Carbon materials in environmental applications," In: Radovic L. R. (ed.), *Chemistry and Physics of Carbon*, Vol. 27. Marcel Dekker: New York; pp. 1-66.

Domingues, V., Alves, A., Cabral, M., and Delerue-Matos, C. (2005). "Sorption of behaviour of bifenthrin on cork," *J. Chromatogr. A* 1069, 127-132.

Elizalde-González, M. P., and Hernández-Montoya, V. (2007). "Characterization of mango pit as raw material in the preparation of activated carbon for wastewater treatment," *Biochem. Eng. J.* 36, 230-238.

Fernández-González, V., Concha-Graña, E., Muniategui-Lorenzo, S., López-Mahía, P., and Prada-Rodríguez, D. (2007). "Solid-phase microextraction-gas chromatography-

tandem mass pectrometric analysis of polycyclic aromatic hydrocarbons towards the European Union Water Directive 2006/0129 EC," *J. Chromatogr. A* 1176, 48-56.

García-Falcón, M. S., and Simal-Gándara, J. (2005). "Polycyclic aromatic hydrocarbons in smoke from different woods and their transfer during traditional smoking into chorizo sausages with collagen and tripe casings," *Food Addit. Contam.* 22, 1-8.

García-Falcón, M. S., Cancho-Grande, B., and Simal-Gándara, J. (2005). "Determination of polycyclic aromatic hydrocarbons in alcoholic drinks and identification of their potential sources,".*Food Addit. Contam.* 22, 791-797.

Giles, C. H., MacEwan, T. H., Nakhwa, S. N., and Smith, D. (1960). "Studies in adsorption. Part XI. A system of classification of solution adsorption isotherms, and its use in diagnosis of adsorption mechanisms and in measurement of specific surface areas of solids," *J. Chem. Soc.* 111, 3973-3993.

Huang, L., Boving, T. B., and Xing, B. (2006). "Sorption of PAHs by aspen wood fibers as affected by chemical alterations," *Environ. Sci. Technol.* 40, 3279-3284.

Iglesias-Jiménez, E., Poveda, E., Sánchez-Martín, M. J., and Sánchez-Camazano, M. (1997). "Effect of the nature of exogenous organic matter on pesticide adsorption by the soil," *Arch. Environ. Contam. Toxicol.* 33, 127-134.

Jové P., Olivella M. À., and Cano, L. (2011). "Study of the variability in chemical composition of bark layers of cork from different production areas," *BioResources* 6(2), 1806-1815.

Kyriakopoulos, G., and Doulia, D. (2006). "Adsorption of pesticides on carbonaceous and polymeric materials from aqueous solutions: A review," *Sep. Purif. Rev.* 35, 97-191.

Mackay, D., Shiu, W. Y., Ma, K. C., and Lee, S. C. (2004). *Handbook of Physical-Chemical Properties and Environmental Fate for Organic Chemicals*. CD-Rom.

Mendonça, E., Pereira, P., Martins, A., and Anselmo, M. (2004). "Fungal biodegradation and detoxification of cork boiling wastewaters," *Eng. Life. Sci.* 4(2), 144-148.

Microbics Corporation (1992). Microtox® Manual, Carlsbad CA, USA.

Olivella, M. À. (2006). "Polycyclic aromatic hydrocarbons (PAHs) in rainwater and surface waters of Lake Maggiore, a subalpine lake in northern Italy," *Chemosphere* 63, 116-131.

Olivella, M. À., Jové, P., and Oliveras, A. (2011). "The use of cork waste as a biosorbent for persistent organic pollutants - Study of adsorption/desorption of polycyclic aromatic hydrocarbons," *J. Environ. Sci. Health Part A.* 46, 1-9.

Olivella, M. À., Fernández, I., Cano, L., Jové, P., and Oliveras, A. (submitted) "Role of biopolymers of cork on sorption of polycyclic aromatic hydrocarbons from water," *J. Environ. Qual.*

Psareva, T. S., Zakutevskyy, O. I., Chubar, N. I., Strelko,V. V., Shaposhnikova, T. O., Carvalho, J. R., and Joana Neiva Correia, M. (2005). "Uranium sorption on cork biomass," *Colloids and Surfaces A: Physicochem. Eng. Aspects* 252, 231-236.

Pereira, H. (2007). *Cork: Biology, Production and Uses*, Elsevier, pp. 85-90.

Ratola, N. Botelho, C., and Alves, A. (2003). "The use of pine bark as a natural adsorbent for persistent organic pollutants - Study of lindane and heptachlor adsorption," *J. Chem. Technol. Biotechnol.* 78, 347-351.

Rey-Salgueiro, L., Martínez-Carballo, E., García-Falcón, M. S., and Simal-Gándara, J. (2007). "Effects of a chemical company fire on the occurrence of polycyclic aromatic hydrocarbons in plant foods," *Food Chem.* 108, 347-353.

Rey-Salgueiro, L., Martínez-Carballo, E., García-Falcón, M.S., and Simal-Gándara, J. (2009a). "Survey of polycyclic aromatic hydrocarbons in canned bivalves and investigation of their potential sources," *Food Res. Inter.* 42, 983-988.

Rey-Salgueiro, L., Martínez-Carballo, E., García-Falcón, M. S., González- Barreiro, C., and Simal-Gándara, J. (2009b). "Occurrence of polycyclic aromatic hydrocarbons and their hydroxylated metabolites in infant foods," *Food Chem.* 115, 814-819.

Rodríguez-Cruz, S., Andrades, S. M., Sánchez-Camazano, M., and Sánchez-Martín, M. (2007). "Relationship between the adsorption capacity of pesticides by wood residues and the properties of woods and pesticides," *Environ. Sci. Technol.* 41, 3613-3619.

Rodríguez-Cruz, S., Valderrábano, M., and Hoyo, C. (2009). "Physicochemical study of the sorption of pesticides by wood components," *J. Environ. Quality* 38, 719-728.

Şen, A., Quilhó, T., and Pereira, H. (2011a). "Bark anatomy of *Quercus cerris* L. var. *cerris* from Turkey," *Turk. J. Bot.* 35, 45-55.

Şen, A., Quilhó, T., and Pereira, H. (2011b). "The cellular structure of cork from *Quercus cerris* var. cerris bark in a materials' perspective," *Ind. Crop. Prod.* In press.

Şen, A., Miranda, I., Santos, S., Graça, J., and Pereira, H. (2010). "The chemical composition of cork and phloem in the rhytidome of *Quercus cerris* bark," *Ind. Crops Prod.* 31, 417-422.

Severtson, S. J., and Banerjee, S. (1996). "Sorption of chlorophenols to wood pulp," *Environ. Sci. Tecnol.* 30, 1961-1969.

Wang, X., Cook, R., Tao, S., and Baoshan, X. (2007). "Sorption of organic contaminants by biopolymers: Role of polarity, structure and domain spatial arrangement," *Chemosphere* 66, 1476-1484.

Zeledón-Toruño, Z. C., Lao-Luque, C., and de las Heras, F. X. C. (2007). "Removal of PAHs from water using an immature coal (leonardite)," *Chemosphere* 67, 505-512.

Article submitted: May 12, 2011; Peer review completed: June 28, 2011; Revised version received: July 9, 2011; Further corrections: July 14, 2011; Accepted: July 17, 2011; Published: July 19, 2011.

3.2.7. Removal of chromium (VI) in aqueous environments using cork and heat treated cork samples from *Quercus cerris* and *Quercus suber*

Şen, A., Olivella, M. A., Fiol, N., Miranda, I., Villaescusa, I., & Pereira, H.

BioResources, 7(4). 4843-4857

2012

REMOVAL OF CHROMIUM (VI) IN AQUEOUS ENVIRONMENTS USING CORK AND HEAT-TREATED CORK SAMPLES FROM *QUERCUS CERRIS* AND *QUERCUS SUBER*

Ali Şen,[a] M. Àngels Olivella,[b] Nuria Fiol,[b] Isabel Miranda,[a] Isabel Villaescusa,[b] and Helena Pereira [a,*]

Chromium (VI) removal and its reduction to chromium (III) from aqueous solution by untreated and heat-treated *Quercus cerris* and heat-treated *Quercus suber* black agglomerate cork granules was investigated. Initial screening studies revealed that among the sorbents tested, untreated *Q. cerris* and *Q. suber* black agglomerate are the most efficient in the removal of Cr(VI) ions and were selected for adsorption essays. Heat treatment adversely affected chromium adsorption and chromium (VI) reduction in *Q. cerris* cork. The highest metal uptake was found at pH 3.0 for *Q. cerris* and pH 2.0 for black agglomerate. The experimental data fitted the Langmuir model and the calculated q_{max} was 22.98 mg/g in black agglomerate and 21.69 mg/g in untreated *Q. cerris* cork. The FTIR results indicated that while in black agglomerate, lignin is the sole component responsible for Cr(VI) sorption, and in untreated *Q. cerris* cork, suberin and polysaccharides also play a significant role on the sorption. The SEM-EDX results imply that chromium has a homogenous distribution within both cork granules. Also, phloemic residues in *Q. cerris* granules showed higher chromium concentration. The results obtained in this study show that untreated *Q. cerris* and black agglomerate cork granules can be an effective and economical alternative to more costly materials for the treatment of liquid wastes containing chromium.

Keywords: Cork; Quercus cerris; Quercus suber; Black Agglomerate; Biosorbent; Chromium; Heat treatment

*Contact information: a: Centro de Estudos Florestais, Instituto Superior de Agronomia, Universidade Técnica de Lisboa, Tapada da Ajuda, 1349-017, Lisbon, Portugal; b: Department of Chemical Engineering, Escola Politècnica Superior, University of Girona, Avda Lluis Santaló , s/n 17071, Girona, Spain. *Corresponding author: hpereira@isa.utl.pt*

INTRODUCTION

Chromium-polluted wastewaters include those from industries of dyes and pigments, film and photography, galvanometry, metal cleaning, plating and electro-plating, leather, and mining. Chromium is found in hexavalent and trivalent forms in the industrial wastewaters. The hexavalent form is of particular concern because of its greater toxicity. Unlike other toxic pollutants, metals are not biodegradable and can accumulate in living tissues, causing various diseases and disorders in a variety of living species.

Conventional methods for removing metals from industrial effluents are chemical precipitation, coagulation, solvent extraction, electrolysis, membrane separation, ion exchange, and adsorption (Villaescusa *et al.* 2004). The industrial practices for chromium removal such as stabilization ponds are only slightly efficient (Üstün 2009). For the adsorption methods, mostly activated carbon and different types of ion-exchange resins

are applied. However, the high capital and regeneration costs of these materials limit their large-scale use for the removal of metals. In recent years, studies have focused on finding new low-cost sorbing materials, including many of lignocellulosic nature. A recent review has been made on the cellulosic substrates that have been researched for the removal of metals in aqueous systems (Hubbe *et al.* 2011).

Tree barks have been considered for this purpose, such as pine, Douglas fir, eucalypts, teak (Sarin and Pant 2006; Oh and Tshabalala 2007; Kehinde *et al.* 2009; Jauberty *et al.* 2011), as well as cork (Villaescusa *et al.*, 2002). Cork is one important bark component in some species, namely in cork oak (*Quercus suber*). Because of its unique anatomical and chemical properties, cork is a polyvalent material and a valuable industrial raw material with numerous usage possibilities, the most important being cork stoppers production.

Cork was tested for adsorption of heavy metals in aqueous solutions such as Cu(II), Ni(II), and Zn(II), but the adsorption capacity was found to be lower than that of other lignocellulosic materials (Chubar *et al.* 2004a). However, cork has properties that may be interesting for wastewater treatments, *i.e.* low density and floatability. The important metal binding sites are carboxylic groups, and the adsorption capacity can be increased by pre-treatments such as thermal activation (Chubar *et al.* 2004b).

Heating treatments can significantly change the chemical and anatomical composition of cork. Extractives and hemicelluloses degrade in early phases of heating, while the heat-treated samples increase their suberin and lignin ratios in relation to untreated cork (Pereira 2007). One commercial example of heat-treated cork is the expanded or black cork agglomerates that are used for insulation purposes.

One important aspect of economical and ecological relevance in the use of biological materials is to make a close-to-source material selection. This is the approach taken here regarding chromium contamination that was found at high concentrations in industrial wastewaters in Turkey (Yılmaz *et al.* 2010) by studying the adsorption potential of a local bark source, that of the Turkey oak (*Quercus cerris*).

Turkey oak grows naturally in central and south-eastern Europe and Asia Minor, and its thick bark contains substantial, albeit not continuous, regions of cork. The investigations on *Q. cerris* cork showed that it has similar chemical and anatomical characteristics with those of *Q. suber*, including the response to heating treatments (Şen *et al.* 2012a). These findings triggered the interest to find application areas, including adsorption (Olivella *et al.*, 2011) to *Q. cerris* cork, which is currently unused in Turkey

In the present study, chromium (VI) adsorption was investigated for the first time on heat-treated and untreated cork granules obtained from *Q. cerris* bark and on commercial black agglomerate produced from *Q. suber* cork. The study involved: a) chemical characterisation of the adsorbents *i.e.* elemental analysis and atomic ratios; b) screening of adsorption through a selected pH range; c) determination of adsorption kinetics and adsorption isotherms; d) determination of Cr(VI) reduction capacity of selected granules; e) analysis of functional groups involved in adsorption through FT-IR spectroscopy; and f) microscopic characterization by SEM.

EXPERIMENTAL PROCEDURE

Preparation of Adsorbents

Cork granules were extracted from the bark of mature, 70- to 80-year-old *Q. cerris* trees from southeastern Turkey. The bark samples were granulated with an industry-type hammer and sieved with a Retsch Analytical Sieve Shaker AS 200. The granulometric fraction over 2 mm was fractionated by suspending cork granules (floating layer) from the phloem (sedimenting material) in water for a short time. Cork samples were dried at 60°C for 3 days and inspected visually to separate any conspicuous residual phloem particles. Then, samples were submitted to different thermal treatments.

The heat-treated samples of *Q. cerris* cork were prepared by submitting 2 g samples to four different isothermal heating treatments (200°C, 250°C, 300°C, and 350°C) in a temperature controlled furnace (Heraeus MR 170 E) for 20 min. An untreated sample (coded UN) was also used.

A cork black granulate (BA) was obtained by granulating a commercial insulation cork board (ICB) sample. This board is produced from cork granulates of *Quercus suber* that are treated in an autoclave with 300ºC superheated steam during 20 min (Pereira, 2007). The resulting granules were sieved to a 40-60 mesh size to be used in adsorption tests. Cork samples used in this study are detailed in Table 1.

Table 1. Treatments and Codification of the Sorbents

Sample	Treatment type	Code
Q. cerris cork (QC)	Untreated	UN
	200°C treated	200°C
	250°C treated	250°C
	300°C treated	300°C
	350°C treated	350°C
Q. suber cork from commercial black agglomerate (QS)	Over 300°C steam-heated	BA

Elemental Characterization of the Adsorbents

The C, H, N, and S contents of the cork samples were determined using a Perkin Elmer EA2400 series II Elemental Analyzer. Limits of detection for N and S were 1.20% and 0.44%, respectively. Oxygen content was calculated by the difference. The H/C, O/C, C/N, and (O + N)/C atomic ratios were also calculated.

Batch Equilibrium Studies

Hexavalent chromium solutions were prepared by dissolving appropriate amounts of potassium dichromate ($K_2Cr_2O_7$) in distilled water. A 0.1 M HCl solution was used for initial pH adjustment. All reagents were analytical grade and were purchased from Panreac (Barcelona, Spain). Chromium standard 1.000 mg/L solutions from Merck (Damstadt, Germany) were used for flame atomic absorption (FAAS) calibrations.

Adsorption screening

Adsorption screening was applied to compare chromium (VI) adsorption features of untreated and heat-treated *Quercus cerris* cork (QC) granules and black agglomerate (BA) granules (*Quercus suber*, QS). Experiments within a selected 1.0 to 5.0 initial pH range were carried out to determine the influence of initial pH on performance of the six sorbents. In these experiments, 15 mL of 25 mg/L Cr(VI) solutions were put into contact with 0.1 g of sorbents (particle size 0.25 to 0.42 mm) in glass tapered tubes and agitated at 30 rpm on a rotary shaker for 24 hours (Rotator STR4, Stuart Scientific Bibby) at room temperature (20 ± 2 °C).

Chromium (VI) adsorption experiments

Untreated (UN) and black agglomerate (BA) samples were selected after adsorption screening, since maximum chromium adsorption was obtained with these samples. Batch experiments were conducted on UN and BA samples at 20 ± 2 °C in stoppered glass tubes by agitating a 0.1 g sample with 15 mL of 25 mg/L chromium(VI) solution in a rotary mixer at 30 rpm. After agitation, the sorbents were removed by filtration through a 0.45 µm cellulose paper (Millipore Corporation). The total chromium concentration, *i.e.*, Cr(VI) + Cr(III), in filtrates was determined by flame atomic absorption spectrometry using a Varian Spectrometer (Model 220FS). Control experiments (blank) were conducted under the same experimental conditions using deionized water. In all sets of experiments, each test was carried out in duplicate and the average results are presented.

The initial solution pH was 2.0 and 3.0 when BA and UN samples were used respectively. No efforts were made to maintain the solution pH during the adsorption process. The adsorbed metal concentration was obtained from the difference between initial and final metal concentration in solution. The pH variation during the sorption process was monitored using a pH meter (Crison Model Digilab 517).

In order to obtain the sorption isotherms, the time necessary for the system to reach equilibrium was determined. For this purpose, kinetics experiments were performed by putting each of the two sorbents into contact with a 25 mg/L Cr(VI) solution for different times within the range 0 to 96 hours.

For isotherm experiments initial Cr(VI) concentrations were 25, 50, 100, 200, 300, 500, 750, and 1000 mg/L, respectively, and the agitation time was 48 h. The following equation was used to compute the specific uptake by the sorbent, q (mg/g of dry solid):

$$q = (Ci - Cf) \times V \div w \quad (1)$$

where Ci and Cf are initial and final (equilibrium) concentration, V (L) is the solution volume, and w (g) is the mass of dry sorbent used.

Point of Zero Charge (PZC) test

The point of zero charge (pH_{pzc}) was determined in UN and BA samples by mass titration following the procedure described by Fiol and Villaescusa (2009). Different masses of sorbent materials within the concentration range 20 to 90 g/L were put into contact with a 0.03 M KNO_3 solution. The aqueous suspensions were shaken for 24 h in a shaker at 200 rpm until pH equilibrium was reached. The pH_{pzc} is the pH at which a plateau is achieved when plotting equilibrium pH versus sorbent mass concentration.

Cr(VI) Reduction Assay

It is well demonstrated that, at acidic pH, Cr(VI) can be reduced to Cr(III) after contact with lignocellulosic materials, and the converted Cr(III) could be totally or partially released into the solution (Fiol *et al.* 2008; Park *et al.* 2008). Therefore, it is important to determine if reduction of Cr(VI) takes place when in contact with QC and BA sorbents to understand the mechanism of Cr(VI) removal when using these natural sorbents.

Total chromium and Cr(VI) in the liquid phase were quantified by using two different techniques: total chromium was analyzed by Flame Atomic Absorption Spectroscopy (FAAS) and Cr(VI) by the standard colorimetric 1,5-diphenylcarbazide method, in a spectrophotometer (Cecil, CE2021) (Clesceri *et al.* 1998). Cr(III) was calculated as the difference between total chromium and Cr(VI). The Cr(VI) standard solution used for obtaining the calibration curve in the diphenylcarbazide method was analysed by FAAS. Analytical measurements made by the two techniques were comparable within 5%.

Fourier Transform Infrared (FTIR) Analysis

Fourier transform infrared spectra (FTIR) were used to investigate changes in the functional groups of the adsorbents due to Cr(VI) adsorption. Elucidating the functional group involved in a sorption process is one of the key factors to understand the mechanism of metal binding by natural adsorbents. Each initial and each Cr(VI)-loaded adsorbent was mixed separately with spectroscopic grade KBr (Acros, New Jersey, U.S.A.) and made in the form of pellets. FTIR spectra were recorded on a Galaxy 5000 FTIR spectrometer (Mattson Instrument Co., Madison, WI). All FTIR spectra were measured in the 4000 to 400 cm^{-1} range by co-addition of 32 scans with a resolution of 4 cm^{-1}.

For FTIR analysis, UN and BA cork granules were loaded with 1000 mg/L of Cr(VI) solutions following the batch procedure described above. As a blank, the same procedure was made using Milli-Q water adjusted at pH 2.0 and pH 3.0 for BA and UN cork, respectively. The blank and the chromium loaded samples were dried until constant weight and kept in a desiccator until the moment of analysis.

Scanning Electronic Microscopic (SEM-EDX) Analysis

The same samples used for FTIR were used for SEM analysis. The granules were deposited on a double-sided carbon tape, and a layer of Au/Pd with approximately 450° A thickness was deposited using a Quorum Technologies E5100 (former Polaron) sputter coater. The samples were observed with a Hitachi S-2400 scanning electron microscope with a Bruker EDX (Energy Dispersive X-Ray Spectroscopy) detector attached using an acceleration voltage of 20 kV at magnifications of 50 to 1000x. The images were recorded in digital format.

RESULTS AND DISCUSSION

Elemental Composition of the Sorbents

The elemental composition of the sorbents is important to clarify the affinity of cork components to chromium. The results indicate that with heat treatment, the carbon

ratio increases rapidly in QC samples from 48% (UN) to 64% (200°C) and reaches a limit of 68% (350°C). The BA shows the same carbon ratio as the 350°C treatment, probably because of the similarity of the heating temperatures. As a consequence of this, the oxygen ratio decreases rapidly with heating (UN 45%, 200°C 26%) until 23% (350°C and BA). Heating also modifies the elemental H/C ratio (1.49 in UN, 1.67 in 200°C and 1.38 in 350°C treatments). It is interesting to note that UN and BA exhibited similar H/C ratios (UN 1.49 and BA 1.48). The O/C and (N+O)/C ratios also showed similar pattern, but UN and BA values were quite different (0.70 to 0.26 O/C and (N+O)/C ratios for UN and BA, respectively) (Table 2.).

Table 2. Elemental Composition, Atomic Ratios (H/C and O/C) and Polarity Index ((N+O)/C) of the Cork Samples

Samples	C (%)	H (%)	O (%)	H/C	O/C	(N+O)/C
200°C	64.28	8.96	26.76	1.67	0.31	0.31
250°C	68.12	9.02	22.87	1.59	0.25	0.25
300°C	67.20	7.97	24.83	1.42	0.28	0.28
350°C	68.98	7.94	23.08	1.38	0.25	0.25
BA	68.28	8.45	23.28	1.48	0.26	0.26
UN	48.64	6.05	45.32	1.49	0.70	0.70
UNCr	43.38	5.47	51.16	1.51	0.88	0.88
BACr	64.05	6.97	28.98	1.31	0.34	0.34

Chromium Sorption and Mechanism

It is well recognised that metal biosorption processes are pH-dependent, as the proton concentration influences the sorbent ionization and the chemical speciation of metal in solution. Additionally, in the case of Cr(VI) sorption, the knowledge of the protons role in the sorption process is of great importance to assess the mechanism involved.

Figure 2 shows the amount of chromium sorbed for an initial 25 mg/L Cr(VI) concentration within the pH range 1.0 to 5.0 and a contact time of 24 h. The results show that the highest sorption was found at pH 3.0 for UN and 200°C treated and at pH 2.0 for BA. These results are consistent with those obtained previously in which it was described that the acidic conditions are more favourable to the sorption of chromium (Seng *et al.* 2001; Fiol *et al.* 2003).

There was almost no difference in the chromium(VI) sorption between these sorbents at pH 4.0 and pH 5.0 for 350°C and BA sample, respectively. The maximum Cr(VI) removal for 350°C was 26.2 % at pH 3.0, while for BA it was 69.4% at pH 2.0.

Because the net charge on the sorbent surface determines the protonation or deprotonation of the sorbent in aqueous media, the zero point charge (pHpzc) was determined. The pHpzc values, 4.40 (UN) and 5.54 (BA), show that sorbent surfaces were positively charged in interaction with chromium solutions.

At the optimal sorption pH, Cr(VI) is present as the negative species $Cr_2O_7^{2-}$ and $HCrO_4^-$. Therefore, the adsorption observed at pH lower than the pH_{pzc} of UN (pH 4.40) and BA (pH 5.54) must be due to the electrostatic attraction between these negative ionic species and the positive surface charge.

As shown in Fig. 2, the increase of temperature treatment had an adverse effect on Cr(VI) sorption onto *Q. cerris*. Thus, it seems that the heat treatment may modify some surface functional groups that are involved in chromium sorption. Indeed, both H/C and

O/C ratios decreased with the increase of temperature (Table 2), confirming that the temperature affects the nature of binding sites (*e.g.* dehydroxylation of –OH groups of lignin) with the subsequent Cr(VI) sorption decrease.

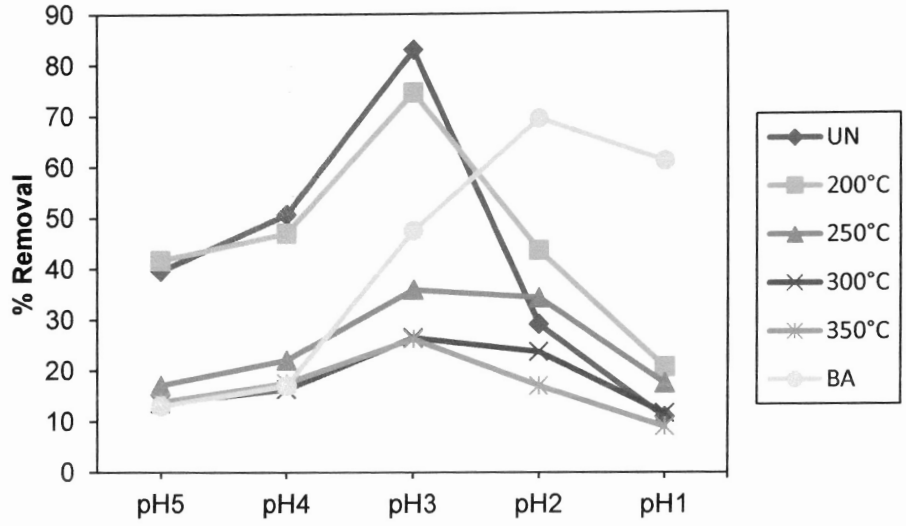

Fig. 2. Chromium removal (%) in the pH range (1.0 to 5.0). Initial Cr(VI) concentration: 25 mg/L, sorbent particle size: 0.25 to 0.42 mm, contact time: 24 hours

Though BA was also subjected to heat treatment (over 300°C), results shown in Fig. 2 indicate that this sorbent presents quite high sorption yields at the lowest pH values. This could be due to the fact that BA heat treatment was performed under steam in autoclave (Pereira and Ferreira 1989; Pereira 1992), and the possible modification of the binding sites favours chromium sorption. It seems that sorption is more related to binding sites containing hydrogen than oxygen (Table 2).

Reduction of Cr(VI) by the sorbents was observed by analysing the residual chromium in solution. Cr(VI) and Cr(III) concentrations of the residual solutions from experiments performed at initial pH 3.0 are presented in Fig. 3. As reduction is a proton-consuming reaction, the final pH of these solutions was measured and is also shown in the same figure.

As can be seen in Fig. 3, UN was the only sample able to render the residual chromium in its trivalent form. Conversely, in the case of BA, the remaining chromium in solution was almost exclusively as Cr(VI), indicating that at pH 3.0, this sorbent has almost null capacity to reduce Cr(VI).

Temperature treatment higher than 200°C negatively affected the Cr(VI) reduction, as observed in Fig. 3. The variation of pH (ΔpH 1.0 to 2.5) observed in Fig. 3 must be due to proton consumption as a consequence of chromium reduction because the corresponding sorbent blanks did not present any change in the pH. Indeed the highest pH variation was found for UN and 200°C samples and the lowest for the samples that suffered the highest heat treatments. These pH variations (ΔpH) correlate very well with Cr(III) concentration in the residual solutions. The results presented in Fig. 3 confirm that the heat treatment of QC provokes a modification on the surface functional groups involved in Cr(VI) reduction, which seems to play an important role in chromium elimination and explains the differences observed on chromium removal between QC

sorbents. Also in the QS sample BA the heating treatment has a high adverse effect on chromium reduction.

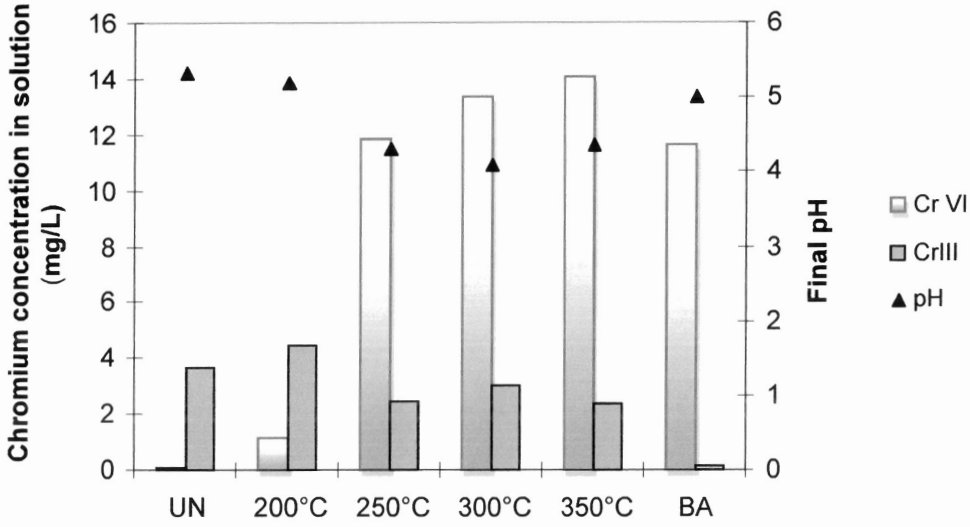

Fig. 3. Concentrations of Cr(VI) and Cr(III) and final pH in the remaining solutions after contact with the sorbents. Cr(VI) initial concentration: 25 mg/ L; Initial pH: 3.

FTIR spectroscopy was applied to identify the functional groups responsible for Cr(VI) sorption. FTIR spectra were obtained with the optimal sorbents UN and BA for chromium removal (Fig. 4). By comparing the spectra before and after adsorption, it was observed that the strong bands at 3426.36 cm^{-1} and 3431.76 cm^{-1} indicating the presence of hydroxyl groups in QC (UN) and black agglomerate (BA) were shifted to 3441.22 cm^{-1} and 3443.73 cm^{-1}, respectively and decreased after the adsorption of chromium. This indicates that surface aliphatic hydroxyl groups are involved in the adsorption of chromium.

Infrared absorption spectra of both samples show that the aromatic skeletal vibrations derived from C=C vibration of aromatic lignin moieties at around 1600 cm^{-1} were affected by chromium sorption. This is confirmed by the shift of the peaks from 1600.8 cm^{-1} to 1585.3 cm^{-1} in the case of BA and from 1516.14 cm^{-1} to 1506 cm^{-1} in UN. The decrease in wave number could be due to the higher steric hindrance for the formation of hexavalent chromium complexes on positively charged groups of the lignin moieties (*e.g.* hydroxyl). The functional groups of the lignin moieties seem to play a significant role on sorption of chromium. This is shown by a decrease in the intensities of the peaks at 1271 cm^{-1} in the case of UN and 1261 cm^{-1} in BA, attributed to C-O-CH_3 (methoxyl deformation). This could indicate the oxidation of lignin in these sorbents upon addition of Cr(VI). Then the adsorbed Cr(VI) might be partially reduced to Cr(III) with the oxidation of neighboring electron-donor functional groups (*e.g.* the O-CH_3 group) (Albadarin *et al.* 2011).

Therefore, these results indicate that lignin plays a significant role in the sorption of Cr(VI) and its reduction to Cr(III).

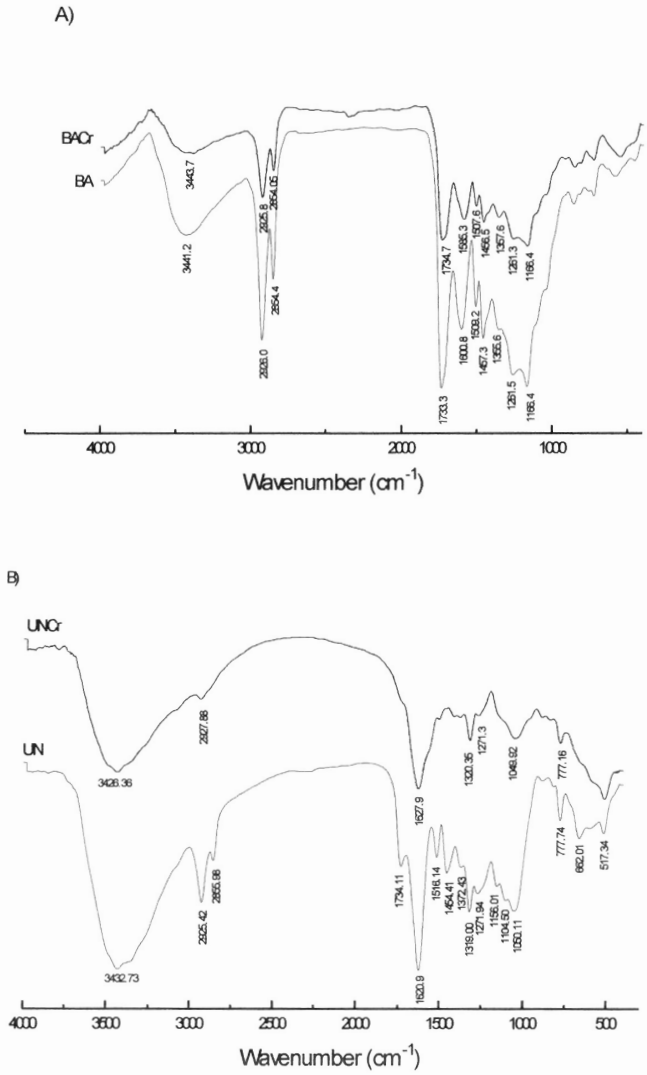

Fig. 4. FTIR spectra of the A) BA and BA treated with 1000 mg/L Cr(VI) solution (BACr) at pH 2 for 24 h. and B) UN and UN treated with 1000 mg/L Cr(VI) solution (UNCr) at pH 3 for 24 h

In the case of the UN sample, other compounds were also involved in the chromium sorption process. The UN sample interaction of carbonyl oxygen (C=O) of suberin with chromium was reflected by the disappearance of the peak at 1734.11 cm^{-1} (Marques *et al.* 1994). According to Shen *et al.* (2010), carbonyl groups may provide binding sites for Cr(III) resulting from Cr(VI) reduction. The carbonyl groups were not affected by chromium sorption on BA. It is also shown that while the intensities of the peaks contributed by cellulose and hemicelluloses in BA were insignificantly affected (*e.g.* 1166 cm^{-1} corresponding to C-O bond), the intensity of the peak at 1052 cm^{-1} in UN characteristic to polysaccharides (cellulose and hemicelluloses) is clearly affected by Cr(VI), indicating it could play an important role of the adsorption. A strong band at

around 1627.88 cm^{-1} is assigned to calcium oxalate ions present in phloem residues in the QC cork (Şen *et al.* 2012b).

The two bands in the 2800 to 2900 cm^{-1} region can be associated with the presence of suberin corresponding to the asymmetric and symmetric vibration, respectively, of C-H in the olephinic chains. In BA, a minor shift of these bands was observed, and a clear decrease of these bands was shown in UN, indicating that these groups were involved in the sorption. This is also consistent with the variations of C-H stretching in UN with a shift from 1454.41 cm^{-1} and 1372.43 cm^{-1} to 1418.09 cm^{-1} and 1383 cm^{-1}, respectively.

Therefore, while in the case of BA, lignin is taken to be the main component responsible for Cr(VI) sorption, in the case of UN, suberin and polysaccharides play significant roles in the sorption. The O-H groups, C=O groups, and C-O groups (as evidenced by the stretching absorption band) seem to contribute to the chromium adsorption (Vinodhini and Das 2009).

A complementary SEM-EDX analysis was applied to analyze the distribution of the chromium adsorption on the cork granules (Hossain *et al.* 2010). The spectra obtained show the presence of chromium in the UN and BA samples. The scanning along the surface of the samples indicated that chromium had a homogenous distribution within the cork granule (Fig. 5).

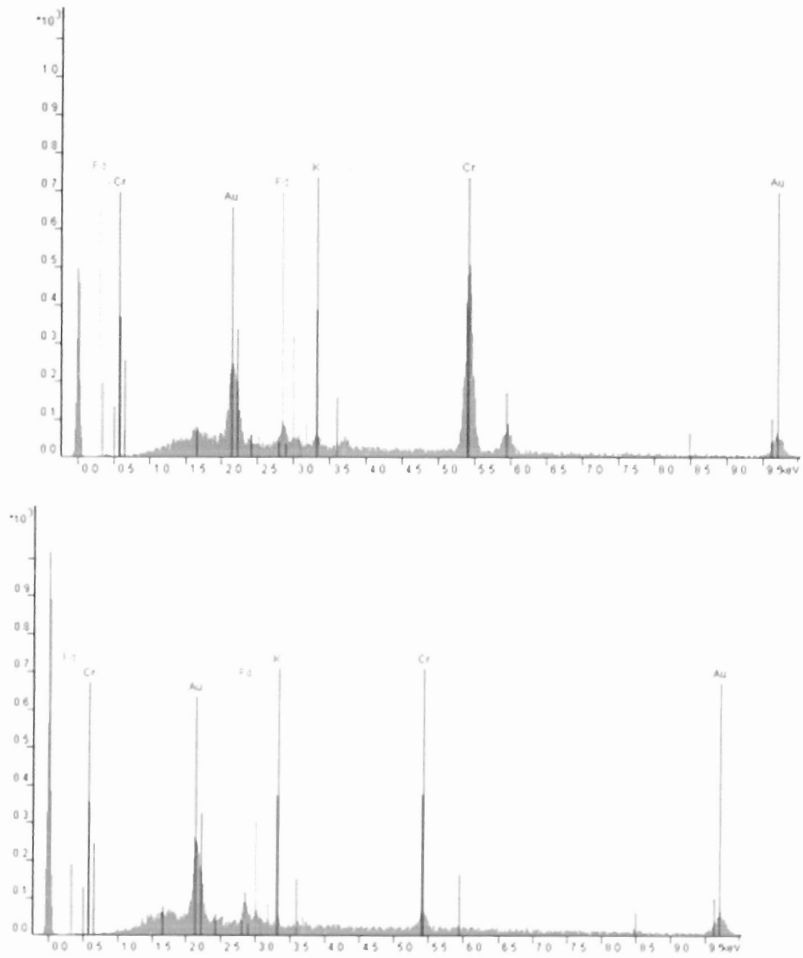

Fig. 5. EDX spectra of *Q. cerris* (above) and *Q. suber* black agglomerate (below) cork samples

No difference in chromium density was observed between the cross-sectioned cell wall and the surface of cell base both in UN and BA samples (Figs. 6 and 7). The UN sample was found to contain phloemic residues (Fig. 8), which also contained a high amount of chromium similar as in cork.

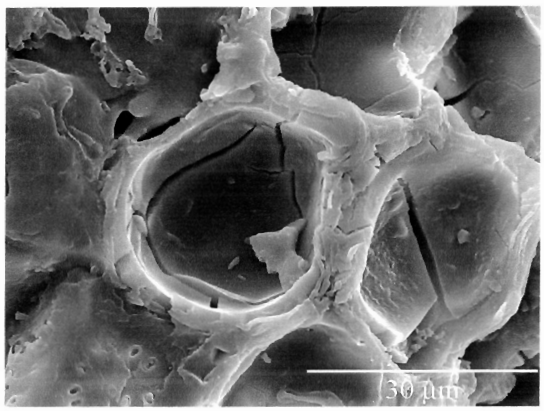

Fig. 6. *Q. cerris* cork cell from UN granule treated with 1000 mg/L chromium solution

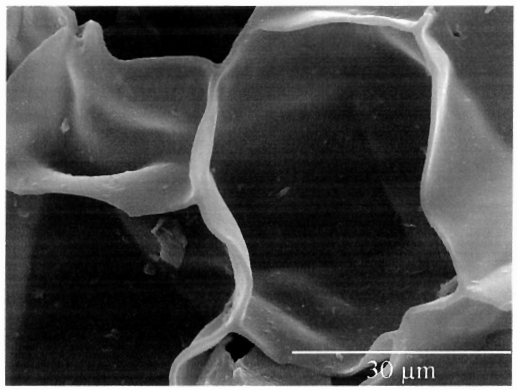

Fig. 7. Cork cell from BA granule treated with 1000 mg/L chromium solution

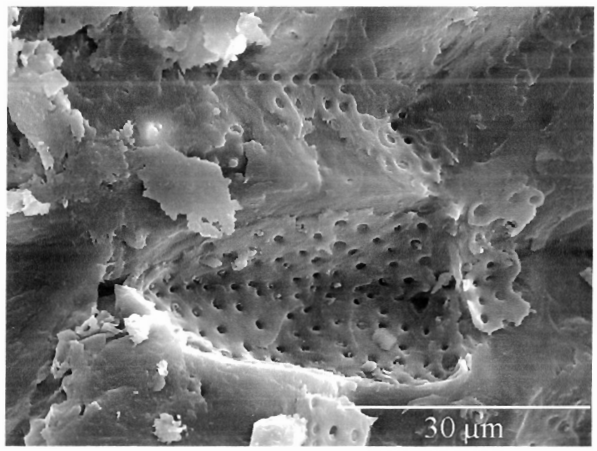

Fig. 8. Phloemic portions in a UN granule

Adsorption Isotherms

The adsorption isotherm tests were conducted based on the equilibrium time found in kinetics experiments (Fig. 9). The equilibrium time was reached at 24 h for BA and 48 h for UN. Thus, an agitation time of 48 h was selected to ensure that equilibrium adsorption had been reached.

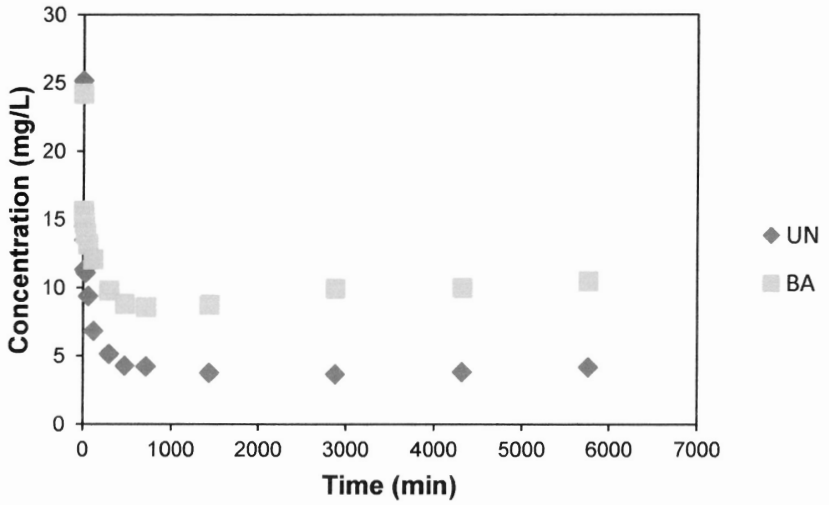

Fig. 9. Chromium concentration in solution as a function of time. Initial Cr(VI) concentration: 25 mg/L. Initial pH : 2.0 (BA) or 3.0 (UN).

Chromium sorption isotherms when using UN and BA are presented in Fig. 10. The experimental data were fitted to the Langmuir model (Equation 1) and its linearized form (Equation 2). The Langmuir parameters were calculated and are plotted together with the experimental data in Fig. 10. The q_{max}, b, and the regression coefficient parameters are presented in Table 3.

$$q = (qmax \times b \times Ceq) \div (1 + b \times Ceq) \quad (2)$$

$$1 \div q = 1 \div qmax + 1 \div (Ceq \times qmax \times b) \quad (3)$$

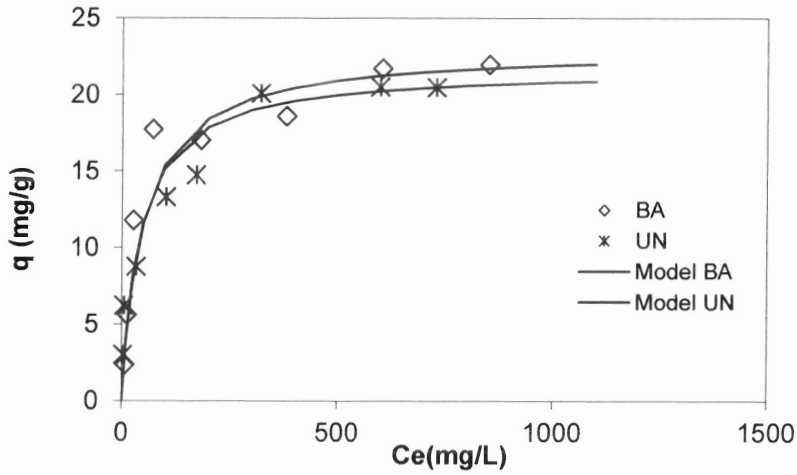

Fig. 10. Fitting of the Langmuir isotherm equation (lines) to the data gathered from the experiments (symbols). Initial pH: 2.0 (BA) or 3.0 (UN)

As can be observed, the experimental isotherm data fitted well with the Langmuir model, and the calculated maximum uptakes (q_{max}) were found to be 22.98 mg/g in BA and 21.69 mg/g in UN. Therefore, no significant differences were found in maximum sorption capacity between the two sorbents. The maximum uptake (q_{max}) values of both granules UN and BA were higher than that of untreated *Q. suber* cork (17.0 mg/g, Fiol *et al.* 2003) and comparable with other lignocellulosic materials like coconut shell (18.69) and saw dust (20.70) (Singha *et al.* 2011). The *b* values indicating the affinity of sorbents toward the metal were similar, although slightly lower in BA (0.023 and 0.020, respectively), *i.e.* having higher affinity.

Table 3. Langmuir Parameters for Cr(VI) Uptake

Sorbents	Calculated Langmuir Values		
	q_{max} (mg/g)	*b* (L/mg)	R^2
UN	21.69	0.023	0.9940
BA	22.98	0.020	0.9938

CONCLUSIONS

Removal of aqueous chromium(VI) by *Quercus cerris* and *Quercus suber* cork samples were performed. The following conclusions arise from this work:

1. Among the granules tested, untreated *Q. cerris* (UN) cork granules were the most efficient, followed by 200°C treated *Q. cerris* and black agglomerate *Q. suber* (BA) granules in the removal of Cr(VI) ions from aqueous solutions. Sorption was strongly dependent on initial pH of solution.
2. The experimental data were well fitted to the Langmuir model, and a similar maximum uptake was found (21.69 mg/g for UN and 22.98 mg/g for BA).
3. Heat treatment of *Q. cerris* cork at temperatures higher than 200°C resulted in a decrease of the total amount of chromium removed and Cr(VI) reduced.
4. FTIR spectra indicate that lignin plays a significant role in sorption of Cr(VI) onto both BA and UN. Suberin and polysaccharides also contribute to metal binding onto UN.
5. SEM–EDX analysis showed that chromium was homogeneously distributed on the cork granules surface.

These findings will be used in further works to optimize the experimental sorption conditions in continuous processes, since the results obtained in this study underline that the studied corks can be an alternative to more costly materials for the treatment of liquid wastes containing metals.

ACKNOWLEDGMENTS

This research was funded by the Spanish Ministerio de Ciencia e Innovación as part of the project CTM 2010-15185 and by the Strategic Project PEst-OE/AGR/UI0239/2011 by the Portuguese Fundação para a Ciência e Tecnologia (FCT).

REFERENCES CITED

Albadarin, A. B., Al-Muhtaseb, A. H., Walker, G. M., Allen, S. J., and Ahmad, M. N. M. (2011). "Retention of toxic chromium from aqueous phase by H_3PO_4-activated lignin: Effect of salts and desorption studies," *Desalination* 274, 64-73.

Chubar, N., Carvalho, J. R., and Correia, M. J. N. (2004a). "Cork biomass as biosorbent for Cu(II), Zn(II) and Ni(II),"*Colloid Surface A* 230, 57-65.

Chubar, N., Carvalho, J. R., and Correia, M. J. N. (2004b). "Heavy metals biosorption on cork biomass: Effect of pre-treatment,"*Colloid Surface A*. 238, 51-58.

Clesceri, S. L., Greenberg, A. E., and Eaton, A. D., (eds.). (1998). *Standard Methods for the Examination of Water and Wastewater*, American Public Health Association, Washington DC, 65-67.

Fiol, N., Villaescusa, I., Martínez, M., Miralles, N., Poch J., and Serarols, J. (2003). "Biosorption of Cr(VI) using low cost sorbents,"*Environ Chem Lett.* 1, 135-139.

Fiol, N., Escudero, C., and Villaescusa, I. (2008). "Chromium sorption and Cr(VI) reduction to Cr(III) by grape stalks and yohimbe bark," *Bioresource Technol.* 99(11), 5030-5036.

Fiol, N., and Villaescusa, I. (2009). "Determination of sorbent point zero charge: Usefulness in sorption studies," *Environ. Chem. Lett.* 7, 79-84.

Hossain, M. A., Kumita, M., and Mori, S. (2010). "SEM Characterization of the mass transfer of Cr(VI) during the adsorption on used black tea leaves," *Afr. J. Pure Appl. Chem.* 4(7), 135-141.

Hubbe, M. A., Hasan, S. H., and Ducoste, J. J. (2011). "Cellulosic substrates for removal of pollutants from aqueous systems: A review. 1. Metals," *BioResources.* 6(2), 2161-2287.

Jauberty, L., Gloaguen, V., Astier, C., Krausz, P., Delpech, V., Berland, A., Granger, V., Niort, I., Royer, A., and Decossas, J. L. (2011). "Bark, a suitable biosorbent for the removal of uranium from wastewater – From laboratory to industry," *Radioprotection* 46(4), 443-456

Kehinde, O. O., Oluwatoyin, T. A., and Aderonke, O. O. (2009). "Comparative analysis of the efficiencies of two low cost adsorbents in the removal of Cr(VI) and Ni(II) from aqueous solution," *Afr. J. of Environ. Sci. Technol.* 3(11), 360-369.

Marques, A. V., Pereira, H., Meier, D., and Faix, O. (1994). "Quantative analysis of cork (*Quercus suber* L.) and milled cork lignin by FTIR spectroscopy, analytical pyrolysis and total hydrolysis," *Holzforschung* 48 (suppl.), 43-50.

Oh, M., and Tshabalala, M. A. (2007). "Pelletized ponderosa pine bark for adsorption of toxic heavy metals from water," *BioResources* 2(1), 66-81.

Olivella, M. À., Jové. P., Şen, A., Pereira, H., Villaescusa, I., and Fiol, N. (2011). "Sorption performance of *Quercus cerris* with polycyclic aromatic hydrocarbons and toxicity testing," *BioResources* 6(3), 3363-3375.

Park, D., Ahn, C. K., Kim, Y. M., Yun, Y. S., and Park, J. M. (2008). "Enhanced abiotic reduction of Cr(VI) in a soil slurry system by natural biomaterial addition," *J. Hazard. Mater.* 160, 422-427.

Pereira, H., and Ferreira, E. (1989). "Scanning electron microscopy observations in insulation cork agglomerates," *Mater. Sci. Eng.* A 111, 217-225.

Pereira, H. (1992). "The thermochemical degradation of cork," *Wood Sci. Techno.* 26, 259-269.

Pereira, H. (2007). *Cork: Biology, Production and Uses*, Elsevier Public., Amsterdam.

Sarin, V., and Pant, K. K. (2006). "Removal of chromium from industrial waste by using eucalyptus bark," *Bioresour. Technol.* 97, 15-20.

Şen, A., Miranda, I., and Pereira, H. (2012a). "Temperature-induced structural and chemical changes in cork from *Quercus cerris*," *Ind. Crop. Prod.* 37, 508-513.

Şen, A.,Velez Marquez, A., Gominho, J., and Pereira, H. (2012b). "Study of thermochemical treatments 1 of cork in the 150-400ºC range using colour analysis and FTIR spectroscopy," *Ind. Crop. Prod.* 38, 132-138.

Seng, C. E., Lee, C. G., and Liew, K. Y. (2001). "Adsorption of chromium (VI) and nickel (II) ions on acid- and heat-activated deoiled spent bleaching clay," *J. Am. Oil Chem. Soc.* 78, 831-835.

Shen, Y. S., Wang, S. L., Huang, S. T., Tzou, Y. M., and Huang, J. H. (2010). "Biosorption of Cr(VI) by coconut coir: Spectroscopic investigation on the reaction mechanism of Cr(VI) with lignocellulosic material," *J. Hazard. Mater.* 179(1-3), 160-165.

Singha, B., Naiya, T. K., Bhattacharya, A. K., and Das, S. K. (2011). "Cr(VI) ions removal from aqueous solutions using natural adsorbents-FTIR studies" *JEP.* 2, 729-735.

Üstün, G. E. (2009). "Occurence and removal of metals in urban wastewater treatment plants," *J. Hazard. Mater.* 172(2-3), 833-838.

Villaescusa, I., Fiol, F., Cristiani, F., Floris, C., Lai, S., and Nurchi, V. M. (2002). "Copper(II) and nickel(II) uptake from aqueous solutions by cork wastes: A NMR and potentiometric study," *Polyhedron.* 21, 1363-1367.

Villaescusa, I., Fiol. N., Martínez, M., Miralles, N., Poch, J.,and Serarols, J. (2004). "Removal of copper an nickel ions from aqueous solutions by grape stalks wastes," *Water Res.* 38, 992-1002.

Vinodhini, V., and Das, N. (2009). "Mechanism of Cr(VI) biosorption by neem sawdust," *AEJSR.* 4(4), 324-329.

Yılmaz, S., Türe, M., Sadıkoğlu, M., and Duran, A. (2010). "Determination of total Cr in wastewaters of Cr electroplating factories in the I. organize industry region (Kayseri, Turkey) by ICP-AES," *Environ. Monit. Assess.* 167, 235-242.

Article submitted: February 20, 2012; Peer review completed: June 2, 2012; Revised version received: June 29, 2012; Second revision: July 5, 2012; Third revision received and accepted: August 10, 2012; Published: August 15, 2012.

3.2.8. Heavy Metal Removal in Aqueous Environments Using Bark as a Biosorbent: A review

Şen, A., Pereira, H., Olivella, M. A., &Villaescusa, I.

Submetido a Water Research

2012

Heavy Metal Removal in Aqueous Environments Using Bark as a Biosorbent: A review

Ali Şen[1*], Helena Pereira[1], M. Àngels Olivella[2], Isabel Villaescusa[3]

[1]Centro de Estudos Florestais, Instituto Superior de Agronomia, Universidade Técnica de Lisboa, Tapada da Ajuda, 1349-017 Lisboa, Portugal. [2] Department of Chemistry, Sciences Faculty, University of Girona, Campus Montilivi, s/n 17071, Girona, Spain. [3]Department of Chemical Engineering, Escola Politècnica Superior, University of Girona, Mª Aurelia Campmany, 61, 17071, Girona, Spain.

*Corresponding Author. Tel. +351213634662; fax: 213653338

Email address: umutsen@isa.utl.pt (A.U. Şen)

Abstract

Barks are among the widely available and low cost sorbents for metal adsorption. Various studies were made on the utilization of barks in treatment of effluents, particularly to remove heavy metals. A review is made on the research carried out on the biosorption of heavy metals onto barks, including a characterization of bark structure and chemistry. This review highlights and provides an overview of the research on metals sorption on barks over the last 12 years.

From a comprehensive literature review, it was found that biosorption is gaining importance for bark valorization purposes and have promising specific uptake values for heavy metal ions comparable to some commercial activated carbons. In addition, barks have low cost and can be used without any pre-treatment, thus they are green alternatives for heavy metal treatments of industrial waters.

A brief survey of the chemical composition of different barks is presented. Given the bark's structural complexity some considerations are made on the information obtained from the knowledge of the bark structure to better screen bark species for specific metals ions uptake.

Keywords: Bark, adsorption, heavy metal, water effluents, low-cost sorbents

1. Introduction

Tree barks are among the most abundant and under-utilized biosources in the world. Because bark is traditionally considered as a waste product from forest operations and forest industrial processes, statistics on bark production and availability are scarce and usually estimated indirectly using total round wood production. Barks constitute between 9-15 % of stem volume (Harkin and Rowe, 1971) but in some trees may reach up to 22% of log volume (Lu et al., 2006). A factor of 0.13 was proposed to estimate total bark volume by using wood production (Corder, 1976). In 2008, about 1.542 million m^3 of round wood were produced worldwide which implies that approximately 200 million m^3 of bark were produced (Anonymous, 2011). In the U.S., bark generation is estimated to reach 32.6 million tonnes by 2050 (Lu et al., 2006).

Barks are usually treated as a waste stream in timber processing and their disposal or use is a major concern because of the high volumes involved. Bark is known to be either left in the forest after tree felling or used as a fuel by the forest industry (Lu et al., 2006). However, solid waste management methods vary between the countries and depend on economical reasons and market availability. Landfill is the cheapest option in countries with available areas such as the USA, while incineration is the choice in countries where real estate is expensive as in Japan. Recycling is the option in countries with reliable markets such as Switzerland (Anonymous, 2012).

Incineration of bark is not economically viable as the bark has relatively lower calorific value and its considerable water content reduces further this value (9500 and 19000 btu/lb calorific values of crude bark and fuel oils respectively) (Gaballah and Kilbertus, 1998). Environmental

concerns on the burning of bark in relation to soil and air quality are also at stake (Villeneuve, 2004).

In the recent years there was a renewed interest in biomass utilization as a raw-material for production of chemicals, materials and energy, and studies developed focused on the concept of bio-refineries (i.e., to use biomass more efficiently by extracting valuable chemicals and materials) (Tuck et al., 2012). In this bio-refineries concept, bark offers many possibilities because of its complex chemical composition. Main utilization possibilities of bark are summarized in Fig 1. The more traditional routes of energy generation by incineration or other thermochemical processes (such as charcoal production or pyrolysis), or of a raw-material for composting, are complemented by an increased use for materials using the whole bark or fractions (e.g. cork and fibers) as well as a source of chemicals by extraction of soluble materials or chemical modification. A new approach is to use bark as an adsorption substrate for removal of pollutants, namely of heavy metals, from liquid streams.

Fig. 1. Main platforms for bark utilization

Metal adsorption onto bark is an accumulation of metals from a liquid solution (solute) on the surface of the solid bark (adsorbent) forming an atomic or a molecular layer (adsorbate). The term “heavy metal” has been defined differently in the literature: some authors consider heavy metals as metal and semi-metals (metalloids) that cause toxicity while others use the parameters such as density, atomic mass or atomic number. Some metals are not heavy according to these parameters while others such as arsenic are metalloids (Naja et al., 2010). In this review the term heavy metal includes all metals except Group I and Group II elements of the periodic table.

Heavy metal removal from waters is a crucial issue for human health. Heavy metals are not biodegradable and accumulate in living organisms causing various diseases (Bailey et al., 1999). Heavy metal contamination occurs in the effluents of many industries but the important contributors can be grouped as iron and steel production, mining and mineral processing, painting and photography and metal processing and finishing (electroplating) industries (Gaballah and Kilbertus, 1998).

Traditionally treatments of industrial effluents for heavy metal removal have applied precipitation, or adsorption on ion exchange resins or activated carbons. Precipitation is not as effective as ion exchange resins or activated carbon and the need to treat large volumes of sludge after the precipitation causes a further problem. Ion-exchange resins and activated carbon are very effective for heavy metal treatments but they are expensive.

Biosorption is an option to tackle this problem. Bioadsorbents or dead biomass are highly efficient as heavy metal adsorbents, often require little processing, they are abundant in nature as waste material or by-product and have low cost (Bailey et al., 1999). Also, they have advantages over living biomass (e.g. phytoremediation or microbial treatments) since they do not need nutrient supply or maintenance of healthy microbial populations and allow the recovery of metals (Park et al., 2010). Various biomass types were tested for heavy metal adsorption including fungal biomass, bacterial biomass, algae, peat, wood, bark, leaves, pulp, exhausted coffee, etc. (Naja et al., 2010; Kumar, 2006).

The utilization of barks in heavy metal adsorption is a promising research line as barks have shown high capacity to remove metal ions from aqueous solutions. Because barks are abundant, renewable and low cost sources, they appear as excellent alternatives to ion exchange resins and activated carbon for industrial applications. Other less emphasized but yet

101 important advantages of barks as biosorbents are their capability to be used for the removal of
102 low metal concentrations (below 100 ppm) (Vazquez et al., 2002) and their reductive ability
103 which is important in the case of chromium (VI) treatment (Aoyama et al., 2004; Şen et al.,
104 2012).
105
106 The low density and floatability of bark are important factors that must be considered in the
107 high scale industrial applications of bark. The density of bark is similar to that of wood (Ragland
108 and Aerts, 1991) which implies that bark will float if it is used in pond treatments and its metal
109 removal efficiency will be reduced. Applications of packed column systems may solve this
110 problem. The metal recovery after the adsorption can easily be made by acidic washing of the
111 bark and retrieving the metals from the concentrate using electrolytic techniques. Also,
112 incineration or landfill options can be considered since the adsorbent is of low cost (Naja et al.,
113 2010). In order to re-use the bark, a dilute acidic treatment seems to be the best option
114 (Horsfall et al., 2006).
115
116
117
118 There are limited references analyzing the specific bark adsorbents and their heavy metal
119 adsorption features (Bailey et al., 1999; Kumar, 2006). The knowledge on the anatomical and
120 chemical characteristics of barks, the adsorption process and mechanism will allow a screening
121 for higher adsorption efficiency and contribute for bark valorization in the bioadsorption
122 platform.
123
124 The aim of the present paper is to survey the past research over the last 40 years and the
125 recent studies in this matter, and make a state-of-the-art of research on metal sorption by
126 barks having in background the anatomical structure of barks and their chemistry.

2. Bark structure and chemistry

2.1 Bark structure

Barks include all the tissues outside the vascular cambium and constitute the external region of tree stems and branches (Fig. 2). Bark is structurally heterogeneous and includes the phloem (with inner functional region for conduction and an outer non-functional region), the periderm (including phelloderm, phellogen and phellem) and rhytidome. Often bark is also divided into inner bark (including the conducting phloem) and outer bark (non-conducting phloem, periderm and rhytidome)

Fig.2. Schematic diagram of bark: young bark with periderm and epidermis (above) and older bark with a rhytidome (below) (Pereira, 2012a).

Two meristems play the major role in bark formation: the vascular cambium that forms the phloem, and the phellogen that produces the phellem (cork) and the phelloderm, together building up the bark periderm.

The periderm is most often short lived and in most trees, with aging, the rhytidome is formed including various superposed periderms and phloem tissues between them. However, in a few species such as the cork oak (*Quercus suber*) only one periderm is active throughout the life of the tree and no rhytidome is formed (Pereira, 2007). Fig. 3 shows an example of a bark from *Quercus cerris* with a thick rhytidome and the bark of *Q. suber* with only one periderm.

Fig. 3. Bark of *Q.cerris* with a thick rhytidome (above) and bark of *Q.suber* with only one periderm (below)

The bark thickness is closely related to tree species. It increases with age and it is also variable along the tree trunk. In general bark thickness increases with increasing stem diameter but climatic and nutritional conditions as well as silvicultural practices determine the final bark thickness (Roth, 1981).

Phloem percentage also depends on tree species and on growth conditions (Cole, 1973). In some species the phloem is very thin and only comprises a few millimeters but in other species its thickness is at cm scale. Only a small part (usually from 0.1 to 1 mm but also up to 6 mm) of the phloem is physiologically functional for conduction in trees (Esau, 2006).

The cells forming the structure of phloem are sieve elements, axial and radial parenchyma, fibers, sclereids and secretory cells (Roth, 1981). Sieve elements function for water and organic material transfer while axial parenchyma cells function for organic material storage and radial parenchyma cells for transport and storage. Fibers and sclereids are sclerenchyma cells that function as a mechanical support.

The phloem is usually more complex in hardwoods (broad leaved trees) than in softwoods (needle leaved trees) in terms of cell arrangement and cell components. The proportions of cell types differ between bark species. For instance, Quilhó et al. (2000) reported proportions

177 of cell types in *Eucalyptus globulus* phloem as 50% axial parenchyma, 28% fibres, 12% rays
178 (radial parenchyma), 3% sieve elements and 7% sclereids.
179
180
181 *2.2. Bark chemical composition*
182
183 The chemical composition of bark differs from other biomass resources (Table 1). From a
184 chemical point of view, barks are considerably more heterogeneous than wood as regards
185 proportion of the main components as well as their composition. Chemical differences are
186 found between hardwood and softwood barks as exemplified in Table 2 for birch and pine
187 barks (Miranda et al., 2012, 2013).
188
189 In spite of the large diversity found between species, in general, barks contain high amounts of
190 inorganic material that is determined as ash. The most common elements in the inorganic
191 fraction are calcium, magnesium and potassium.
192
193 The non-structural components that may be solubilized by appropriate solvents, the so-called
194 extractives, appear also in larger amounts in barks, and usually show a considerable diversity in
195 terms of chemical families and molecules. The extractives of bark include in general 3 to 5
196 times more hydrophilic compounds than lipophilic compounds (Harkin and Rowe, 1971).
197
198 Another important chemical feature of barks is the presence of suberin as a structural
199 component of the phellem cells. Suberin is a macromolecule with structural functions in the
200 cell wall that is chemically characterized by an interesterified polymer of glycerol to long chain
201 carboxylic hidroxy-acids and diacidos, that constitute a main component of the cork cell wall
202 e.g. about 40% of *Q. suber* cork (Pereira, 2007). Suberin is not found in woods and in the barks

it is included only in the phellem. Therefore the relative amounts of the different anatomical tissues in the bark, namely the proportion of the cork tissue in the periderm and in the rhytidome will result in differences in the chemical composition of whole bark. Depending on the species, suberin may represent between 2 to 45% of the structural chemical components of barks.

Table 1. Range of chemical composition of barks, wood and leaves (Pereira, 2012b)

Table 2. Chemical compositions of barks from a hardwood (*Betula pendula*) and a softwood (*Pinus sylvestris*) barks (Miranda et al., 2012, 2013)

Lignin composition seems highly variable but it must be noted that studies on barks are scarce and mainly made on sclereid cells (Fengel and Wegener, 1989). However bark is heterogeneous and its components can have different lignin compositions. For instance, the cork lignin in the periderm of the hardwood bark of *Q. suber*, has a composition similar to that of softwood lignins (Marques et al., 2005).

Cellulose content of bark is lower than of wood while hemicelluloses content is nearly equal (Table 1). The principal hemicelluloses in softwood and hardwood barks are galactoglucomannans and arabino-4-O-methyl-glucuronoxylan respectively, and are similar to those found in the corresponding woods (Rowell, 2012).

The different types of cells in the bark have different cell wall structures: parenchyma cells and sieve elements have thin primary cell walls dominated by cellulose; fibres and sclereids have

thick cell walls with high proportion of lignin; and cork cells have secondary walls dominated by suberin.

3. Heavy metal adsorption onto bark

Barks have shown among the tree biomass components the highest capacity for heavy metal sorption followed by cones, needles and wood. For instance, Al-Asheh and Duvnjak (1997) found Cd^{2+} uptake rates of 9.2, 7.5 and 7.1 μg/mg for pine bark, cones, and needles, respectively. Shin et al. (2007) compared Cd^{2+} uptakes of juniper wood and bark and concluded that bark had 3-4 times higher adsorption capacity than wood. Boving et al. (2008) studied various agricultural wastes including bark in relation to Cu^{2+} adsorption and concluded that barks were the most effective filtration media from all the adsorbents tested.

Shin (2005) found higher Cd^{2+} adsorption in bark than in wood in *Juniperus monosperma* and explained it by the contribution of calcium oxalate to adsorption as confirmed by x-ray diffraction. Barks contain calcium oxalate monohydrate crystals while in wood this structure is generally absent (Trockenbrodt, 1995) (Fig. 4).

Fig. 4. Calcium oxalate crystals in teak bark

Heavy metals adsorption on biomass is defined as a physicochemical process. Three factors seem to play an important role in heavy metal adsorption on barks, i.e., solution system related, metal related and adsorbent related factors.

3.1 Adsorption system parameters

253 The pH, temperature and adsorption time are the most important adsorption system
254 parameters.
255
256 The pH can influence metal adsorption in three ways. First, the state of active sites can change
257 with pH; and at lower pH the active sites are protonated and a competition starts between
258 metal ions and protons for the active sites. Second, extreme pH values can alter the surface of
259 the adsorbent. Third, the metal speciation in solution is pH dependent and at higher pH values
260 metal hydroxide complexes and precipitates can be formed (Naja et al., 2010). Metal
261 adsorption onto barks normally occurs under slightly acidic conditions and within the first
262 minutes of contact time (Martin-Dupont et al., 2002).
263
264 Temperature can also alter the adsorption results. With temperature increase the adsorption
265 of metals increases, although the effect of temperature is small in the 4-25°C range (Martin-
266 Dupont et al., 2002). Ghodbane et al (2008) showed that maximum cadmium (II) uptake
267 capacity of Eucalyptus bark increased from 14.53 mg/g to 16.47 mg/g when the temperature
268 increased from 20 to 50°C. Higher temperatures can change the structure of the adsorbent
269 and the adsorption capacity may be reduced (Naja et al., 2010). The effect of structure change
270 was observed in cork granules of *Q.cerris* where 200 to 350°C heat treated cork granules
271 showed reduced adsorption capacity (Şen et al., 2012).
272
273 *3.2 Metal related factors*
274
275 Metal related factors are sorption type i.e., non-competitive or competitive sorption, cation
276 hydration enthalphy, polarisability and number of unpaired electrons (Martin-Dupont et al.,
277 2002).
278

279 The metal cations in solution may compete with other ions for the adsoption sites. When there
280 is only one metal available, the adsorption is non-competitive but in treatments of industrial
281 effluents, there are many metals available for the adsorption. These metals may suppress each
282 other (competitive adsorption) (Gloaguen and Morvan, 1997). In contrast, Hanzlik et al (2008)
283 reported that copper and silver were adsorbed better when both existed in solution and total
284 metal uptake was higher than in single metal ion solutions. Li and Li (2003) reported that
285 spruce bark showed a selectivity order Cd<Cu<Pb in multielement complex adsorption.
286
287 When the hydration energy is smaller, the cation can more easily lose water ligands to bind the
288 adsorbent. Larger ions are more polarisable than smaller ions because part of their electrons is
289 less retained. The more polarisable the metal, the easier is the adsorption.
290
291 The number of unpaired electrons also influences the adsorption. Martin-Dupont et al (2002)
292 showed that Cr (III) had a higher affinity to bind to bark than cations with lower hydration
293 enthalpy because of its unpaired electrons.
294
295
296 *3.3 Adsorbent related factors*
297
298 Adsorbent related factors are a consequence of the anatomical and chemical properties of
299 barks. It is important to note that the quantity of the adsorbent also alters the adsorption by
300 changing the adsorption capacity. Alves et al. (1993) proposed an optimal loading for the
301 chromium removal of 1-2 mg/L by *Pinus sylvestris* bark.
302

303 The different cell types in bark may be important in adsorption due to their different chemical
304 composition. The difference between the phloem and rhytidome particularly affects
305 adsorption. However, the heterogeneity of bark structure has seldom been taken into account.
306
307 Only in one research (Aoyama et al., 2004) the inner (phloem) and outer (rhytidome) barks of
308 *Cryptomeria japonica* were tested separately for heavy metal adsorption and concluded that
309 adsorption capacity was higher in the rhytidome than in the phloem. However, more studies
310 are needed before making a generalization on the different adsorption performances of
311 phloem and rhytidome.
312
313 Scanning electron microscopy (SEM) images of *Q.suber* cork before and after Cd(II) and Pb(II)
314 treatments did not shown any difference of the cork morphology (López-Mesas et al., 2011).
315 TheSEM-EDX results of Cr^{6+} laden cork-enriched rhytidome granules of *Q.cerris* showed that
316 the metal ions were homogeneously adsorbed by the different cell types of rhytidome (Şen et
317 al., 2012).
318
319 Rowell (2006) reported that adsorptive sites of the lignocellulosic materials increase only
320 slightly with grinding of the material and concluded that heavy metal sorption by
321 lignocellulosic materials does not depend on particle size. Therefore differences in adsorption
322 performance may result mainly from chemical differences of bark cell wall components such as
323 crystal bearing cells in bark (Shin, 2005).
324
325 Chemical composition differences between bark and other biomass may play an important role
326 in heavy metal adsorption, particularly the higher inorganic (ash) and extractive contents of
327 bark.
328

329 The ash content of barks was often ignored in heavy metal adsorption studies even if the
330 mineral content may affect ionic interaction between the metal and the bark structure and
331 contribute to ion-exchange mechanism. Escudero et al (2008) confirmed potassium ions
332 release from Yohimbe bark during copper (II) adsorption.
333
334 Extractives have often been considered in heavy metal adsorption onto the bark (Martin-
335 Dupont et al. 2006). Extractives have advantages in heavy metal treatments: some extractives
336 such as flavanoids (particularly the B ring) can complex with metals in water (Vazquez et al.,
337 2002) while tannins and pectins are considered the active ion-exchange compounds with their
338 carboxylic and phenolic groups providing active sites for metal binding (Gloaguen and Morvan,
339 1997). On the other hand, extractives originate coloring problems in water by leaching of
340 compounds such as hydrolysable tannins that may be harmful to the aquatic life (Aoyama and
341 Tsuda, 2001).
342
343 To avoid the release of soluble tannins from the bark into water several treatments were
344 tested: Haussard et al., (2003) treated the bark with microorganisms or with copper or
345 chromium solution; Vázquez et al., (2002) used acidified formaldehyde; Oh and Tshabalala
346 (2007) consolidated bark pine into pellets using citric acid as cross-linking agent before
347 removing Cd II), Cu (II), Zn (II) and Ni (II).
348 Freer et al. (1989) showed that the uranium adsorption capacity of *Pinus radiata* bark
349 improved with acidified formaldehyde treatments. The acid type is important in these
350 treatments i.e. nitric acid/ formaldehyde treatment gave better results than sulphuric
351 acid/formaldehyde (Freer et al., 1989). Martin-Dupont et al. (2004) used peroxide
352 functionalization followed by 4,4'-diamino-2,2'-stilbene disulfonic acid derivatization in
353 presence of aspartic acid with Douglas fir bark. However the toxicity of formaldehyde must
354 also be taken into account in these treatments (Martin-Dupont et al., 2004). Palma et al (2003)

355 reported that acidified formaldehyde treated tannins had lower adsorption capacity than the
356 bark treated in the same way.
357
358 Lignin was always regarded along with tannins and pectins as the main responsible for heavy
359 metal adsorption onto the barks (Martin-Dupont et al. 2006; Rowell, 2006; Şen et al., 2012).
360 Some cations have shown different selectivity to bark components: Cu (II) was bound to
361 phenolic groups of lignins and tannins while Pb(II) was bound to carboxylic groups in
362 polysaccharides (Martin-Dupont et al., 2006). Şen et al. (2012) indicated that Cr (VI) reacts with
363 polysaccharides of cork as well as with lignin and suberin. A NMR study of cork showed that
364 carbohydrate moieties of cork produced metal complexations (Villaescusa et al., 2002). Heat
365 modified lignin structure was also reacted with chromium (Şen et al. 2012).
366
367 Suberin is also involved in heavy metal adsorption. Psareva et al. (2005) suggested the
368 importanc e of acidic monomers of suberin in heavy metal adsorption. Şen et al (2012)
369 analyzed untreated and Cr (VI) treated *Q.cerris* cork samples with FT-IR spectroscopy and
370 concluded that Cr(VI) was adsorbed onto suberin. The different monomeric composition of
371 two suberins from *Q. suber* and *Q.cerris* corks as well as differences in chemical compositions
372 of different cork layers may affect the adsorption. Şen et al (2010) showed that *Q. cerris*
373 suberin is formed primarily by ω-hidroxyacids (90%) and α,ω-diacids (8%) while *Q. suber*
374 suberin is constituted by ω-hidroxyacids (36%) and α,ω-diacids (62%). Jové et al. (2011) found
375 significant differences in chemical composition between outer, center and inner cork layers
376 with suberin content increasing from the outer to the inner part of cork while holocellulose
377 content was decreased.
378
379 Surface acidic groups in the barks are thought to play an important role in heavy metal
380 adsorption by ion-exchange mechanism. Chubar (2004b) showed that metal cations bind to

carboxylic groups in cork. A total acidic group content of 1.64 meq/g (López-Mesas et al., 2011) and 1.88 mmol/g (Olivella et al., 2011) were detected on the cork surface. *Q. cerris* cork had lower total acidic (1.55 mmol/g) but higher strong acidic groups (0.85 to 0.73 mmol/g) than *Q.suber* cork. Phenolic hydroxyl groups as well as weak acid groups were also higher in *Q. suber* cork (Olivella et al., 2011). Psareva et al. (2005) treated cork with hydrochloric acid solution and increased uranium adsorption due to increase of strong and weak acidic groups.

The pH at which the adsorbent surface charge is equal to zero is defined as the point of zero charge (pHpzc). The pHpzc gives information on the ionization of functional groups and their interaction with metal species in solution; at solution pHs higher than pHpzc, the sorbent surface is negatively charged and could interact with positive metal species while at pHs lower than pHpzc, the solid surface is positively charged (Fiol and Villaescusa, 2009). Bark surfaces were found to be positively charged (pHpzc= 6.8 for *Pausinystalia yohimbe*) or negatively charged (pH_{pzc}= 3.6 for *Q. suber*) with interaction of Cu^{2+} or (pHpzc=4.4, *Q. cerris*) with interaction of Cr^{6+} (Fiol and Villaescusa, 2009; Şen et al., 2012).

The elemental compositions of the untreated *Q.cerris* and heat treated *Q.suber* corks were investigated in chromium (VI) adsorption to explain the similar maximum uptake values of the two sorbents. The H/C ratios of the two adsorbents were similar (1.49 and 1.48) (Şen et al., 2012).

4. Mechanism, models and determination of adsorption

The ion-exchange or complex formation mechanisms are often used to explain metal binding onto barks (Randall et al.,1974; Martin-Dupont et al., 2002; Vazquez, 2002; Escudero et al., 2008; Nurchi et al., 2010). In the ion-exchange mechanism, metal cations exchange with deprotonated groups on the adsorbent surface. Some functional groups of bark such as hydroxyl and carboxyl groups loose the associated proton and behave as an acid while other groups such as carbonyl behave as a base because of its electronegative oxygen atom (Brás et al, 2004).

The carboxylic acid group is the main functional group involved in metal adsorption by biomass, followed by hydroxyl group, aromatic rings and amine group (Nurchi et al., 2010). These four groups make approximately 85% of the total groups involved in adsorption.

Adsorption isotherms are used to describe the adsorption process of metal ions at constant temperature. Mainly Langmuir or Freundlich adsorption isotherm models are used to calculate metal binding as a function of equilibrium concentration of the metal ion in solution without considering pH or the other ions in the system (Naja et al., 2010). The Freundlich isotherm assumes that the stronger binding sites are occupied first and binding strength decreases with increasing site occupation. The following equation is used to define Freundlich isotherm (Naja et al., 2010):

$$Mq = K \times [M]^{\frac{1}{n}}$$

where the constant K is related to maximum binding capacity and constant n is related to binding strength.

Langmuir isotherm is based on the assumption that adsorption is a chemical phenomenon. According to Langmuir isotherm the sorption is restricted to a monolayer, all sorption sites are uniform, there is only one adsorbent, one sorbet molecule reacts with one active site and there is no interaction between the sorbed species (Naja et al., 2010).

The Langmuir isotherm is defined by the following equation:

$$q = (qmax \times b \times Cf) \div (1 + b \times Cf)$$

where q is the amount of metal adsorbed (mg/g, mmol/g, meq/g), qmax is the maximum metal uptake by the adsorbent, b is the Langmuir constant and Cf is the final (equilibrium) concentration of the metal. The b parameter reflects the affinity (the lower b value, the higher affinity) of the adsorbent for the metal. The Langmuir model is useful in bark metal adsorption studies because it gives the *qmax* and b information. Generally higher qmax and lower b values are sought in adsorbents.

In most sorption studies reported in the literature, authors use some of the available isotherm models and calculate the isotherm parameters by using different regression methods. Recently, Poch and Villaescusa (2012) reported that the Orthogonal Distance Regression (ODR) method gives the most accurate estimates of the Langmuir isotherm parameters among the different methods when the experimental data have an error.

The metal uptake of the bark may be determined with batch adsorption essays or using packed column. In laboratory conditions batchwise experiments are generally conducted and according to results upflow or downflow packed bed tests are made to predict industrial

utilization possibilities of the adsorbents. In batch experiments, the metal adsorption is determined by introducing the metal solutions onto bark and calculating the difference of initial and final metal concentrations of the filtrates. The column experiments generally give higher adsorption results than the batch tests (Palma et al., 2003).

For the determination of metal concentration, generally Flame Atomic Absorption Spectroscopy (FAAS) is applied but inductively coupled plasma atomic emission spectroscopy (ICP-AES) and spectrophotometric methods are also commonly used. To determine the active sites of the adsorbent Fourier Transformed Infrared Spectroscopy (FT-IR), Diffuse Reflectance Infrared Fourier Transform Spectroscopy (DRIFTS), Nuclear Magnetic Resonance Spectroscopy (NMR), Electron Spin Resonance Spectroscopy (ESR) or potentiometric titration methods are applied (Park et al., 2010; Nurchi et al., 2010). Metal localizations and their bindings on the adsorbent surface are evaluated with Scanning Electron Microscopy Energy-dispersive X-ray Spectroscopy (SEM-EDX), X-ray Absorption Spectroscopy (XAS) or X-ray Photoelectron Spectroscopy (XPS) (Nurchi et al., 2010).

The metal adsorption study usually involves determination of the equilibrium time and pH effect on the adsorption followed by the determination of the maximum uptake study with different metal concentrations.

5. Overview of adsorption studies

5.1 Barks and metals tested

Although it is estimated that heavy metal adsorption studies have been conducted as early as the 1920´s scientists started testing new biosorbents including bark only after the 1970´s. It is noteworthy that bark adsorption tests with bark as adsorbent gained importance between 1970 and 1980 (Fig. 5). One of the oldest publications on bark adsorption was the study of Masri et al. (1974). In that study Douglas fir and black oak barks were treated with mercury solutions and the adsorption quantities were 100mg Hg/g for Douglas fir bark and 400 mg Hg/ g for black oak bark.

From that period on, research publications increased substantially, especially between the periods 1990-2000 and 2000-2010. The fact that many of the research publications are very recent (in the last 10 years), is indicative of the interest in bark valorization and on the use of biosorbents for water treatments (Figs. 5-6).

Fig. 5 Number of search results using *bark*, *adsorption* and *heavy metal* keywords on bark adsorption with heavy metals based on Google Scholar Data.

Fig. 6 Number of search results (two year averages) using *bark*, *adsorption* and *heavy* metal keywords on bark adsorption with heavy metals in the last 10 years based on Google Scholar Data.

Google Trends analysis in 2011 and Google Insights for Search between years 2004-2012 showed that bark was studied mostly in USA, Canada, Australia and UK, while adsorption was searched in South Korea, India, Malaysia and Thailand. The keyword heavy metal was searched mostly in India, USA, Canada and Brazil. Nurchi and Villaescusa (2008) reported increasing

510 interest on the use of agricultural biomass in the emerging countries of India, Brazil, Turkey,
511 Argentina and Nigeria. These results indicate the current problems of the countries (e.g. bark
512 in large timber producing countries such as the USA) and industrialization process (metal
513 effluents in India).
514
515 In the last four decades more than 60 research studies were reported on the biosorption of
516 heavy metals with barks. More than 40 bark species were tested (mainly softwood barks) and
517 over 10 heavy metals were studied (Table 3-4). The adsorption tests were conducted mainly
518 using locally available low cost tree barks.
519
520 **Table 3.** Research on softwood barks as biosorbents: Metal cations and corresponding *qmax*
521 (mmol/g) values
522
523 **Table 4.** Research on hardwood barks as biosorbents: Metal cations and corresponding qmax
524 (mmol/g) values
525
526 Copper and cadmium are the most studied metals followed by zinc and chromium. Lead and
527 nickel were also studied to some extent. Nurchi and Villaescusa (2008) reported that these six
528 metals account for 90% of the adsorption studies with agricultural biomass. Studies with iron
529 and mercury are rare and there is only one study with uranium and vanadium.
530
531
532
533 *5.2 Critical evaluation aspects*
534

Several authors have tested barks of different species for heavy metal adsorption. However, most ignored bark origin, structure and chemistry which might be important aspects regarding adsorption performance.

The reporting of the species scientific names of the barks used was sometimes neglected and in some cases dubious common names were used such as black oak, redwood or eucalypt bark. This is a drawback for comparing adsorption performances of different barks.

The heterogeneity of the bark structure was also often ignored in the heavy metal adsorption tests. In most cases whole samples (phloem and rhytidome milled together) were used in the laboratory adsorption tests.

The metal solutions were usually prepared in the laboratory but industrial effluents were also tested. Sarin and Pant (2006) studied chromium adsorption in industrial effluent from a metal finishing auto ancillary unit with *Eucalyptus globulus* bark.

Chemical compositions of the barks used for adsorption were generally not studied although usually barks with higher lignin or tannin contents were used. Martin-Dupont et al. (2006) studied the chemical composition of the barks to analyze $Cu^{2+}$and Pb^{2+} interactions with bark active groups.

In metal removing studies with bark, important parameters seem to be metal uptake values, maximum uptake and metal uptake affinity of the adsorbent. The metal uptake values varied between 50 to 99% (Gaballah and Kilbertus, 1998). These values can be altered by changing the sorption parameters and therefore are not adsorbent specific. Metal adsorption models are therefore used to describe the adsorption process. Langmuir parameters of maximum

561 uptake (*qmax*) and metal uptake affinity (b) have often been used although, some authors also
562 used the Freundlich model. Other types of models were not encountered.
563
564 The values of *qmax* and *b* are related to the adsorbents. In barks, the highest *qmax* values
565 were usually obtained with mercury (400 mg/g) followed by uranium (138 mg/g) and
566 chromium (71.9 mg/g). However, mg/g unit may mislead the real effectiveness of the
567 adsorbents because it does not consider the atomic mass of the metals (Nurchi and
568 Villaescusa, 2012). Therefore, qmax values with different barks were compared using mmol/g
569 units (Table 3 and 4).
570
571 Bark had equal or even more metal uptake capacity than activated carbon (Seki et al., 1997;
572 Aoyama and Tsuda, 2001). For instance, Cd^{2+} removal values were: for *Abies sachalinesis*: 6.7
573 mg/g, *Taxus cuspidata* 14.4 mg/g, activated carbon (granular) 7.3 mg/g, activated carbon
574 (powder) 7.1 mg/g (Table 3). Likewise Cu^{2+} adsorption of activated carbon varied between 5.8
575 and 6.5 mg/g while Zn^{2+} adsorption was 5.7 and 2.5 mg/g for granular and powder forms
576 respectively. Higher values were achieved with barks (Table 3).
577
578 Among the low cost bio-sorbents, lignin, chitosan and cotton have shown higher metal uptake
579 capacities than bark. The uptake values were 1587 mg Pb/g lignin, 796 mg Pg/g chitosan, 1123
580 mg Hg/ g chitosan and 1000 mg Hg/ g crosslinked polyethylenimine (CPEI) cotton (Bailey et al.,
581 1999)
582
583 Different bark granulometries were used in adsorption tests ranging from 150 µm (Gundogdu
584 et al, 2009) to 4 mm (Jauberty et al.2011, López-Mesas et al., 2011). For the batch tests usually
585 smaller granulometries were used but in column tests larger particles were preferred to
586 prevent clogging of the column (Jauberty et al., 2011). The adsorption was higher with smaller

587 particles because of the higher surface area, but the adsorption might also have been favored
588 by the mineral content of smaller particles. Liu and Bi (2011) and Miranda et al. (2012-2013)
589 reported that smaller bark particles have higher mineral contents than bigger particles in pine,
590 eucalypt, birch and spruce barks.
591
592
593 **6. Conclusions and prospects**

594 There is an increasing interest in using barks and other biomasses for heavy metal effluent
595 treatments because they provide a low-cost green alternative without pre-treatments.
596 Adsorption studies using barks are gaining importance also for valorization purposes of bark.

597 Generally softwood barks were studied more than hardwood barks. Softwood barks of Pinus,
598 Picea and Larix species were among the most studied species.

599 Among the metals tested, copper and cadmium were the most studied metals followed by zinc
600 and chromium. Barks of *Acacia leucephala*, *Cryptomeria japonica* and *Sequoia sempervirens*
601 showed higher potential in the removal of copper, chromium and mercury, respectively. In
602 addition *Abies sachalinesis* and *Taxus cuspidata* barks revealed promising specific uptake
603 values for the heavy metal ions that are comparable with commercial activated carbons.

604 However the studies done until now are far from being complete and more data are needed to
605 better screen bark species for specific metals. Special attention should be given to the
606 heterogeneity of bark and the adsorption assays should better explore this structural
607 complexity and its associated chemical composition. There is a need for mechanistic studies
608 that include such issues as binding sites nature, coordination chemistry, oxidation states and
609 the speciation of metals in solution. It is also advisable that scientific names should be used
610 when reporting the studied bark species.

611 Careful bark type-metal combinations, as well as good selection of adsorption parameters may
612 substantially improve the adsorption processes. Furthermore the high sorption efficiency
613 proved by some barks in packed column systems underline a promising field of research to
614 transfer the technology from laboratory scale to industrial scale for detoxification of liquid
615 wastes containing metal ions.

616

617

618 **References**

619 Acemioglu, B., 2004. Removal of Fe (II) ions from aqueous solution by Calabrian pine bark
620 wastes. Bioresource Technology 93 (1), 99-102.

621 Alves, M.M., González Beça, C.G., Guedes de Carvalho, R., Castanheira, J.M., Sol Pereira, M.C.,
622 Vasconcelos, L.A.T., 1993. Chromium removal in tannery wastewaters"polishing" by *Pinus*
623 *sylverstris* bark. Water Research 27 (8), 1333-1338.

624 Anonymous., 2011. State of World's Forests 2011. Food and Agriculture Organization of the
625 United Nations. Rome.

626 Anonymous., 2012. World of waste. Science 337, 664-667. Date of Access: 30.08.2012.
627 www.sciencemag.org/special/waste

628 Argun M.E., Dursun, S., 2008. A new approach to modification of natural adsorbent for heavy
629 metal adsorption. Bioresource Technology, 99 (7), 2516.

630 Al-Asheh, S., Duvnjak, Z., 1997. Sorption of cadmium and other heavy metals by pine bark.
631 Journal of Hazardous Materials 56, 35-51.

632 Aoyama, M., Tsuda, M., 2001. Removal of Cr(VI) from aqueous solutions by larch bark. Wood
633 Science and Technology 35, 425-434.

634 Aoyama, M., Kishino, M., Jo, T.S., 2004. Biosorption of Cr(VI)on Japanese cedar bark.
635 Separation Science and Technology 39 (5), 1149-1162.

636 Bailey, S.E., Olin, T.J., Bricka, R.M., Adrian, D.D., 1999. A review of potentially low-cost sorbents
637 for heavy metals. Water Research 33, 2469–2479.

638 Boving, T.B., Klement, J., Rowell, R., Xing, B., 2008. Effectiveness of wood and bark in removing
639 organic and inorganic contaminates from aqueous solution. Molecular Crystals and Liquid
640 Crystals 483 (1), 339-347.

641 Brás, I., Lemos, L.T., Alves, A., Pereira, M.F.R., 2004. Application of pine bark as a sorbent for
642 organic pollutants in effluents. Management of Environmental Quality 15 (5), 491-501.

643 Chubar, N., Carvalho, J.R., Correia, M.J.N., 2004a. Cork biomass as biosorbent for Cu(II), Zn(II)
644 and Ni(II). Colloids and Surfaces A: Physicochemical and Engineering Aspects 230, 57-65.

645 Chubar, N., Carvalho, J.R., Correia, M.J.N., 2004b. Heavy metals biosorption on cork biomass:
646 effect of the pre-treatment. Colloids and Surfaces A: Physicochemical and Engineering Aspects
647 238, 51-58.

648 Cole, D.M., 1973. Estimation of phloem thickness in lodgepole pine. USDA Forest Service
649 Research Paper. INT-148.

650 Corder, S.E., 1976. Properties and uses of bark as an energy source. XVI IUFRO World Congress,
651 Oslo, Norway.

652 Escudero, C., Fiol., N., Poch, J., Villaescusa, I., 2008. The kinetics of copper sorption onto
653 yohimbe bark wastes. International Journal of Environment and Pollution 34 (1-4), 215-230.

654 Fengel, D., Wegener, G., 1989. Wood: Chemistry, Ultrastructure, Reactions.

655 Fiol, N., Villaescusa, I., Martinez, M., Miralles, N., Poch, J., Serarols, J., 2003. Biosorption of Cr
656 (VI) using low cost sorbents. Environmental Chemistry Letters 1, 135–139.

657 Fiol, N., Villaescusa, I., 2009. Determination of sorbent point zero charge: usefulness in
658 adsorption studies. Environmental Chemistry Letters 7, 79-84.

659 Freer, J., Baeza, J., Maturana, H., Palma, G., Duran, N., 1989. Removal and recovery of uranium
660 by modified *Pinus radiata* D. Don. bark. Journal of chemical technology and biotechnology 46
661 (1), 41-48.

662 Gaballah, I., Kilbertus, G., 1998. Recovery of heavy metal ions through decontamination of
663 synthetic solutions and industrial effluents using modified barks. Journal of Geochemical
664 Exploration 62 (1-3), 241-286.

665 Ghodbane, I., Nouri, K., Hamdaoui, O., Chiha, M., 2008. Kinetic and equilibrium study for the
666 sorption of cadmium (II) ions from aqueous phase by eucalyptus bark. Journal of hazardous
667 materials 152, 148-158.

668 Gloaguen, V., Morvan, H., 1997. Removal of heavy metal ions from aqueous solution by
669 modified barks. Journal of Environmental Science and Health. Part A: Environmenal Science
670 and Engineering and Toxicology 32 (4), 901-912.

671 Gundogdu, A., Ozdes, D., Duran, C., Bulut V.N., Soylak, M., Senturk, H.B., 2009. Biosorption of
672 Pb(II) ions from aqueous solution by pine bark (*Pinus brutia* Ten.). Chemical Engineering
673 Journal 153, 62-69.

674 Harkin. J.M., Rowe, J.W., 1971. Bark and its possible uses. Research note. FPL.

675 Hanzlik, J. Jehlicka, J., Sebek, O., Weishauptova, Z., Machovic, V., 2004. Multi-component
676 adsorption of Ag (I), Cd (II) and Cu (II) by natural carbonaceous materials. Water Research 38,
677 2178-2184.

678 Haussard, M., Gaballah, I., Kanari, N., De Donato, O., Barres, O., Villieras, F., 2003. Separation
679 of hydrocarbons and lipid from water using treated bark. Water Research 37 (2), 362-374.

680 Hosrsfall, M., Ogban, F.E., Akporhonor, E.E., 2006. Recovery of lead and cadmium ions from
681 metal-loaded biomass of wild cocoyam (*Caladium bicolor*) using acidic, basic and neutral
682 eluent solutions. Electronic Journal of Biotechnology 9 (2), 152-156.

683 Jauberty, L., Gloaguen, V., Astier, C., Krausz, P., Delpech, V., Berland, A., Granger, V., Niort, I.,
684 Royer, A., Decossas, J.L., 2011. Bark, a suitable biosorbent for the removal of uranium from
685 waste water-From laboratory to industry. Radioprotection 46 (4), 443-456.

686 Jové, P. Olivella, M.A., Cano, L., 2011. Study of the variability in chemical composition of bark
687 layers of *Quercus suber* L. From different production areas. BioResources 6 (2), 1806-1815.

688 Kumar, U., 2006. Agricultural products and by-products as a low-cost adsorbent for heavy
689 metal removal from water and waste-water: A review. Scientific Research and Essay 1 (2), 33-
690 37.

691 Li, F., Li, L.Y., 2003. An equation characterizing multi-heavy-metal sorption onto bentonite,
692 forest soil and spruce bark. Environmental Technology 24, 1479-1490.

693 Liu, X., Bi, X.T., 2011. Removal of inorganic constituents from pine barks and switchgrass. Fuel
694 Processing Technology 92 (7), 1273-1279.

695 Lohani, M.B., Singh, A., Rupainwar, D.C., Dhar, D.N., 2008. Studies on efficiency of guava
696 (Psidium guajava) bark as bioadsorbent for removal of Hg (II) from aqueous solutions. Journal
697 of Hazardous Materials 159 (2-3), 626-629.

López-Mesas, M., Navarrete, E.R., Carrillo, F., Palet, C., 2011. Bioseparation of Pb (II) and Cd (II) from aqueous solution using cork waste biomass. Modelling and optimization of the parameters of the biosorption step. Chemical Engineering Journal 174, 9-17.

Lu, W., Sibley,J.L., Gilliam, C.H., Bannon, J.S., Zhang, Y., 2006. Estimation of U.S. bark generation and implications for horticultural industries. Journal of Environmental Horticulture 24 (1), 29-34.

Martin-Dupont, F., Gloaguen, V., Granet, R., Guilloton, M., Morvan, H., Krausz, P., 2002. Heavy metal adsorption by crude coniferous barks: A modelling study. Journal of Environmental Science and Health Part A 37 (6), 1063-1073.

Martin-Dupont, F., Gloaguen, V., Granet, R., Guilloton, M., Krausz, P., 2004. Chemical modifications of Douglas fir bark, a lignocellulosic by-product-enhancement of their lead (II) binding capacities. Separation Science and Technology 39 (7), 1595-1610.

Martin-Dupont, F., Gloaguen, V., Guilloton, M., Granet, R., Krausz, P., 2006. Study of the chemical interaction between the barks and heavy metal cations in the sorption process. Journal of Environmental Science and Health Part A 41 (2), 149-160.

Marques, A.V., Pereira, H., Meier, D., Faix, O., 2005. Structural characterization of cork lignin by thioacidolysis and permanganate oxidation. Holzforschung 53 (2), 167-174.

Masri, M.S., Reuter, F.W., Friedman, M., 1974. Binding of metal cations by natural substances. Journal of Applied Polymer Science 18, 675-681.

Miranda, I., Gominho, J., Mirra, I., Pereira, H., 2012. Chemical characterization of barks from *Picea abies* and *Pinus sylvestris* after fractioning into different particle sizes. Industrial Crops and Products 36, 395-400.

720 Miranda, I., Gominho, J., Mirra, I., Pereira, H., 2013. Fractioning and chemical characterization
721 of barks of *Betula pendula* and *Eucalyptus globulus*. Industrial Crops and Products 41, 299-305.

722 Munagapati, V.S., Yarramuthi, V., Nadavala, S.K., Alla, S.R., Abburi, K., 2010. Biosorption of Cu
723 (II), Cd (II) and Pb (II) by *Acacia leucephala* bark powder:Kinetics, equilibrium and
724 thermodynamics. Chemical Engineering Journal 157, 357-365.

725 Mohan, S., Sumitha, K., 2008. Removal of Cu (II) by adsorption using *Casuarina equisetifolia*
726 bark. Environmental Engineering Science 25 (4), 497-506.

727 Naja, G.M., Volesky, B., Murphy, V., 2010. Biosorption, metals. In: Encyclopedia of Industrial
728 Biotechnology, Flickinger, M., ed. Wiley Interscience, NY.

729 Nurchi, V.M., Villaescusa, I., 2008. Agricultural biomasses as sorbents of some trace metals.
730 Coordination Chemistry Reviews 252, 1178-1188.

731 Nurchi, V.M., Crisponi, G., Villaescusa, I., 2010. Chemical equilibria in wastewaters during toxic
732 metal ion removal by agricultural biomass. Coordination Chemistry Reviews 254, 2181-2192.

733 Nurchi, V.M., Villaescusa, I., 2012. Sorption of toxic metal ions by solid sorbents: A predictive
734 speciation approach based on complex formation constants in aqueous solution. Coordination
735 Chemistry Reviews 256, 212-221.

736 Oh, M., Tshabalala, M., 2007. Pelletized ponderosa pine bark for adsorption of toxic heavy
737 metals from water. BioResources 2 (1), 66-81.

738 Olivella, M.A., Jové, P., Şen, A., Pereira, H., Villaescusa,I., Fiol, N., 2011. Sorption performance
739 of *Quercus cerris* cork with polycyclic aromatic hydrocarbons and toxicity testing. BioResources
740 6 (3), 3363-3375.

741 Palma, G., Freer, J., Baeza, J., 2003. Removal of metal ions by modified *Pinus radiata* bark and
742 tannins from water solutions. Water Research 37, 4974-4980.

743 Park, D., Yun, Y.S., Park, J.M., 2010. The past, present, and future trends of biosorption.
744 Biotechnology and Bioprocess Engineering 15, 86-102.

745 Pereira, H., 2007. Cork: Biology, Production and Uses. Elsevier Publications, Amsterdam.

746 Pereira, H., 2012a. Anatomical studies of barks. I SINBOT, International Symposium on Applied
747 Botany. Federal University of Lavras, 4-6 Oct, Lavras, Brasil.

748 Pereira, H., 2012b. The importance of biomass structure and chemical composition for
749 biorefineries. 2012 IUFRO Conference. 8-13 Jul, Lisbon, Portugal.

750 Poch, J., and Villaescusa, I., 2012. Orthogonal distance regression: A good alternative to least
751 squares for modelling sorption data. Journal of Chemical & Engineering Data 57, 490-499.

752 Prasad, A.G.D., Abdullah, M.A., 2009. Biosorption of Fe (II) from aqueous solution using
753 tamarind bark and potato peel waste: Equilibrium and kinetic studies. Journal of Applied
754 Sciences in Environmental Sanitation 4 (3), 273-282.

755 Psareva, T.S., Zakutevskyy, O.I., Chubar, N.I., Strelko, V.V., Shaposhinikova, T.O., Carvalho, J.R.,
756 Correia, M.J.N., 2005. Uranium sorption on cork biomass. Colloids and Surfaces A:
757 Physicochemical and Engineering Aspects 252, 231-236.

758 Quilhó, T., Pereira, H. Richter, H.G., 2000. Within-tree variation in phloem cell dimensions and
759 proportions in *Eucalyptus globulus*. IAWA Journal 21 (1), 31-40.

760 Ragland, K.W., Aerts, D.J., 1991. Properties of wood for combustion analysis. Bioresource
761 Technology 37, 161-168.

762 Roth, I., 1981. Structural patterns of tropical barks. Gebruder Borntraeger, Berlin.

763 Rowell, R.M., 2006. Removal of metal ions from contaminated water using agricultural
764 residues. Ecowood 2006: 2nd International Conference on Environmentally-Compatible Forest
765 Products. Fernando Pessoa University. Oporto, Portugal.

766 Rowell, R.M., 2012. Handbook of wood chemistry and wood composites. CRC Press.

767 Sarin, V., Pant, K.K., 2006. Removal of chromium from industrial waste by using eucalyptus
768 bark. Bioresource Technology. 97. 15-20.

769 Seki, K., Saito, N. Aoyama, M., 1997. Removal of heavy metal ions from solutions by coniferous
770 barks. Wood Science and Technology 31, 441-447.

771 Shin, E,W., 2005. Cadmium removal by *Juniperus monosperma*. The role of calcium oxalate
772 monohydrate structure in bark. Korean Journal of Chemical Engineering 22 (4), 599-604.

773 Shin, E.W., Karthikeyan, K.G., Tshabalala, M.A., 2007. Adsorption mechanism of cadmium on
774 juniper bark and wood. Bioresource Technology 98, 588-594.

775 Şen, A., Miranda I., Santos, S., Graça, J., Pereira, H., 2010. The chemical composition of cork
776 and phloem in the rhytidome of *Quercus cerris* bark. Industrial Crops and Products 31, 417-
777 422.

778 Şen, A., Olivella, M.A., Fiol, N., Miranda, I., Villaescusa, I., Pereira, H., 2012. Removal of
779 chromium (VI) in aquaeus environments using cork and heat treated cork samples from
780 *Quercus cerris* and *Quercus suber*. BioResources 7 (4), 4843-4857.

781 Trockenbrotd, M., 1995. Calcium oxalate crystals in the Bark of *Quercus robur*, *Ulmus glabra*,
782 *Populus tremula* and *Betula pendula*. Annals of Botany, 75. 281-284.

783 Tuck, C.O., Pérez, E., Horváth, I.T., Sheldon, R.A., Poliakoff, M., 2012. Valorization of biomass:
784 Deriving more value from waste. Science 337, 695-699.

785 Vázquez, G., González-Álvarez, J., Freire, S., López-Lorenzo, M., Antorrena, G., 2002. Removal
786 of cadmium and mercury ions from aqueous solution by sorption on treated *Pinus pinaster*
787 bark: Kinetics and isotherms. Bioresource Technology 82, 247-251.

788 Villaescusa, I., Martinez, M., Miralles, N., 2000. Heavy metal uptake from aqueous solution by
789 cork and yohimbe bark wastes. Journal of Chemical Technology and Biotechnology 75, 812-
790 816.

791 Villaescusa, I., Fiol, N., Cristiani, F., Floris, C., Lai, S., Nurchi, V.M., 2002. Copper (II) and nickel
792 (II) uptake from aqueous solutions by cork wastes: a NMR and potentiometric study.
793 Polyhedron 21., 1363-1367.

794 Villeneuve, E., 2004. Utilization de l'écorce de peuplier faux-tremble pour la fabrication de
795 panneaux de particules. MSc Thesis, Université Laval, Canada.

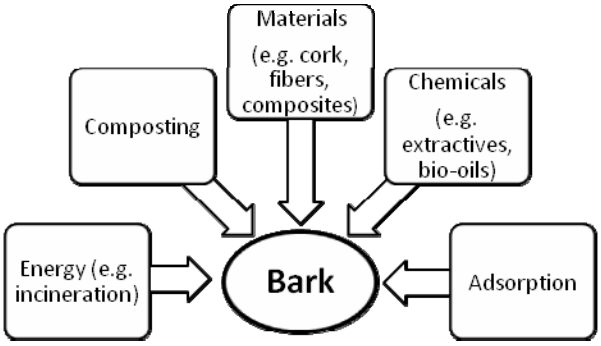

Fig. 1. Main platforms for bark utilization

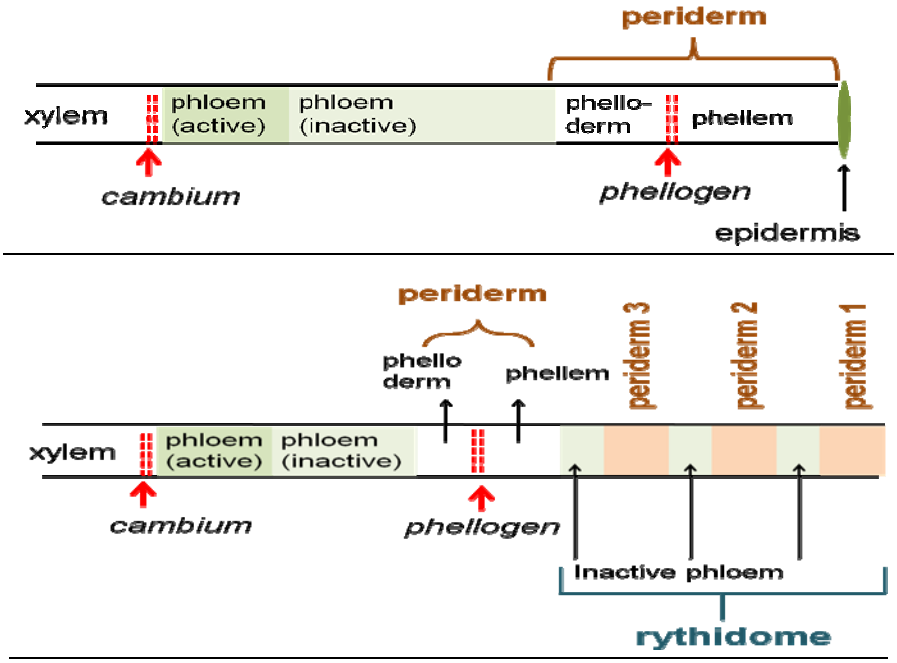

Fig.2. Schematic diagram of bark: young bark with periderm and epidermis (above) and older bark with a rhytidome (below) (Pereira, 2012a).

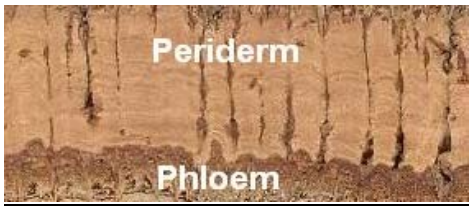

Fig. 3. Bark of *Q.cerris* with a thick rhytidome (above) and bark of *Q.suber* with only one periderm (below)

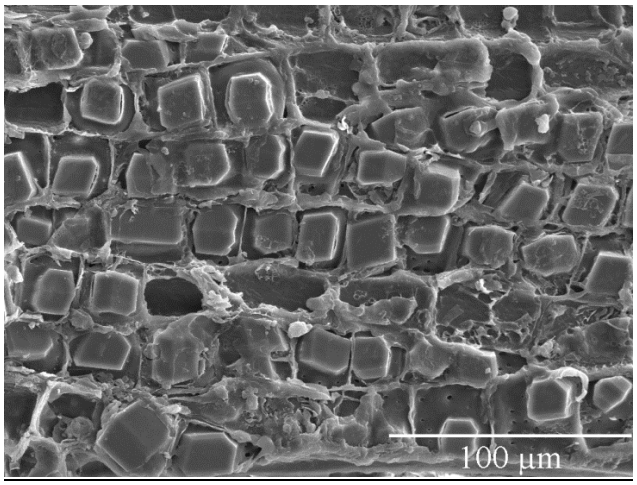

Fig. 4. Calcium oxalate crystals in teak bark

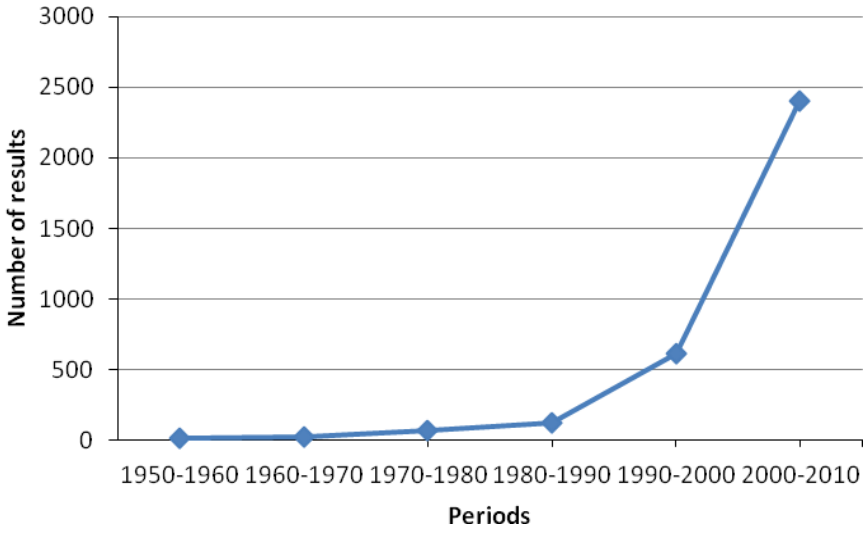

Fig. 5 Number of search results using *bark*, *adsorption* and *heavy metal* keywords on bark adsorption with heavy metals based on Google Scholar Data.

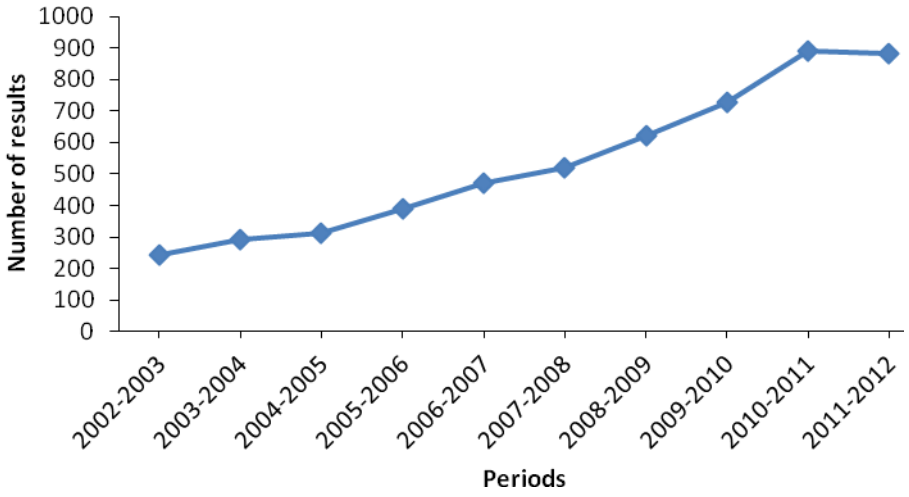

Fig. 6 Number of search results (two year averages) using *bark*, *adsorption* and *heavy* metal keywords on bark adsorption with heavy metals in the last 10 years based on Google Scholar Data.

Table 1. Range of chemical composition of barks, wood and leaves (Pereira, 2012b)

	Barks	Wood	Leaves
Ash	2-15%	>1%	2-7%
Extractives	5-30%	1-10%	15-50%
Lignin	20-30%	20-35%	10-15%
Cellulose	20-40%	40-60%	15-35%
Hemicelluloses	20-30%	15-30%	10-15%
Suberin/Cutin	2-45%	-	1-4%

Table 2. Chemical compositions of barks from a hardwood (*Betula pendula*) and a softwood (*Pinus sylvestris*) barks (Miranda et al., 2012, 2013)

	Betula pendula	*Pinus sylvestris*
Ash	2.9%	4.6%
Extractives	17.6%	18.8%
Lignin	27.9%	33.7%
Holocellulose	49.8%	37.6%
Suberin	5.9%	1.6%

Table 3. Research on softwood barks as biosorbents: Metal cations and corresponding *qmax* (mmol/g) values

Species	**Metal cations, qmax (mmol/g)**									**References**
	Cd^{2+}	Cr^{3+}	Cr^{6+}	Cu^{2+}	Fe^{2+}	Hg^{2+}	Ni^{2+}	Pb^{2+}	Zn^{2+}	
Abies sachalinensis	0.06			0.07					0.05	Seki et al., 1997
Chamaecyparis obtusa	0.10			0.08					0.09	Seki et al., 1997
Cryptomeria japonica			1.38							Aoyama et al., 2004
Juniperus monosperma	0.09									Shin et al., 2007
Larix gmelinii var. *japonica*	0.09			0.10					0.08	Seki et al., 1997
Larix leptolepis			0.30							Aoyama and Tsuda, 2001
	0.08			0.08					0.07	Seki et al., 1997
Picea abies		0.07		0.12			0.09	0.16	0.10	Martin-Dupont et al., 2006
	0.14			0.15					0.12	Seki et al., 1997
Picea glehnii	0.11			0.12					0.11	Seki et al., 1997
Picea jeozensis	0.11			0.11					0.11	Seki et al., 1997
Pinus brutia					0.04					Acemioglu et al., 2004
								0.37		Gundogdu et al., 2009.
Pinus densiflora	0.09			0.07					0.07	Seki et al., 1997
Pinus nigra	0.09									Argun and Dursun,

									2008
Pinus pinaster	0.07	0.37					0.02		Kumar, 2006
Pinus ponderosa	0.45			0.89		0.46		0.81	Oh and Tsabalala, 2007
Pinus radiata					0.47				Palma et al., 2003
							0.01		Vazquez et al., 1994
Pinus strobus	0.08			0.09				0.06	Seki et al., 1997
Pinus sylvestris		0.16							Alves et al., 1993
		0.03		0.04		0.03	0.05	0.03	Martin-Dupont et al., 2006
Pinus thunberghii	0.06			0.10				0.08	Seki et al.,1997
Pseudotsuga menziesii					0.50				Masri et al., 1974
		0.03		0.06		0.06	0.06	0.06	Martin-Dupont et al., 2006
Sciadopitys verticillata	0.09			0.12				0.10	Seki et al., 1997
Sequoia sempervirens					1.25				Kumar, 2006
Taxus cuspidata	0.13			0.12				0.12	Seki et al., 1997
Thujopsis dolabrata var. *hondae*	0.12			0.09				0.09	Seki et al., 1997

Table 4. Research on hardwood barks as biosorbents: Metal cations and corresponding qmax (mmol/g) values

Species	**Metal cations, qmax (mmol/g)**									**References**
	Cd^{2+}	Cr^{3+}	Cr^{6+}	Cu^{2+}	Fe^{2+}	Hg^{2+}	Ni^{2+}	Pb^{2+}	Zn^{2+}	
Acacia leucephala	1.49			2.31				0.89		Munagapati et al., 2010
Afzelia africana			0.19	0.40	0.16		0.16	0.2		Gloaguen and Morvan, 1997
Castanea sativa		0.08		0.24			0.06	0.16	0.10	Martin-Dupont et al., 2006
Casuarina equisetifolia				0.26						Mohan and Sumitha, 2008
Harwickia binata	0.30									Kumar, 2006
Eucalyptus (globulus)	0.13									Ghodbane et al., 2008
Pausinystalia yohimbe				0.15			0.15			Villaescusa et al., 2000
			0.82							Fiol el al., 2003
Psidium guajava						0.02				Lohani et al., 2008
Quercus cerris cork			0.41							Sen et al., 2012
Quercus		0.05		0.09			0.06	0.08	0.06	Martin-

pedunculata							Dupont et al., 2006
Quercus suber cork		0.05		0.07			Villaescusa et al., 2000
	0.32						Fiol et al., 2003
		0.32		0.17		0.38	Chubar et al., 2004a
Quercus (velutina)			2				Masri et al.,1974
Tamarindus indicas			0.21				Prasad and Abdullah, 2009
Tectona grandis	0.26	0.49	0.24	0.19	0.22		Gloaguen and Morvan, 1997

Not: Scientific names in paranthesis indicate probable species, in the corresponding References the species was not mentioned.

Capítulo 4. Conclusões e perspetivas de trabalhos futuros

Neste trabalho, cujo objetivo geral foi o de aumentar o conhecimento sobre a casca de *Quercus cerris* de modo a contribuir para a sua valorização económica, foi analisada a constituição da sua casca e as propriedades da fração de cortiça do ritidoma, após amostragem direta em florestas na região de distribuição da espécie na Turquia.

Os trabalhos realizados permitiram obter, pela primeira vez, uma caracterização sistemática da cortiça de *Q. cerris*, quanto à sua formação na casca, estrutura e composição química, para além de propriedades de comportamento durante tratamento termoquímico e como bioadsorvente de poluentes, como potenciais indicadores de vias de utilização.

Foi possível obter as seguintes conclusões específicas:

1. A casca de *Q. cerris* é constituída pelo floema, periderme e ritidoma, contendo este uma proporção apreciável de cortiça, que se encontra localizada em camadas descontínuas axial e tangencialmente. Devido ao facto da casca ser estruturalmente heterogénea, ela terá de ser fracionada por trituração em grânulos para separar a fração de cortiça.

2. A cortiça de *Q. cerris* é semelhante anatomica e quimicamente à cortiça de *Q. suber*. As principais diferenças anatómicas são as seguintes: as células de cortiça de *Q. cerris* são mais pequenas, tem a parede mais espessa e a fração sólida do material é mais elevada. As principais diferenças químicas são: a cortiça de *Q. cerris* tem um teor de lenhina mais alto e o teor de suberina mais baixo do que a cortiça de *Q. suber*, apresentando também algumas diferenças na composição monomérica da suberina.

3. A cortiça de *Q. cerris* possui um comportamento térmico semelhante ao da cortiça de *Q. suber*. Assim, a cortiça é estável a temperaturas inferiores a 200 °C, mas com o aumento de temperatura e a duração de tratamento inicia-se a degradação termoquímica. Os extrativos e polissacáridos são os componentes mais sensíveis a tratamento térmico e a suberina é o componente mais estável. A suberina de *Q. cerris* mostrou ser mais estável do que a suberina de *Q. suber*.

4. Durante o tratamento térmico ocorreu alteração de cor que foi medida por parâmetros *Cielab*, e que se mostrou correlacionada com a perda de massa até 40%. Foi possível desenvolver um modelo para a perda de massa por tratamento térmico utilizando os valores da alteração de cor, o que pode ser utilizado na indústria de aglomerados puros de cortiça como controlo industrial.

5. Procuraram-se valorizações para a fração de cortiça da casca de *Q. cerris* tendo em conta a sua semelhança com a cortiça de *Q. suber*, através da sua utilização como adsorvente de poluentes, em testes de adsorção com hidrocarbonetos aromáticos policíclicos e com crómio (VI). A cortiça demonstrou ter uma alta eficiência para adsorver hidrocarbonetos aromáticos policíclicos e crómio (VI) de soluções aquosas. A capacidade da cortiça para reduzir crómio (VI) para crómio (III), que é menos tóxico, é particularmente importante. O trabalho de revisão sobre a utilização de cascas como adsorventes de metais pesados mostra o seu potencial e o facto de muito haver ainda a investigar.

Deste modo mostrou-se que a casca de *Q. cerris*, nomeadamente o seu ritidoma, apresenta potencial para aproveitamento da fração de cortiça que poderá ser utilizada após trituração e separação de outros componentes da casca em aglomerados e como bioadsorvente de poluentes.

No futuro pretende-se investigar o modo de fracionamento da casca de *Q. cerris* tendo em vista a separação da componente de cortiça como uma fração com elevado grau de pureza, tendo por base as diferenças de propriedades (nomeadamente de densidade e de permeabilidade) dos diferentes componentes anatómicos da casca. Este ponto é importante para viabilizar a utilização industrial da cortiça da casca de *Q. cerris*.

Por outro lado, também se planeia pesquisar as potencialidades de cascas de outras espécies que possuem cortiça, continuando trabalhos já iniciados para algumas das espécies ou estudando outras espécies pela primeira vez (por exemplo *Quercus variabilis* da China; *Kielmeyra coriacea, Agonandra brasiliensis, Enterolobium ellipticum, Connarus suberosus, Erythrina mulungu* e *Symplocas lanceolata* do Brasil), aumentando o conhecimento

sobre as suas propriedades anatómicas e químicas, assim como desenvolver novos compósitos com base na combinação de cortiças destas espécies.

Pretende-se ainda analisar as transformações das macromoléculas da cortiça durante o tratamento térmico, utilizando por exemplo análises de DSC e TGA, para além de investigar a obtenção de subprodutos do tipo bio-óleos através de tratamento térmico.

Bibliografia

Abi-Saleh, B., Safi, S., 1988. Carte de la Végétation du Liban. Ecologia Mediterranea XIV (1/2), 123-142.

Almeida, D.G. de., 1946. Cortiças. Revista Florestal 5 (3-4), 10-24.

Almeida, D.G. de., 1948. Test of some corks from Brazil. Tropical Woods 93, 40-48.

Almeida, S.P., Proença, C.E., Sano, S.M., Ribeiro, J.F., 1998. Cerrado: espécies vegetais úteis. EMBRAPA. Planaltina-DF: 183-186.

Aoyama, M., Tsuda, M., 2001. Removal of Cr (VI) from aqueous solutions by larch bark. Wood Science and Technology 35, 425-434.

Associação Portuguesa da Cortiça (Apcor), 2012. Anuário. Cortiça, Cork, 2012.

Azevedo Gomes, M., 1960. Monografia do Parque da Pena. Estudo Dendrológico-Florestal. Grafitécnica. Lisboa.

Babos, K., 1979. Anatomische Untersuchungen der Rinde bei den Stammen von *Quercus cerris* var. cerris Loud. und *Quercus cerris* var. *austrica* (Willd.) Loud. Folia Dendrol 6, 60-78.

Bagnoli, F., Fineschi, S., Simeone, G.G., Vendramin, G.G., 2009. Phylogeography of *Quercus cerris* L. (Fagaceae) based on cpDNA markers. VII Congresso Nazionale SISEF: Sviluppo e adattamento naturalità e conservazione. Isernia-Pesche. 29 Setembro- 3 Outubro.

Bartha, S., 2011. Cercatări Privind Factorii De Variaţie A Calităţii Lemnului De Cer Din Pădurea Boboştea (Jud. Bihor). Rezumatul tezei de doctorat. Universitatea Transilvania Din Braşov.

Beck, C.B., 2010. An Introduction to plant structure and development. Plant anatomy for the twenty-first century. 2nd Ed. Cambridge University Press.

Berkel, A., Bozkurt, Y., 1961. Untersuchungen über die makroskopischen und anatomischen holzmerkmale der wichtigsten Türkischen Eichenarten. Istanbul Universitesi Orman Fakultesi Yayinlari, 78. Kutulmus Matbaasi. Istanbul.

Bozkurt, Y., Göker, Y., 1986. Orman Urunlerinden Faydalanma. Istanbul Universitesi Orman Fakultesi Yayinlari, 379. Istanbul.

Brüggemann, W., Bergmann, M., Nierbauer, K.U., Pflug, E., Schmidt, C., Weber, D., 2009. Photosynthesis studies on European evergreen and decidous oaks under Central European climate conditions: II. Photoinhibitory and light-independent violaxanthin deepoxidation and downregulation of photosystem II in evergreen, winter-acclimated European *Quercus* taxa. Trees. 23, 1091-1100.

Buttrick, P.L., 1941. Note on Brazilian cork. Tropical Woods 68, 11-13.

Camus, A. 1934. Les Chênes. Monographie du genre *Quercus*. Paris. Ed. Paul le Chavalier.

Centre de documentation, de recherche, et d'expérimentationssur les pollutions acciedentelles des eaux (Cedre). 2012a. Sorbents. Disponível em http://www.cedre.fr/en/response/sorbent.php. Acesso em 20/09/2012.

Centre de documentation, de recherche, et d'expérimentationssur les pollutions acciedentelles des eaux (Cedre). 2012b. Characteristics of floating sorbent to be used at sea and inland waters adapted according to Afnor norm NFT 90-360. Disponível em: http://www.cedre.fr/en/response/sorbent-gb.pdf. Acesso em 20/09/2012.

Çekiç, T.I., 2011. Redefining Turkey´s regional economic disparities through social participation. 51st Congress of the European Regional Science Association International. 30 August-4 September, Barcelona, Spain.

Chang, Y. P., 1954. Anatomy of common North American pulpwood barks. Tappi Monograph Series 14, 127-146.

Chubar, N., Carvalho, J.R., Correia, M.J.N., 2004a. Cork biomass as biosorbent for Cu(II), Zn(II) and Ni(II). Colloids and Surfaces A: Physicochemical and Engineering Aspects 230, 57-65.

Chubar, N., Carvalho, J.R., Correia, M.J.N., 2004b. Heavy metals biosorption on cork biomass: effect of the pre-treatment. Colloids and Surfaces A: Physicochemical and Engineering Aspects 238, 51-58.

Corticeira Amorim SGPS. 2012a. Aglomerados compósitos. Disponível em: www.amorim.com/cor_neg_aglomerados.php. Acesso em 28/09/2012.

Corticeira Amorim SGPS. 2012b. Corksorb. Sustainable absorbents. Disponível em www.corksorb.com. Acesso em 29/09/2012.

Cotti, C., 2008. Molecular markers for the assessment of genetic variability in the threatened plant species. Tese de Doutoramento. Università degli studi di Bologna.

Çuhadar, M.T., 2010. Regional development agencies in Europe and in Turkey: A case study on Çukurova RDA. Governship of Ordu, Turkey.

Damas, H. 1949. Estudo comparative das cortiças portuguesas e brasileiras. Portugal Junta Nacional da Cortiça B 128, 365-370.

Dickinson, W.C., 2000. Interactive Plant Anatomy. USA. Elsevier Publ.

Di Filippo, A., Alessandrini, A., Biondi, F., Blasi, S., Portoghesi, L., Piovesan, G., 2010. Climate change and oak growth decline: Dendroecology and stand

productivity of a Turkey oak (*Quercus cerris* L.) old stored coppice in Central Italy. Annals of Forest Science 67, 706. DOI: 10.1051/forest/2010031.

Domingues, V., Alves, A., Cabral, M., Delerue-Matos, C., 2005. Sorption behaviour of bifenthrin on cork. Journal of Chromatography A 1069, 127-132.

Evert, R. F., Kozlowski, T. T., 1967. Effect of isolation of bark on cambial activity and development of xylem and phloem in trembling aspen. American Journal of Botany 54, 1045–1055.

Evert, R.F., 2006. Esau's Plant Anatomy. Meristems, cells and tissues of the plant body-Their structure, function and development. 3rd ed. John Wiley & Sons, Inc.

Fahn, A., 1990. Plant anatomy. 4th Ed. Pergamon.

Fineschi, S., Bagnoli, F., Simeone, M.C., Vendramin, G.G., 2011. La diversità cloroplastica del cerro (*Quercus cerris*) rivela un forte segnale filogeografico e il ruolo della Turchia como serbatoio di diversità. VIII Congresso Nazionale SISEF. Selvicoltora e conservazione del suolo : la sfida europea per una gestione territoriale integrata. Arcavata di Rende. 4-7 Outubro.

Fiol, N., Villaescusa, I., Martinez, M., Miralles, N., Poch, J., Serarols, J., 2003. Biosorption of Cr (VI) using low cost sorbents. Environmental Chemistry Letters 1, 135–139.

Fortes, M.A., Rosa, M.E., Pereira, H., 2004. A cortiça. IST Press. Lisboa.

Gete, A.R., 2008. Tecnología del Corcho. Visión Libros. Madrid.

Gibson, L.J., Easterling, K.E., Ashby, M.F., 1981. The structure and mechanics of cork. Proceedings of the Royal Society of London. A377, 99-117.

Gil, L., 2009. Cork composites: A review. Materials 2, 776-789.

Gorian, F., Bertolasi, B., Meloni, M., Binelli, G., Fineschi, S., Sebastiani, F., Vendramin, G.G., 2012. Toward a synthetic map of the genetic diversity of *Quercus cerris* in Italy. PMS.07-P16. Dispoível em: www3.corpoforestale.it. Acesso em 10/10/2012.

Graça, J., Pereira, H., 1999. Glyceryl-Acyl and Aryl-Acyl dimers in *Pseudotsuga menziesii* bark suberin. Holzforschung 53, 395-402.

Graça, J., Pereira, H., 2000. Methanolysis of bark suberins: Analysis of glycerol and acid monomers. Phytochemical Analysis 11, 45-51.

Graça, J., Pereira, H., 2004. The periderm development in *Quercus suber*. IAWA Journal 25, 325-335.

Guerra, F., Santos, A., Sanquetta, C., Bittencourt, A., Almeida, A., 2009. Quantificação e valoração de produtos florestais não-madereiros. Floresta, Curitiba PR., 39 (2), 431-439.

Hedge, I.C. Yaltırık, F., 1982. Flora of Turkey and the East Aegean Islands. Edinburg. Edinburg Univ Press.

Holdheide, W., 1951. Anatomie mitteleuropäischer Gehölzrinden (mit mikrophotographischem Atlas). In: Handbuch der Mikroskopie in der Technik, Band 5, Heft 1, pp. 193–367, H. Freund, ed. Umschau Verlag, Frankfurt am Main.

Howard, E.T., 1977. Bark structure of the Southern Upland Oaks. Wood and Fiber 9, 172-183.

Huber, B., 1958. Anatomical and physiological investigations on food translocation in trees. In K. V. Thimann, ed., The physiology of forest trees. Ronald Press, New York.

Instituto Nacional Da Propriedade Industrial (INPI) 2012a. PT 104704. Fibre-reinforced cork-based composites. Dispoível em: http://servicosonline.inpi.pt/pesquisas/main/patentes.jsp?lang=PT. Acesso em 10/10/2012.

Instituto Nacional Da Propriedade Industrial (INPI) 2012b. PT 103492. Meio de absorção/adsorção à base de derivados de cortiça para absorção/adsorção de óleos. Dispoível em: http://servicosonline.inpi.pt/pesquisas/main/patentes.jsp?lang=PT. Acesso em 10/10/2012.

International Oak Society, 2012. *Quercus cerris* L. (1753). Dispoível em: www.oaknames.org/search/alpha/asp. Acesso em 10/10/2012.

Jardim Botânico-UTAD, 2012. *Quercus cerris*. Dispoível em: http://jb.utad.pt/especie/quercus_cerris. Acesso em 15/10/2012.

Junikka, L., 1994. Survey of English macroscopic bark terminology. IAWA Journal 15 (1), 3-45.

Karastergiou, S., Barboutis, J., Vassilou, V., 2006. Effect of the PVA gluing on bending strength properties of finger jointed turkey oakwood (*Quercus cerris* L.). Holz als Roh-und Werkstoff 64 (4), 339-340.

Kasaplıgil, B., 1981. Past and present oaks of Turkey. Phytologia 49, 95-146.

Kumar, U., 2006. Agricultural products and by-products as a low-cost adsorbent for heavy metal removal from water and waste-water: A review. Scientific Research and Essay 1 (2), 33-37.

La Marca, O., Totolo, M., Uzielli, L., Zanuttini, R. 1983. Possibilità di impegio del legname di cerro (*Quercus cerris* L.) in Italia. Indagini preliminari su alcuni popolamenti e prove sperimentali per l'industria dei compensati. L'Italia Florestale e Montana 1, 33-62.

Lavisci, P., Scalbert, A., 1991. Quality of Turkey Oak (*Quercus cerris* L.) Wood I. Soluble and Insoluble Proanthocyanidins. Holzforschung 45 (4), 291-296.

Lavisci, P., Masson, D., Deglise, X., 1991. Quality of Turkey Oak (*Quercus cerris* L.) Wood II. Analysis of some Physico-Chemical Parameters Related to its Gluability. Holzforschung 45 (6), 415-418.

Lavisci, P., Masson, D., 1992. Quality of Turkey Oak (*Quercus cerris* L.) Wood III. Microscopy and X-Ray Spectroscopy of Fractured Surfaces.Holzforschung 46 (2), 103-107.

Liberato, M.C., Caixinhas, M.L., Lousã, M., Vasconcelos, T. 2003. Mediterranean flora in some botanic gardens and parks in Portugal. Bocconea 16 (2), 1123-1130.

Lo Monaco, A., Todaro, L., Sarlatto, M., Spina, R., Calienno, L., Picchio, R., 2011. Effect of moisture on physical parameters of timber from Turkey oak (*Quercus cerris* L.) coppice in Central Italy. Forestry Studies in China 13 (4), 276-284.

Martin-Dupont, F., Gloaguen, V., Guilloton, M., Granet, R., Krausz, P., 2006. Study of the chemical interaction between the barks and heavy metal cations in the sorption process. Journal of Environmental Science and Health Part A 41 (2), 149-160.

Marques, A.V., Pereira, H., Meier, D., Faix, O., 1994. Quantative analysis of cork (*Quercus suber* L.) and milled cork lignin by FTIR spectroscopy, analytical pyrolysis and total hydrolysis. Holzforschung 48 (suppl.), 43-50.

Marques, A.V., Pereira, H., Meier, D., Faix, O., 1999. Structural characterization of cork lignin by thioacidolysis and permanganate oxidation. Holzforschung 53, 167-174.

Matheus, M.T., Bacelar, M., Oliveira, S.A, Lopes, J.C., 2009. Morfologia de frutos, sementes e desenvolvimento pós-seminal de cabelo-de-negro *Connarus suberosus* Planch. (Connaraceae). Cerne, Lavras 15 (4), 407-412.

Mauseth, J.D. 2011. Botany. An Introduction To Plant Biology. 4th Ed. Jones and Bartlett Publishers.

Mıhçıoğlu, K., 1942. Turkiye de saçli meseden mantar istihsaline dair bir arastirma. Orman ve Av 1, 151–166.

Miranda, I., Gominho, J., Pereira, H., 2012. Cellular structure and chemical composition of cork from the Chinese cork oak (*Quercus variabilis*). Journal of Wood Science, DOI: 10.1007/s10086-012-1300-8.

Natividade, J.V., 1950. Subericultura. Lisboa. Direção Geral dos Serviços Florestais e Aquícolas.

Nunes, E., Quilhó, T., Pereira, H., 1996. Anatomy and chemical composition of *Pinus pinaster* bark. IAWA Journal 17 (2), 141-149.

Nunes, E., Quilhó, T., Pereira, H., 1999. Variability of bark structure in plantation-grown *Eucalyptus globulus* Labill. Annals of Forest Science, 56, 479-484

Orman Genel Müdürlüğü (OGM), 2006. Türkiye orman varlığı. Disponível em: http://www.ogm.gov.tr/orm_var.htm. Acesso em 20/09/2011.

Orman Genel Müdürlüğü (OGM), 2012. Bölge Müdürlükleri. Disponível em: http://web.ogm.gov.tr/Sayfalar/BolgeMudurlukleri.aspx. Acesso em: 10/10/2012.

Pereira, H., 1988a. Chemical composition and variability of cork form *Quercus suber* L. Wood Science and Technoly 22 (3), 211–218.

Pereira, H., 1988b. Structure and chemical composition of cork from *Calotropis procera* (Ait.) R. Br. IAWA Bulletin 9 (1), 53–58.

Pereira, H., Ferreira, E., 1989. Scanning electron microscopy observations in insulation cork agglomerates. Materials Science and Engineering A 111, 217-225.

Pereira, H., 1992. The thermochemical degradation of cork. Wood Science and Technology 26, 259-269.

Pereira, H., 2007. Cork: Biology, Production and Uses. Elsevier Publications. Amsterdam.

Pintor, A.M.A., Ferreira, C.I.A., Pereira, J.C., Correia, P., Silva, S.P., Vilar, V.J.P., Botelho, C.M.S., Boaventura, R.A.R. 2012. Use of cork powder and granules for the adsorption of pollutants: A review. Water Research. 46. 3152-3166.

Quilhó, T., Pereira, H., Richter, H.G., 1999. Variability of bark structure in plantation-grown *Eucalyptus globulus*. IAWA Journal 20, 171-180.

Quilhó, T., Sousa, V., Tavares, F., Pereira, H., 2012. Bark anatomy and cell size variation in *Quercus faginea*. Turkish Journal of Botany DOI: 10.3906/bot-1201-54.

Rameau, J.C., Mansion,D., Dumé, G., 1989. Flore Forestière Française. Guide écologique illustré. Plaines et collines. IDF Éditions. Paris.

Richter, H.G., Mazzoni-Viveiros, S.C., Alves, E.S., Luchi, A.E., Costa, C.G., 1996. Padronização de critérios para a descrição anatómica da casca: lista de características e glossário de termos. Revista do Instituto Florestal e IF Série Registros 16, 1-25.

Rios, P.D.A., 2007. Caracterizção tecnólogica e produção de painéis de cortiça de *Kilmeyera coriacea* (Pau-santo). Universidade Federal de Lavras. Tese de Mestrado.

Rios, P.D.A., 2011. Estrutura anatômica e caracterização química da cortiça de árvores de Kielmeyera coriacea Mart. (Pau-Santo). Tese Doutoramento. Universidade Federal De Lavras.

Rios, P.D.A., Mori, F.A., Barbosa, A.C.M.C., 2011. Morphological characterization of *Kielmeyera coriacea* Mart. cork from Brazilian Cerrado. Cerne, Lavras 17 (3), 387-392.

Rizzini, C.T., Mors, W.B., 1995. Botânica econômica brasileira. 2ª edição. Rio de Janeiro, Âmbito Cultural.

Röckle , H., 1986. Veränderungen der Rindenstruktur in Abhängigkeit von der Topographie, am Beispiel von *Quercus rubra* L. Dipl-Arbeit, Universidade Hamburg.

Romagnoli, M., Codipietro, G., 1996. Pointer years and growth in Turkey oak (*Quercus cerris* L.) in Latium (central Italy). A dendroclimatic approach. Annals of Forest Science 53, 671-684.

Roth, I., 1981. Structural patterns of tropical barks. Gebruder Borntraeger, Berlin.

Royal Botanic Gardens-Kew, 2012. Turkey oak *Quercus cerris*. Dispoível em http://apps.kew.org/trees/?page_id=89. Acesso em:10/10/2012.

Tanılır, M.N., 2010. TR 63 (Hatay-Kahramanmaras-Osmaniye) Bölge Planı 2010-2013. 10 Ağustos, 2010.

Teixeira, R.T., Pereira, H., 2009. Ultrastructural observations reveal the presence of channels between cork cells. Microscopy and Microanalysis 15 (6), 539-544.

Telgeren, G. 1976. Memleketimizde yetişen saçlı meşe ağaçlarının kabuklarından yararlanma olanakları. Ormancılık Araştırma Enstitüsü Dergisi 22, 114-127.

Todaro, L., Zanuttini, R., Scopa, A., Moretti, N., 2012a. Influence of combined hydro-thermal treatments on selected properties of Turkey oak (*Quercus cerris L*.) wood. Wood Science and Technology 46, 563-578.

Todaro, L., Zuccaro, L., Marra, M., Basso, B., Scopa, A., 2012b. Steaming effects on selected wood properties of Turkey oak by spectral analysis. Wood Science and Technology 46, 89-100.

Trockenbrodt, M., 1990. Survey and discussion of the terminology used in bark anatomy. IAWA Bulletin 11 (2), 141-166.

Trockenbrodt, M., 1991. Qualitative structural changes during bark development in *Quercus robur*, *Ulmus glabra*, *Populus tremula* and *Betula pendula*. IAWA Bulletin 12(1), 5-22.

Trockenbrodt, M., 1994. Quantitative changes of some anatomical characters during bark development in *Quercus robur*, *Ulmus glabra*, *Populus tremula* and *Betula pendula*. IAWA Journal 15 (4), 387-398.

Trockenbrodt, M., 1995. Calcium oxalate crystals in the bark of *Quercus robur*, *Ulmus glabra*, *Populus tremula* and *Betula pendula*. Annals of Botany. 75, 281-284.

Vázquez, G., González-Álvarez, J., Freire, S., López-Lorenzo, M., Antorrena, G., 2002. Removal of cadmium and mercury ions from aqueous solution by sorption on treated *Pinus pinaster* bark: Kinetics and isotherms. Bioresource Technology, 82. 247-251

Villaescusa, I., Martinez, M., Miralles, N., 2000. Heavy metal uptake from aqueous solution by cork and yohimbe bark wastes. Journal of Chemical Technology and Biotechnology 75, 812-816.

Whitmore, T.C., 1962. Studies in systematic bark morphology IV. The bark of beech, oak and sweet chesnut. New Phytologist 62, 161-169.

Williams, L.O., Erlanson, C.O., 1959. Brazilian cork. Qualitas Plantarum et Materiae Vegetabiles 6 (2), 114-120.

Yafang, L., Yanzhen, L., Wei, Z., Jingfeng, Z., 2009. The microstructure of cork from *Quercus variabilis*. Scientia Silvae Sinicae 45 (1), 167-170.

Yaltırık, F., 1984. Türkiye meşeleri teşhis kılavuzu.Tarım Orman ve Köyişleri Bakanlığı Genel Müdürlüğü Yayınları. Yenilik Basimevi. Istanbul.

Anexos: Resumos dos trabalhos apresentados em congressos internacionais

Chromium (VI) sorption onto granulated cork from *Quercus suber* and *Quercus cerris*

Şen, A., Olivella, M.A., Fiol, N., Miranda, I., Villaescusa,I, & Pereira, H.

International Symposium on Metal Complexes (ISMEC) Lisboa, 18-22 de Junho de 2012.

Adsorção do crómio (VI) foi estudada com grânulos de cortiças de *Q. cerris* submetidas a tratamento térmico a temperaturas 200°C, 250°C*, 300*°C e *350*°C e não tratada*,* e com aglomerados negros da cortiça de *Q. suber* (tratada a temperatura aproximadamente 300°C).

A maior adsorção foi obtida com grânulos não tratados de *Q. cerris* em pH 3, seguido com aglomerado negro de *Q. suber*. Com o tratamento térmico a eliminação do crómio total e a redução de crómio (VI) de solução reduziram. As isotermas de adsorção seguem o modelo de Langmuir e os valores máximos de adsorção foram 21.69 mg/g para grânulos não tratados de *Q. cerris* e 22.98 mg/g para os aglomerados negros de *Q. suber*.

Espectros de FTIR indicaram que a lenhina desempenha um papel significativo para adsorção de crómio nas ambas cortiças. No entanto, a suberina e os polissacáridos também contribuem a adsorção na cortiça de *Q. cerris*.

Conclui-se que as cortiças não tratadas de *Q. cerris* e aglomerados negros de *Q. suber* são adsorventes eficientes a remoção do crómio nas soluções aquosas.

Bark Fibre Dimensions of *Quercus cerris* var. *cerris*.

Şen, A., Quilhó, T. & Pereira, H.

International Union of Forest Research Organizations (IUFRO)

Congress Lisboa, 8-13 de Julho de 2012.

A casca de *Q. cerris* tem uma quantidade considerável de fibras. As amostras das cascas foram recolhidas em 4 localidades na Turquia. O comprimento, a largura e a espessura da parede das fibras variou entre localidades, designadamente 1.06-1.16 mm, 21-22 µm e 9-10 µm, respetivamente. Os resultados da análise de variância revelaram diferenças significativas ($P<0.05$) nas dimensões das fibras entre localidades de amostragem. Seguidamente, a análise de Student-Newman-Keuls (SNK) demonstrou que a espessura do lúmen vária entre todas as localidades enquanto a espessura da parede vária apenas entre as localidades 1 e 2. A espessura da parede e o comprimento das fibras têm diferenças significativas na localidade 2. Os resultados demonstraram a influência das localidades sobre as dimensões das fibras.

Treatment of Textile Industry Effluents with *Quercus cerris* Cork.

Ali Şen, Elena Lygina, Ahmet Çelebi, Isabel Fonseca, Helena Pereira, Bülent Şengörür, Terencio Junior,& Svetlana Lyubchik

International Union of Pure and Applied Chemistry (IUPAC) Congress
Foz de Iguaçu, 25-29 de Agosto de 2012.

As amostras dos efluentes, adquiridas em 4 fábricas do ramo têxtil na Turquia, foram analisadas quanto à presença de metais e a demanda química de oxigênio (DQO) antes de se efetuar o tratamento com grânulos de cortiça de *Q. cerris*. Foram encontrados 26 metais nos efluentes. O crómio e o manganês foram os metais tóxicos com concentrações mais altas do que a autorizada pela legislação referente a potabilidade de água (a concentração do crómio não deve ultrapassar 0.1 ppm e a concentração de manganês não deve ultrapassar 0.05 ppm, contudo nos efluentes a concentração do crómio foi 1.08 ppm na fábrica 3 e as concentrações de manganês foram 0.121 e 0.139 ppm nas fábricas 3 e 4). O tratamento dos efluentes com a cortiça eliminou entre 14% e 98% (chumbo-vanádio) de metais dos efluentes. A demanda química de oxigênio também diminuiu (os valores antes e depois, 535-374 ppm, 1420-279 ppm, 1460-674 ppm e 494-72 ppm, nas 4 fábricas respetivamente) o que significa que, além de metais a cortiça adsorveu também os materiais orgânicos dos efluentes.

A eficiência da cortiça na eliminação de metais nos efluentes foi comparada com o tratamento efetuado atualmente na fábrica 4, o que revelou a eficiência da cortiça (94%-28%, 88%-66%, 81%-57%, 93%-46%, as eliminações de B, Cr, Cu e Ni respetivamente).

Concluiu-se que a carga da cortiça mais adequada para o tratamento dos efluentes foi de 2-4 mg/L. A cortiça pode ser utilizada como adsorvente de metais pesados sem pré-tratamento e os metais podem ser recuperados após tratamento.

Modelling mass loss of cork during thermal treatments using colour analysis

Şen, A., Gominho, J., Knapic, S., & Pereira, H

The Sixth European Conference on Wood Modification (ECWM6)

Ljubljana, 16-18 de Setembro de 2012.

Os grânulos suberosos foram obtidos por trituração da casca do carvalho da Turquia (*Quercus cerris*), seguido a crivação e flutuação em água. Tratamento térmico foi efetuado com os grânulos a temperaturas entre 150°C e 400°C durante entre 5 e 90 minutos. Após o tratamento, foi calculada a perda de massa e foram medidos os parâmetros de cor utilizando o sistema de CIELAB.

Foi desenvolvido um modelo de perda de massa empregando a análise de cor até 40% de perda de massa. Este modelo é aplicável em monitoração da produção dos aglomerados negros de cortiça e outros tratamentos térmicos, fornecendo informação sobre intensidade do tratamento (perda de massa).